MicroRNAs and orphan nuclear receptor GCNF as novel regulators of human neural stem cell differentiation and neuronal subtype specification

DISSERTATION

zur Erlangung des Doktorgrades (Dr. rer. nat.)
der Mathematisch-Naturwissenschaftlichen Fakultät
der Rheinischen Friedrich-Wilhelms-Universität Bonn

vorgelegt von

Laura Stappert

aus Andernach

Bonn, 2014

Angefertigt mit Genehmigung der Mathematisch-Naturwissenschaftlichen Fakultät
der Rheinischen Friedrich-Wilhelms-Universität Bonn
am Institut für Rekonstruktive Neurobiologie

1. Gutachter: Prof. Dr. Oliver Brüstle

2. Gutachter: Prof. Dr. Michael Hoch

Tag der Mündlichen Prüfung: 19.08.2015

Erscheinungsjahr: 2015

SUMMARY

MicroRNAs (miRNAs) are currently recognized as important regulators of neural development. However, given the large number of miRNA species in existence, our understanding of miRNA-based regulation during neurogenesis remains incomplete, in particular with regard to human neural development. Human pluripotent stem cell (hPSC)-based neural stem cells (NSCs) now offer the possibility to study the function of miRNAs in association with early human neuronal differentiation. Thus, the aim of this study was to analyze the impact of miRNAs and their downstream effectors on human neuronal differentiation and subtype specification using a specific population of long-term self-renewing neuroepithelial-like stem (lt-NES) cells.

First, a miRNA profiling analysis was performed covering the progression from human embryonic stem cells to neurons with lt-NES cells as a stable intermediate. Subsequent functional analyses demonstrated that miR-153, miR-181a/a* and miR-324-5p/3p are able to promote neuronal differentiation of lt-NES cells, similar to the impact of the neuronal-associated miR-124 and miR-125b. In addition, miR-124, miR-125b and miR-181a/a* were found to modulate the neuronal subtype composition of differentiating lt-NES cells, and transfection with respective miRNA oligonucleotides induced differentiation towards a dopaminergic phenotype. Further experiments using hPSC-derived floor plate progenitor cells, a more authentic source for midbrain dopaminergic neurons, confirmed the positive function of miR-181a and the negative function of miR-124 during dopaminergic differentiation. The last part of the thesis focused on deciphering the targets and down-stream effectors of miR-181a. With regard to its role as promoter of neuronal differentiation, miR-181a down-regulates several factors involved in NSC maintenance, including the orphan nuclear receptor GCNF. GCNF is a known transcriptional repressor of pluripotency genes, however, evidence collected in this work points to a yet unrecognized role for GCNF in human NSCs. Specifically, direct targeting of GCNF by miR-181a resulted in an increased rate of neuronal differentiation. Conversely, GCNF overexpression interfered with neuronal differentiation, while preserving the characteristic neural rosette morphology of undifferentiated lt-NES cells. On a mechanistic level, GCNF might act as a suppressor of pro-neural bHLH gene expression, similar to the role of Notch signaling. Indeed, ectopic expression of GCNF partially compensated for Notch inhibition by the gamma-secretase inhibitor DAPT. In addition to this general effect on neuronal differentiation, GCNF has a specific negative effect on the dopaminergic lineage. Thus, the action of miR-181a on GCNF might also account for the miR-181a-induced dopaminergic differentiation. Overexpression of miR-181a in lt-NES cells also increased Wnt activity, which might further contribute to the generation of dopaminergic neurons.

Taken together, this work describes a comprehensive analysis from miRNA profiling to the functional study of specific miRNAs in the context of human neuronal differentiation. Based on these analyses, a mechanistic interaction between miR-181a and GCNF in regulating human NSC fate was discovered. Furthermore, this study is the first to describe a miRNA – miR-181a – that promotes the generation of dopaminergic neurons. These findings could be exploited to develop novel approaches for human neural stem cell maintenance as well as the *in vitro* differentiation of dopaminergic neurons.

TABLE OF CONTENTS

1 INTRODUCTION

1.1 Human pluripotent stem cell-based neural stem cells as a tool to access key aspects of early human neural development

Stem cells are defined as cells capable of both self-renewal and differentiation into one or more distinct cell types along a developmental path. There are several types of stem cells, which can be distinguished by their origin and their potency defining the spectrum of derivatives they can give rise to. Pluripotent stem cells (hPSCs), which can be derived from early embryonic stages (embryonic stem cells; Evans et al. 1981; Thomson et al. 1998) or by reprogramming of somatic cells (induced pluripotent stem cells; Takahashi & Yamanaka 2006; Takahashi et al. 2007), can differentiate into any cell type of the three germ layers. Multipotent stem cells are usually restricted to a particular germ layer but possess the potential to differentiate into various cell types. For instance, multipotent neural stem cells (NSCs) are capable of differentiating into the three major cell types of the CNS, i.e. neurons, astrocytes and oligodendrocytes (Reynolds et al. 1992; Breunig et al. 2011).

During the last decade several protocols have been developed that enable the generation of distinct neural cell types from hPSCs. However, the direct production of mature neural cells from hPSCs via so-called run-through protocols is prone to variability. Proliferative NSCs that can be easily derived from hPSCs and propagated in culture might be used to minimize this variability and also allow the generation of bulk amounts of the desired cell type. Furthermore, NSCs offer the opportunity to study stage-dependent functions during early human neural development, which was previously hardly attainable, due to the limited access to primary human neural tissue (reviewed by Koch et al. 2009a; Roese-Koerner et al. 2013). With regard to applied research, NSCs and the mature neural cells thereof could be harnessed for drug-screening approaches or cell-replacement strategies. In this context, one main interest is to generate dopaminergic neurons, which are the cell type affected in Parkinson's disease.

In fact, the understanding of how neural progenitor cells differentiate into distinct mature neuronal cell types in response to a few developmental signals is still scarce. MicroRNAs (miRNAs), as post-transcriptional regulators of gene expression, have emerged as important fate determinants during this process. However, so far only a small proportion of the miRNA repertoire known to be expressed during neural development has been functionally studied. Furthermore, most of the experiments leading to the identification of specific miRNAs implicated in neurogenesis were restricted to animal models. Thus, the knowledge on the role of miRNAs during human neural development is still limited – a gap that could be closed by the increasing availability of human neural cell types generated from human pluripotent stem cells (reviewed by Benchoua et al. 2013).

1.1.1 Human embryonic and induced pluripotent stem cells

Classically, embryonic stem cells (ESCs) have been derived from the inner cell mass (ICM) of the blastocyst embryo. Specifically, ICM cells have been plated on a layer of mitotically inactivated fibroblast feeder cells and further propagated to establish a stable cell line (Evans et al. 1981; Thomson et al. 1998). Until now, hundreds of mouse and human ESC lines have been established and the culture conditions have improved towards chemically defined xeno-free media and feeder-free culture systems (reviewed by Villa-Diaz et al. 2012). In parallel, many researchers have started to investigate the mechanisms underlying pluripotency, which led to the discovery of transcription factors importantly required for pluripotency and stemness (reviewed by Jaenisch et al. 2008). In the center of the so-called pluripotency network are OCT4 (POU5F1), Nanog and SOX2, which form an auto-regulatory transcriptional circuitry. Furthermore, they regulate numerous other genes including miRNA genes, and drive the expression of stemness factors while repressing the expression of differentiation-associated genes in conjunction with Polycomb group proteins (Pietersen et al. 2008; Marson et al. 2008). These findings were the basis for the landmark discovery by Takahasi and Yamanka, who showed that adult somatic cells can be reprogrammed into induced pluripotent stem cells (iPSCs) by retroviral overexpression of a specific set of pluripotency factors (OCT4, SOX2, KLF4 and MYC) (Takahashi & Yamanaka 2006; Takahashi et al. 2007). During the last years the reprogramming technique has been further improved involving the use of different transcription factor combinations, chemical compounds and miRNAs to increase the reprogramming efficiency. In addition, alternative integration-free reprogramming delivery methods have been developed (reviewed by Bayart & Cohen-Haguenauer 2013). Induced PSCs evade the ethical and legal issues related to hESC research. The iPSC technology further provides the unique opportunity to derive disease- and patient-specific cells for a different range of applications, like cellular disease modeling, drug screening and autologous cell transplantation. In general, both embryonic and induced PSCs represent a valuable source to overcome the restricted supply of human neural cells. However, it is still challenging to master the differentiation of hPSCs into authentic neural cell types.

1.1.2 Directing human pluripotent stem cells towards the neural lineage

When induced to enter neural differentiation, hPSCs undergo specific fate transitions reminiscent of the *in vivo* neural development. This includes the transition of hPSCs to neuroepithelial cells, their segregation into distinct neural progenitors and terminal differentiation into specific neuronal and glial lineages (reviewed by Conti & Cattaneo 2010; Gaspard et al. 2010). Earlier studies have demonstrated that PSCs show a strong “default” bias towards neural differentiation when withdrawn from their self-renewal environment (Reubinoff et al. 2001; Tropepe et al. 2001). However, this undirected differentiation results in insufficient purity and variable subcomposition of the neural populations. Thus, individual protocols have been developed to efficiently derive distinct neural cell types from hPSCs. The classic approach for neural induction of hESCs consists of the formation of embryoid bodies, which are then plated and further cultivated in the presence of FGF2 (Okabe et al. 1996; Zhang et al. 2001). Under these conditions, hPSCs can give rise to Nestin-positive

neuroepithelial cells, which self-assemble to blossom-like “neural rosette” structures, reminiscent of the radial organization of the neural tube-forming cells (Fig. 1.1 A). More recent protocols rely on the pharmacological modulation of key signals known to regulate neural induction *in vivo*. For instance, it is known from developmental studies, that neural induction depends on the inhibition of the Activin/TGFβ-mediated pluripotency pathways and the anti-neural effects of BMP (reviewed by Stern 2005). Accordingly, pharmacological blockage of BMP/TGFβ-signaling is now widely used to further promote the differentiation of hPSCs towards primitive neuroepithelial cells (e.g. Chambers et al. 2009; Kim et al. 2010; Zhou et al. 2010). Chambers et al. (2009) have coined the term “dual SMAD inhibition” for this approach, since both BMP and Activin/TGFβ signaling converge on SMAD proteins as main signal-transduction molecules.

1.1.3 Different types of neural stem cells generated from human pluripotent stem cells

Nowadays, a diverse set of proliferative neural stem/precursor cell (NSC/NPC) populations can be generated from hPSCs (reviewed by Conti & Cattaneo 2010; Karus et al. 2014; Fig. 1.1 A). These populations can be discriminated based on their morphology, their ability to form neural rosettes and their propensity to give mainly rise to neurons (neurogenesis) or astrocytes and oligodendrocytes (gliogenesis). Furthermore, *in vitro* generated NSCs display distinct regional identities – in analogy to the subdivision of the neural tube along the antero-posterior and dorso-ventral axes – and differ in their responsiveness to morphogens defining their range of neuronal subtype progenies. It is believed that the different types of *in vitro* generated NSCs might be a reflection of the distinct NSC/NPC populations that are sequentially generated during neural development. However, it is still unclear whether the direct interrelation observed *in vivo* can be transferred to the different *in vitro* NSC populations.

The earliest type of *in vitro* generated NSCs are the primitive neuroepithelial cells, which can be captured and maintained in a proliferative stage in the presence of pharmacological modulators of either Wnt and LIF signaling (Li et al. 2011a) or Wnt and SHH signaling (Reinhardt et al. 2013). These primitive neuroepithelial stem cells grow as large colonies and show uniform, non-polarized expression of the tight-junction protein ZO1 (TJP1) and the cell-adhesion molecule N-cadherin (CDH2). However, they can also self-organize into neural rosettes upon FGF2 treatment (Reinhardt et al. 2013), indicating that they might represent an early “pre-rosette” stage. In line with this theory, pre-rosette NES cells have a broad differentiation potential and can give rise to CNS as well as neural crest progeny (Reinhardt et al. 2013). Neural rosettes generated during hPSC differentiation can be also isolated and propagated in culture (Fig. 1.1) as first indicated by Elkabetz et al. (2008), who reported on a specific population of rosette-forming R-NSCs. These R-NSCs typically grow in large rosette structures, which are characterized by expression of ZO1 and N-cadherin in the lumen. This spatially restricted expression pattern points to an apico-basal polarization of the R-NSCs (Elkabetz et al. 2008; Abranches et al. 2009). Furthermore, R-NSCs express neural precursor markers (SOX1, SOX2, PAX6, Nestin, NCAM) as well as rosette markers (PLZF, DACH1) and show evidence of interkinetic nuclear migration (Elkabetz et al. 2008; Abranches et al. 2009; Nasu et al. 2012). However, R-NSCs

can only be kept in culture for a few passages when treated with SHH and Notch ligands. When exposed to the commonly used mitogens FGF2 and EGF, instead, R-NSCs loose their rosette morphology and convert into cells with an elongated bipolar morphology (Elkabetz et al. 2008) and acquire properties comparable to radial glial. Indeed, during development neuroepithelial cells eventually convert to radial glia cells, which express both neuroepithelial markers (Nestin, SOX2, PAX6) as well as astroglial markers (BLBP, GLAST, Vimentin, GFAP) and are responsible for the main wave of neurogenesis and gliogenesis (Götz & Barde 2005). Cells with similar characteristics can be generated from hPSCs and are, henced, named radia-glial like RGL-NSCs (Glaser et al. 2007; Nat et al. 2007; Gorris et al. in submission). In contrast to neuroepithelial NSCs, radia-glial like NSCs are characterized by a higher gliogenic potential, a restricted range of neuronal subtype progenies and a reduced amenability to patterning signals.

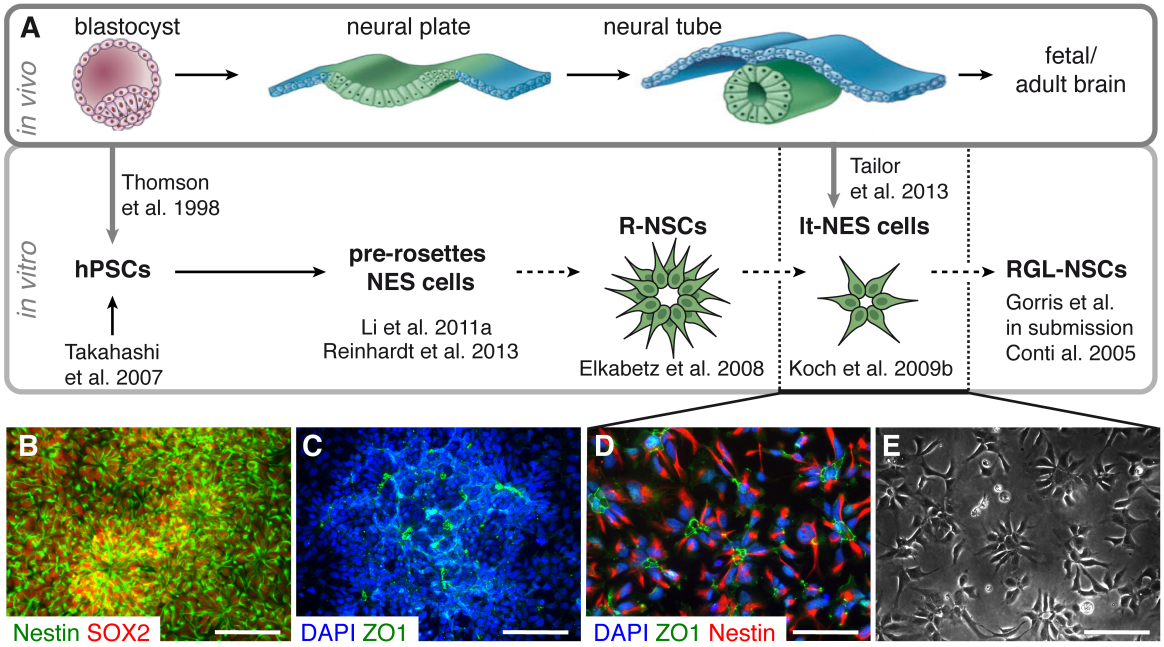

Fig. 1.1: Different types of human neural stem cell populations. (A) Both during embryonal development and hPSC-based culture systems different NSC populations are generated. These NSC populations differ in their morphology, marker expression profile and their self-renewal and differentiation abilities. *In vitro* generated NSCs may reflect specific *in vivo* developmental stages. However, this still needs to be experimentally validated. Illustration is adapted from Conti & Cattaneo (2010). **(B-E)** Human PSCs give rise to neural rosette-forming neuroepithelial cells, which can be isolated to generate a stable NSC line. **(B, C)** Plated neurospheres contain Nestin/SOX2-positive neural rosettes with characteristic ZO1 expression in their lumen. **(E, E)** Lt-NES cell cultures generated from these neurospheres contain small neural rosettes and show expression of ZO1 and Nestin. Scale bars in B, C = 50 μm; in D, E = 100 μm.

In our institute Phillip Koch and his colleagues succeeded in isolating yet a second type of neuroepithelial rosette-forming NSCs, which in contrast to R-NSCs show an extensive self-renewal capacity (Koch et al. 2009b). Hence, these NSCs were designated long-term self-renewing neuroepithelial-like stem (lt-NES) cells. As recently shown, lt-NES cells can be robustly derived both from hESCs and iPSCs independent from the parental hPSC line (Falk et al. 2012). Lt-NES cells represent a valuable *in vitro* model of early human neural development as emphasized by a recent

study describing the direct isolation of hindbrain neural stem cells with lt-NES cell-like characteristics from human fetal tissue (Tailor et al. 2013). Moreover, lt-NES cells have been successfully used to model human neurodegenerative diseases (Koch et al. 2011; Koch et al. 2012). To generate lt-NES cells, neural rosettes formed during hPSC differentiation (Fig. 1.1 B, C), are mechanically isolated and first propagated as floating neurospheres. The neurospheres are then dissociated to single cells, plated as monolayer and further cultured in neural medium containing FGF2, EGF, N2 supplement and low concentrations of B27 supplement (Koch et al. 2009b). Under these conditions, lt-NES cells form small rosettes with accentuated ZO1 expression in their center and show expression of neural precursor markers (e.g. SOX1, SOX2, Nestin; Fig. 1.1 D, E). Upon growth factor withdrawal, lt-NES cells differentiate primarily into GABAergic neurons and may also give rise to astrocytes and oligodendrocytes after prolonged differentiation. Lt-NES cell-derived neurons form neuronal networks, and engrafted neurons can functionally integrate into the host brain tissue (Koch et al. 2009b; Falk et al. 2012). Like other types of NSCs, lt-NES cells depend on Notch signaling in order to maintain their self-renewal capacity (Yoon et al. 2005; Louvi et al. 2006; Borghese et al. 2010). Consequently, inhibition of the endogenous Notch activity by the γ-secretase inhibitor DAPT, which interferes with the release of the Notch intracellular domain (NICD), can be used to accelerate neuronal differentiation of lt-NES cells (Borghese et al. 2010).

1.1.4 Strategies for the in vitro generation of dopaminergic neurons

Given the loss of midbrain/mesencephalic dopaminergic (mDA) neurons in Parkinson's disease (PD), much effort has been made to derive this neuronal subtype *in vitro*. So far two different strategies have been pursued, the direct derivation of mDA neuron from hPSCs or from an intermediate NSC population that is then patterned towards the dopaminergic lineage (reviewed by Lindvall 2013).

During development, mDA neurons emerge from midbrain floor plate progenitors that are located at the ventral midline of the neural tube in response to SHH, FGF8 and Wnt signaling (Ono et al. 2007). SHH, secreted from the floor plate, and FGF8, secreted from the isthmic organizer at the midbrain-hindbrain boundary, are important for both ventral mesencephalic patterning and dopaminergic fate induction (Ye et al. 1998). In addition, Wnt signaling, originating from the isthmic organizer and the developing midbrain itself, is required for mDA neuron induction (reviewed by Hegarty et al. 2013). As recently shown, these signals can be used to induce midbrain floor plate progenitor cells from hPSCs (Fasano et al. 2010). These floor plate cells can be then efficiently differentiated into mDA neurons expressing key markers of the lineage, such as FOXA2, LMX1A, NURR1 (NR4A2), EN1 and PITX3 as well as tyrosine hydroxylase (TH), the rate-limiting enzyme of dopamine synthesis (Kriks et al. 2011; Kirkeby et al. 2012; Xi et al. 2012). However, the floor plate progenitors cannot be propagated in an undifferentiated stage but directly undergo terminal differentiation. This run-through approach has several drawbacks, in that it is difficult to standardize and less suitable for bulk production. Proliferative progenitor populations like hPSC-derived neural stem cells may represent an alternative cell source of dopaminergic neurons, which would not only circumvent these problems but also allow for a greater accessibility for functional experiments.

Although hPSC-derived neuroepithelial cells possess specific positional identities recapitulating neural tube patterning (reviewed by Conti & Cattaneo 2010), they are still sensitive to patterning cues and can be shifted towards other neuronal subtypes (Elkabetz et al. 2008; Koch et al. 2009b). Specifically, lt-NES cells possess a default anterior hindbrain identity and have a differentiation bias towards GABAergic neurons but they can also adopt other regional identies (Koch et al. 2009b; Falk et al. 2012). For instance, they can give rise to TH-positive neurons, which occasionally show co-expression of FOXA2 and LMX1A, upon exposure to SHH and FGF8b (Falk et al. 2012). However, these neurons do not faithfully express the full mDA neuron marker set and might be rather considered as "dopaminergic-like neurons". In fact, the authenticity of the generated neurons is the major drawback of using NSCs as source for dopaminergic neurons. It is currently discussed whether the very recently described pre-rosette NES cells might be more suitable for generating mDA neurons, since they may be more responsive to SHH, FGF8b and Wnt patterning (Reinhardt et al. 2013).

1.2 MicroRNAs as important regulators of cell fate

Initially considered as "junk RNAs", non-coding RNAs (ncRNAs) are currently recognized as critical regulators of the cellular homeostasis (reviewed by Esteller 2011). In particular, miRNAs, which constitute a distinct class of small ncRNAs, have emerged as important post-transcriptional gene regulators. MicroRNAs bind to specific target messenger RNAs (mRNAs) with imperfect complementarity, which typically results in mRNA degradation or repression of translation. Since the discovery of the first miRNAs (lin-4 and let-7; Lee et al. 1993; Reinhart et al. 2000), hundreds of miRNAs have been identified across all species showing a high degree of conservation throughout evolution. To date more than 2500 miRNAs have been annotated for the human genome (miRBase annotation v20; Kozomara et al. 2013). Considering that each of these miRNA is predicted to recognize several hundreds of target mRNAs, a large proportion of the transcriptome and consequently many cellular processes might be subjected to miRNA-based regulation (Lewis et al. 2005). Therefore, connecting miRNAs to specific functions has a great value for the deeper understanding of both physiological and pathological processes.

1.2.1 MicroRNA biogenesis and function

The characteristic feature of a miRNA gene is the folding of its primary RNA transcript into hairpin structures that are further processed by the sequential action of two ribonuclease (RNase III) enzymes (canonical miRNA biogenesis, Fig. 1.2). Most mammalian miRNA genes are encoded in introns of protein coding-genes or ncRNA genes, whereas some miRNA genes are also located in intergenic regions (Rodriguez et al. 2004; Godnic et al. 2013). Intronic miRNAs may be transcribed together with their host genes or may have their own promoters and transcription initiation sites (Ozsolak et al. 2008). Like protein-coding genes, the majority of miRNA genes is transcribed by the RNA-polymerase II to produce the so-called primary miRNA (pri-miRNA), which carries a 5' cap structure and a polyA-tail, like conventional transcripts (Lee et al. 2004; Cai et al. 2004). The hairpin region within the pri-miRNA is excised by the microprocessor complex formed around the RNase III enzyme

Drosha and the double-stranded (ds)RNA-binding protein DGCR8 to produce the ~70 nucleotide long precursor (pre-miRNA) molecule (Denli et al. 2004; Han et al. 2004). Polycistronic miRNAs harboring multiple pri-miRNA hairpins are also processed by Drosha to liberate the individual pre-miRNAs (Lee et al. 2002). Most miRNAs encoded in intronic sequences are processed co-transcriptionally without interfering with the splicing process of the respective host pre-mRNAs (Kim et al. 2007b; Kataoka et al. 2009). There is, however, a class of unconventional intronic miRNAs, the so-called mirtrons, which are processed independently of Drosha using the pre-mRNA splicing machinery (Ruby et al. 2007; Berezikov et al. 2007). The pre-miRNA is subsequently exported into the cytoplasm by Exportin 5 (XPO5) (Bohnsack et al. 2004), where it is further processed by the RNase III enzyme Dicer together with the dsRNA-binding protein TRBP (TARBP2). Dicer binds to the hairpin structure and cleaves the loop to produce the ~22 nucleotide long intermediate miRNA:miRNA* duplex (Zhang et al. 2002; Zhang et al. 2004a). The miRNA:miRNA* duplex is then loaded into the RNA-induced silencing complex (RISC) containing Argonaute proteins, which are responsible for dsRNA binding and duplex unwinding (Hutvagner et al. 2007; Kwak et al. 2012). Generally, it is assumed that during this process only one strand, the guide strand, of the miRNA duplex remains incorporated in the RISC, whereas the passenger strand is removed and degraded (Fig. 1.2). Strand selection is believed to depend on the thermodynamic properties of the miRNA duplex and the strand with the relatively less stable 5' end is more often retained (Khvorova et al. 2003). However, recent findings suggest that quite a large proportion of the miRNA duplexes is actually bifunctional giving rise to two active sister miRNAs (Okamura et al. 2008; Yang et al. 2011; Fig 1.2). According to the miRNA nomenclature the preferred strand is called the miRNA strand, while the non-preferred passenger strand is called the star (miRNA*) strand. When it is not possible to identify the predominant product or when both miRNA strands are expressed at comparable levels they are instead called by their position within the duplex, i.e. miR-X-5p (from the 5' arm) and miR-X-3p (from the 3' arm; Kozomara et al. 2011).

Most miRNAs bind with semi-complementarity to specific target sites that usually lie within the 3' untranslated region (UTR) of mRNAs and are often present in multiple copies. However, perfect and contiguous base-pairing to the miRNA seed sequence stretching from nucleotides 2-8 is the key requirement for mRNA target recognition (Brennecke et al. 2005; Grimson et al. 2007). Many miRNAs come in families, which encompass different miRNA isoforms sharing the same seed sequence and accordingly a similar set of mRNA targets (Kamanu et al. 2013). MicroRNAs repress the protein synthesis of targeted mRNAs by either directly interfering with mRNA translation or by promoting mRNA degradation, whereby the exact mechanisms are still unknown. MicroRNA-induced repression of translation can occur at several stages ranging from translation initiation, ribosome assembly to elongation (Humphreys et al. 2005; Petersen et al. 2006; Chendrimada et al. 2007; Kiriakidou et al. 2007). MicroRNA targeting can also lead to transcript degradation by inducing mRNA deadenylation and decapping (Wu et al. 2006b; Behm-Ansmant et al. 2006). The destabilized mRNAs are then marked for mRNA decay, which in part takes place in so-called processing "P" bodies (Eulalio et al. 2006; Parker et al. 2007).

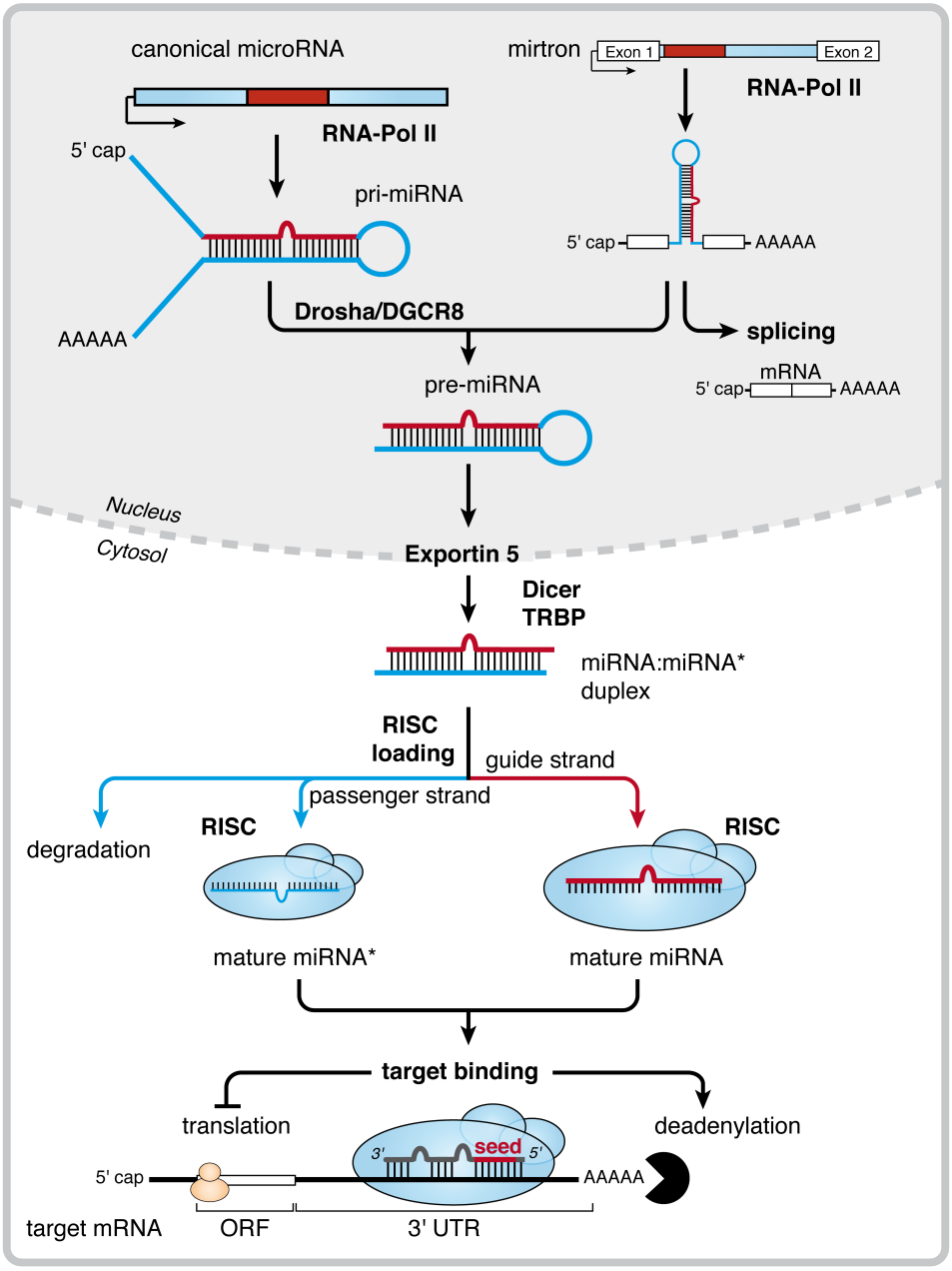

Fig. 1.2: MicroRNA biogenesis and function. The mature miRNA duplex is generated from primary transcripts by the sequential actions of Drosha and Dicer (mirtrons are processed independently from Drosha). The miRNA duplex is then loaded into the RNA-induced silencing complex (RISC), whereby one strand is eliminated. As part of the RISC, the miRNA can bind to specific target mRNAs by sequence specificity and repress their protein synthesis by directly interfering with translation or by inducing mRNA degradation.

MicroRNA biogenesis is tightly regulated at the level of transcription and at various steps during miRNA maturation to ensure tissue- or developmental-specific miRNA expression profiles (reviewed by Slezak-Prochazka et al. 2010; Treiber et al. 2012). The main factors implicated in post-transcriptional regulation of miRNA expression are accessory proteins for Drosha and Dicer as well as terminal loop RNA-binding proteins. Among them, LIN28A, as regulator of let-7 processing, has been extensively studied. Mature let-7 is present only at relatively low levels in pluripotent stem cells, despite the abundant expression of pri-let-7 transcripts. This is due to LIN28A and its homolog

LIN28B, which interfere with both pri- and pre-let-7 processing (Viswanathan et al. 2008; Rybak et al. 2008; Piskounova et al. 2011). LIN28A binds to the terminal loop of let-7 precursors and recruits the uridylyl transferase TUT4 leading to the rapid decay of oligouridylated pre-let-7 species (Heo et al. 2009). LIN28B, instead, acts on the primary let-7 RNAs and prevents Drosha processing (Piskounova et al. 2011). MicroRNA processing is also coupled to signaling pathways, and the signaling molecules SMAD2, p53 and estrogen receptor ER-α have been shown to modulate Drosha-mediated pre-miRNA cleavage (Davis et al. 2008; Suzuki et al. 2009; Yamagata et al. 2009; Davis et al. 2010). Furthermore, sequence-editing enzymes and ribonucleases control the abundance of miRNA processing intermediates and, hence, modulate mature miRNA expression levels (Yang et al. 2005; Kawahara et al. 2007; Suzuki et al. 2011).

1.2.2 The role of miRNAs during pluripotency, neuronal differentiation and neuronal subspecification

The central nervous system (CNS) expresses a large fraction of all known miRNAs (Shao et al. 2010), and many of these miRNAs show temporal and spatial dynamic expression patterns (Miska et al. 2004; Sempere et al. 2004; Krichevsky et al. 2006; Moreau et al. 2013). The emerging concept is that miRNAs are importantly involved throughout neural development starting from neural lineage entry to neural progenitor expansion, differentiation and neuronal subtype specification (reviewed by Roese-Koerner et al. 2013; Sun et al. 2013; Bian et al. 2013; Stappert et al. 2014), and there is a growing list of miRNAs assigned to each of these steps. During these processes miRNAs are embedded in gene regulatory circuits to modulate cell fate decisions (reviewed by Herranz et al. 2010; Ivey et al. 2010; Fig. 1.3).

Although several miRNAs have been found to influence pluripotent stem cells, the balance between self-renewal and differentiation might be mainly regulated by the opposing actions of the ES cell cycle (ESCC) regulating miRNA superfamily and the let-7 family (reviewed by Greve et al. 2013; Fig. 1.3 A). The ESCC miRNA superfamily encompasses several miRNAs clusters, including the miR-302/367, the miR-371-3, and the large C19MC miRNA cluster (Chromosome 19 microRNA cluster), which all share the same seed sequence or derivatives (Laurent et al. 2008; Stadler et al. 2010; Greve et al. 2013). While ESCC miRNAs act in concert with the pluripotency network to maintain pluripotency, let-7 miRNAs promote differentiation by destabilizing the pluripotency network (Melton et al. 2010). Undifferentiated hPSCs display high expression of ESCC miRNAs due to the direct binding of OCT4 and SOX2 to the respective loci (Marson et al. 2008). Conversely, hPSCs express only low levels of mature let-7 due to the blockage of let-7 maturation by LIN28 (Viswanathan et al. 2008; Rybak et al. 2008; see also 1.2.1). However, when hPSCs differentiate, the core pluripotency factors (OCT4, SOX2, Nanog) are down-regulated concomitantly with a decrease of ESCC miRNAs and LIN28 expression. This leads to the up-regulation of mature let-7 that is reinforced by let-7 targeting LIN28 (Rybak et al. 2008). ESCC miRNAs and let-7 also have opposing functions on cellular reprogramming, in that ESCC miRNAs promote or can even induce iPSC generation, while let-7 acts as barrier of the reprogramming process (reviewed by Greve et al. 2013).

In addition to their negative role during general hPSC differentiation, miR-302 and miR-371 specifically interfere with differentiation into the neuroectoderm (Rosa et al. 2009; Rosa et al. 2011; Kim et al. 2011; Lipchina et al. 2012; Fig 1.3 B, B'). Both miR-302 and miR-371 contribute to a higher ground-state level of BMP signaling by targeting several endogenous inhibitors of the pathway and thereby raise the threshold for neural induction. In contrast, miR-125b promotes neural induction by targeting SMAD4, a key factor of BMP/TGFβ-signaling (Boissart et al. 2012). MicroRNAs also modulate neural lineage entry by directly regulating the expression of factors either implicated in pluripotency or neuroectoderm specification (Fig 1.3 B'). For instance, miR-302/367 acts in concert with OCT4 to ensure the repression of pro-neural NR2F2 expression (Rosa & Brivanlou 2011). In turn, NR2F2 represses OCT4 transcription during differentiation and thus reinforces its own expression. MicroRNA-125b and let-7 instead repress the expression of LIN28A allowing mature let-7 to accumulate (Guo et al. 2006; Rybak et al. 2008; Zhong et al. 2010).

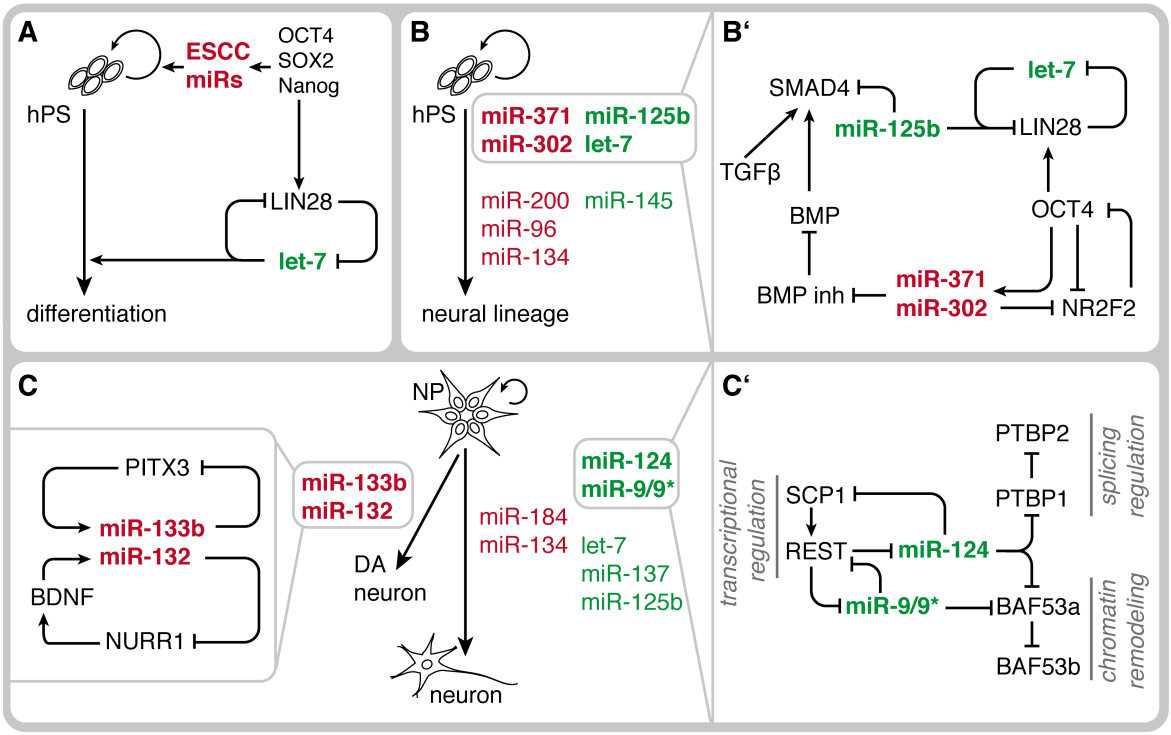

Fig. 1.3: MicroRNAs act on various levels throughout neuronal development. MicroRNAs labeled in red have an inhibitory and miRNAs in green a promoting effect on human pluripotent stem (hPS) cell differentiation **(A)**, neural lineage entry **(B)**, neuronal differentiation of neural progenitors (NP) and dopaminergic (DA) differentiation **(C)**, respectively. Inserts show the action of selected miRNAs within gene regulatory networks. For more details see text and for a detailed description of the function of the specific miRNAs see the reviews by Bian et al. (2013) and Stappert et al. (2014).

Once the neural fate is induced, a highly orchestrated network of intrinsic mechanisms including miRNAs and other developmental signals regulates the balance between neural progenitor proliferation and differentiation. For instance, miR-124, miR-125b, miR-137, miR-9 and let-7 promote neuronal differentiation, while miR-134 and miR-184, are implicated in neural progenitor maintenance and proliferation (for a detailed review see e.g. Bian et al. 2013; Fig 1.3 C). In addition, miRNAs are

also involved in regulating the shift from neuronal to glial fate and the generation of astrocytes and oligodendrocytes (reviewed by He et al. 2012; Zheng et al. 2012). Among the brain-enriched miRNAs, the functions of miR-124 and miR-9 as neuronal-promoting miRNAs have been extensively studied (reviewed by e.g. Coolen et al. 2013; Akerblom et al. 2013). MicroRNA-124 has been subject to intense research since Lim et al. (2005) demonstrated that overexpression of miR-124 in HeLa cells is sufficient to induce a neuronal-like gene expression program. In 2011, the Wernig group showed that it is actually possible to transdifferentiate human fibroblasts into so-called induced neurons by overexpression of specific neurogenic transcription factors (ASCL1, BRN2/POU3F2, MYT1L, NEUROD1; Pang et al. 2011). In two independent follow-up studies it was shown that overexpression of either miR-124 together with BRN2 and MYTL1 or overexpression of miR-124 and miR-9/9* alone is also sufficient to induce the direct neuronal conversion of fibroblasts (Ambasudhan et al. 2011; Yoo et al. 2011). These data underline the relevance of miRNA-based regulation on neuronal fate determination and indicate that miR-124 and miR-9/9* might have an instructive role in this context. Indeed, both miR-124 and miR-9/9* have been repeatedly shown to promote neuronal differentiation by modulating the activity of several anti-neuronal factors (reviewed by e.g. Coolen et al. 2013; Akerblom et al. 2013; Fig 1.3 C'). The expression of miR-124, miR-9/9* and other neuronal-associated miRNAs is regulated by the transcriptional repressor REST, which prevents premature expression of neuronal genes in neural progenitors and mediates long-term silencing of these genes in non-neural cells (Wu et al. 2006a; Conaco et al. 2006; Otto et al. 2007; Packer et al. 2008; Fig 1.3 C'). In turn, miR-124 represses the activity of REST through targeting REST-cofactor SCP1 (CTDSP1) and, thus, reinforces its own expression (Visvanathan et al. 2007). Similarly, miR-9/9* and REST together with CoREST (RCOR1) reciprocally regulate each other to control neuronal differentiation (Packer et al. 2008). Cell cycle exit and neuronal differentiation of NSCs is accompanied by global chromatin changes and requires a subunit switch in the ATP-dependent chromatin remodeling complex BAF (Lessard et al. 2007). This switch from the BAF53a subunit in the neural-progenitor npBAF complex to BAF53b in the neuronal-specific nBAF complex, is induced by miR-124 and miR-9*, which repress the expression of BAF53a (Yoo et al. 2009). Similarly, miR-124 induces a switch in the expression of two RNA splicing regulators – PTBP1 and PTBP2 (Makeyev et al. 2007). PTBP1 is expressed in neural progenitors and is down-regulated during neuronal differentiation, which is in part mediated by miR-124. This leads to the expression of the neuron-enriched homolog PTBP2, which favors a neuron-specific pre-mRNA splicing pattern (Makeyev et al. 2007). Other relevant miR-124 targets are the Notch ligand JAG1 and the transcription factor SOX9, which are both important for NSC maintenance (Cheng et al. 2009; Farrell et al. 2011). MicroRNA-9 regulates NSC fate as part of an auto-regulatory network including REST, HES1 and the orphan nuclear receptor TLX (NR2E1), all of which act as transcriptional repressors of miR-9/9* and other neural genes. Reciprocally, miR-9/9* targets HES1, REST, CoREST and TLX leading to an enhanced neuronal differentiation at the expense of NSC self-renewal (Wu & Xie 2006a; Packer et al. 2008; Zhao et al. 2009; Bonev et al. 2012).

Besides their role during neural progenitor self-renewal and differentiation, miRNAs also contribute to the development of specific neuronal subtypes. In this context, miRNAs act in concert with gene regulatory motifs and control genetic switches to regulate the spatial and temporal expression dimensions of important cell fate determinants. Based on *in vivo* studies in model organisms, specific miRNAs have been identified to regulate the temporal fate of neural progenitors or their spatial identity along the antero-posterior and dorso-ventral coordinates in the CNS (reviewed by Cremisi 2013; Stappert et al. 2014). MicroRNAs are also involved in the development of murine midbrain dopaminergic (mDA) neurons. As shown by Dicer knock-out experiments, miRNA activity is required for the generation and maintenance of mDA neurons (Kim et al. 2007a; Pang et al. 2014). So far, two specific miRNAs, i.e. miR-133b and miR-132, were found to impair dopaminergic differentiation of mouse ESCs (Kim et al. 2007a; Yang et al. 2012; Fig 1.3 C, left insert). However, the actual role of miR-133b on mDA neuron differentiation is unclear, since miR-133b knock-out mice display normal midbrain development (Heyer et al. 2012). Interestingly, miR-133b is embedded in a negative feedback loop in which the expression of miR-133b is induced by PITX3, while miR-133b reciprocally represses PITX3 expression (Kim et al. 2007a). Similarly, expression of miR-132 is indirectly induced by NURR1 via the up-regulation of BDNF. MicroRNA-132, in turn, targets NURR1 mRNA also forming a negative feedback loop (Klein et al. 2007; Yang et al. 2012).

In summary, miRNAs are emerging as important cell fate determinants as elegantly shown by the efficacy of miRNA modulation during cellular reprogramming and direct neuronal conversion. However, considering the large number of miRNA species expressed in the CNS, the knowledge on the function of these miRNAs is still scarce. For instance, although the miR-181 family is expressed in the CNS (Miska et al. 2004; Chen et al. 2004; Kane et al. 2012), its is still unknown whether it also contributes to neurogenesis.

1.3 MicroRNA-181 family as potential regulator of neuronal differentiation

The miR-181 family is highly conserved from teleosts to mammals (Otto 2008; Ji et al. 2009) and most species contain four mature miR-181 isoforms, namely miR-181a, miR-181b, miR-181c and miR-181d, which arise as the major products from the 5' arm of the respective miRNA precursors. In addition, there are four minor miRNA* products (miR-181a*, miR-181b*, miR-181c* and miR-181d*) from the 3' arm of the miRNA precursors (Fig. 1.4; Ji et al. 2009). The miR-181 precursors are expressed from three paralog clusters on three distinct chromosomal sites, i.e. MIR181A1/MIR181B1, MIR181A2/MIR181B2 and MIR181C/MIR181D (Fig. 1.4 A). The miR-181 family is expressed in a variety of tissues, with highest expression in brain, heart, lung and thymus (mouse: Miska et al. 2004; Chen et al. 2004; human: Kane et al. 2012) and contributes to the development of various cell lineages. MicroRNA-181 promotes myoblast, osteoblast and endothelial differentiation (Naguibneva et al. 2006; Kazenwadel et al. 2010; Kane et al. 2012; Bhushan et al. 2013), while inhibiting hepatic stem cell differentiation (Ji et al. 2009). Furthermore, miR-181 has diverse functions in the hematopoietic system and regulates the development of both lymphoid and myeloid lineages (reviewed by Seoudi et al. 2012). As recently indicated, miR-181 also impacts on the balance between ESC self-renewal and

differentiation by targeting factors importantly involved in the maintenance of pluripotency, i.e. Sirt1, Cbx7 and CARM1 (Saunders et al. 2010; O'Loghlen et al. 2012; Xu et al. 2013b). Accordingly, expression of miR-181 is very low in self-renewing ESCs and becomes only induced upon differentiation (Krichevsky et al. 2006; Saunders et al. 2010; Xu et al. 2013a). Intriguingly and in apparent contrast to its role during ESC differentiation, miR-181 has been recently shown to enhance transcription factor-based generation of induced pluripotent stem cells (Judson et al. 2013).

A

Gene	Chromosomal location	Mature miRs	Overlapping transcripts
MIR181A1	1: 198828173 - 198828282 [−]	181a, 181a*	RP11-31E23.1 (LincRNA)
MIR181B1	1: 198828002 - 198828111 [−]	181b, *181b**	
MIR181A2	9: 127454721 - 127454830 [+]	181a, 181a*	**GCNF (NR6A1)** (protein-coding)
MIR181B2	9: 127455989 - 127445607 [+]	181b, *181b**	
MIR181C	19: 13985513 - 13985622 [+]	181c, 181c*	NANOS3 (protein-coding)
MIR181D	19: 13985689 - 13985825 [+]	181d, 181d	

B

major miRNAs arising from 5' arms		minor miRNAs arising from 3' arms	
181a	A**ACAUUCA**ACGCUGUCGGUGAGU	181a*	A**CCACU-GA**CCGUUGACUGUACC
181c	A**ACAUUCA**AC-CUGUCGGUGAGU	181c*	A**ACCAUCG**ACCGUUGAGUGGAC
181b	A**ACAUUCA**UUGCUGUCGGUGGGU	181b*	C**UCACUGA**ACAAUGAAUGCAA
181d	A**ACAUUCA**UUGUUGUCGGUGGGU	181d*	C**CACCGGG**GG-AUGAAUGUCAC

Fig. 1.4: The members of the human miR-181 family. (A) Genomic organization of the miR-181 family. Clustered genes are highlighted with the same color. The existence of miR-181b* (in italic) has so far not been verified experimentally. **(B)** Sequence homology of the major and minor miR-181 family members. The seed sequences are displayed in bold. The blue shading indicates conserved bases among the different miR-181 isoforms. Data were obtained from the miRBase annotation, release 20 (www.mirbase.org).

Aberrant expression of the miR-181 family has been linked to different types of cancers, whereby miR-181 might act as tumor suppressor or oncogene dependent on the cellular context. In glioblastoma, expression of miR-181 is strongly down-regulated compared to normal brain tissue (Shi et al. 2008; Wang et al. 2011; Shi et al. 2013). Accordingly, miR-181 acts as a tumor suppressor and impairs tumor proliferation and migration through targeting components of the oncogenic MAPK/ERK and FOS/miR-21 pathways (Wang et al. 2011; Shi et al. 2013; Wang et al. 2013b; Tao et al. 2013). Restoration of miR-181 expression in glioblastoma enhances the sensitivity of the tumor cells to anti-tumor treatment and increases apoptosis by down-regulating members of the pro-survival BCL2 family (Chen et al. 2010; Wang et al. 2013b).

The miR-181 family is strongly expressed in the CNS (Miska et al. 2004; Chen et al. 2004; Kane et al. 2012), where it is implicated in multiple processes. For instance, miR-181 has been reported to impair the inflammatory response in the CNS triggered by astrocytes and microglia (Zhang et al. 2012b; Hutchison et al. 2013). During ischemia, miR-181 promotes cell apoptosis, and accordingly inhibition of miR-181a was found to have a neuroprotective effect and resulted in smaller infarct areas and ameliorated neurological deficits (Ouyang et al. 2012b; Peng et al. 2013). In neurons, miR-181 is involved in the regulation of synaptic transmission through targeting the AMPA-type glutamate receptor GluA2 subunit, the GABA receptor α1-subunit and the calcium sensor protein

VSNL1 (Beveridge et al. 2008; Saba et al. 2012; Zhao et al. 2012). Furthermore, elevated miR-181b expression has been associated with schizophrenia (Beveridge et al. 2008; Shi et al. 2012) and decreased miR-181c expression with Alzheimer's disease (Schonrock et al. 2010; Nunez-Iglesias et al. 2010; Geekiyanage et al. 2011). Considering that the expression of miR-181 increases during human brain development and *in vitro* neuronal differentiation (Landgraf et al. 2007; Wu et al. 2007; Moreau et al. 2013), it is very likely that miR-181a may also contribute to neurogenesis. In order to test this hypothesis, miR-181 was chosen as candidate for further functional studies in lt-NES cells. Furthermore, several putative miR-181 target genes were analyzed for their responsiveness towards miR-181a overexpression and their function in neuronal differentiation. In this context, the putative miR-181a target GCNF (germ cell nuclear factor) was especially interesting since the GCNF locus overlaps with the MIR181A2/MIR181B2 host gene (Fig. 1.4, Fig. 1.5).

1.4 The role of GCNF during embryonic and neural development

GCNF (official gene symbol NR6A1) is a member of the nuclear receptor (NR) family of ligand-dependent transcription factors. The nuclear receptor family comprises 48 different transcription factors, which are involved in diverse physiological events, including embryonic development and NSC fate decision (reviewed by Wagner et al. 2013; Stergiopoulos et al. 2013). Since no ligand has been identified to date for GCNF, it is designated an orphan receptor. GCNF is essential for normal embryonic development, during which it represses the expression of pluripotency factors such as OCT4 and Nanog (reviewed by Wang et al. 2013c). In addition, GCNF plays a role during gametogenesis and neurogenesis (reviewed by Zechel 2005; Wang et al. 2013c).

1.4.1 Structure and mode of action of the orphan nuclear receptor GCNF

GCNF was first cloned by several labs from mouse cDNA libraries (Hirose et al. 1995; Bauer et al. 1997) and was designated germ cell nuclear factor based on its predominant expression in germ cells (Chen et al. 1994). GCNF is highly conserved throughout vertebrates, and human GCNF shares 98.3% and 82.7% amino acid identity with its homologs in mouse and frog, respectively (Kapelle et al. 1997). The genomic co-localization of GCNF with the MIR181A2 host gene (MIR181A2HG) and the nuclear receptor NR5A1 is also conserved between mouse and human (Zhang et al. 2004b; Fig. 1.5 A). Although GCNF shares the common structural makeup of nuclear receptors, it is distantly related to the other NR members and represents the sole member of the NR6 subgroup. Nuclear receptors typically consist of four major domains as shown in Fig. 1.5 B and as reviewed by Bain et al. (2007). The C-terminal ligand-binding domain (LDB) of GCNF is relatively divergent to that of other nuclear receptors and lacks the typical canonical activation function-2 (AF2) motif (Kapelle et al. 1997). Since the AF2 motif is usually involved in transcriptional activation and the recruitment of co-activators in a ligand-dependent manner, GCNF is assumed to act as a transcriptional repressor, also in the absence of a ligand (Cooney et al. 1998). In fact, all target genes identified so far were found to be repressed by GCNF (reviewed by Wang et al. 2013c). GCNF binds to a specific nuclear receptor response element (GCNF-RE), which is a direct repeat of the core motif AG(G/T)TCA with zero

spacing (DR0) as depicted in Fig. 1.5 C (Borgmeyer 1997; Yan et al. 1997; Cooney et al. 1998). Upon binding to its response elements, GCNF forms a hexameric complex known as the transiently retinoid acid (RA)-induced factor (TRIF) complex (Fuhrmann et al. 2001; Gu et al. 2005b; Fig. 1.5 D). GCNF may exert its repressive function in part by competing with other nuclear receptors and transcription activators, such as ERRα, SF-1 (NR5A1), LRH-1 (NR5A2) and CREMτ (Yan et al. 2000; Hummelke et al. 2004; Rajkovic et al. 2004; Gu et al. 2005a; Rajkovic et al. 2010; Fig. 1.5 D). Furthermore, GCNF may interact with several co-repressors, such as NCoR and SMRT (Yan & Jetten 2000; Fuhrmann et al. 2001; Fig. 1.5 D). In addition, GCNF may recruit DNA methyltransferase to the promoter of target genes to induce promoter methylation and silencing (Gu et al. 2011; Fig. 1.5 E).

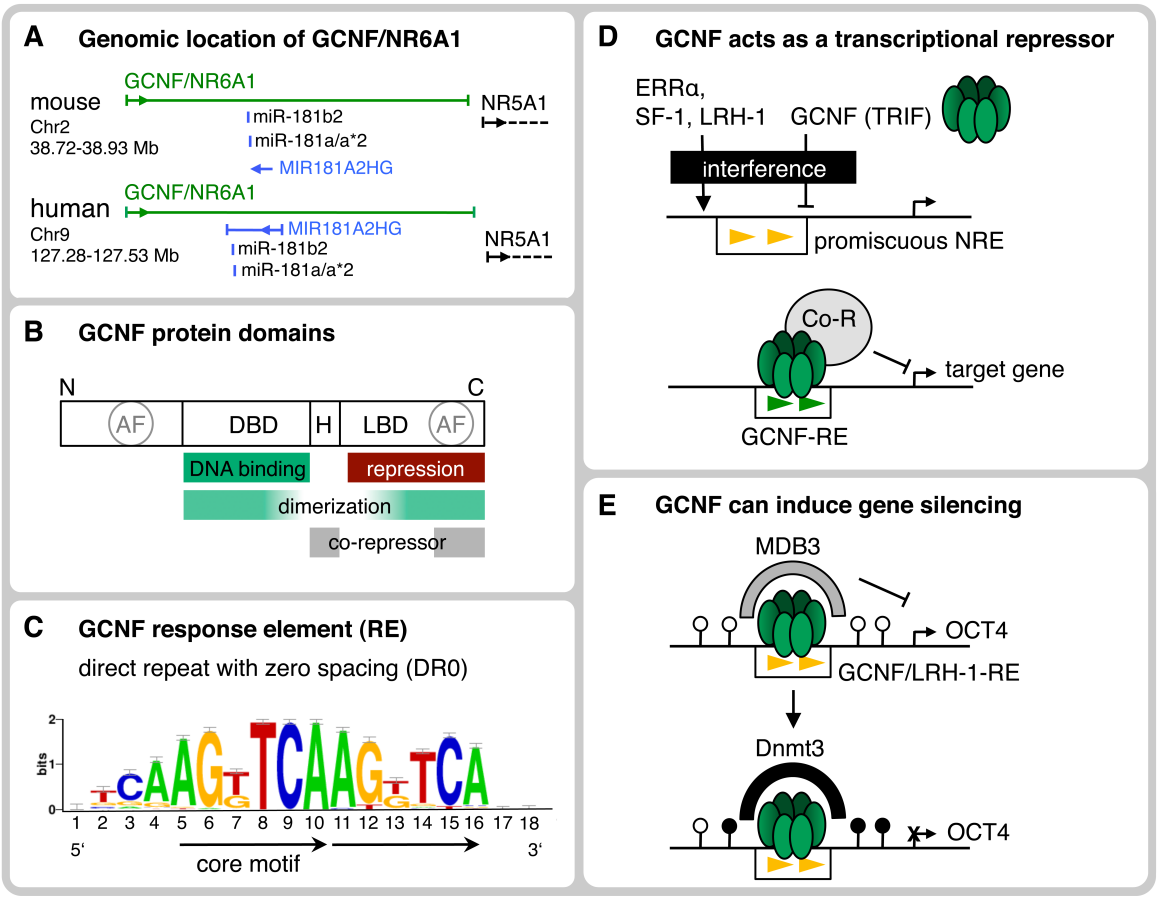

Fig. 1.5 GCNF acts as transcriptional repressor through binding to GCNF response elements within gene regulatory sequences. (A) Schematic depiction of the GCNF/NR6A1 locus in mouse and human. **(B)** Schematic depiction of the GCNF protein domains and their associated functions. The activation function (AF) motifs (in grey) typically located at the N-terminus (N) and in the ligand-binding domain (LBD) of nuclear receptors, are not present in GCNF. C, C-terminus; DBD, DNA-binding domain; H, hinge domain. **(C)** Bitscore model of the GCNF response element. Occurrence frequencies of the 4 nucleotides are indicated by variable letter sizes. **(D)** GCNF regulates the transcription of its target genes by distinct mechanisms. The hexameric GCNF-TRIF complex can compete with other nuclear receptors for binding to promiscuous response elements. GCNF may also interact with co-repressors (Co-R) to repress target gene expression. Schematic in D is adapted from Zechel (2005). **(E)** OCT4 gene repression is initiated by GCNF, which recruits MDB3 to unmethylated CpG sites. Then, the DNA-methyltransferase Dnmt3 is recruited, which triggers de novo DNA methylation to silence the OCT4 promoter. Schematic in E is adapted from Gu et al. (2011).

1.4.2 Expression and function of GCNF during embryonic and neural development

GCNF was found to be predominantly expressed in the germ cells of several adult vertebrates (Chen et al. 1994; Hirose et al. 1995; Joos et al. 1996; Süsens et al. 1996; Zhang et al. 1998). Detailed expression analyses and functional studies revealed that GCNF is expressed in spermatogonial cells and in growing oocytes and might influence both male and female fertility (Lan et al. 2002; Xu et al. 2004; for review see Zechel 2005). GCNF is also expressed in unfertilized oocytes, fertilized ova and in mouse pre-implantation embryos (Lan et al. 2002). In the post-implantation embryo at embryonic day (E)6.5, GCNF is expressed in all three germ layers and in the extraembryonic tissue (Fuhrmann et al. 2001). At E8.5 expression of GCNF is enriched in the proliferating neuroepithelium and in the underlying mesoderm (Süsens et al. 1997; Chung et al. 2001b; Fuhrmann et al. 2001). With ongoing development expression of GCNF declines and is restricted to the developing nervous system at E9.5 with low expression levels in the forebrain and midbrain (Chung et al. 2001b; Chung et al. 2006). GCNF expression in the embryo is further down-regulated by E10.5 but persists in the embryonic part of the placenta (Süsens et al. 1997; Chung et al. 2001b; Mehta et al. 2002). Although it is generally assumed that GCNF expression is diminished after E10.5, there is one paper reporting on a persistent expression of GCNF in the marginal zone of the neuroepithelium at E15 (Bauer et al. 1997).

GCNF knock-out mice, generated through gene targeting in mouse ESCs, show a normal pre-implantation development, but display gross morphological abnormalities from E8.5 onwards and die at E10.5 due to cardiovascular failure (Chung et al. 2001b). GCNF knock-out embryos also suffer from other defects, including failure of body axis turning, failure of neural tube closure and an impaired somitogenesis. Furthermore, GCNF knock-out embryos have a protruding tailbud, which is pushed out of the yolk sac (Chung et al. 2001b; Chung et al. 2001a). Subsequently, it was shown that GCNF is required for the repression of Oct4 and Nanog, which were identified as direct GCNF target genes (Fuhrmann et al. 2001; Gu et al. 2005b). Upon inactivation of GCNF, Oct4 expression is no longer restricted to the germ cell lineage after gastrulation but is also expressed in somatic tissues, including the early neuroectoderm. GCNF-mediated repression of pluripotency genes is also indispensable for mouse ESC differentiation. On a mechanistic level, GCNF might inhibit Oct4 expression by competing with the transcription activators LRH-1 (Nr5a2) and SF-1 (Nr5a1), which bind to the same promiscuous NR element in the proximal Oct4 promoter (Barnea et al. 2000; Gu et al. 2005a). In addition, GCNF initiates DNA methylation and silencing of the Oct4 proximal promoter via recruiting methyl-DNA binding proteins (MBD3, MBD2) and the DNA methyltransferase Dnmt3A (Gu et al. 2011; Fig. 1.5 E).

The spatially and temporally regulated expression pattern of GCNF in the developing murine nervous system points to an additional function of GCNF in neurogenesis. This further is supported by the finding that GCNF knock-out mice embryos display a disrupted neural tube formation (Chung et al. 2001b). Furthermore, GCNF expression in mouse ESCs and embryonic carcinoma (EC) cells is induced upon retinoic acid (RA) treatment (Sattler et al. 2004; Gu et al. 2005), which is known to promote neuronal differentiation (Jones-Villeneuve et al. 1983). Functional analyses during mouse

embryonic development revealed that GCNF-mediated repression of Oct4 is required to allow the transition of primitive neuroepithelial stem cells, which can still give rise to non-neural cell types, to fully neural-committed neuroepithelial stem cells (Akamatsu et al. 2009). In addition, GCNF might affect later stages of neurogenesis. Knock-down of GCNF during RA-induced differentiation of mouse EC cells impaired the generation of neurons, whereas overexpression of GCNF promoted neuronal differentiation (Sattler et al. 2004). While these data point to a pro-differentiation effect of GCNF with regard to neuronal differentiation, another study performing GCNF gain- and loss-of-function experiments in human EC cells proposed a negative role for GCNF (Schmitz 2000).

The role of GCNF was also studied in *Xenopus leavis,* where GCNF is predominantly expressed at the neurula stages (Joos et al. 1996; David et al. 1998). GCNF gain- and loss-of-function experiments demonstrated that it has an important role during Xenopus organogenesis and the establishment of the anterior-posterior axis (David et al. 1998; Barreto et al. 2003a; Barreto et al. 2003b). In particular, neural development was impaired upon GCNF depletion as indicated by a defective neural plate cell migration and a failure of neural tube closure (Barreto et al. 2003b). Like shown for mouse, GCNF expression is induced upon RA treatment of Xenopus embryos. In this context, GCNF might even act as a stabilizer of RA signaling by down-regulating the expression of the RA-degrading enzyme CYP26 (cyp26a1; David et al. 1998; Barreto et al. 2003a). Indeed, knock-down of GCNF interfered with RA-mediated up-regulation of neural genes, indicating that GCNF is required for the neuralizing activity of RA signaling (Barreto et al. 2003a).

In addition, GCNF might be involved in regulating the regionalization of the developing nervous system. *In situ* hybridization analysis in GCNF knock-out mouse embryos revealed a down-regulation of several genes involved in the development of the isthmic organizer forming the midbrain-hindbrain boundary. This was accompanied by an underdeveloped midbrain in GCNF-depleted embryos (Chung et al. 2006). GCNF was also found to be enriched in the midbrain-hindbrain boundary in Xenopus embryos, and knock-down of GCNF resulted in a caudal shift of the midbrain-hindbrain boundary and affected the expression of several important marker genes (Song et al. 1999; Barreto et al. 2003a).

In summary, GCNF seems to affect several steps during neural development, ranging from neural stem cell specification, to neuronal differentiation and regionalization. However, the data discussed above were collected in different animal models and immortalized cell lines, and it is not clear whether the functions of GCNF are conserved throughout the different systems.

1.5 Aims and objectives

It is becoming increasingly evident that miRNAs are crucially involved in cell fate decisions, and studies in several model organisms have identified specific miRNAs as regulators of neural stem cell proliferation, differentiation and fate choice. However, due to the restricted access to human primary neural cells, the role of miRNAs during human neuronal differentiation is largely unknown. A deeper insight into the function of miRNAs and their target genes during human neural fate determination could in the end be exploited to develop new protocols for the generation of human neurons and medically relevant neuronal subtypes. Given their stable self-renewal and neurogenic capacity, hPSC-derived lt-NES cells represent one of the most accessible cellular models to study miRNAs in association with human neural development. Thus, the aim of this thesis was to use these lt-NES cells to identify and functional characterize miRNAs regulating human neural stem cell differentiation and neuronal subtype specification. In pursuit of this goal the following objectives were addressed:

1. Analysis of miRNA expression changes during human neuronal differentiation

The first part of the thesis aimed at annotating miRNA expression profiles along the differentiation route from hPSCs to neurons using lt-NES cells as a stable intermediate stage. Data acquisition for the miRNA profiling analysis was performed in a joint project with researchers from the Institute of Transplantation Diagnostics and Cell Therapeutics at the University of Düsseldorf, and first analyses were done as part of my Diploma thesis (Muertz 2009). In this thesis the data were then analyzed in depth and experimentally validated.

2. Functional analysis of selected miRNAs with regard to neuronal differentiation

Based on the miRNA profiling analysis and evidence collected from the literature, several miRNAs including miR-181a were chosen as candidates for further functional studies. The selected miRNAs were investigated for their potential to promote neuronal differentiation of lt-NES cells. Furthermore, the impact of miRNA manipulation on neuronal lineage decisions, in particular with regard to the dopaminergic lineage, was assessed.

3. Targets genes responsible for the miR-181a-mediated phenotypes

Once the impact of miR-181a on lt-NES cell differentiation and dopaminergic differentiation was established, the next task was to identify functionally relevant miR-181a targets. In this context, the main focus was to validate and assess the functional relevance of the potential regulatory interaction between miR-181a and GCNF.

4. Role of the miR-181a target GCNF on lt-NES cell maintenance and neuronal differentiation

There are several reports, which suggest a considerable role for GCNF on the neural lineage. However, its exact function during human neuronal differentiation has so far not been addressed. Thus, the last part of the study set out to explore the function of GCNF in human neural stem cells by using RNA interference and overexpression approaches.

2 MATERIAL & METHODS

2.1 Cell culture

Cell culture was performed under sterile conditions in a sterile laminar flow hood and the cells were cultivated at 37 °C in a humified incubator with 5% CO_2. Regular cell culture plastic ware (reaction tubes, tissue culture (TC) dishes, pipette tips, serological pipettes and cryovials) was purchased from PAA, Greiner Bio-One, BD Falcon, BD Bioscience and Nunc.

2.1.1 Cell lines

Table 2.1: Cell lines

Abbreviation	Cell line	Source/generated by
I3 hESC	I3 human embryonic stem cells	(Amit et al. 2002)
H9.2 hESC	H9.2 human embryonic stem cells	(Amit et al. 2000)
hiPSC	iLB-C-31F-r1 induced pluripotent stem cells	Matthias Brandt
I3 lt-NES	long-term self-renewing neuroepithelial-like stem cells derived from I3 hESCs	(Koch et al. 2009b)
H9.2 lt-NES	long-term self-renewing neuroepithelial-like stem cells derived from H9.2 hESCs	
DCX::EGFP lt-NES	DCX-EGFP reporter H9.2 lt-NES cells	(Ladewig et al. 2008)
HEK-293 FT	Human embryonic kidney cells transformed with the SV40 large T antigen	LifeTechnologies
MEF	Primary mouse embryonic fibroblasts	Anke Leinhaas
astro	Primary post-natal mouse astrocytes	Jaideep Kesavan

2.1.2 Reagents and media for cell culture work

All cell culture reagents and media were prepared under sterile conditions or sterilized before usage.

Table 2.2: Media and cell culture solutions

Medium/Reagent	Manufacturer	Medium/Reagent	Manufacturer
Accutase (StemPro)	Gibco	2-Mercaptoethanol (50 mM)	Gibco
B27 supplement (50x)	Gibco	mTESR1	Stemcell Technologies
DMEM high glucose	Gibco		
DMEM high glucose	Gibco	N2 supplement (100x)	Gibco or PAA
DMEM-F12	Gibco	Neurobasal	Gibco
DMSO	Sigma-Aldrich	Non-essential amino acids (NEAA)	Gibco
Fetal bovine serum (FBS)	Gibco	OptiMEM	Gibco
Glutamine (200 mM)	Gibco	PBS	Gibco
HBSS buffer	Gibco	Penicilin Streptomycin (Pen/Strep)	Gibco
Knockout DMEM	Gibco	Sodium pyruvate (100 mM)	Gibco
Knockout Serum Replacement (SR)	Gibco	Trypan Blue Stain (0.4%)	Gibco
Laminin	Sigma-Aldrich	Trypsin/EDTA (10x)	Gibco
Matrigel	BD Bioscience	BSA Fraction V (7.5%)	Gibco

Table 2.3: Cell culture additives. The following reagents were purchased as powder and resuspended in an appropriate solvent to create a stock solution.

Reagent	Manufacturer	Concentration (stock)	Solvent
Ascorbic acid	Sigma-Aldrich	200 mM	H_2O
BDNF	PeproTech	10 µg/ml	0.1% BSA in PBS
BrdU	Sigma-Aldrich	10 mM	H_2O
CHIR-99021	Axon Medchem	10 mM	DMSO
Chloroquin	Sigma-Aldrich	50 mM	H_2O
Collagenase	Gibco	1 mg/ml	DMEM-F12
Cyclic(c)AMP	Sigma-Aldrich	300 µg/ml	H_2O
DAPT	Sigma-Aldrich	2.5 mM	DMSO
dibuturyl (db)cAMP	Enzo Life Science	100 mM	H_2O
DNAse	Worthington	10 mg/ml	PBS
Doxycycline	Sigma-Aldrich	10 mg/ml	H_2O
EGF	R&D Systems	10 µg/ml	0.1 M Acetic acid 0.1% BSA/PBS
FGF2	R&D Systems	10 µg/ml	0.1% BSA in PBS
FGF8b	PeproTech	100 µg/ml	0.1% BSA in PBS
FGFb	Gibco	10 µg/ml	0.1% BSA in PBS
Fibronectin	Invitrogen	1 mg/ml	H_2O
Floxuridine	Sigma-Aldrich	10 mM	H_2O
G418	Calbiochem	200 mg/ml	H_2O
GDNF	PeproTech	10 µg/ml	0.1% BSA in H_2O
Gelatine[1]	Invitrogen	0.1 mg/ml	H_2O
Glucose	Sigma-Aldrich	160 mg/ml	DMEM-F12
Insulin	Sigma-Aldrich	5 mg/ml	10 mM NaOH in H_2O
IWR-1	Sigma-Aldrich	10 mM	DMSO
LDN193184[2]	Axon Medchem	200 µM	DMSO
Poly-L-Lysine	Sigma-Aldrich	2 mg/ml	H_2O
Poly-L-Ornithine[1]	Sigma-Aldrich	1.5 µg/ml	H_2O
Polybrene	Sigma-Aldrich	5 mg/ml	H_2O
Purmorphamine[2]	Merck	10 mM	Ethanol:DMSO (1:1)
Puromycin	Clontech	10 mg/ml	H_2O
ROCK Inhibitor Y-27632	Tocris	10 mM	H_2O
SAG	Calbiochem	1 mM	DMSO
SB431542	Sigma-Aldrich	50 mM	DMSO
SHH(C25II)-N	Pelo Biotech	100 µg/ml	0.1% BSA in PBS
TGFβ3	PeproTech	2 µg/ml	4 mM HCl, 0.1% BSA in H_2O
Trypsin inhibitor	Gibco	0.5 mg/ml	PBS
Uridine	Sigma-Aldrich	100 mM	H_2O

[1] stored at 4 °C; [2] stored at -80 °C. All other stock solutions were stored at -20 °C.

Table 2.4: Cell culture media for It-NES cells

NES maintenance N2 medium		Neuronal differentiation ND medium		Neuroprotective enzyme mix		NES freezing medium	
98%	DMEM-F12	49%	N2 medium	78%	HBSS buffer	90%	DMEM-F12
1%	N2 supplement	49%	Neurobasal	10%	Trypsin/EDTA	10%	DMSO
1.6 mg/ml	Glucose	1%	B27 supplement	10%	Accutase		
20 µg/ml	Insulin	100 ng/ml	cAMP	2%	B27 supplement		
1%	Pen/Strep	0.5%	Pen/Strep				

Table 2.5: Cell culture media for hESCs

hPSC maintenance SR medium		MEF-conditioned SR medium	mTeSR1 medium		hPS freezing medium	
77%	Knockout DMEM	50 ml of SR medium per 10^6 γ-irradiated MEFs Overnight incubation Harvesting and filtration	90%	mTeSR1 basal	70%	Knockout DMEM
20%	Knockout SR		10%	mTesR1 supplement	20%	Knockout SR
1%	NEAA		1%	Pen/Strep	10%	DMSO
2 mM	Glutamine					
0.1 mM	2-Mercaptoethanol					
1%	Pen/Strep					

Table 2.6: Cell culture media for MEFs/HEK cells

MEF/HEK maintenance medium		MEF/HEK freezing medium	
86%	DMEM high glucose	70%	DMEM high glucose
10%	FBS (heat inactivated)	20%	FBS
1 mM	Sodium pyruvate	10%	DMSO
1%	NEAA		
1%	Pen/Strep		

Table 2.7: Cell culture coatings

Gelatine-coating	Poly-L-Ornithine/Laminin (PO/LN)-coating
Incubation with 0.1 mg/ml gelatine in H_2O for 20 min at 37 °C	1) Overnight incubation with 1.5 µg/ml Poly-L-Ornithine in H_2O at 37 °C or 4 °C 2) Wash twice with PBS 3) Overnight incubation with 1 µg/ml Laminin in PBS at 37 °C or 4 °C
Matrigel (MG)-coating	
Overnight incubation with 33.3 µg/ml Matrigel in DMEM-F12 at 4 °C	
Poly-L-Lysine-coating	
1) Incubation with 0.1 mg/ml Poly-L-Lysine in H_2O for at least 20 min, 37 °C 2) Wash twice with H_2O	

2.1.3 Cryopreservation and thawing of cells

For cryopreservation, cells were resuspended in DMSO-containing freezing medium (Table 2.4-6) and transferred to cryovials, which were then placed in freezing containers and shifted to a -80 °C freezer. For long-term storage, vials were transferred to a liquid nitrogen storage tank. For thawing, cyrovials with frozen cells were warmed-up in a 37 °C water bath until only a small frozen clump remained. The cell suspension was then immediately transferred to appropriate wash medium, pelleted by centrifugation and suspended in appropriate culture medium.

2.1.4 Maintenance of human pluripotent stem cells

Classically, hESCs have been expanded on a feeder cell layer of mouse embryonic fibroblast (MEF). However, during the last years the culture conditions of hESCs have been improved, and nowadays hESCs are cultured in defined culture conditions without the need for feeder cells (reviewed Villa-Diaz et al. 2012). In this work, both the feeder-dependent cultivation method in SR medium as well as the feeder-free cultivation in mTeSR1 medium has been used.

Feeder-dependent culturing of hESCs

Human ESCs were cultivated on a layer of γ-irradiated mouse embryonic fibroblasts (MEFs), which provide essential growth factors and extracellular matrices to the hESCs. One day prior to thawing or replating hESCs, MEFs were thawed in MEF medium and plated on gelatine-coated 6-well plates at a density of 200.000 cells/well. The hESCs were then plated on top of the MEF layer and cultivated in SR medium supplemented with 4 ng/ml FGFb. Medium was changed daily and the hESCs were passaged every third to sixth day. To this end, cells were incubated with 1 mg/ml/well collagenase solution for 1 hour at 37 °C. Using this approach the MEFs mainly remained on the plate, while the hESC colonies detached from the feeder layer and could be rinsed off with medium. The cell suspension was then pelleted by centrifugation (800 rpm, 3 min; Heraeus Megafuge 1.0 R[1]) and carefully resuspended in an appropriate amount of culture medium to dissociate the colonies into smaller aggregates and distributed in a ratio of 1:1 up to 1:6 on fresh MEF-coated 6-well plates. For feeder-free cultivation of hESCs, as it was done prior to RNA isolation for the miRNA profiling analysis, hESCs were replated on MG-coated plates after splitting and cultivated in MEF-conditioned medium supplemented with 4 ng/ml FGFb for two passages to get rid of any remaining MEFs. If necessary, morphological differentiated hESCs were manually removed by scraping them off with a sterile injection needle in a horizontal sterile hood using a microscope.

Feeder-independent culturing of hPSCs in mTeSR1 medium

Human ESCs and iPSCs were cultivated on MG-coated TC dishes in mTeSR1 medium. The medium was changed daily and the cells were splitted approximately every third day at a ratio of 1:10 using Accutase treatment. For that purpose, hPSCs were incubated with Accutase for 5 min at 37 °C. The dissociated colonies were rinsed off and pelleted by centrifugation (1000 rpm, 5 min). The cells were then suspended in mTeSR1 medium and plated as single cell solution on MG-coated dishes. During this step, the ROCK inhibitor Y-27632 was added at a concentration of 10 mM to prevent cell death (Watanabe et al. 2007). For plating a defined number of cells, the total cell amount was determined using trypan blue vital staining and a Neubauer counting chamber. When the cells were frozen after Accutase splitting, ROCK inhibitor was also added during the thawing and replating process.

2.1.5 Floor plate-based differentiation of hPSCs into dopaminergic neurons

Differentiation of hPSCs into dopaminergic (DA) neurons via inducing floor plate progenitors was performed as described by Kriks et al. (2011). Briefly, hPSCs were plated onto MG-coated TC dishes and cultivated in mTeSR1 medium until 90% confluence. Subsequently, the cells were cultured in SR medium supplemented with pharmacological inhibitors against BMP/TGFβ receptors, i.e. LDN193189 (100 nM) and SB431542 (10 μm) to direct them towards neural differentiation by dual SMAD inhibition. To further direct the cells towards the floor plate identity, hPSCs were additionally treated with 100 ng/ml SHH(C25II)-N, 100 ng/ml FGF8b, 2 μm Purmorphamine (PMA) and 3 μm CHIR, which were

[1] Since the same centrifuge was used for all cell culture work, it will be not listed again in the following descriptions.

added at specific time points of the protocol (see Fig. 2.1). From day 5 on, the SR medium was mixed in 25% steps with N2 medium, which is beneficial for the expansion of neural precursor cells. From day 11 on, cells were cultured in Neurobasal-based (NB) differentiation medium containing 1x B27 supplement (devoid of retinoic acid (RA)) as well as 20 ng/ml BDNF, 200 μM ascorbic acid (AA), 20 ng/ml GDNF, 0.5 mM dibuturyl(db)cAMP, 1 ng/ml TGFβ3 and 10 μm DAPT. On day 13, the cultures were spilt 1:1 onto PO/LN-coated TC dishes with 45 min of Accutase treatment. From this day on, the medium was changed every other day until day 20 when the cells were splitted and replated at a density of 400.000 cells/cm^2 on MG-coated dishes. The cells were then finally fixed or harvested at day 25. Cell culturing and subsequent analyses were done in collaboration with Beate Roese-Koerner.

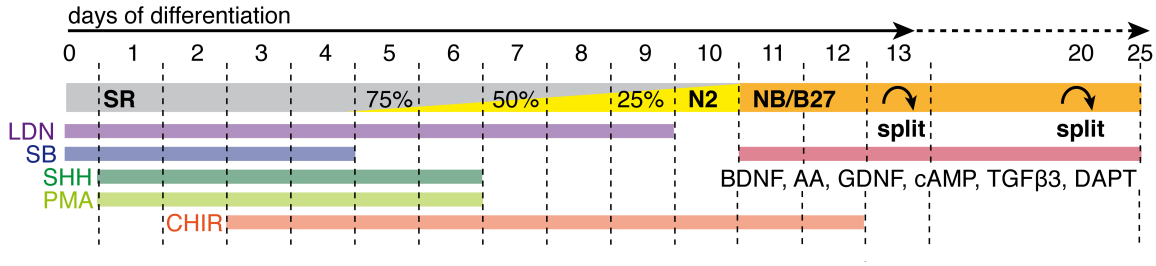

Fig. 2.1: Flowchart of the floor plate/DA differentiation paradigm according to Kriks et al. (2011). Percentages indicate the mixing ratio of SR to N2 medium. For more see the original publication and the text above.

2.1.6 Maintenance of long-term self-renewing neuroepithelial-like stem cells

Lt-NES cells were cultured and differentiated according to previously established protocols (Koch et al. 2009b). For lt-NES cell propagation, cells were cultivated on PO/LN-coated TC dishes in N2 medium supplemented with 10 ng/ml FGF2, 10 ng/ml EGF and 1 μl/ml B27 supplement (with RA). B27 supplement and growth factors were replenished every day, while the medium was exchanged every second day. Lt-NES cells were splitted approximately every third day at a ratio of 1:2 or 1:3. To this end, lt-NES cells were incubated for approximately 5 min with a 1x Trypsin/EDTA solution. When the cells started to detach, Trypsin inhibitor was added to stop the reaction and the cells were collected in DMEM-F12 and pelleted by centrifugation (1000 rpm, 5 min). Afterwards, lt-NES cells were resuspended in an appropriate amount of fresh N2 medium including the supplements and plated on PO/LN-coated or MG-coated dishes.

2.1.7 Neuronal differentiation of lt-NES cells

Default neuronal differentiation

For default neuronal differentiation, lt-NES cells were plated on MG-coated TC dishes and first cultivated under self-renewing conditions as previously described until confluence reached approximately 80%. Then, the N2 medium was replaced by ND medium (devoid of the growth factors EGF and FGF2), which was changed every other day. If the differentiation rate needed to be further enhanced, cultures were additionally treated with the γ-secretase inhibitor DAPT (2.5 μM).

Differentiation in the presence of factors inducing dopaminergic differentiation (DA-factors)

The protocol used here to increase the amount of TH-positive neurons generated during lt-NES cell differentiation was based on the protocol published by Perrier et al. (2004). In detail, lt-NES cells were first cultivated in N2 medium supplemented with 0.5 μm SAG or 1μm Purmorphamine (both SHH activators), 100 ng/ml FGF8b, 20 ng/ml BDNF and 0.2 mM ascorbic acid for 7 days. The cells were then cultured for another 7 days in ND medium supplemented with 20 ng/ml BDNF, 20 ng/ml GDNF, 2 ng/ml TGFβ3, 0.2 mM ascorbic acid and 0.5 mM dbcAMP.

Differentiation in the presence of pharmacological Wnt modulation

For activation of Wnt/β-catenin signaling, lt-NES cells were cultured with 3 μM CHIR-99021, which inhibits the GSK3 kinase and leads to an accumulation of β-catenin mimicking Wnt signaling (Ring et al. 2003). For inhibition of Wnt/β-catenin activity, cells were treated with 10 μM IWR-1, which stabilizes the scaffold of the β-catenin disruption complex (Chen et al. 2009). These factors were applied in ND medium with daily medium changes. ND medium supplemented with 0.1% DMSO was used as vehicle control.

Neuroprotective splitting

For splitting differentiating neuronal cultures, a specific protocol was used to enhance the survival of the neurons. Differentiating lt-NES cell cultures were first gently washed with HBSS buffer and then incubated for 4 min at 37 °C with the neuroprotective enzyme mix containing 1x Accutase, 1x Trypsin/EDTA and 2 μl/ml B27 supplement (Table 2.4). The reaction was stopped by adding Trypsin inhibitor and the cells were rinsed off with HBSS supplemented with 100 μg/ml DNAse to avoid cell clumping. After centrifugation (1200 rpm, 3 min), the cells were resuspended in an appropriate amount of ND medium containing 10 mM ROCK inhibitor to increase cell survival.

2.1.8 Clonal capacity assay of pre-differentiated lt-NES cells

To determine the clonal capacity (i.e the ability to generate clone from single cells) of two-weeks pre-differentiated lt-NES cell cultures, the cells were dissociated to single cells using the neuroprotective splitting method and replated at a density of 3125 cells/cm^2 on primary mitotically inactivated mouse astrocytes. Primary astrocytes obtained from mouse pups (post-natal day 3) were kindly provided by Jaideep Kesavan. Astrocytes were propagated in MEF medium on gelatine-coated TC dishes for at least four passages before mitotically inactivating them by 24 hours exposure to the nucleotide-analogs floxuridine (40 μM) and uridine (1 mM). Afterwards, the astrocytes were washed several times with MEF medium before plating lt-NES cells on top of them. Since after two weeks of differentiation, lt-NES cell cultures consisted of approximately 70% post-mitotic neurons, the actual density of undifferentiated cells was below 1000 cells/cm^2, which is considered to be suitable for clonal assays (Coles-Takabe et al. 2008).

The lt-NES/astrocytes co-cultures were cultivated for two weeks in normal N2 culture medium with growth factors and 2.5 µg/ml doxycycline, whereby the medium was replenished every third day. For follow-up differentiation assays lt-NES/astrocytes co-cultures were differentiated under default conditions as described for up to 3 months.

2.2 Lentiviral-based transgenesis of hPSCs and lt-NES cells

Table 2.8: Plasmids

Plasmid	Source or parental DNA origin	Antibiotic resist.
pMD2.G	Gift from Didier Trono (Wiznerowicz et al. 2003)	Ampicillin (Amp)
psPAX2	Gift from Didier Trono (Wiznerowicz et al. 2003)	Amp
pLVTHM	Gift from Didier Trono (Wiznerowicz et al. 2003)	Amp
pLVTHM-Puro	Modified from pLVTHM, described in Roese-Koerner et al. (2013)	Amp/Puromycin
pLVTHM-miR	miRNA loci were amplified from lt-NES cell genomic DNA	Amp/Puromycin
pLVTHM-ctr	shRNA ctr sequence was obtained from the pSilencer construct (Ambion)	Amp/Puromycin
pLVX-Tet-ON-Advanced	From Clontech (part of the Lenti-X Tet-ON Advanced Inducible Expression System)	Amp/G418
pLVX-EtO	Modified from pLVX-Tet-ON-Advanced as described in Mertens et al. (2013a)	Amp/G418
pLVX-Tight-Puro	From Clontech (part of the Lenti-X Tet-ON Advanced Inducible Expression System)	Amp/Puromycin
pCAG-mir30	Gift from Paddison et al. (2004) via Addgene (#14758)	Amp/Puromycin
pTight-miR-30:shRNA-ctr	miR-30 sequence was modified from pCAG-mir30 to include a scrambled ctr sequence	Amp
pTight-miR	miRNA loci were cloned from the respective pLVTHM contructs	Amp/Puromycin
pTight-GCNF	Amplified from cDNA generated from lt-NES cell total RNA	Amp/Puromycin
pTight-GFP	Cloned by Jérôme Mertens	Amp/Puromycin
7TGP	Gift from Fuerer & Nusse (2009) via Addgene (#24305)	Amp/Puromycin

2.2.1 Cloning and expansion of lentiviral constructs

Cloning and DNA plasmid preparation was performed using competent *E. coli* cells (strains DH5α, STLB2, STBL3; all from Invitrogen) and DNA isolation kits following manufacturer's instruction. The *E. coli* cells were grown on LB Agar plates or in LB medium with 100 µg/ml Ampicillin. For long-term storage of plasmids, bacteria glycerol stocks were prepared as described by Addgene.

Table 2.9: Reagents and recipes for DNA amplification in bacteria

LB medium		LB Agar plates
10 g	Tryptone	Dissolve 15 g Agar in 1000 ml LB, autoclave, cool to 50 °C pour into sterile plates, store at 4 °C
5 g	Yeast extract	
10 g	NaCl	**Bacteria glycerol stock**
1 ml	NaOH solution (1 M)	Mix 700 µl Bacteria solution with 500 µl glycerol, store at -80 °C
Add H_2O to 1000 ml, autoclave and store at 4 °C		
Ampicillin		
100 mg/ml Ampicillin sodium salt in H_2O		All components purchased from Roth or Sigma-Aldrich.

Table 2.10: Solutions for agarose gel electrophoresis

50x TAE buffer		6x DNA loading buffer	
242 g	Tris	3 ml	Glycerol
100 ml	EDTA (0. 5 M sol., pH 8.5)	0.25 mg	Bromophenol blue
57 ml	Acetic Acid (100%)	0.25 mg	Xylene cyanol
Add H_2O to 1000 ml		Add H_2O to 10 ml	

All components purchased from Sigma-Aldrich.

Table 2.11: Reagents and kits for cloning

Reagent/Kit	Manufacturer	Reagent/Kit	Manufacturer
Agarose	Peqlab	peqGOLD Gel Extraction Kit	Peqlab
Alkaline Phosphatase, Calf Intestine (CIP)	NEB	peqGOLD Plasmid Miniprep Kit	Peqlab
DNA ladders (100 bp & 1 kb)	Peqlab	Phusion High-Fidelity PCR Kit	NEB
dNTPs	Peqlab	Restriction enzymes	NEB
Ethidium bromide	Sigma-Aldrich	T4 ligase	NEB
NucleoBond Xtra EF Maxiprep Kit	Machery-Nagel	Taq DNA Polymerase	Invitrogen

For constant miRNA overexpression a lentiviral expression system based on the pLVTHM vector developed by Wiznerowicz et al. (2003) was used. This system was originally designed for conditional doxycycline-regulated shRNA expression. However, it can be also used for constant transgene expression, when the cells are only transduced with the pLVTHM construct, but not with the repressor tTR-KRAB construct. Here, a modified version of the pLVTHM vector expressing a puromycin resistance gene instead of the original GFP cassette was used. The genomic pre-miRNA loci plus ~150 basepairs up- and downstream flanking regions were amplified by PCR from the genomic DNA of lt-NES cells (cloning primers are listed in Table 2.38). PCR products were then isolated by agarose gel electrophoresis and gel extraction, digested using appropriate restriction enzymes and ligated into the multiple cloning site (MCS) of a linearized and dephosphorylated pLVTHM vector. As control, a short scrambled RNA sequence (sequence information was obtained from the pSilencer construct, Ambion) was cloned into the pLVTHM vector.

For conditional miRNA overexpression the Lenti-X Tet-ON Advanced Inducible Expression System from Clontech was used. The pLVX-Tet-ON plasmid was modified to carry the EF1α promoter instead of the original CMV promoter as described by Mertens et al. (2013a). For cloning the miRNA loci into the pLVX-Tight-Puro (pTight) plasmid, their expression cassettes were amplified by PCR from the respective pLVTHM plasmids and the different cloning steps were performed as described above. The coding DNA sequence for GCNF/NR6A1 was amplified from lt-NES cell cDNA and cloned into the pLVX-Tight-Puro backbone. The amplified sequence matched with the GCNF/NR6A1 transcript variant (ENST00000344523). For cloning the miR-30:shRNA-ctr hybrid cassette first an oligonucleotide sequence (containing the sense-ctr and the antisense-ctr sequence separated by the miR-30 loop sequence and flanked by parts of pre-miR-30) was designed and ordered from Invitrogen. The oligonucleotide was then amplified and elongated using common miR-30 primers, and cloned into the linearized pCAG-mir30 backbone (Paddison et al. 2004) and from there transferred to the pLVTHM and pTight vectors (for more details see Fig. 2.2 and Table 2.38).

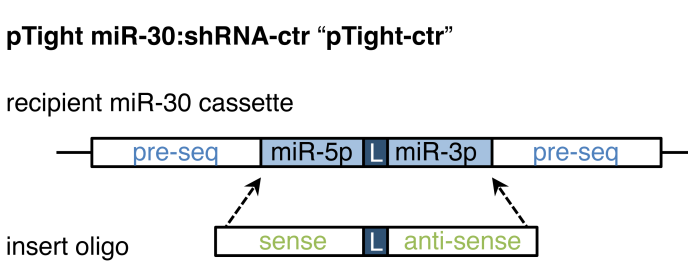

Fig. 2.2: Cloning of miR-30:shRNA-ctr hybrid as artificial non-targeting control miRNA. The mature miR-30-5p/3p sequences in the pre-miR-30 cassette were replaced by the siRNA sequences of the non-targeting control shRNA obtained from the pSilencer construct (Ambion). pre-seq: precursor sequence, L: miRNA loop.

The final plasmids were expanded in STBL3 or STBL2 *E. coli* and the DNA was isolated using the NucleoBond Xtra EF Maxiprep Kit following the manufacturer's instruction. The isolated DNA was analyzed by endonuclease digestion followed by agarose gel electrophoresis and sequencing (Seqlab). The DNA concentration was determined using the NanoDrop (Peqlab) spectrophotometer.

2.2.2 Production of lentiviral particles

Lentiviral particle production and transduction of cells was performed under S2 safety-conditions. Lentiviral particles were produced using the HEK-293FT cells (Invitrogen), which were, for regular maintenance, cultivated in MEF medium with 5% FBS on gelatine-coated TC dishes. One day prior transfection the cells were plated at a density of 120,000 cells/cm^2 on TC dishes coated with 0.1 mg/ml Poly-L-Lysine. The next day, the cells were transfected with lentiviral plasmids either by calcium phosphate precipitation as described by Koch et al. (2006) or by FuGENE-based (Promega) lipofection (see Table 2.12). The FuGENE-transfection mix was incubated for 15 min at room-temperature (RT) before adding 3 µl Chloroquin (final concentration 25 µM). In the meantime, the normal MEF culture medium on the cells was replaced with only 2% FBS-containing MEF medium. The transfection solution was briefly mixed and added dropwise to the cells. The cells were then incubated at 37 °C for 6 hours (h) and afterwards the medium was replaced by normal MEF medium. Transfected 293FT cells were cultivated for another three days with daily medium changes, during which they produced and secreted the lentiviral particles. The HEK-293FT supernatants from up to day 3 post-transfection were collected, filtered through 0.45 µm syringe filters (Corning) and concentrated by precipitation using PEG6000 as described by Kutner et al. (2009); see also Table 2.13. In brief, PEG6000 (final concentration 8.6%) and NaCl (final concentration 0.3 M) solutions were added to the supernatant and the mixture was incubated at 4 °C for 1.5 h and mixed every 20 min. Then, the solution was centrifuged at 4500g for 30 min at 4 °C (Heraeus Megafuge 16R). The pellet containing the viral particles was resuspended in 1 ml HBSS buffer, distributed into aliquots and stored at -80 °C.

Table 2.12: Lentiviral transfection mix

55 µl	FuGENE (Promega)
4.6 µg	psPAX2 (packaging plasmid)
4.6 µg	psMD2.G (envelop plasmid)
9.25 µg	Transfer vector containing the gene of interest
	Add PBS to 1000 µl

Table 2.13: PEG6000 precipitation mix

25 ml	HEK supernatant
6.8 ml	Polyethylenglycol 6000 (50%) (Sigma-Aldrich)
3 ml	4 M NaCl
Add PBS to 40 ml	

2.2.3 Transduction of hPSCs and lt-NES cells with lentiviral particles

Generally, lentiviral transduction was allowed to take place overnight at 37 °C. For lentiviral transduction of hPSCs, 1.5 million cells were resuspended in 2 ml mTeSR1 medium supplemented with 10 nM ROCK inhibitor and 5 µg/ml polybrene, and seeded into MG-coated 6-well TC plates. 100 µl of the concentrated viral particles were added to each dish while the cells were still in suspension. The next day, medium was changed to normal mTeSR1 culture medium. For lentiviral transduction of lt-NES cells, the cells were first seeded and cultivated as previously described until reaching 70% confluence. Then, the medium was changed to fresh N2 medium supplemented with 1 µl/ml B27, 10 ng/ml EGF, 10 ng/ml FGF2 (N2 culture medium) and 5 µg/ml polybrene and the respective lentiviral particles were added. The next day, medium was changed to normal N2 culture medium. Antibiotic selection to enrich for transduced cells by treatment with 200 µg/ml G418 and/or 5-2.5 µg/ml puromycin was started 72 h post-transduction and maintained during further propagation of the cells. To generate cell lines transduced with the Lenti-X Tet-ON Advanced Inducible Expression System, cells were first transduced with the pLVXTP-Eto virus and thereafter propagated in the presence of G418. Subsequently, pLVXTP-Eto cells were transduced with the different pLVX-Tight-Puro variants and cultivated with G418 and puromycin. To activate transgene expression, 2.5-5 µg/ml doxycycline was added and replenished every or every other day depending on the experimental set-up.

2.3 Oligonucleotide transfection experiments

2.3.1 Transfection procedure

All miRNA mimics, inhibitors, controls and siRNAs used in this work were purchased from Qiagen and are displayed in Table 2.14.

Table 2.14: RNA oligonucleotides[1] used for transfection experiments

Name	Catalog no.	Final conc.	Name	Catalog no.	Final conc.
AllStars Neg. Control siRNA	1027281	10-100 nM	**AllStars Neg. siRNA AF 555**	1027286	10 nM
miScript Inhibitor Neg. Control	1027272	100 nM	**Syn-hsa-miR-124-3p**	MSY0000422	10 nM
			Syn-hsa-miR-125b-5p	MSY0000423	10 nM
Anti-hsa-miR-124-3p	MIN0000422	100 nM	**Syn-hsa-miR-181a-3p**	MSY0000270	10 nM
Anti-hsa-miR-125b-5p	MIN0000423	100 nM	**Syn-hsa-miR-181a-5p**	MSY0000256	10 nM
Anti-hsa-miR-181a-3p	MIN0000270	100 nM	**Hs_NR6A1_3**	SI00146153	100 nM
Anti-hsa-miR-181a-5p	MIN0000256	100 nM	**Hs_NR6A1_6**	SI02626358	100 nM
miR-181a mut ds[2]	Purchased as custom oligonucleotide: AACA**GC**CAACGCUGUCGGUGAGU				10 nM

[1] MicroRNA mimics, and siRNAs are double-stranded RNA oligonucleotides, while miRNA inhibitors are single-stranded 2' O-methyl-modified RNAs. [2] Mutated nucleotides in the miR-181a seed region are indicated by bold letters.

Lt-NES cells were plated on MG-coated 12-well TC dishes (60,000 cells/cm^2) and either transfected on the same day (4 h after plating) or on the next day using Lipofectamine 2000 (Invitrogen) following the manufacturer's instruction. One hour before transfection, the medium was changed to 400 µl Pen/Strep-free culture medium. The Lipofectamine reaction mix was prepared in OptiMEM, incubated with the diluted oligonucleotides for 20 min at RT and added dropwise to the cells (see Table 2.15 for an overview). Four hours after transfection, medium was changed to normal culture medium. For serial transfections, cells were transfected every other day and splitted after every third transfection using the neuroprotective splitting method (see page 23). To monitor the transfection efficiency, one well was transfected with a fluorophore-labeled (AF 555) siRNA and the amount of fluorescent cells was determined by microscopy or flow cytometry analysis (as described in 0). For GCNF RNA interference, lt-NES cells were simultaneously transfected with two different GCNF siRNAs (Table 2.14).

Table 2.15: Short protocol for Lipofectamine-based transfection (12-well plate)
1. Change medium to 400 µl antibiotic free medium
2. Dilute 1 µl Lipofectamine in 49 µl OptiMEM (Solution 1)
3. Mix oligonucleotides/plasmid with OptiMEM in a total volume of 50 µl (Solution 2)
4. Incubate for 5 min at room-temperature
5. Combine the two solutions (100 µl) and incubate for another 20 min
6. Add oligomer-Lipofectamine complexes dropwise to the cells
7. Incubate for 4 h at 37 °C
8. Change to normal culture medium

2.3.2 Luciferase reporter assays

For Luciferase reporter assays, derivatives of the dual luciferase vector psiCHECK2 (Promega) were used. The psiCHECK2 plasmid contains a multiple cloning site (MCS) downstream of the stop codon of a Renilla luciferase gene (regulated luciferase) and an additional unregulated Firefly luciferase gene to normalize for transfection variability.

Table 2.16: Luciferase reporter plasmids

Plasmid	Source or parent DNA
psiCHECK2	Promega
psiCHECK2-GCNF 3' UTR	3' UTR was amplified from lt-NES cell genomic DNA
psiCHECK2-miR-181a biosensor (psiCHECK2-181BS)	Oligonucleotides were purchased from Invitrogen

The miR-181a biosensor was cloned following the instructionS from Promega. In brief, the biosensor containing two tandem-repeats of the reverse complement miR-181a sequence was purchased as oligonucleotides (forward and reverse), which were annealed following the instruction from Invitrogen and subsequently cloned into the MCS of the linearized psiCHECK2 plasmid using the restriction endonucleases Xho1 and Not1. To generate the GCNF 3' UTR reporter, the 3' UTR sequence of

GCNF/NR6A1 transcript variant (ENST00000344523) was amplified from genomic DNA isolated from lt-NES cells and cloned into the psiCHECK2 plasmid using Xho1 and Not1 restriction endonucleases.
For luciferase reporter assays, lt-NES cells were first transfected with 10 ng/ml of the respective psiCHECK2 plasmids with Lipofectamine as described. The next day, cells were transfected with the different RNA oligonucleotides. After 24 h, cells were detached by Trypsin/EDTA treatment and incubated for 20 min in Passive Lysis Buffer (Promega) while rocking, before freezing the lysates at -20 °C overnight. Before luciferase activity measurement, lysates were thawed and centrifuged briefly to pellet cell debris (1000 rpm, 3 min; Heraeus Megafuge 1.0 R). 10 μl of lysate was transferred to a white 96-well plate (Falcon), whereby three wells, i.e. three technical replicates, each were loaded for Renilla and Firefly luciferase reactions, respectively. Luminescence reaction was performed using the Lumino2000 luminometer (Bio-Rad). Renilla luciferase was initiated by automatically injecting Colenterazin solution and Firefly luciferase reaction by injecting Luciferin solution (Table 2.17).

Table 2.17: Reagents for luciferase reporter assays

Solution (in H_2O)	**Components**	**Manufacturer**	**Concentration**
Passive Lysis Buffer	Passive Lysis 5x Buffer	Promega	1x
Colenterazin solution	Colenterazine	PJK	40 μM
	Methanol	Sigma-Aldrich	2%
Luciferin solution	ATP	Sigma-Aldrich	0.75 mM
	Coenzyme A	Sigma-Aldrich	67.5 μM
	D-Luciferin Sodium-salt	PJK	0.5 mM
	DTT	Sigma-Aldrich	1.25 mM
	MgSO4	Sigma-Aldrich	3.75 mM
	Tricine (pH 7.8)	Sigma-Aldrich	30 mM

In order to determine the impact of RNA oligonucleotide transfection on Renilla luciferase activity the following formulas were used. First, the luminescence signal (measured as relative light units (RLU)) of Renilla luciferase was normalized to the luminescence signal of Firefly luciferase to correct for differences in transfection efficiency (Formula 2.1). Second, the relative Renilla activity (RRA) of the experimental group (e.g. psiCHECK-GCNF 3' UTR or psiCHECK-181BS) was normalized to the control group (psiCHECK2) to determine the plasmid-dependent response ratio (PRR; Formula 2.2). Third, the transfection-dependent response ratio (TRR) was determined by dividing the PRR for the different miRNA transfection conditions by the PRR of cells transfected with a scrambled (scr) control siRNA (Formula 2.3).

Formula 2.1

$$\mathrm{RRA} = \frac{\mathrm{RLU\ (Renilla)}}{\mathrm{RLU\ (Firefly)}}$$

Formula 2.2

$$\mathrm{PRR} = \frac{\mathrm{mean\ RRA\ (psiCHECK-reg)}}{\mathrm{mean\ RRA\ (psiCHECK)}}$$

Formula 2.3

$$\mathrm{TRR} = \frac{\mathrm{PRR\ (miRNA\ )}}{\mathrm{PRR\ (scr\ transfection)}}$$

2.4 Flow cytometry-based assays

Flow cytometry analyses were performed using the BD FACSCalibur flow cytometer (BD Bioscience) and data analysis was done with the FlowJo Software. The workflow was as follows: First, lt-NES cells were treated with the respective compounds (see description below) before harvesting them by trypsinization as described in 2.1.6. The resulting cell pellet was washed, resuspended in appropriate amounts of PBS/wash buffer and filtered through a nylon mesh (40 μm) into FACS tubes. The tubes were kept on ice in the dark until the analysis. Instrument settings for FACSCalibur were calibrated using positive and negative samples and lt-NES cells were gated based on their size (forward scatter, FSC) and granularity (side scatter, SSC) to exclude aggregates and debris from the analysis. FITC (fluorescein isothiocyanate) and EGFP fluorescence was determined using the FL1 channel (515-545 nm) and AF 555 fluorescence from fluorophore-labled siRNAs with the FL2 channel (564-601 nm).

2.4.1 Doublecortin-EGFP reporter assay

H9.2 DCX::EGFP lt-NES cells, expressing EGFP under the human doublecortin (DCX) promoter were kindly provided by Julia Ladewig (Ladewig et al. 2008). DCX is an early neuronal marker and the reporter cells were used here to monitor the degree of neuronal differentiation after transient miRNA modulation. In brief, differentiating H9.2 DCX::EGFP lt-NES cells were transfected twice with RNA oligonucleotides as described above. The cells were then harvested at day 5 and the amount of EGFP-positive cells was determined by flow cytometry.

2.4.2 CaspGLOW fluorescein active caspase assay

To determine the amount of apoptotic cells in differentiating lt-NES cell cultures, the CaspGLOW Kit from eBioscience was used. This kit contains a pan-Caspase inhibitor Z-VAD-FMK coupled to FITC. The inhibitor-FITC conjugate only binds to active Caspases enabling direct fluorescent labeling of apoptotic cells. The original manufacturer's protocol was adapted to adherent cell culture conditions: First, 1 μl of inhibitor-FITC conjugate was added to approximately 1 million lt-NES cells and incubated for one hour at 37 °C. Afterwards, the supernatant was collected and the cells were harvested with Trypsin/EDTA. The cell pellet was washed twice with CaspGLOW wash buffer and resuspended in the same buffer for flow cytometry analysis.

2.4.3 Wnt/β-catenin reporter assay

In order to monitor the degree of Wnt/β-catenin signaling, the lentiviral 7TGP Wnt reporter construct developed by Fuerer & Nusse et al. (2009) was used. The 7TGP Wnt reporter constructs contains an EGFP expression cassette downstream of the β-catenin-dependent 7xTCF promoter. Lentiviral particles were produced as described (see 2.2.2) and used to transduce l3 lt-NES cells to generate a stable reporter cell line. The 7TGP Wnt reporter system was first tested by treating lt-NES cells with increasing concentrations (0.09-3 μM) of the Wnt activator CHIR-99021 in N2 culture medium (Ring et al. 2003). Culture medium supplemented with 0.1% DMSO was used as vehicle control. The cells were treated for 48 h and then harvested for flow cytometry-based quantification of

EGFP-positive cells. In order to determine the impact of miR-181a/a* overexpression on Wnt activity, 7TGP lt-NES cells were subsequently transduced with pLVXTP-Eto and the different pTight-constructs. Transgene expression was activated by doxycycline treatment and the cells were cultured for 4 days in the presence of doxycycline before harvesting them for flow cytometry analysis. The Wnt reporter experiments were done in collaboration with Katharina Doll.

2.5 RNA-based expression analyses

To avoid RNA degradation by RNases, disposable plastic ware, RNase-free H_2O treated with DEPC, and surface a RNase decontaminant (RNase-ExitusPlus, Labomedic) was used.

2.5.1 RNA isolation

The total RNA used for reverse transcription (RT)-PCR or Northern blotting was extracted using PeqGOLD TriFast (Peqlab) following the manufacturer's instructions with minor changes. In brief, cells were first washed once with PBS and then directly lysed on the TC dish by adding at least 1 ml TriFast (the volume was increased according to the surface harvested). Lysates were stored at -80 °C for at least 24 h before proceeding with the RNA extraction. For this purpose, samples were thawed at RT and mixed with 200 µl/ml chloroform. After incubation for 7 min at RT, tubes were centrifuged at 12,000 rpm (Centrifuge 5415R, Eppendorf) for 5 min to facilitate phase separation. The hydrous upper phase was transferred to a fresh tube and RNA was precipitated by adding 500 µl isopropanol and 70 µg/ml glycogen. Precipitation was allowed to take place for at least 30 min on ice. Subsequently, RNA was pelleted by centrifugation at 12,000 rpm for 10 min at 4 °C and washed twice with ice-cold 75% ethanol in DEPC-H_2O. Afterwards, the RNA pellet was dried and resuspended in DEPC-H_2O. At the end of the RNA extraction procedure samples were subjected to DNaseI treatment (Invitrogen) following the manufacturer's instructions to remove any contaminating DNA.

Table 2.18: Kits and reagents for RNA extraction

Reagent/Kit	Manufacturer
Chloroform	Roth
DEPC	Sigma-Aldrich
DNaseI Amplification Grade Kit	Invitrogen
Ethanol for molecular biology	Roth
Glycogen (35 mg/ml)	Peqlab
Isopropyl alcohol	Roth
PeqGOLD TriFast	Peqlab
RNase-ExitusPlus	Labomedic

Table 2.19: Recipe for DEPC-H2O
1 ml/l DEPC in H_2O
Incubate overnight while stirring in the dark, under the hood, lid open
Autoclave the next day

2.5.2 Northern blot analysis

The non-radioactive Northern blot method used here was developed by combining two published protocols (Ramkissoon et al. 2006; Várallyay et al. 2008). Here, RNA detection relied on the hybridization with DIG-labeled RNAs probes that are complementary to the mature miRNA sequence. It is important to note that these probes can hybridize to the precursor and mature miRNA species. DIG-11-UTPs (Roche Applied Science) were incorporated during T7-mediated *in vitro* transcription of DNA oligonucleotides (Table 2.20) using the mirVana Probe Construction Kit (Applied Biosystems, Life Technologies) and following manufacturer's instructions. At the end of the procedure, unincorporated nucleotides were removed by ammonium acetate (5 M in DEPC-H_2O)-ethanol precipitation. The amount of DIG-labeled RNA probes was quantified with the NanoDrop spectrophotometer and aliquoted as 400 ng (miRNA) or 100 ng (RNU6B snRNA) portions in 50 μl DEPC-H_2O containing 10 μm EDTA and stored at -80 °C.

Table 2.20: DNA oligonucleotides used as templates for DIG-RNA probes (purchased from Invitrogen).

Name	DNA Template	Antisense RNA probe
miR-124-3p	TTAAGGCACGCGGTGAATGCCACCTGTCTC	**AATTCCGTGCGCCACTTACGGT**GGACAGAGGG
miR-125b-5p	TCCCTGAGACCCTAACTTGTGACCTGTCTC	**AGGGACTCTGGGATTGAACACT**GGACAGAGGG
miR-181a-3p	ACCATCGACCGTTGATTGTACCCCTGTCTC	**TGGTAGCTGGCAACTAACATG**GGGACAGAGGG
miR-181a-5p	AACATTCAACGCTGTCGGTGAGTCCTGTCTC	**TTGTAAGTTGCGACAGCCACTCA**GGACAGAGGG
miR-302b-5p	ACTTTAACATGGAAGTGCTTTCCCTGTCTC	**TGAAATTGTACCTTCACGAAAG**GGACAGAGGG
miR-371a-3p	AAGTGCCGCCATCTTTTGAGTGTCCTGTCTC	**TTCACGGCGGTAGAAAACTCACA**GGACAGAGGG
miR-520c-3p	AAAGTGCTTCCTTTTAGAGGGTCCTGTCTC	**TTTCACGAAGGAAAATCTCCCA**GGACAGAGGG
miR-9-5p	TCTTTGGTTATCTAGCTGTATGACCTGTCTC	**AGAAACCAATAGATCGACATACT**GGACAGAGGG
RNU6B (U6)	AATTCGTGAAGCGTTCCATATCCTGTCTC	TTAAGCACTTCGCAAGGTATAGGACAGAGGG

DNA templates contain a sequence stretch complementary to the T7 promoter (5'-CCTGTCTC-3') and two extra Gs are added during the T7 transcription reaction. Sequence complementary to the mature miRNAs is indicated in bold.

Table 2.21: Reagents for RNA polyacrylamide gel separation

Solution	Components	Manufacturer	Concentration/Amount
10x TBE (DEPC-H_2O)	Tris	Sigma-Aldrich	0.9 M
	Boric acid	Sigma-Aldrich	0.9 M
	EDTA	Sigma-Aldrich	0.02 M
PAGE-Urea gel (40 ml)	Urea	Roth	20 g
	Acrylamide/Bis 19:1	Sigma-Aldrich	15 ml
	APS (10%)	Sigma-Aldrich	240 μl
	TEMED	Sigma-Aldrich	16 μl
	10x TBE	-	5 ml
	DEPC-H_2O	-	4 ml
RNA-loading buffer [Color maker solution]	Deionized formamide	Applied Biosystems	10 ml
	EDTA (0.5 M)	Sigma-Aldrich	200 μl
	Xylene cyanol	Bio-Rad	1 mg [10 mg]
	Bromophenol blue	Sigma-Aldrich	1 mg [10 mg]

For Northern blot analysis, first RNA was separated on a 15% denaturing polyacrylamide gel (see Table 2.21) using the Owl P10DS-1 gel casting and vertical electrophoresis system (Thermo Scientific). The gel was pre-run in 1x TBE for 1 h at 400 mV. For RNA loading, 40 µg total RNA was mixed 1:1 with RNA-loading buffer and denatured at 65 °C for 20 min. RNA samples were cooled on ice and then loaded on the PAGE-Urea gel using Gel-Loading Pipet Tips (1-200 µl, VWR). Empty wells were loaded with 10 µl color marker solution to monitor the electrophoresis and 10 µl RNA Low Molecular Weight Marker (USB) was loaded as size standard. To allow the samples to gently enter the gel, it was first run at 200 mV for about 15 min and then run at 400 mV for 2 h, while attached to a water-cooling unit. For visualization of the RNA, the gel was afterwards incubated for 10 min in 1x TBE containing 1 µg/ml ethidium bromide, washed twice with 1x TBE and images were taken using the GelDoc2000 (Bio-Rad) UV transilluminator.

Table 2.22: Reagents for capillary blotting and northern blot detection

Solution	Components	Manufacturer	Concentration/Amount
10x SSC (in DEPC-H_2O, pH 7.0)	Sodium chloride	Roth	3 M
	Sodium citrate	Fluka	0.3 M
Acetic acid 5%	Acetic acid	Roth	5% in H_2O
Methylene blue staining solution (in DEPC-H_2O, pH 5.5)	Methylene blue	Sigma-Aldrich	0.02% (w/v)
	Sodium actetate	Roth	0.3 M
Destaining solution (in DEPC-H_2O)	20x SSC	-	1%
	SDS	Roth	1%
Hybridization buffer (in DEPC-H_2O)	Deionized formamide	Applied Biosystems	50%
	SDS	Roth	0.02%
	N-laurolysarcosine	Sigma-Aldrich	0.1%
	10x Blocking solution	Roche Applied Science[#]	20%
	20x SSC	-	25%
Hybrdization wash buffer (in DEPC-H_2O)	20x SSC	-	10%
	SDS	Roth	0.1%
Maleic acid buffer (in DEPC-H_2O, pH 7.0)	Maleic acid	Fluka	0.1 M
	NaCl	Sigma-Aldrich	0.15 M
1x Blocking solution (BS)	10x Blocking solution	Roche Applied Science[#]	10%
	Maleic acid buffer	-	90%
Antibody solution	Anti-Digoxigenin-AP	Roche Applied Science[#]	1:10,000 in 1x BS
Antibody washing buffer	Maleic acid buffer	-	99.7%
	Tween20	Sigma-Aldrich	0.3%
Detection buffer (in DEPC-H_2O, pH 9.5)	Tris HCl	Sigma-Aldrich	0.1 M
	NaCl	Sigma-Aldrich	5 M
Chemiluminescence substrate	CSPDstar	Roche Applied Science	2 ml/membrane
Stripping buffer (in DEPC-H_2O)	Deionized formamide	Applied Biosystems	50%
	SDS	Roth	5%
	Tris HCl (pH 7.5)	Sigma-Aldrich	50 mM

[#] Part of the DIG Luminescent Detection Kit from Roche Applied Science.

Next, RNA samples were transferred onto a nylon membrane (Roche Applied Science) using capillary blotting in 20x SSC as described by Várallyay et al. (2008). Transfer was allowed to proceed overnight at RT. Afterwards, the membrane was washed in 2x SSC for 2 min and the RNA was fixed on the membrane by UV-cross-linking with 1200 mJ using a UV Hybridizer (Straterlinker from Stratagene). The quality of the RNA transfer was controlled by methylene blue staining. To that end, the membrane was first soaked in 5% acetic acid for 15 min and then incubated for 5 min in methylene blue staining solution until the tRNA bands and the ladder became visible. The membrane was rinsed several times with DEPC-H_2O and photographed. The ladder was cut out and stored in 20x SSC for later reference. The rest of the membrane was washed with destaining solution for 15 min. Subsequently, the membrane was hybridized with the DIG-RNA probes and probe detection was performed using the DIG Luminescent Detection Kit (Roche Applied Science) following the manufacturer's protocol. In brief, the membrane was first equilibrated in 2x SSC and pre-hybridized in 10 ml hybridization buffer at 65 °C for at least 1 h in a hybridization oven (OV3 Biometra) under agitation. For each membrane an aliquot of 100 ng RNU6B or 400 ng miRNA probe was denatured at 95 °C for 2 min, cooled on ice and diluted in 2 ml hybridization buffer. Hybridization was allowed to take place overnight at RT under agitation. The next day, the membrane was rinsed in DEPC-H_2O, washed twice for 5 min in hybridization wash buffer and then prepared for alkaline phosphatase immunodetection using anti-digoxigenin Fab fragments conjugated to alkaline phosphatase (AP). In brief, the membrane was first incubated for 30 min in blocking solution followed by 30 min incubation with the antibody solution containing anti-DIG-AP conjugates. Afterwards, the membrane was washed with antibody washing buffer, equilibrated with detection buffer, incubated with the chemiluminescence substrate CSPDstar and exposed to CL-XPosure films overnight at RT. X-ray films were developed using the XOMAT1000 processor (Kodak). For re-probing, membranes were incubated two times with 5 ml stripping buffer for 1 h at 80 °C followed by washing in 2x SSC for 5 min and pre-hybridization as described above.

2.5.3 Quantitative RT-PCR analysis

RNA expression levels were quantified using SYBR Green-based quantitative real-time RT-PCR (qRT-PCR). Extracted RNA was first reverse transcribed (RT) to generate cDNA, whereby different kits were used for pri-, pre- and mature miRNA-cDNA and mRNA-cDNA synthesis (Table 2.23).

Table 2.23: Kits for cDNA synthesis

Target RNA species	cDNA synthesis kit	Manufacturer
Pri-, pre-, mature miRNAs	miScript Reverse Transcription Kit II	Qiagen
mRNAs	iScript cDNA Synthesis Kit	Bio-Rad

The qPCR reactions were run in an Eppendorf Realplex Mastercycler using SYBR Green-based reaction mixtures. The specificity of PCR products was verified by melting curve analysis and agarose gel electrophoresis. Data were analyzed using the comparative ΔΔCt method (Livak et al. 2001). RT-PCR primers were designed with Primer3web to span exon-exon junctions and are listed in Table 2.41. Primer amplification efficiency was initially determined by applying serial dilutions of template cDNA.

Quantitative RT-PCR analysis of miRNA precursors and mature miRNAs

In order to measure the expression of small RNAs, like miRNAs, specific systems have been developed to increase the size of the template RNA during reverse transcription. With the miScript Reverse Transcription Kit II (Qiagen) used in this work the small RNAs are first polyadenylated and subsequently converted into elongated miRNA-cDNAs using a poly(T)-universal tag primer. The reverse transcription reaction was performed following manufacturer's instructions with 500 ng RNA in a 10 µl reaction using the HiFlex buffer, which enables the simultaneous reverse transcription of pre-miRNAs, mature miRNAs and mRNAs. The cDNA was quantified by NanoDrop spectrophotometer and the cDNA concentration was adjusted to 25-50 ng/µl. Between 50 and 200 ng of template cDNA was applied for each qRT-PCR reaction using the miScript SYBR Green PCR Kit (Qiagen) and reactions were set up in a 20 µl volume according to the manufacturer's protocol. For mature miRNA detection, miRNA-specific forward primers and the miScript Universal Reverse Primer, which binds to the poly(T)-universal tag, were used. For pre-miRNA expression analysis, miScript Precursor Assays (Qiagen), which contain pre-miRNA-specific forward and reverse primer were used (see Table 2.40). The cycling parameters applied for miScript qRT-PCR are listed in Table 2.24.

Table 2.24: Cycling conditions for miScript qRT-PCR

Step		Temperature	Time
Initial activation		95 °C	15 min
Denaturation	40-45x	94 °C	15 s
Annealing		55 °C	30 s
Extension		70 °C	30 s
Final denaturation		95 °C	15 s
Dissociation curve		55-95 °C	

All measurements were carried out in technical duplicates or triplicates and expression data of the genes of interest (measured as cycle threshold (ct) values) were normalized to miR-16, RNU5A or SNORD25 reference levels, respectively.

Quantitative RT-PCR analysis of primary miRNAs and messenger RNAs

For detection of pri-miRNAs, cDNA was generated using the miScript Reverse Transcription Kit II as described. The qRT-PCR reactions were set up using a self-made SYBR Green-based qPCR mix (Table 2.25, 2.26) and Taq Polymerase (Invitrogen); in the following referred to as "Taq qRT-PCR".

Table 2.25: Recipe for 2x qPCR mix (for 10 ml stock)

Component	Manufacturer	Amount
10x PCR buffer (-$MgCl_2$)	Invitrogen	2 ml
$MgCl_2$ Solution (50 mM)	Invitrogen	1.2 ml
dNTPs (each 100 mM)	Peqlab	Each 40 µl
SYBR Green I nucleic acid gel stain (1000x)	Sigma-Aldrich	15 µl
Fluorescein calibration dye (100 µM)	Bio-Rad	2 µl
H_2O	-	6.623 ml

Table 2.26: Reaction set up for Taq qRT-PCR

Component	Amount
2x qPCR mix	10 µl
Taq polymerase	0.12 µl
cDNA (150-500 ng/µl)	2 µl
Forward/reverse primer (3 mM each)	2 µl
Add H_2O to 20 µl final volume	

Table 2.27: Cycling conditions for Taq qRT-PCR

Step		Temperature	Time
Initial activation		95 °C	3 min
Denaturation		95 °C	15 s
Annealing	40-45x	60 °C	20 s
Extension		72 °C	30 s
Final denaturation		72 °C	10 min
Dissociation curve		55-95 °C	

For mRNA expression analysis, cDNA was synthesized using the iScript cDNA Synthesis Kit (Bio-Rad) and the respective qRT-PCR reactions were performed using the Taq qRT-PCR reaction set up. The cycling program for Taq qRT-PCR reactions is given in Table 2.27. Pri-miRNA and mRNA expression data were normalized to 18s rRNA reference levels.

Human brain RNA samples used for qRT-PCR

For qRT-PCR analysis of human brain samples, RNA was extracted from human midbrain samples (CS18-20, provided by the Human Developmental Biology Resource) as previously described (see 2.5.1). For comparison, total RNA extracts from whole fetal brain (purchased from Agilent) was used.

2.5.4 Semi-quantitative RT-PCR analysis

Template cDNA was generated from total RNA extracts as described and adjusted to 50-75 ng/µl. Semi-quantitative RT-PCR was performed using the GoTaq Flexi DNA Polymerase (Promega). PCR reactions were set up using the 5x Green GoTaq Flexi Buffer, which already contains gel loading dyes, following the manufacturer's protocol (Table 2.28, 2.29). PCR products were separated by agarose gel electrophoresis in TAE buffer and visualized with ethidium bromide (1:10,000).

Table 2.28: Reaction set up for GoTaq RT-PCR

Component	Amount
5x Green GoTaq Flexi Buffer	5 µl
$MgCl_2$ Solution (25 mM)	1.5 µl
PCR Nucleotide Mix, 10 mM each	0.5 µl
GoTaq DNA Polymerase (5 U/µl)	0.125 µl
cDNA (50-75 ng/µl)	2 µl
Primers (20 mM)	1 µl
Add H_2O to 25 µl final volume	

Table 2.29: Cycling conditions for GoTaq RT-PCR

Step		Temperature	Time
Initial activation		95 °C	2 min
Denaturation		95 °C	30 s
Annealing	25-40x[#]	60 °C	30 s
Extension		72 °C	30 s
Final denaturation		72 °C	10 min

[#] Amount of cycles depends on the primers used. See Table 2.41 for more information.

2.6 Western blot analysis

Cells lysates were prepared by first mechanically detaching the cells from the TC dishes using a cell scraper (Cell lifter, Corning) followed by lysis in RIPA buffer (Table 2.30). Lysates were cleared by centrifugation (12,000 rpm, 15 min, 4 °C; Eppendorf Centrifuge 5415R) and protein concentration was determined using Bradford Reagent (Sigma-Aldrich) according to manufacturer's protocol. The samples were then either stored at -80 °C or distributed as 40 µg aliquots and heat-denatured with 5x Laemmli buffer (Table 2.30) at 95 °C for 10 min for subsequent electrophoresis. Protein samples

were separated by SDS-polyacrylamide gel electrophoresis (SDS-PAGE) using the Mini-PROTEAN vertical electrophoresis system from Bio-Rad. Gels were prepared according to manufacturer's instructions and consisted of a stacking gel and a separating gel (8% acrylamide; Table 2.31). 40 µg of each protein sample was loaded per lane and one lane was loaded with 10 µl of a size marker (Color Plus Prestained Protein Ladder (10-230 kDa, NEB). The gel was run in running buffer at 100 V for 2 h.

Table 2.30: Reagents for preparing protein lysates

RIPA buffer	
Tris HCl	50 mM (pH 7.5)
EDTA	1 mM
Deoxycholic acid sodium salt	0.5%
NaCl	150 mM
SDS	0.1%
Igepal CA-639	1%
Protease inhibitor cocktail	1:100
5x Laemmli buffer	
Tris HCl	312.5 mM (pH 6.8)
SDS	10%
Glycerol	50%
Bromophenol blue	0.1%
2-Mercaptoethanol (add fresh)	10%

Table 2.31: Recipes for polyacrylamide gels

Separating gel (8%, 10 ml)	
H_2O	4.6 ml
Acrylamide Mix (30%)	2.6 ml
Tris HCl (pH 8.8)	2.6 ml
SDS (10%)	100 µl
APS (10%)	100 µl
TEMED	6 µl
Stacking gel (2 ml)	
H_2O	1.15 ml
Acrylamide Mix (30%)	330 µl
Tris HCl (pH 6.8)	500 µl
SDS (10%)	20 µl
APS (10%)	20 µl
TEMED	2 µl

All reagents were purchased from Sigma-Aldrich or Roth, except for the Halt Protease Inhibitor Cocktail, which was purchased from Thermo Scientific.

Table 2.32: Recipes for Western blotting. All reagents purchased from Sigmal-Aldrich or Roth.

10x Running buffer (in H_2O)		**Ponceau staining solution** (in H_2O)		**Stripping buffer** (in H_2O)	
Trizma-Base	25 mM	Ponceau S	0.1% (w/v)	SDS	2% (w/v)
Glycin	193 mM	Acetic Acid	5%	Tris HCl	62.5 mM (pH 6.7)
SDS	0.1% (w/v)			2-Mercap-toethanol	7 mM
1x Transfer buffer (in H_2O)		**TBS-[T]** (in H_2O)			Add fresh
Trizma-Base	2.5 mM	Tris HCl	10 mM (pH 7.5)		
Glycin	19.3 mM	NaCl	150 mM (TBS_{50}: 50 mM)		
Methanol	20%	[Tween20]	0.1%		

Separated proteins were blotted onto a nitrocellulose membrane applying the wet blot technique and using the Mini Trans-Blot Cell from Bio-Rad. Blotting was run in transfer buffer at 70 V for 2 h, while cooled with an ice pack. The efficacy of protein transfer was surveyed by Ponceau staining. Afterwards, the membrane was blocked in blocking solution containing 2.5-5% milk powder in TBS-(T), incubated with the primary antibody solution followed by several washing steps in TBS-T, and incubation with an HRP-linked secondary antibody (for details see Table 2.33.) Finally, the membrane was again washed with TBS-T and HRP-signal was detected with a chemiluminometer (ChemiDoc, Bio-Rad) using the Luminata Forte Western HRP substrate (Merck Millipore).

Table 2.33: Conditions used for GCNF, NLK, Beta-Actin Western blot analysis

Condition	GCNF	NLK
Blocking	5% milk powder in TBS-T, 2 h at RT	5% milk powder in TBS without Tween20, 1 h at RT
1° antibody solution	GCNF mouse antibody, 1:1000 in 5% milk powder in TBS-T, 2 h at RT	NLK mouse antibody, 1:100 in 2.5% milk powder in TBS-T_{50}, overnight at 4 °C followed by 30 min at RT
Washing	TBS-T	TBS-T_{50}
2° antibody solution	HRP-goat anti-mouse, 1:1000 in 5% milk powder in TBS-T, 1 h at RT	HRP-goat anti-mouse, 1:500 in 2.5% milk powder in TBS-T_{50}, 1 h at RT
Condition	**β-actin**	
Blocking	10% milk powder in TBS-T, 1 h at RT	
1° antibody solution	β-actin mouse antibody, 1:2000 in 5% milk powder in TBS-T, overnight at 4°C	
Washing	TBS-T	
2° antibody solution	HRP-goat anti-mouse, 1:1000 in 5% milk powder in TBS-T, 1 h at RT	

2.7 Immunocytochemistry

Chemical substances used for immunochemistry were purchased from Sigma-Aldrich or Merck, if not stated otherwise (Table 2.34). For immunocytochemistry, cells were washed once with PBS, fixed with 4% PFA (20 min, RT) and washed again three times with PBS. The plates were then either stored at 4 °C in PBS with 1% Sodium azide (PBSaz) or directly used for immunostainings. To that end, cells were permeabilized with 0.1% Triton-X-100 in PBSaz for 10 min. Afterwards, cells were incubated in blocking solution (5-10% fetal bovine serum (FBS) in 0.1% Triton/PBSaz) for up to 2 h at RT. The respective primary antibodies listed in Table 2.42 were applied in blocking solution for either 2 h at RT or for overnight incubation at 4 °C. Cells were washed twice in PBS before secondary antibodies (listed in Table 2.43) were applied in blocking solution for 2 h at RT. Cell nuclei were counterstained with DAPI (4',6-diamidino-2-phenylindole, 1:10,000 in PBS), and the cells were finally embedded in Mowiol and covered with a glass cover slip.

Table 2.34: Recipes for immunocytochemistry

4% PFA solution	**0.1 M Borate Buffer**		
Dissolve 40 g PFA in 1000 ml PBS by heating	3.8 g Sodium borate in 100 ml H_2O		
	Adjust pH to 8.5 with HCl		
Filter, adjust pH to 7.4	**Permeabilization solution (in PBS)**		**Mowiol**
	Triton-X-100 sol	0.1-0.5%	Dissolve 2.49 g Mowiol and 6 g Glycerol in 6 ml H_2O
Aliquot and store at -20 °C	Sodium azide	1% (w/v)	
2 N HCl	**Blocking solution** (in PBS)		Add 12 ml of 0.2 M Tris HCl (pH 8.5)
Add 167 ml HCl to 833 ml H_2O	FBS	5-10%	Heat to 50 °C for 10 min
	Triton	0.1%	Clarify by centrifugation
	Sodium azide	1% (w/v)	Aliquot and store at -20 °C

2.7.1 BrdU incorporation assay

Lt-NES cells were incubated with BrdU (Bromdesoxyuridin, 10 μM) for 3.5 h in a cell culture incubator and subsequently fixed with 4% PFA as described. After washing, cells were permeabilized with 0.5% Triton/PBSaz for 30 min at RT. For DNA denaturation, cells were treated with 2 N HCl for 10 min at RT, washed three times with PBS and subsequently incubated with 0.1 M borate buffer for 10 min at RT. After washing again three times in PBS, cells were incubated with 5% FBS-blocking solution for 30 min. The primary antibody (BrdU mouse IgG, Becton Dickinson) was applied 1:50 in blocking solution and incubated overnight at RT. Secondary antibody staining and DAPI counterstaining were performed as described above.

2.7.2 Image analysis and processing

At least three pictures were taken randomly per condition using Zeiss microscopes (see Table 2.36) and processed using Adobe Photoshop and ImageJ (Schneider et al. 2012). Cell counting was performed using ImageJ, whereby each picture was first scored for DAPI-labeled nuclei and subsequently for the markers of interest. For each condition three images and at least 1000 cells were scored. For quantification of β-III Tubulin-positive cells, only cells with neurites longer than the cell soma were counted. Neurite length was determined using the ImageJ plugin NeuronJ (Meijering et al. 2004). To generate whole well overview pictures, the automated microscopy device CellaVista (SynenTec) was used and images were taken using the “Cell Cluster” application and the 10x objective. Images were further processed with ImageJ and converted to binary images.

2.8 In silico analyses

2.8.1 MicroRNA profiling analysis

MicroRNA expression analysis was done by Sandra Weinhold (Institute for Transplantation Diagnostics and Cell Therapeutics, University Düsseldorf) using the TaqMan MicroRNA Multiplex qRT-PCR Assay from Applied Biosystems (Lao et al. 2007). The assay was run according to the manufacturer’s protocol. Briefly, small RNA fractions from two independent collections of, respectively, I3 hESCs, self-renewing lt-NES cells and neuronal cultures (generated after 15 and 30 days of differentiation (ND15, ND30)) were extracted using the miRVana miRNA Isolation Kit (Ambion, Life Technologies). Aliquots of the small RNA fractions corresponding to 5000 cells were subjected to reverse transcription employing 330 different miRNA-specific stem-loop primers followed by a multiplex pre-amplification PCR step. Subsequently, miRNA expression was determined by TaqMan qRT-PCR using the ABI Prism 7900 HT Sequence Detection System (Applied Biosystems, Life Technologies). The generated raw miRNAs expression values (Ct values) were analyzed using a multi-step approach (Fig. 2.3). First, miRNAs with Ct values over 28 were considered as not significantly expressed following suggestions from Applied Biosystems. According to this cutoff, 75 of the miRNAs analyzed appeared to be absent in all samples, including miRNAs that are encoded by the human cytomegalovirus (miR-UL-, miR-US-species), which were used as negative controls.

Second, the raw miRNA expression values were normalized to the mean Ct value of the respective multiplex PCR plate in order to correct for plate-to-plate variations. The normalized values were subsequently analyzed by the comparative ΔΔCt method using the hES cell samples as baseline. Since two independent biological replicates for each cell sample (hES, NES, ND15 and ND30) were analyzed, and both hES cell samples were used as baseline, four combinatorial data sets for each stage (e.g. NES_1 vs ES_1, NES_1 vs ES_2, NES_2 vs ES_1, NES_2 vs ES_2; Fig. 2.2) were generated. The four data sets for each stage were compared with each other and only miRNAs with similar expression profiles in all four stage-specific combinatorial data sets were considered for further analyses. From those, only miRNAs with a minimum 2-fold expression difference across the neural cell samples compared to the ESC reference sample were considered as differentially expressed. According to these requirements 69 miRNAs were designated as not significantly differentially expressed. Third, the expression data (as log2 ratios) of the differentially expressed miRNAs were further analyzed by a two-step hierarchical clustering using the Cluster 3.0 software (Eisen et al. 1998; de Hoon et al. 2004). Java TreeView software (Saldanha 2004) was used to visualize clustering results, whereby the miRNA expression ratios were displayed in a heat-map with yellow-blue color coding (as shown in Fig. 3.1).

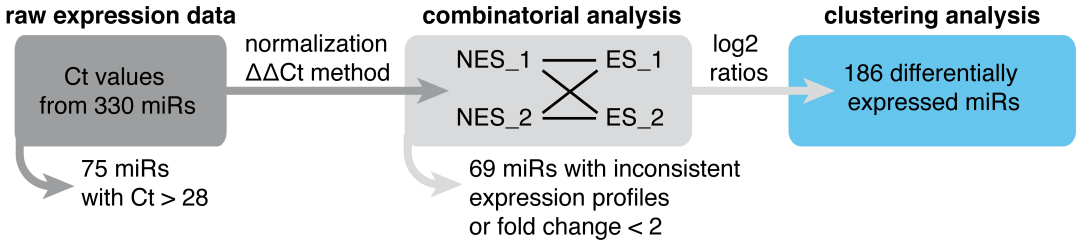

Fig. 2.3: Workflow of the approach used to analyze the miRNA profiling data. For more details see text.

2.8.2 MicroRNA target gene prediction

MicroRNA target prediction was performed using the comprehensive miRWalk database, which enables the comparison of different target prediction algorithms, e.g. miRanda, PICTAR5 and Targetscan (Dweep et al. 2011). The list of predicted miRNA target genes was matched to the Gene Ontology and KEGG pathway repositories using the DAVID Bioinformatics Resources 6.7 (Huang et al. 2009).

2.8.3 GCNF target gene prediction

To identify genes with putative GCNF transcription factor binding sites on a global scale, the MAPPER platform was used (Marinescu et al. 2005). This platform generates a list of the 1000 best scoring putative targets. This list was then analyzed with the functional annotation tool of the DAVID Bioinformatics Resources 6.7, which calculates an enrichment score for the different functional terms, mainly based on Gene Ontology annotations, associated with a given gene list (Huang et al. 2009). To identify putative GCNF binding sites in the promoters of specific genes, the Transcriptional Regulatory Element Database (Jiang et al. 2007) was used. Since the consensus sequence of the GCNF

response element was not annotated in TRED, its positional weight matrix, generated based on the TRANSFAC annotation (M00526, V$GCNF_01; Table 2.35), was manually inserted. Cutoff score for the binding site search was set to 9.

Table 2.35: Positional weight matrix of the GCNF consensus sequence

	Position																	
	1	2	3	4	5	6	7	8	9	10	11	12	13	14	15	16	17	18
Nucleotide A	0.2	0.1	0.1	0.8	0.9	0.0	0.0	0.0	0.0	1.0	1.0	0.0	0.0	0.0	0.0	0.9	0.2	0.2
C	0.4	0.1	0.7	0.0	0.0	0.0	0.0	0.0	1.0	0.0	0.0	0.0	0.0	0.0	0.9	0.0	0.4	0.4
G	0.2	0.2	0.1	0.1	0.0	1.0	0.3	0.0	0.0	0.0	0.0	0.9	0.5	0.1	0.0	0.0	0.2	0.2
T	0.1	0.6	0.0	0.0	0.0	0.0	0.6	1.0	0.0	0.0	0.0	0.1	0.5	0.9	0.1	0.0	0.2	0.3
		T	C	A	A	G	G/T	T	C	A	A	G	G/T	T	C	A		

Consensus sequence

2.8.4 Software and online tools

Table 2.36: Software and online tools

Program/Database	Manufacturer/Source
Adobe Photoshop, Illustrator CS3	Adobe
APE – A Plasmid Editor 1.17	M. Wayne Davis
Cluster 3.0	Michael Eisen (Eisen et al. 1998; de Hoon et al. 2004)
FlowJo 6.8	Tree Star
Image J 1.44o	NIH (Schneider et al. 2012)
Java TreeView	(Saldanha 2004)
Microsoft Office 2008 for Mac	Microsoft
Papers 2.73	Mekentosj
Prism 5.0c	Graphpad
DAVID Bioinformatics Resources	http://david.abcc.ncifcrf.gov (Huang et al. 2009)
Ensemble Genome Browser	http://www.ensembl.org/index.html
MAPPER2	http://genome.ufl.edu/mapper/mapper-man (Marinescu et al. 2005)
microRNA.org	http://www.microrna.org/microrna/home.do
miRBase	http://www.mirbase.org
miRWalk	http://www.umm.uni-heidelberg.de/apps/zmf/mirwalk/ (Dweep et al. 2011)
NCBI database	http://www.ncbi.nlm.nih.gov
Primer3web	http://bioinfo.ut.ee/primer3-0.4.0
TargetScan 6.0	http://www.targetscan.org
Transcriptional Regulatory Element Database	http://rulai.cshl.edu/cgi-bin/TRED/tred.cgi?process=home (Jiang et al. 2007)

2.8.5 Statistical analysis

Quantitative data were generated in biological replicates. All results presented as graphs show mean + SEM (standard error of the mean), which was computed using the GraphPad Prism software. Statistical significance, unless otherwise stated, was analyzed by two-tailed Student's t-test for control and experimental conditions, and $p \leq 0.05$ was considered to be statistically significant.

2.9 Supplementary lists

2.9.1 Technical equipment

Table 2.37: Technical equipment – Only equipment that was critical for the success of the experiments and is not part of the general laboratory facilities is listed.

Device		Name	Manufacturer
Automated fluorescence microscope		CellaVista	SynenTec
Centrifuge (bacteria pelleting)		Sorvall RC 6+ Centrifuge	Thermo Scientific
Centrifuge (cell culture)		Heraeus Megafuge 1.0 R	Thermo Scientific
Centrifuge (table top)		Centrifuge 5415R	Eppendorf
Centrifuge (virus concentration)		Heraeus Megafuge 1.6 R	Thermo Scientific
Chemiluminometer		ChemiDoc	Bio-Rad
Flow cytometer		FACSCalibur	BD Bioscience
Fluorescence microscopes	upright	Axioskop2 and Axio Imager X10 with ApoTome	Zeiss
	inverse	Axiovert 200M	Zeiss
Gel documentation		Geldoc2000	Bio-Rad
Gel electrophoresis system used for DNA separation		Agagel	Biometra
Gel electrophoresis system used for Protein separation		Mini-Protean (vertical gel chamber) Mini Trans-Blot Cell (wet blotting cell)	Bio-Rad
Gel electrophoresis system used for RNA separation		Owl Water Cooled, Dual Gel, Electrophoresis System P10DS-1	Thermo Scientific
Horizontal flow hood		HERAguard	Thermo Scientific
Hybridization oven		OV3	Biometra
Incubator for cell culture		HERAcell	Thermo Scientific
Light microscope (inverse)		Axiovert 25	Zeiss
Luminometer		Lumino2000	Bio-Rad
Micropipettes		2 ,10, 20, 100, 1000 μl and multichannel 10 μl	Eppendorf
Real-Time PCR System		Mastercycler realplex	Eppendorf
Spectrophotometer		NanoDrop 1000	Peqlab
Sterile laminar flow hood		HERAsafe	Thermo Scientific
Thermocycler		T3000 Thermocycler	Biometra
UV Hybridizer		Straterlinker	Stratagene
X-Ray developing machine		XOMAT 1000 processor	Kodak

2.9.2 Primers and oligonucleotides for cloning

Table 2.38: Primers and oligonucleotides used to generate recombinant DNA sequences

Target	Recipient plasmid	Name	**Sequence** (5'-3'; restriction sites for endonucleases are highlighted in bold)
MIR124-1	pLVTHM-Puro	3-Mlu1-miR124	TGTACA**ACGCGT**TGGTCCCTTCCTCCGGCGTT
		5-Cla1-miR124	TGTACA**ATCGAT**ACAGGCTGCACACCTCCCCA
MIR125B1	pLVTHM-Puro	3-Mlu1-miR125b	TGTACA**ACGCGT**TATATGCGCCCCCAGATACT
		5-Cla1-miR125b	TGTACA**ATCGAT**CATAGCAGCCAACACGCTAT
MIR153-1	pLVTHM-Puro	3-Mlu1-miR153	TGTACA**ACGCGT**GCTGCCTGTTTCCTCT
		5-Cla1-miR153	TGGAATTC**ATCGAT**AATCCAGAGATCCTCC
MIR181A1	pLVTHM-Puro	3-Mlu1-miR181a	TGTACA**ACGCGT**TGTGATGTGGAGGTTTGC
		5-Cla1-miR181a	TGGAATTC**ATCGAT**AGTCCTGGTGTGTCCA
MIR324	pLVTHM-Puro	3-Mlu1-miR324	TGTACA**ACGCGT**GAGGTTGCATAGTTGGGACA
		5-Cla1-miR324	TGTACA**ATCGAT**CTGGGGCTTTCTTCCCAGT
shRNA control (ctr)	pLVTHM-Puro	Mlu1-shRNA ctr-Cla1	**CGCGT**CCCCACTACCGTTGTTATAGGTGTTCAAGAGACACC TATAACAACGGTAGTTTTTTTGGAA**AT**
		Cla1-antisense-Mlu1	**CGAT**TTCCAAAAAAACTACCGTTGTTATAGGTGTCTCTTGA ACACCTATAACAACGGTAGTGGGG**A**
miR-30: shRNA ctr hybrid	pCAG-mir30	miR30-shRNA ctr hybrid	TGCTGTTGACAGTGAGCGACTACCGTTGTTATAGGTGTAGT GAAGCCACAGATGTACACCTATAACAACGGTAGTTGCCTAC TGCCTCGGA
		5-Xho1-miR30	CAGAAGG**CTCGAG**AAGGTATATTGCTGTTGACAGTGAGCG
		3-EcoR1-miR30	CTAAAGTAGCCCCTT**GAATTC**CGAGGCAGTAGGCA
pCAG-miR30ctr	pLVTHM-Puro	5-Mlu1-pCAG-miR30	TGTACA**ACGCGT**TGTTTGAATGAGGCTTCAGTACTTT
		3-pCAG-miR30	TATTTGTGAGCCAGGGCATT
pLVTHM-miR30ctr	pTight-Puro	5-BamH1-miR30	TGTACA**GGATCC**TGTTTGAATGAGGCTTCAGTACTTT
		3-Not1-pLVTHM	TGTACA**GCGGCCGC**GTTATTCCCATGCGACGGTATCG
pLVTHM-miR124	pTight-Puro[#]	5-BamH1-miR124	ATTCA**GGATCC**TGGTCCCTTCCTCCGGCGTT
		5-EcoR1-miR124	ATTCA**GAATTC**ACAGGCTGCACACCTCCCCA
pLVTHM-miR125b	pTight-Puro[#]	5-Not1-miR125b	ATTCA**GCGGCCGC**TATATGCGCCCCCAGATACT
		3-Mlu1-miR-125b	ATTCA**ACGCGT**CATAGCAGCCAACACGCTAT
pLVTHM-miR181a	pTight-Puro[#]	5-BamH1-miR181a	TGTACA**GGATCC**TGTGATGTGGAGGTTTGC
		5-Not1-miR181a	ATTCA**GCGGCCGC**AGTCCTGGTGTGTCCA
GCNF/ NR6A1	pTight-Puro	5-Not1-GCNF	CA**GCGGCCGC**GTCATGGAGCGGGACGAACCG
		3-EcoR1-GCNF	AC**GAATTC**TTCATTCCTTGCCCACACTGGT
miR-181a biosensor	psiCHECK2	Xho1-181aBS-Not1	**TCGAG**GAGTAGAGCTCTAGTACTCACCGACAGCGTTGAATG TTACTCACCGACAGCGTTGAATGTT**GC**
		Not1-antisense-Xho1	**GGCCGC**AACATTCAACGCTGTCGGTGAGTAACATTCAACGC TGTCGGTGAGTACTAGAGCTCTACTC**C**
miR-181a* biosensor	psiCHECK2	Xho1-181a*BS-Not1	**TCGAG**GAGTAGAGCTCTAGTGGTACAATCAACGGTCGATGG TGGTACAATCAACGGTCGATGGT**GC**
		Not1-antisense-Xho1	**GGCCGC**ACCATCGACCGTTGATTGTACCACCATCGACCGTT GATTGTACCACTAGAGCTCTACTC**C**
GCNF 3' UTR	psiCHECK2	5-Xho1-GCNF3U	TGTACAC**TCGAG**CTCCTCAGGCCAACCACA
		3-Not1-GCNF3U	TGTACA**GCGGCCGC**CTTCACATTCTGTAAACTGTAAGAAAA

[#] The respective pTight-miRNA constructs were cloned by Lars Nolden.

Table 2.39: Additional primers used for sequencing

Target	Name	Sequence (5'-3')
pLVTHM	pLVTHM H1 FOR	GATCAATTCACCATGCTAGTGGATCC
	pLVTHM Cla1 REV	GTTATTCCCATGCGACGGTATCGAT
pTight	pTight FOR	TGTACGGTGGGAGGCCTAT
	pTight REV	AGCGCATGCTCCAGACTGCCT
pTight-GCNF	GCNF FOR1 internal	TGAACCGTCAGATCGCCTGG
	GCNF FOR2 internal	GCAACGGTTTCTGTCAGGAT
	GCNF FOR3 internal	ATTCTGGCCACTCACCACTT
	GCNF REV internal	ATTCTGGCCACTCACCACTT
miR-30	miR-30 FOR	ACTACCGTTGTTATAGGTG
	miR-30 REV	CACCTATAACAACGGTAGT
psiCHECK2	psiCHECK FOR	CGCTCCAGATGAAATGGGTAAG
	psiCHECK REV	CGCGTCAGACAAACCCTAAC

2.9.3 Primers for RT-PCR

Table 2.40: Primers used for pre- and mature miRNA qRT-PCR analysis

miRNA	Primer sequence (5'-3')
let-7a	TGAGGTAGTAGGTTGTATAGTT
miR-124	TAAGGCACGCGGTGAATGCC
miR-125	TCCCTGAGACCCTAACTTGTGA
miR-153	TTGCATAGTCACAAAAGTGATC
miR-16	TAGCAGCACGTAAATATTGGCG
miR-181a	AACATTCAACGCTGTCGGTGAGT
miR-181b	AACATTCATTGCTGTCGGTGGGT
miR-181c	AACATTCAACCTGTCGGTGAGT
miR-181d	AACATTCATTGTTGTCGGTGGGT

miRNA	Primer sequence (5'-3')
miR-324-3p	ACTGCCCCAGGTGCTGCTGG
miR-324-5p	CGCATCCCCTAGGGCATTGGTGT
miR-9	TCTTTGGTTATCTAGCTGTATGA
RNU5A	GTGGAGAGGAACAACTCTGAGTC
Primer assay (from Qiagen)	
miScript Primer Asssay Hs_mir-181a*	
Hs_mir-181a-1_PR_1 miScript Precursor Assay	
Hs_mir-181a-2_PR_1 miScript Precursor Assay	
miScript Primer Assay Hs_SNORD25_11	

Table 2.41: Primers used for mRNA and pri-miRNA RT-PCR analysis

Target	FOR primer sequence (5'-3')	REV primer sequence (5'-3')	# Cycles SQ-RT-PCR
18s rRNA	TTCCTTGGACCGGCGCAAG	GCCGCATCGCCGGTCGG	
ASCL1	GGAGCTTCTCGACTTCACCA	AACGCCACTGACAAGAAAGC	
ATOH1	ATGGCGCAAAAGAATTTGTC	GCCTCATCCGAGTCACTGTAA	
DACH1	GTGGAAAACACCCCTCAGAA	CTTGTTCCACAATTGCAACACC	30
DAT	CATCTACGTCTTCACGCTCCT	GTCATCTGCTGGATGTCGTC	
DLL1	GGAGAAGCATCTGAAAGAAAAAGG	GGGAGTCTTGCCATCTCACTT	
FOXA1	ACACCACTACGCCTTCAACC	GGTAGTGCATCACCTGTTCGT	
GAD1	CTTGTGAGTGCCTTCAAGGAG	TGCTCCTCACCGTTCTTAGC	
GAPDH	ATACTTCTCATGGTTCACACCCAT	ATGACCCCTTCATTGACCTCAACT	25
GCNF	GAGGCCGGAATAAGAGCATT	CAGGGGAACTGTGGTCACTATC	35
GMP6A	TGAGATGGCAAGAACTGCTG	CCAGGCCAACATGAAAAGAT	35
HES1	AAGGCGGACATTCTGGAAAT	GTCACCTCGTTCATGCACTC	
HEY1	CCGAGATCCTGCAGATGA	GCTCAGATAACGCGCAACT	
LIN28A	CGGGCATCTGTAAGTGGTTC	CTGATGCTCTGGCAGAAGTG	
LIN28B	TCTTCCAAAGGCCTTGAGTC	TCAAGGCCACCACAGTTGTA	
LMX1A	AAGGCCTCATTTGAAGTATCCTC	CACTCAGCCCTGTCTCTGC	
MSI1	TACGCCAGCCGGAGTTATAC	CTGGGAGTCGAACCTGGAG	
MSI2	AGCTCAGCCGAAAGAAGTCA	GCCATAGCTTGGAGCAAATC	

Table continues on next page.

Target	FOR primer sequence (5'-3')	REV primer sequence (5'-3')	# Cycles SQ-RT-PCR
NEUROD1	CCGCGCTTAGCATCACTAAC	CCCACTCTCGCTGTACGATT	
NEUROD4	GGGAGACTTGGCTTCTCTGACT	CCAGGATGGTGTGTTGACTAGC	
NEUROG1	GCTCTTCTGACCCCAGTAGCC	CGTTGTGTGGAGCAAGTCTTT	
NEUROG2	CAGGCCAAAGTCACAGCAAC	CCGAGCAGCACTAACACGTC	
NLK	CCAGTGACTTTGAGCCTGTC	GATGGCTGAGCAACAGTGG	
NOTCH1	TGAAGAACGGGGCTAACAAA	TCCATATGATCCGTGATGTCC	
NOTCH2	CTGCCCTTGGACCCATTTAT	CCAGTGGCTGGATCAGTAGC	
NOTCH3	CCTCACTTCACTGCATTCCA	CCCTAGTTCCCAAAGGGAGA	
NURR1	GGGCTGCAAAGGCTTCTTTA	ACAGCCAGGCACTTCTGAAA	
PAX6	AATAACCTGCCTATGCAACCC	AACTTGAACTGGAACTGACACAC	40
PLZF	CTATGGGCGAGAGGAGAGTG	TCAATACAGCGTCAGCCTTG	35
POU3F3	GTTCTCGCAGACCACCATCT	CGATAGAGGTCCGCTTCTTG	30
Pri-181ab-1	ATCGACCGTTGATTGTACCC	GGCCACAGTTGCATTCATT	35
Pri-181ab-2	TGACCCCCTAAGCAAGTGTC	GGGACCTGCTTTTCCTCTTT	32
RFX4	TCTGAGACGGCAAACATCAC	GACTCGATGGGAGACTGCTC	30
SOX1	AGTATTCTTCTGCTCCGGCTGT	TCCCTCCTCTGGACCAAACT	30
TH	ACTGGTTCACGGTGGAGTTC	TCTCAGGCTCCTCAGACAGG	

SQ RT-PCR, semi-quantitative RT-PCR

2.9.4 Antibodies

Table 2.42: Primary antibodies

Target	Host/Isotype	Source	Catalog no.	Dilution[#]
BrdU	Mouse IgG	Becton Dickinson	347580	1:50
FOXA2	Goat IgG	R&D Systems	AF2400	1:100
GABA	Rabbit IgG	Sigma-Aldrich	A-2052	1:500
GAD65/67	Rabbit polyclonal	Merck Millipore	AB1511	1:500
GCNF	Rabbit polyclonal	Santa Cruz Biotechnology	sc-66903	1:500 (WB)
	Mouse IgG	Abcam	ab41894	1:100 (ICC), 1:1000 (WB)
GFAP	Rabbit polyclonal	Dako	Z0334	1:1000
Human Nuclei	Mouse IgG	Merck Millipore	MAB4383	1:250
Ki67	Mouse IgG	Dako	M7240	1:100
LMX1A	Mouse IgG	Merck Millipore	AB10533	1:1000
MAP2ab	Rabbit polyclonal	Merck Millipore	AB5622	1:500
NESTIN	Mouse IgG	R&D Systems	MAB1259	1:1000
	Rabbit polyclonal	Novus	NB300-265	1:500
NLK	Mouse IgG	Santa Cruz Biotechnology	sc-48361	1:100 (WB)
OLIG2	Rabbit polyclonal	Merck Millipore	AB9610	1:200
PH3	Rabbit polyclonal	Merck Millipore	06-570	1:1000
PLZF	Mouse IgG	Merck Millipore	OP128	1:25
SOX2	Mouse IgG	R&D Systems	MAB2018	1:100
TH	Rabbit IgG	Merck Millipore	AB125	1:500
ZO1	Rabbit polyclonal	Invitrogen	61-7300	1:100
β-III Tubulin	Mouse IgG	Covance	MMS-435P	1:4000
	Rabbit polyclonal	Covance	PRB-435P	1:4000
β-Actin	Mouse IgG	Sigma-Aldrich	A1978	1:2000 (WB)

[#] Dilution for immunocytochemistry (ICC), if not stated otherwise. WB, Western blot.

Table 2.43: Secondary antibodies

Antibody	Source	Dilution
Cy3 goat anti-mouse IgG+IgM	Jackson Immuno Research	1:250
Cy5 goat anti-mouse IgG	Jackson Immuno Research	1:250
Alexa488 goat anti-mouse IgG	Invitrogen	1:1000
Alexa488 goat anti-rabbit IgG	Invitrogen	1:1000
Alexa555 goat anti-mouse IgG	Invitrogen	1:1000
Alexa555 goat anti-rabbit IgG	Invitrogen	1:1000
Alexa555 donkey anti-goat IgG	Invitrogen	1:1000
HRP-goat anti-mouse	Jackson Immuno Research	1:500-1000

3 RESULTS

3.1 Identification of miRNA expression patterns associated with human neuronal differentiation

In order to gain first insights into the miRNA expression changes during human neuronal differentiation, a miRNA profiling analysis was performed in hESCs, hESC-derived lt-NES cells and their differentiated neuronal progeny. This was done in a joint project with Dr. Sandra Weinhold and Prof. Wernet (Institute of Transplantation Diagnostics and Cell Therapeutics at the University of Düsseldorf). The resulting miRNA profiling data were then further analyzed and validated in this thesis.

3.1.1 Annotation of miRNA profiles in hESCs, lt-NES cells and neuronal cultures

First, RNA was isolated from four different time points along hESC-based neuronal differentiation, i.e. from undifferentiated I3 hESCs (ES), lt-NES cells (NES) and their differentiated neuronal progeny (ND15, ND30)[1]. Staining for TRA-1-81 surface antigen confirmed the undifferentiated nature of the hESC cultures (Fig. 3.1 A; data not shown). As a stable intermediate stage of neuronal differentiation, hESC-derived lt-NES cells were used, which were cultured under self-renewing conditions in the presence of the growth factors EGF and FGF2 (NES, Fig. 3.1 B). Under these conditions, lt-NES cells expressed the intermediate filament Nestin, a maker for neural progenitors, and showed typical rosette morphology (Fig. 3.1 B). Neuronal differentiation of lt-NES cells was induced by growth factor withdrawal as previously described (Koch et al. 2009b). After 15 days of differentiation, approximately 20% of the cells expressed the pan-neuronal marker β-III Tubulin (Fig. 3.1 C), while after 30 days the fraction of neurons reached more than 50% (Fig. 3.1 D). For each cell type and time point, RNA from two different biological replicates was prepared and subjected to miRNA expression profiling using the ABI TaqMan MicroRNA Multiplex qRT-PCR Assay covering 330 miRNAs (Lao et al. 2007; Fig. 3.1 E). Based on their miRNA profiles, the different cell samples clearly clustered according to the cell type origin. Importantly, lt-NES cells clustered separately from ND15 and ND30 neuronal cultures, proving the reliability of the approach (Fig. 3.1 E). Raw miRNAs expression Ct values were analyzed using a multi-step approach; details are given in the Methods section 2.8.1. First, miRNAs with Ct values above 28 in all samples were defined as not significantly (ns) expressed (Group IV, Fig. 3.1 F). The remaining 255 miRNAs were analyzed by the comparative ΔΔCt method using the hESC samples as reference. Based on this analysis, 186 miRNAs exhibited a minimum 2-fold expression difference in the neural cell samples compared to the hESC samples and were, thus, considered as differentially expressed. While the remaining 69 miRNAs displayed either no significant expression differences or their expression pattern was inconsistent between the two biological replicates (Group 0, Fig. 3.1 F).

[1] Dr. Lodovica Borghese, Dr. Philipp Koch and Dr. Stefanie Terstegge prepared the cell samples used for the initial miRNA profiling analysis. The RNA preparation and multiplex miRNA qRT-PCR assay was carried out by Dr. Sandra Weinhold. The cell samples used for the validation assays were prepared by myself.

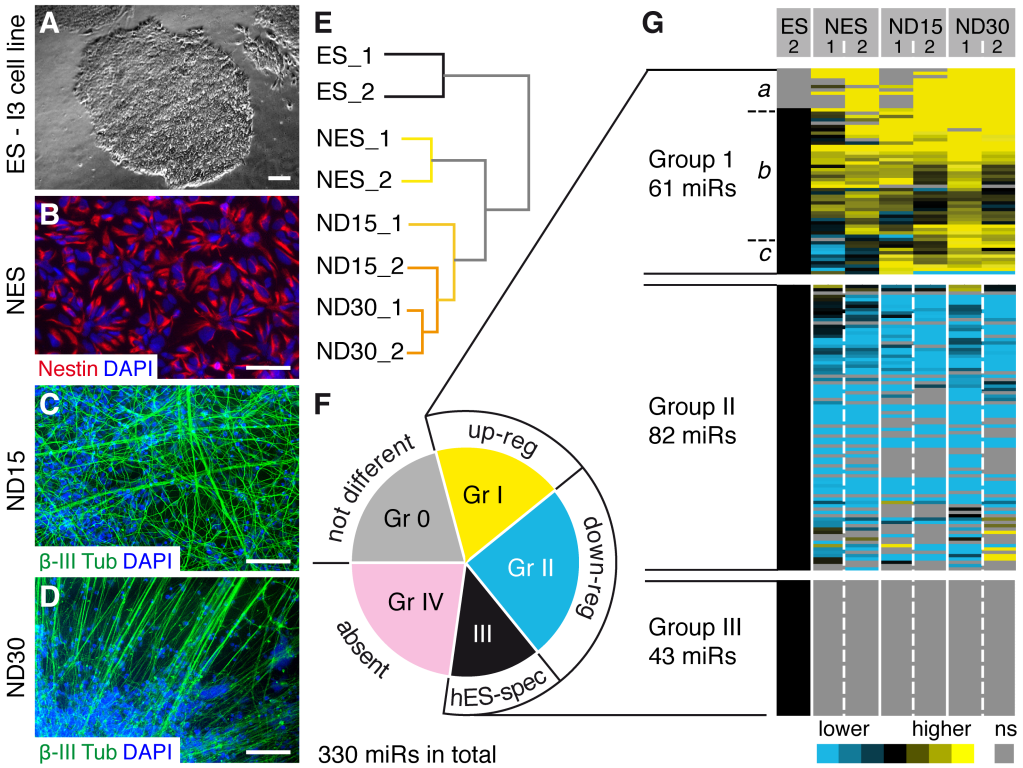

Fig. 3.1: Analysis of miRNA expression in human I3 ESCs, It-NES cells generated therefrom and their derived neuronal progeny. (A) Phase contrast image of a human ESC colony (I3 line). **(B)** Immunofluorescence staining for Nestin in self-renewing It-NES cells. **(C, D)** Immunofluorescence staining for β-III Tubulin in It-NES cell cultures differentiated for 15 days (ND15) and 30 days (ND30). All scale bars = 100 μm. **(E)** Unsupervised hierarchical clustering and correlation analysis of cell samples (hES, NES, ND15, ND30) based on their miRNA expression signatures. **(F)** Pie chart showing the distribution of the analyzed miRNAs to the different expression groups: Group 0, non-differentially expressed miRNAs; Group I-III, differentially expressed miRNAs; Group IV, miRNAs absent in all samples. **(G)** Heat-map showing a hierarchical clustering of the differentially expressed miRNAs. Relative miRNA expression levels in NES, ND15 and ND30 are displayed as log2 ratios compared to ESCs (base line, black; expression increases, yellow; expression decreases, blue; ns, no significant expression). Data were generated in collaboration with Dr. Sandra Weinhold.

The differentially expressed miRNAs were further subdivided into three major groups (Group I-III) according to whether they were up-regulated (Group I) or down-regulated (Group II) in It-NES cells and neuronal differentiated cultures compared to hESCs, or exclusively expressed in hESCs (Group III, Fig. 3.1 F, G). Among the 61 miRNAs found to be up-regulated in neural cells, 12 miRNAs, including miR-7, miR-153 and miR-181a*, were exclusively expressed in It-NES cells and derived neuronal cultures but not in hESCs (Group Ia, Fig. 3.1 G & Fig. 3.2 A). Another 12 miRNAs, including members of the let-7 family showed a decreased expression in It-NES cells compared to hESCs, but were increased again in differentiated neuronal cultures (Group Ic, Fig. 3.1 G & Fig. 3.2 A). In order to assess the reliability of the miRNA expression profiling, identified expression patterns of selected miRNAs were compared to published data on cell type-specific miRNA signatures. In line with the published data on hESC-associated miRNA signatures (Suh et al. 2004; Laurent et al. 2008; Bar et al. 2008), the I3 hESCs used here also showed high expression of miR-302/367, miR-371-373 and C19MC clusters. Members of these clusters were either classified into Group II or into

Group III (Fig. 3.2 C). MicroRNAs, which have been reported to be associated with non-neural lineages, were found to be decreased in neural cells compared to hESCs and were classified into Group II (Fig. 3.2 B). Examples include endodermal-associated miR-122 (Tzur et al. 2008), endothel-specific miR-126 (Wang et al. 2008) as well as muscle-associated miR-133a/b (Ivey et al. 2008). Moreover, miRNAs known to inhibit neural differentiation of hESCs, like miR-200 and miR-96 (Du et al. 2013) were also down-regulated (Fig. 3.2 B). Conversely, miRNAs known to promote neuronal differentiation, such as miR-124, miR-125b and miR-9, were up-regulated in lt-NES cells and derived neuronal cultures (Fig. 3.2 A).

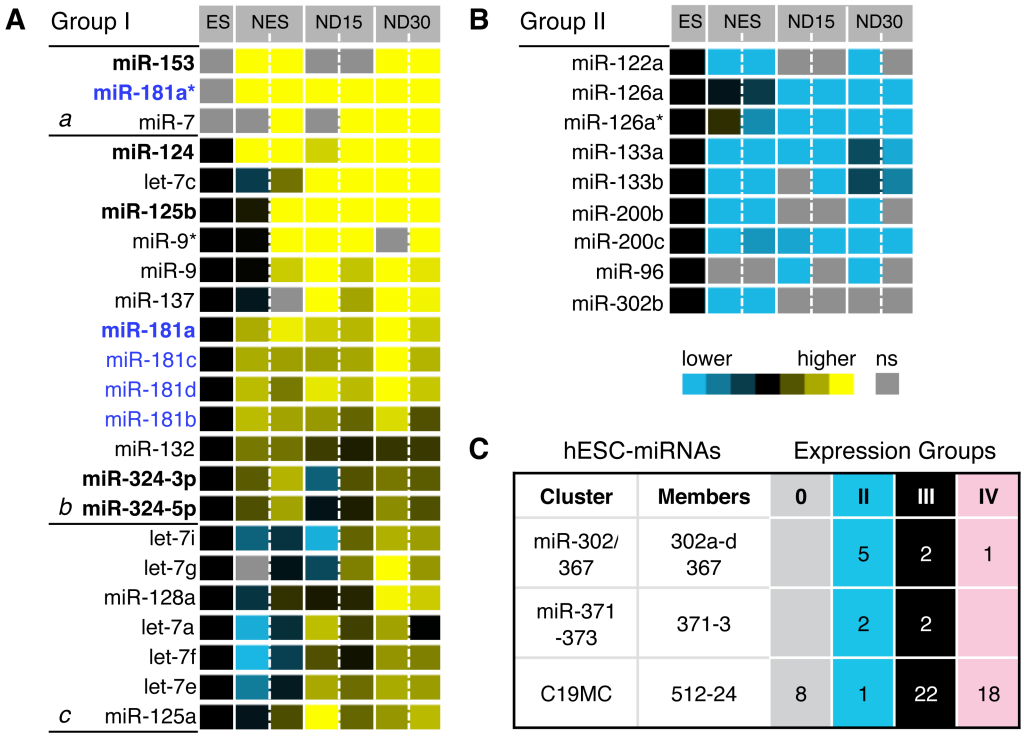

Fig. 3.2: Expression patterns of selected miRNAs. (A, B) Heat-map of miRNA profiling data from I3 hESC-derived samples for a representative selection of miRNAs within Group I **(A)** and Group II **(B)**. Relative expression levels in lt-NES cells and differentiating neuronal cultures (ND15, ND30) are displayed as log2 ratios compared to hESCs. The miRNAs, which were functionally studied in this work, are indicated in bold letters. Members of the miR-181a family are shown in blue letters. **(C)** Table summarizing the expression group affiliations of miRNAs previously annotated as hESC-enriched. Note that none of these miRNAs were assigned to Group I, which is therefore not displayed in the table.

In total, 61 miRNAs showed an increased expression in neural cells compared to hESCs. The expression patterns of some of these miRNAs were validated by SYBR Green-based quantitative real-time RT-PCR (referred to as singleplex qRT-PCR) and non-radioactive Northern blotting. These analyses were performed in an independent collection of cell samples derived from I3 or from H9.2 hESCs, used as an additional cell line. Both qRT-PCR and Northern blotting confirmed the up-regulation of mature miR-124, miR-125b and miR-9 during differentiation of lt-NES cells independent of the ancestral hESC line (Fig. 3.3 A-C). Despite the explicit differential expression of their

corresponding mature miRNAs, pre-miR-124, pre-miR-125b, pre-miR-9/9* were found to be expressed in all cell types analyzed (Fig. 3.3 C). A similar discrepancy in expression patterns of mature and precursor forms was observed for the hESC-associated miRNAs (Fig. 3.3 D). While mature miR-302b, miR-371a and miR-520c were exclusively expressed in the stem cell populations (ES, NES); their corresponding precursors were detected in both stem cells and neuronal differentiating cultures (ND15, ND30; Fig. 3.3 D). These findings indicate a cell type-specific processing of miRNA precursors similar to what has been described for let-7, which has a lower precursor processing rate in ESCs compared to neural cells (Wulczyn et al. 2007; Rybak et al. 2008).

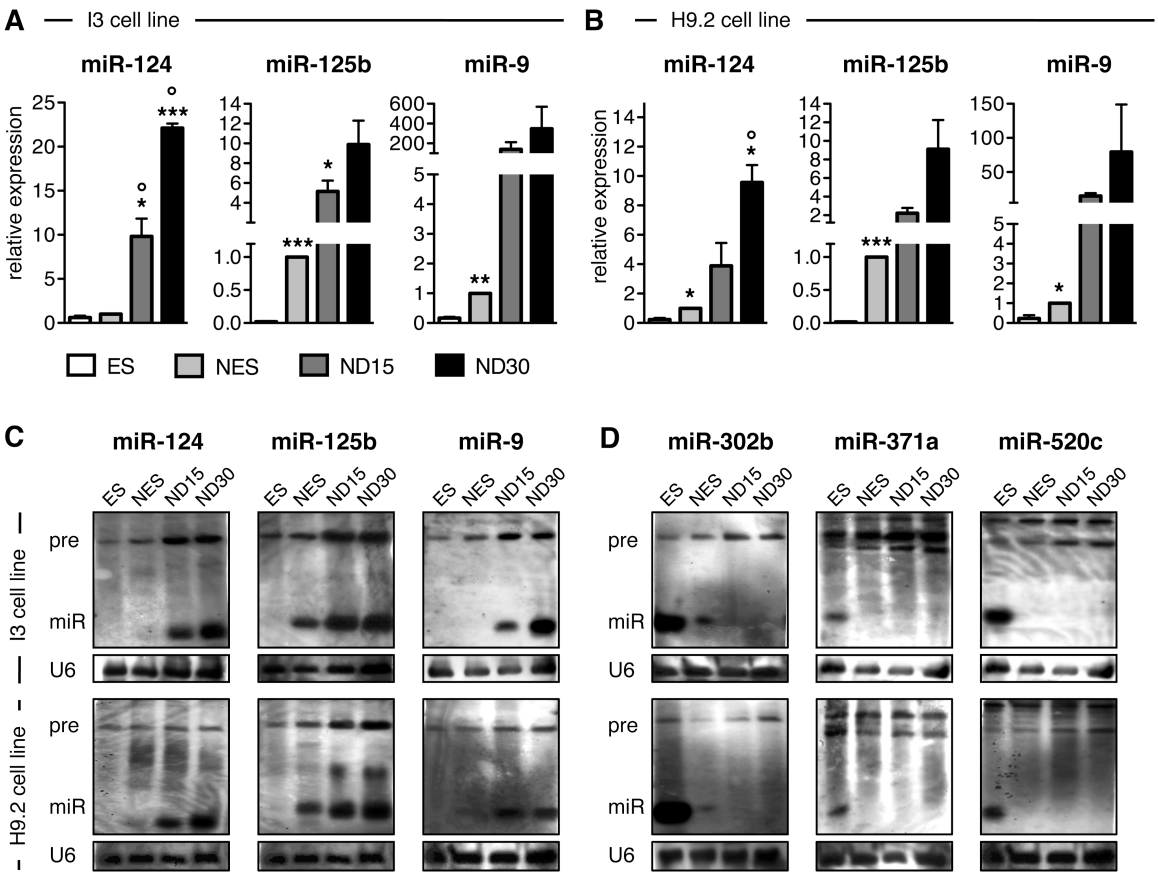

Fig. 3.3: Validation of selected expression patterns of miRNAs by qRT-PCR and Northern blotting. (A, B) Quantitative RT-PCR analysis of neuronal-associated miRNAs in hESCs, lt-NES cells and neuronal cultures (ND15, ND30) derived from I3 **(A)** and H9.2 **(B)** hESCs as measured by singleplex qRT-PCR. Data were normalized to RNU5A snRNA levels and are presented relative to the expression levels in lt-NES cells (equal to 1, n = 3). All data are presented as mean + SEM; *, compared to ES; °, compared to NES; */°, $p \leq 0.05$; **, $p \leq 0.01$; ***, $p \leq 0.0001$. **(C, D)** Northern blot analyses of precursor (pre) and mature (miR) miRNAs in samples from the I3 and H9.2 cell lines. Selected miRNAs known to be associated with neuronal cells **(C)** or pluripotent cells **(D)** are shown. U6 snRNA was used as loading control.

3.1.2 Detailed expression analysis of miR-181 family members and processing intermediates

According to the miRNA profiling, all major miR-181 members were found to be up-regulated in neural cells compared to hESCs (Fig. 3.4 A). Singleplex qRT-PCR further revealed that all members are increased during lt-NES cell differentiation and that miR-181a exhibits the highest expression level within the family (Fig. 3.4 A). Its sister miR-181a* showed the same expression pattern and singleplex qRT-PCR was sensitive enough to detect low miR-181a* expression in the hESCs samples (Fig. 3.4 B). According to multiplex qRT-PCR miR-181a* was not expressed in hESCs (see Fig. 3.2 A).

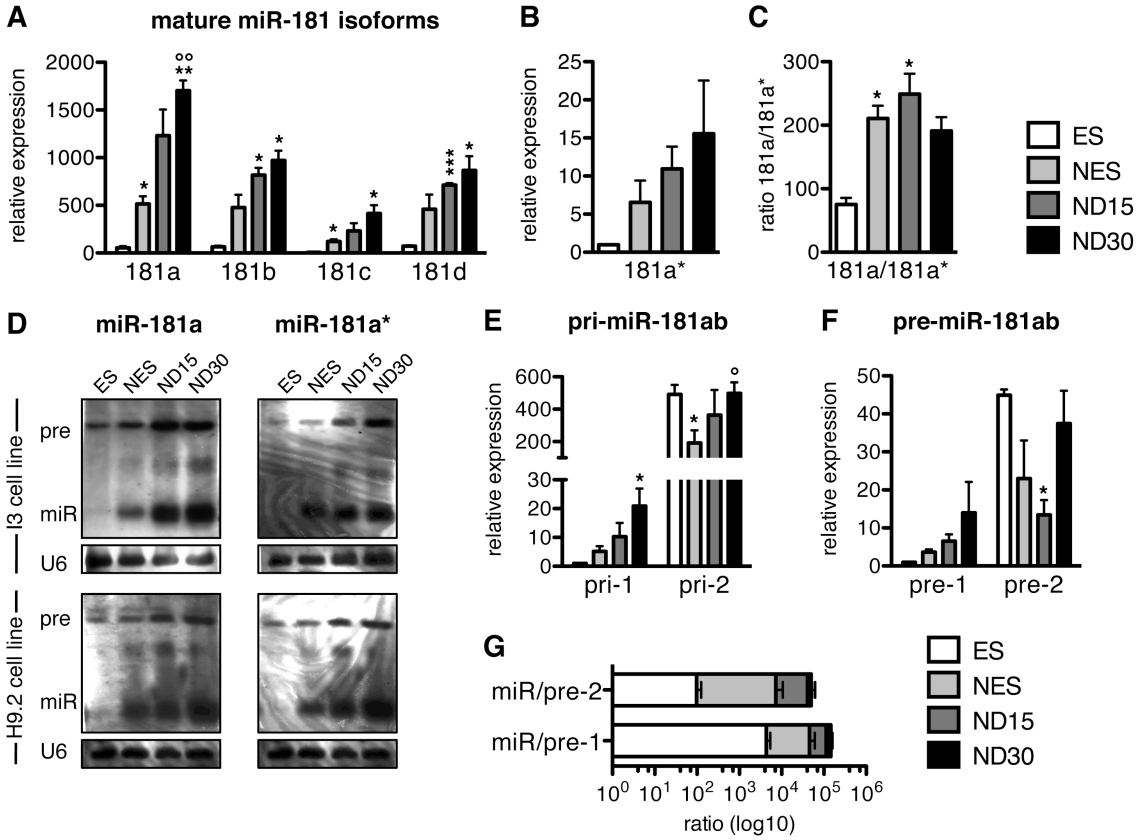

Fig. 3.4: Monitoring expression levels of miR-181 isoforms and miR-181a/a* processing intermediates in hESCs, lt-NES cells and differentiating neuronal cultures. (A, B) Quantitative RT-PCR analysis of miR-181a, -181b, -181c, -181d **(A)** and miR-181a* **(B)** expression levels in human ESCs (ES), lt-NES cells (NES) and differentiated neuronal cultures (ND15, ND30) derived from the I3 hESC line. Data are presented relative to miR-181a* expression in hESCs (equal to 1). **(C)** Ratio of miR-181a to miR-181a* expression levels. **(D)** Northern blot analyses for miRNA-181a and miR-181a* in cell samples derived from the I3 and H9.2 cell lines. U6 snRNA was used as loading control. Note that both miR-181a and miR-181a* Northern blot probes hybridize to pre-miR-181a-1 and pre-miR-181a-2. **(E, F)** Quantitative RT-PCR analysis of primary miRNA transcript (pri) and precursor (pre) levels. **(G)** Ratios of mature miR-181a to pre-1 and -pre-2 expression levels. All PCR data are presented as mean + SEM; n ≥ 3; *, compared to ES; °, compared to NES; */°, p ≤ 0.05; **/°°, p ≤ 0.01; ***, p ≤ 0.0001. Mature and pre-miRNA expression data were normalized to RNU5A snRNA levels; pri-miR expression data were normalized to 18s rRNA levels.

Although the expression of miR-181a* increased in a similar manner as miR-181a during neuronal differentiation, the ratio of the two sister miRNAs showed cell type-dependent variations. While in hESCs miR-181a was around 75 fold more expressed than miR-181a*, this ratio was increased up to 250 fold in ND15 neuronal cultures (Fig. 3.4 C). Northern blotting further demonstrated that, similar to the neuronal-associated miRNAs, pre-181a/a* was expressed in all cell types, while the corresponding mature miR-181a and miR-181a* were detected only in the neural cell types (NES, ND15, ND30; Fig. 3.4 D).

To further test the hypothesis of fate-dependent miRNA processing, the expression patterns of the primary transcripts and the miRNA precursors derived from the two miR-181a/a* loci in the human genome (MIR181A1, MIR181A2) were assessed by qRT-PCR using RNA from I3 ESC, NES, ND15 and ND30 samples (Fig. 3.4 E-G). Expression of pri-181ab-1 as well as expression of pre-181a-1 gradually increased during neuronal differentiation of hESCs (Fig. 3.4 E, F). In contrast to this, pri-181ab-2 was expressed at high levels in hESCs, down-regulated in lt-NES cells and up-regulated again during neuronal differentiation. Except for its low expression level in ND15 cultures, the expression of pre-181a-2 in general followed the pri-181ab-2 profile (Fig. 3.4 E, F). Interestingly, in hESCs pri-181ab-2 was about 500 fold more expressed than pri-181ab-1. This might be due to either a higher transcription activity of the MIR181A2 locus or a higher processing rate of MIR181A1 transcript.

Since the precursors expression levels were detected with a different qRT-PCR method than the expression of primary miRNA transcripts, no conclusions regarding the processing activities of pri-miR-181ab-1 and pri-181ab-2 can be made. Expression levels of precursors and mature miRNAs were instead measured using the same qRT-PCR protocol; therefore the ratios of mature to precursors forms could be calculated (Fig. 3.4 G; see Methods section 2.5.3 for further details). MicroRNA precursors are believed to be rapidly processed by Dicer. In line with this, the overall abundance of pre-181a-1 and pre-181a-2 was very low compared to mature miR-181a expression levels. However, the mature to precursor ratios were lower by one order of magnitude for pre-181a-1 (from 4300 to 67000 fold) and two orders of magnitude (from 100 to 33800 fold) for pre-181a-2 in hESCs compared to the neural cell types (Fig. 3.4 G). These findings confirm the different expression behavior of mature and precursor forms previously observed by the Northern blot analysis and further point to a cell type-specific processing of miRNA precursors.

3.2 The role of distinct miRNAs on human neuronal differentiation and subtype specification

The miRNA profiling analysis revealed a number of distinct miRNAs that could be linked to defined stages of early human neuronal differentiation. During the differentiation process, the transition of self-renewing lt-NES cells towards neuronal differentiation and the subspecification into distinct neuronal subtypes was of particular interest for this thesis. In order to understand how manipulating miRNA expression affects these fate choices, gain- and loss-of-function experiments for a shortlist of miRNAs were performed. More specifically, miR-153, miR-181a/a* and miR-324-5p/3p were selected as potential neuronal-associated miRNAs based on their expression pattern during lt-NES cell differentiation. These miRNAs (in the following referred to as “candidate neuronal miRNAs”) as well the known neuronal-associated miR-124 and miR-125b were analyzed with respect to lt-NES cell maintenance, neuronal differentiation and subtype specification using both stable genetic and transient modification approaches.

3.2.1 Selection of miR-181a, miR-153 and miR-324 as candidates for functional studies

Among the 61 miRNAs that were classified into Group I (i.e. showing an up-regulation during neuronal differentiation), many miRNAs are known to be expressed in neural tissues. However, the specific roles of most of these miRNAs in human neuronal differentiation are still unknown. In particular, the miR-181 family might have a critical function in neuronal differentiation considering the abundant expression of all family members in lt-NES cells and neuronal cultures (Fig. 3.4). MicroRNA-181a was studied in more detail, since this miRNA showed the highest expression in neural cells among the miR-181 family members (Fig. 3.4 A). The known functions of the miR-181 family have been outlined in the Introduction section 1.3. In addition, two other miRNAs, i.e. miR-153 and miR-324-5p/3p, for which evidence from other studies point to roles in the nervous system, were also selected as candidates for functional analyses. MicroRNA-153 is enriched in the brain (Sempere et al. 2004) and is preferentially expressed in neurons (Doxakis 2010). Similar to miR-181, miR-153 induces apoptosis in brain tumors by targeting several anti-apoptotic factors (Xu et al. 2010; Xu et al. 2011a) and decreases the proliferation rate of glioblastoma cells (Xu et al. 2010). Furthermore, miR-153 targets alpha-synuclein (SNCA; Doxakis 2010) and amyloid precursor protein (APP; Liang et al. 2012; Long et al. 2012), which are especially relevant for the pathogenesis of Parkinson’s and Alzheimer’s disease, respectively. MicroRNA-324-5p has been studied in the context of murine cerebellar granule cells and was shown to contribute to neuronal differentiation and growth arrest by suppressing Sonic Hedgehog (SHH) signaling (Ferretti et al. 2008). However, none of these miRNAs have been investigated in the context of human neuronal differentiation.

The expression levels of miR-153 and the sister strands miR-324-5p and miR-324-3p were first validated by singleplex qRT-PCR analysis (Fig. 3.5 A). MicroRNA-153 was up-regulated in neural cells compared to hESCs and was further induced upon differentiation. MicroRNA-324-5p was expressed at similar levels in hESCs and lt-NES cells and was only up-regulated in differentiating neuronal cultures. MicroRNA-324-3p exhibited a distinct expression pattern compared to its sister

strand, which also differed between the two cell lines analyzed. In I3 hESCs, expression of miR-324-3p was relatively high and comparable to the expression in lt-NES and ND15 cultures, whereas in the H9.2 cell line miR-324-3p showed a modest but continuous up-regulation from hESCs to ND30 cultures (Fig. 3.5 A).

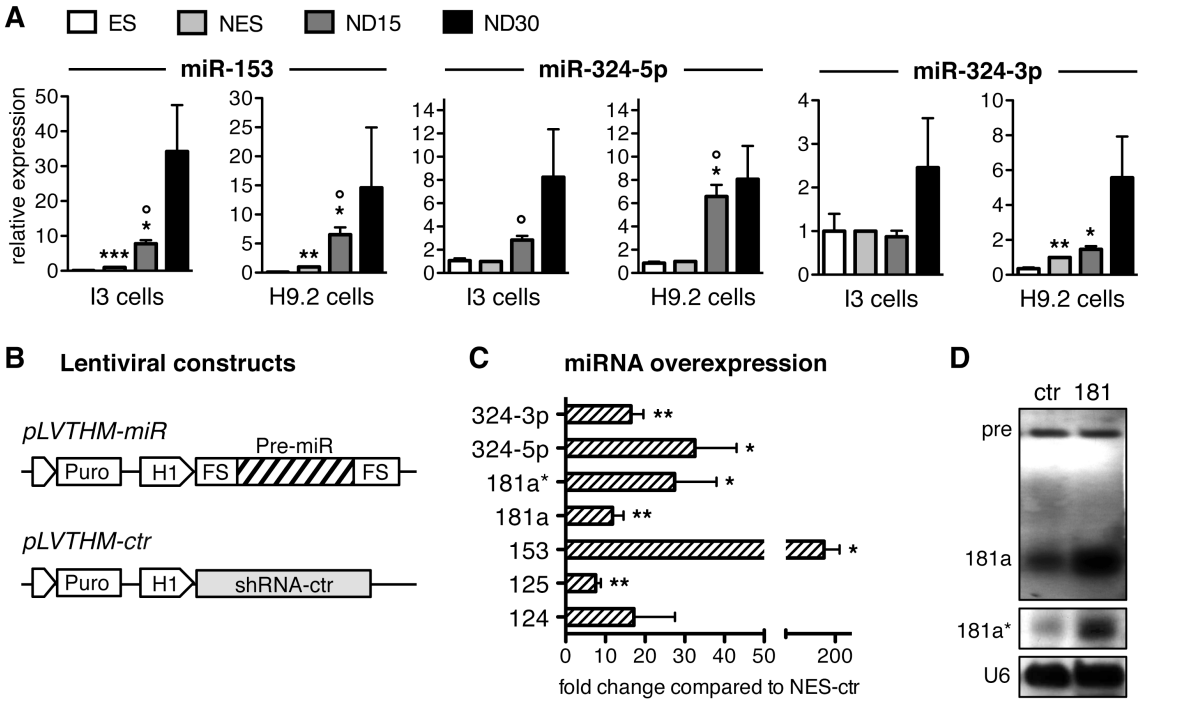

Fig. 3.5: Constitutive overexpression of potentially neuronal-associated miRNAs in lt-NES cells. **(A)** Quantitative RT-PCR analysis of mature miRNA expression levels in hESCs, lt-NES cells (NES) and differentiated neuronal cultures (ND15, ND30) from the I3 and H9.2 cell lines. Data were normalized to RNU5A snRNA levels and are presented as mean + SEM relative to expression in lt-NES cells (equal to 1, n = 3; *, compared to ES; °, compared to NES; */°, $p \leq 0.05$; **, $p \leq 0.01$; ***, $p \leq 0.0001$.) **(B)** Scheme of the pLVTHM vectors containing a puromycin resistance gene (Puro) and a specific pre-miRNA locus plus flanking sequences (FS) or a scrambled shRNA-ctr construct. **(C)** Quantitative RT-PCR analysis showing relative expression levels of miRNAs in lt-NES cells transduced with the different pLVTHM-miR constructs compared to cells transduced with pLVTHM-ctr (NES-ctr). Data were normalized to miR-16 levels and are presented as mean + SEM ($n \geq 4$;*, $p \leq 0.05$; **, $p \leq 0.01$; one-tailed Student's t-test). **(D)** Northern blot detection of pre-miR-181a/a* and mature miR-181a/a* expression in lt-NES cells transduced with pLVTHM-miR-181 or pLVTHM-ctr.

In order to assess the functions of the candidate neuronal miRNAs (miR-153, miR-181a/a* and miR-324-5p/3) in comparison with miR-124 and miR-125b, lt-NES cells were transduced with the pLVTHM lentiviral particles encoding the respective miRNA-overexpression constructs. The miRNA-overexpression constructs were obtained by cloning the respective precursor sequence of each selected miRNA plus flanking regions under the H1 Polymerase-III promoter in the pLVTHM lentiviral backbone obtained from Wiznerowicz & Trono (2003). The pLVTHM vector was further modified to carry a puromycin (Puro) resistance gene to enrich for transduced cells by antibiotic selection (pLVTHM-miR, Fig. 3.5 B). As control, lt-NES cells were transduced with a pLVTHM vector expressing a scrambled non-targeting short-hairpin (sh)RNA (pLVTHM-ctr). Quantitative RT-PCR analyses of

lt-NES cells transduced with each different miRNA overexpression construct showed a stable increase in the expression of each specific miRNA compared to its own endogenous levels (Fig. 3.5 C). In order to assess whether the transgenic miRNA transcripts are processed in a similar manner as the endogenous miRNA, the expression levels of pre- and mature miR-181a/a* were monitored by Northern blot. This analysis showed that the pre-miRNA processing in lt-NES cells did not to seem to be affected by pLVTHM-miR-181a/a* transduction (Fig. 3.5 D).

3.2.2 Overexpression of known and candidate neuronal miRNAs shifts lt-NES cells from self-renewal to neuronal differentiation

First, the effect of ectopic miRNA expression on the rate of cell proliferation and spontaneous differentiation of lt-NES cells cultured in the presence of growth factors was monitored (Fig. 3.6).

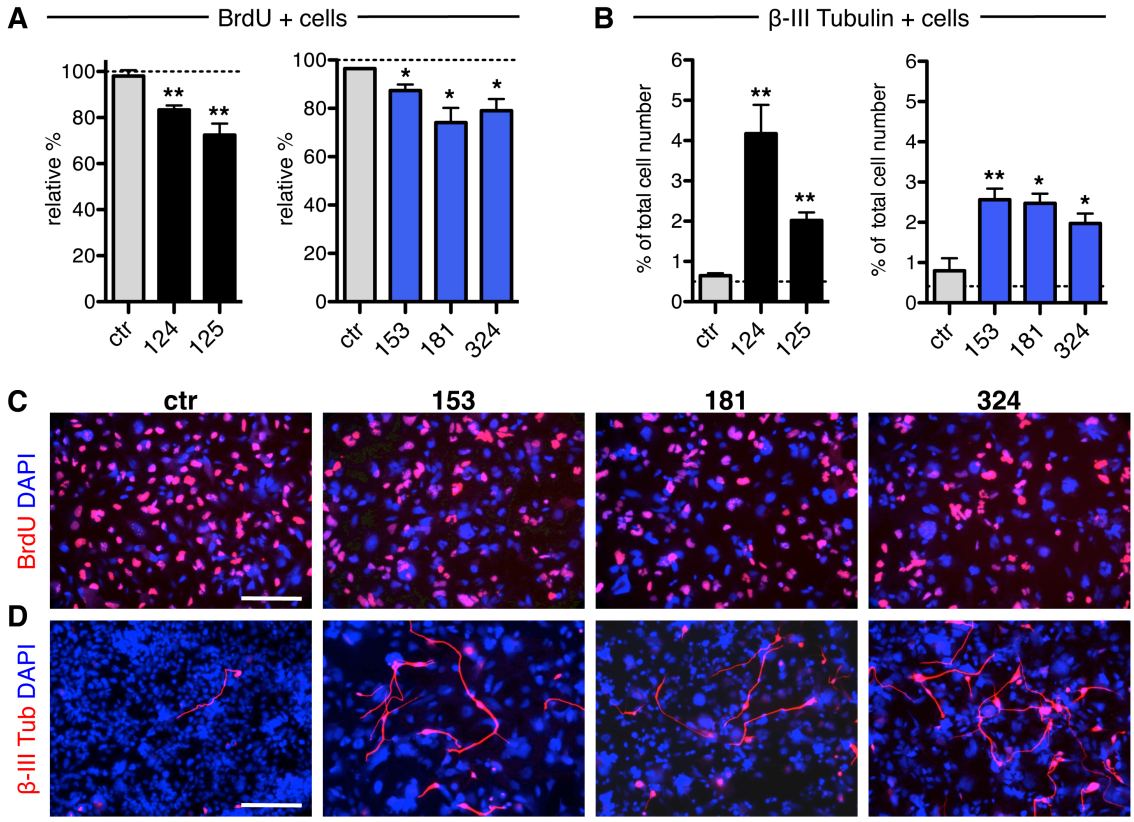

Fig. 3.6: Overexpression of miR-124, miR-125b, miR-153, miR-181a/a* or miR-324-5p/3p inhibits proliferation and promotes neuronal differentiation of lt-NES cells. Lt-NES cells were transduced with either pLVTHM-ctr (ctr) or the respective pLVTHM-miRNA overexpression constructs and cultured under self-renewing conditions in the presence of EGF and FGF2. As an additional control, untransduced lt-NES cells were used (dashed line). **(A)** Quantification of the relative percentage of BrdU-positive in transduced lt-NES cells compared to untransduced cells (dashed line, BrdU-incorporation set to 100%), 2 days after plating. **(B)** Quantification of the percentage of β-III Tubulin-positive cells, 4 days after plating. All data are presented as mean + SEM; $n \geq 3$; *, $p \leq 0.05$; **, $p \leq 0.01$. The percentage of β-III Tubulin-positive cells in untransduced controls is indicated by dashed lines. **(C, D)** Representative immunofluorescence stainings for BrdU **(C)** and β-III Tubulin **(D)** in the conditions described above. Scale bars = 100 μm.

Overexpression of miR-124 or miR-125b (black bars) significantly reduced the rate of BrdU incorporation compared to control cells by 14.7 ± 1.9% and 25.7 ± 4.9%, respectively (Fig. 3.6 A). Similarly, ectopic expression of miR-153, miR-181a/a* or miR-324-5p/3p (blue bars) induced a significant reduction in the rate of BrdU incorporation as well (Fig. 3.6 A, C). Under self-renewing culture conditions only a small proportion of lt-NES cells (0.8 ± 0.3%) differentiated spontaneously into β-III Tubulin-positive neurons (ctr, Fig. 3.6 B, D). The rate of spontaneous neuronal differentiation was, however, increased upon overexpression of the investigated miRNAs. Specifically, overexpression of miR-124 had a strong impact and increased the β-III Tubulin-positive cells up to 4.2 ± 0.7%, while overexpression of the other miRNAs (miR-125b, miR-153, miR-181a/a* and miR-324-5p/3p) induced a significant increase of β-III Tubulin-positive cells of about 2-3% (Fig. 3.6 B).

These data indicate that the miRNAs under study impair lt-NES cell self-renewal and enhance the rate of spontaneous neuronal differentiation in the presence of growth factors. Next, it was assessed whether the miRNAs could further enhance the production of neurons from lt-NES cells, when these are actively directed towards differentiation. To that end, lt-NES cells were cultured in differentiation medium devoid of the growth factors EGF and FGF2. After 7 days under these conditions, control cultures contained around 4% of β-III Tubulin-positive cells (Fig. 3.7 A, C). Ectopic expression of miR-124 or miR-125b strongly increased the proportion of differentiating neuronal cells to 9.6 ± 1.9% and 12.9 ± 1.7%, respectively (Fig. 3.7 A). Likewise, cultures overexpressing miR-153 or miR-181a/a* contained also more neurons (Fig. 3.7 A, C). Noteworthy, ectopic expression of miR-181a/a* appeared to be equally potent as miR-124 and miR-125b and raised the percentage of β-III Tubulin-positive cells to 11.6 ± 1.8% (Fig. 3.7 A). Although overexpression of miR-324-5p/3p enhanced neuronal differentiation of lt-NES cells cultured in the presence of growth factors (Fig. 3.6 B), this effect was lost upon induction of differentiation by growth factor withdrawal (Fig. 3.7 A). Nevertheless, the average neurite length was significantly higher in miR-324-5p/3p-overexpressing cultures than in control cultures (Fig. 3.7 B, D). In general, neurons derived from lt-NES cell cultures overexpressing the investigated miRNAs had significantly longer neurites than the neurons in control cultures (Fig. 3.7 B, D). However, it remains to be clarified whether this phenomenon is caused by a direct impact on neurite development or whether it merely reflects the earlier onset of neuronal differentiation induced by these miRNAs.

In summary, these results confirm that, in agreement with previous studies (see Introduction 1.3) miR-124 promotes neuronal differentiation of human NSCs. The data further prove that miR-125b as well as miR-153, miR-181a/a* and miR-324-5p/3p have a positive effect on neuronal differentiation and contribute to the switch from lt-NES cell self-renewal towards differentiation.

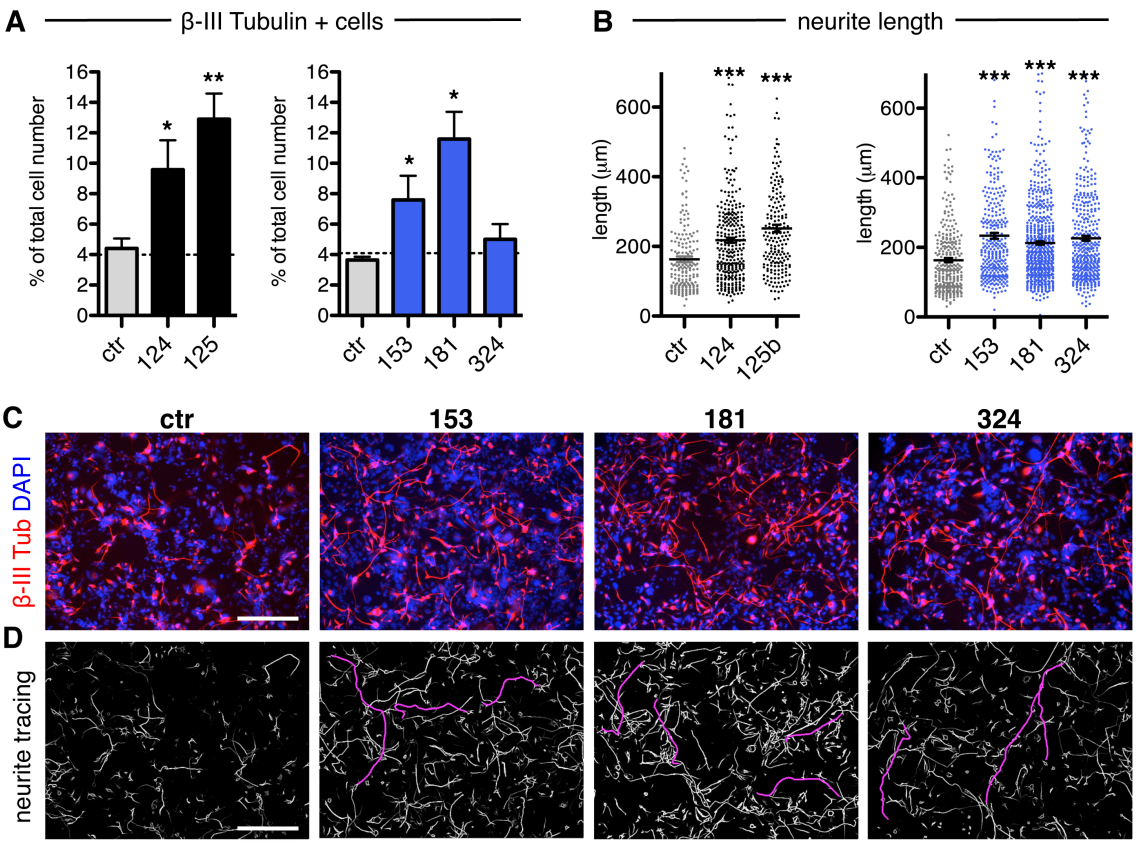

Fig. 3.7: Combination of ectopic expression of distinct miRNAs and growth factor withdrawal further promotes neuronal differentiation of lt-NES cells. (A) Quantification of the percentage of β-III Tubulin-positive cells in lt-NES cells cultures transduced with either pLVTHM-ctr (ctr) or the respective pLVTHM-miRNA overexpression constructs after 7 days of induced neuronal differentiation by growth factor withdrawal. As an additional control, untransduced lt-NES cells were used (dashed line). **(B)** Scatter plots displaying the length of single neurites (in μm) for each of the conditions described above. Data from three independent replicates are shown. Black lines indicate average neurite length. **(C)** Immunofluorescence staining for β-III Tubulin in the conditions described above. **(D)** Representative images of neurite tracings, pink-label indicates neurites of more than 350 μm length. Scale bars = 200 μm. All data are presented as mean + SEM; $n \geq 3$; *, $p \leq 0.05$; **, $p \leq 0.01$; ***, $p \leq 0.0001$.

3.2.3 Transfection with miRNA oligonucleotides modulates neuronal differentiation of lt-NES cells

During the last years, several approaches to modulate miRNA activity by oligonucleotide transfection without the need for genetic manipulations have been developed (reviewed by Zhang et al. 2012a). Here, commercially available miRNA mimics and antisense RNA oligonucleotides, which function as miRNA inhibitors, have been used. The strong impact of miR-181a/a* overexpression on lt-NES cell differentiation raised the question as to whether or not both sister miRNAs influence lt-NES cell differentiation to a similar extent. To assess the individual effects of miR-181a and miR-181a*, their activities were individually modulated using the respective miRNA mimics and inhibitors. These experiments were extended to miR-124, as well as to miR-125b, in order to determine whether these miRNAs are necessary for neuronal differentiation of lt-NES cells. The efficacy of miRNA mimic and inhibitor transfection was validated by qRT-PCR analysis. As expected, transfection of miRNA mimics

resulted in an increased level of the respective mature miRNA in the cells (Fig. 3.8 A). Conversely, the antisense RNA oligonucleotides used here as miRNA inhibitors match perfectly with the targeted miRNA and can reduce its endogenous level in a target-dependent manner (Krützfeldt et al. 2005) as confirmed by qRT-PCR (Fig. 3.8 B).

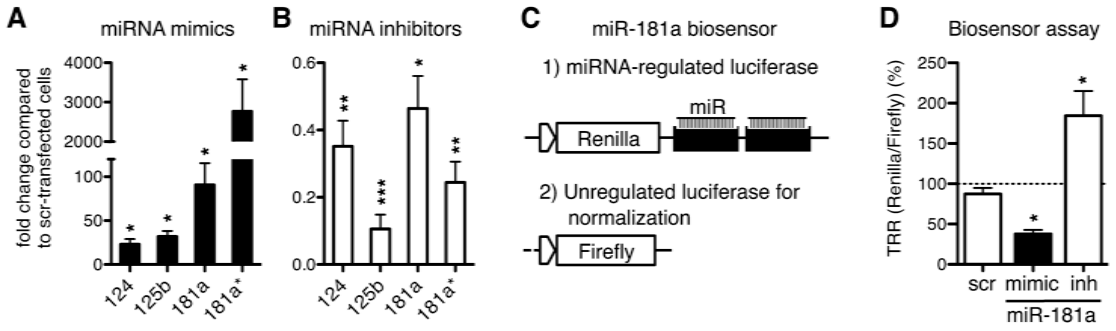

Fig. 3.8: Validation of conditions for miRNA mimic/inhibitor transfections in lt-NES cells. (A, B) Quantitative RT-PCR analyses showing the fold changes in miRNA expression levels in lt-NES cells (I3 cell line) upon transfection with the respective miRNA mimics (**A**) or inhibitors (**B**) compared to cells transfected with a scrambled (scr) control oligonucleotide (set to 1). Data were normalized to RNU5A snRNA levels. **(C)** Scheme of the dual luciferase miR-181a biosensor (psiCHECK-181BS) plasmid including two tandem oligonucleotides with perfect complementarity (compl) to miR-181a. **(D)** Transfection dependent Renilla/Firefly ratios (TRR) in lt-NES cells transfected with the miR-181a biosensor and subsequently transfected with either mock (dashed line), miR-181a mimic, miR-181a inhibitor or a scrambled oligonucleotide (scr). Data are compared to mock-transfected lt-NES cells (set to 100%). All data are presented as mean + SEM; $n \geq 3$; *, $p \leq 0.05$; **, $p \leq 0.01$; ***, $p \leq 0.0001$.

As a more direct approach to measure miRNA activities, a luciferase-based (psiCHECK2) miR-181a biosensor, containing two full-length miR-181a binding sites downstream of a Renilla luciferase gene, was used (Fig. 3.8 C). The vector also encodes for a Firefly luciferase, which is used to normalize for transfection variability. Lt-NES cells were co-transfected with the miR-181a biosensor together with either a miR-181a mimic or an inhibitor followed by a luciferase assay 24 hours post-transfection. Lt-NES cells treated with the miR-181a mimic exhibited a relative reduction of Renilla-miRNA biosensor activity, indicative of an increased miR-181a activity. Lt-NES cells transfected with the miR-181a inhibitor (inh), instead, showed an increased Renilla luciferase activity, indicative of a decreased miR-181a activity (Fig. 3.8 D).

To determine the impact of transfection-based miRNA modulation on lt-NES cell differentiation, I3 hESC-derived lt-NES cells were repeatedly transfected during the time course of neuronal differentiation in order to ensure continuous miRNA modulation (Fig. 3.9 A). Control cells were either transfected with mock or with scrambled control (scr) oligonucleotides (for details see Methods section 2.3.1). The cultures were then analyzed after 7 (ND7) and 15 (ND15) days of differentiation by immunofluorescence staining against β-III Tubulin (Fig. 3.9 B, C). Similar to the genetic gain-of-function experiments, transfection of cells with either a miR-124 or a miR-125b mimic significantly enhanced neuronal differentiation (Fig. 3.9 B, C). Likewise, transfection with the miR-181a mimic significantly increased the number of neurons by 2.3 ± 0.3 fold after 7 days and 1.6 ± 0.2 fold after 15 days of differentiation. In contrast to this, transfection with the miR-181a* mimic only had a

minor effect on the neuron yield (Fig. 3.9 B, C). Nevertheless, inhibition of miR-181a* or miR-181a significantly reduced the number of β-III Tubulin-positive cells by around 0.5 fold as monitored after 15 days of neuronal differentiation (Fig. 3.9 C). Inhibition of miR-124 and miR-125b significantly impaired neuronal differentiation of lt-NES cells already after 7 days of culture (Fig. 3.9 B, C).

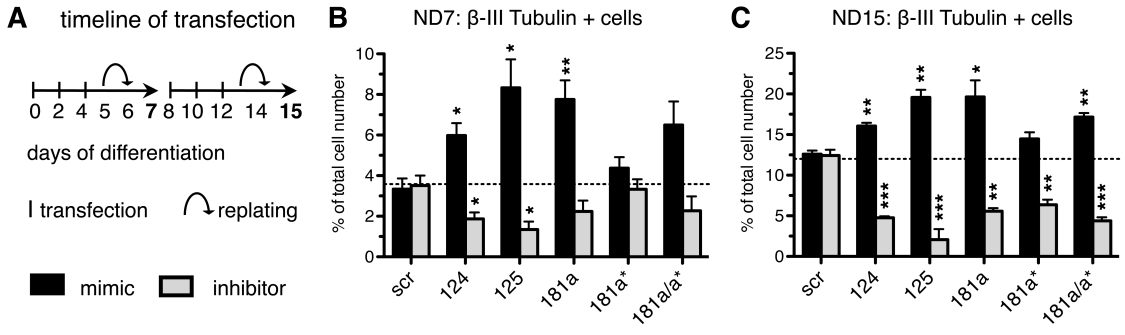

Fig. 3.9: Transfection-based miRNA modulation affects the rate of neuronal differentiation of I3 lt-NES cells. (A) Scheme of the miRNA mimic and inhibitor transfection timeline: Lt-NES cells were cultured under differentiating conditions and transfected 3 or 6 times in 48 hours intervals before replating them for final analysis at day 7 (ND7) and day 15 (ND15), respectively. **(B, C)** Histograms showing the percentages of β-III Tubulin-positive cells in lt-NES cells at ND7 (**B**) or ND15 **(C)**. All data are presented as mean + SEM; n = 3; *, $p \leq 0.05$; **, $p \leq 0.01$; ***, $p \leq 0.0001$.

To exclude that the observed effects are only specific to I3 hES cell-derived lt-NES cells, the miRNA modulation experiments were repeated in H9.2 lt-NES cells. In this case, a different read-out system for neuronal differentiation was used taking advantage of the H9.2 DCX::EGFP lt-NES cell line established in our lab and described in Ladewig et al. (2008). These cells carry an EGFP gene under the control of the human doublecortin (DCX) promoter. Doublecortin is an early neuronal marker, which is already induced after two days of *in vitro* differentiation of lt-NES cells (Ladewig et al. 2008). As shown in Fig. 3.10, lt-NES cell cultures differentiated for 5 days (ND5) show some degree of weak background EGFP expression and contain about 5% of high EGFP-expressing cells, which are also positive for β-III Tubulin (Fig. 3.10 A). The amount of high EGFP-expressing cells was increased upon treatment with the Notch inhibitor DAPT (Fig. 3.10 B), which was previously shown to induce neuronal differentiation of lt-NES cells (Borghese et al. 2010).

Next, H9.2 DCX::EGFP lt-NES cell were transfected with the different miRNA mimics and inhibitors and differentiated for 5 days. In line with the previous results, transfection of mimics for miR-124, miR-125b and miR-181a promoted neuronal differentiation, as indicated by an increase of the high EGFP-expressing cells (Fig. 3.10 C). In particular, transfection with the miR-181a mimic doubled the amount of EGFP-high cells to 8.8% compared to 4.9% in cultures transfected with a scrambled oligonucleotide (Fig. 3.10 D). In contrast, inhibition of miR-124, miR-125b or miR-181a impaired neuronal differentiation (Fig. 3.10 C, D). However, the observed effects were smaller compared to the results generated using I3 lt-NES cells. On the one hand, this could be due to the fact that H9.2 lt-NES cells were only transfected twice with miRNA mimics and inhibitors. On the other hand, H9.2 lt-NES cells are known to exhibit higher differentiation rates than I3 lt-NES cells (data not shown) and the impact of miRNA modulation might be less evident.

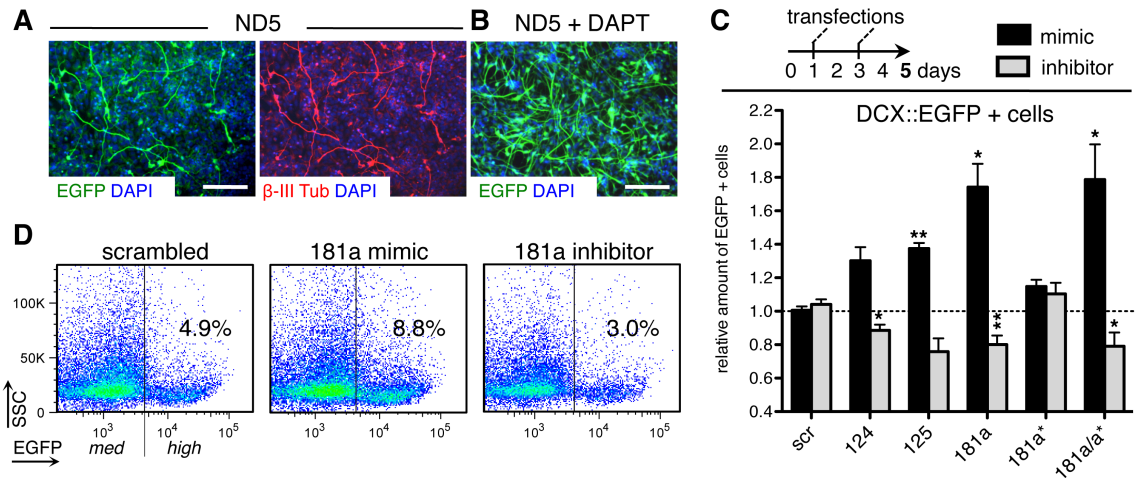

Fig. 3.10: H9.2 DCX::EGFP lt-NES cells as a reporter system to asses the efficacy of miRNA modulation on neuronal differentiation. (A) Co-expression of DCX-promoter driven EGFP and β-III Tubulin in lt-NES cells differentiated for 5 days (ND5). **(B)** DCX::EGFP expression in lt-NES cells differentiated for 5 days in the presence of DAPT. Scale bars = 100 μm. **(C)** DCX::EGFP lt-NE cells were differentiated for 5 days and transfected at day 1 and day 3 with miRNA mimics and inhibitors. Histograms showing the percentages of DCX::EGFP-positive cells as measured by flow cytometry. All data are presented as mean + SEM; n ≥ 3; *, p ≤ 0.05; **, p ≤ 0.01. **(D)** Side scatter (SSC) versus EGFP dot plot analysis of lt-NES cells transfected with scrambled control oligonucleotides, miR-181a mimic or miR-181a inhibitor (med = medium EGFP expression).

In summary, these results demonstrate that transfection-based modulation of miRNA activities suffices to affect lt-NES cell behavior. The loss-of-function experiments further indicate that the neuronal differentiation rate seems to depend on the level of miR-124, miR-125b and miR-181a/a* activity. Furthermore, the data show that DCX::EGFP lt-NES cells could be used as a tool to screen for miRNAs promoting neuronal differentiation.

3.2.4 MicroRNA-181a, miR-125b and miR-124 affect neuronal subspecification of lt-NES cells

Under standard culture conditions, lt-NES cells exhibit an anterior-ventral hindbrain identity and mainly differentiate into GABAergic neurons. They are, however, able to respond to patterning cues and can also give rise to other neuronal subtypes (Koch et al. 2009b; Falk et al. 2012). In order to assess whether the miRNAs under study also affect neuronal subspecification during lt-NES cell differentiation, the differentiation of miRNA-overexpressing lt-NES cell cultures was extended to 15 days. Afterwards, the cultures were stained for β-III Tubulin, the GABAergic marker glutamate decarboxylase (GAD) and for tyrosine hydroxylase (TH), which is the rate-limiting enzyme of dopamine synthesis and is expressed in dopaminergic as well as in noradrenergic neurons. Overexpression of miR-124, miR-125b, miR-153 and miR-181a/a* but not of miR-324-5p/3p resulted in a higher amount of β-III Tubulin-positive neurons compared to control cells (Fig. 3.11 B). However, compared to the short-term neuronal differentiation (ND7, see Fig. 3.7), the effect of miRNA overexpression was attenuated during prolonged differentiation. The basal amount of TH-positive cells generated after standard neuronal differentiation was very low and did not exceed 4% of all neurons (Fig. 3.11 A, C). Surprisingly, the proportion of TH-positive neurons was dramatically changed upon miRNA overexpression (Fig. 3.11 A, C). In detail, miR-125b and miR-181a/a*-overexpressing cultures

contained 9.2 ± 1,4% and 16.2 ± 2.2% of TH-positive neurons, respectively (Fig. 3.11 C). The amount of GAD-positive neurons as well as GAD1 expression levels was instead not affected by these miRNAs (Fig. 3.11 D, E). On the contrary, the relative numbers of both neuronal subtypes (TH- and GAD1-postive neurons) were reduced upon miR-124 overexpression (Fig. 3.11 C, D). In agreement with the immunostainings, TH transcript levels were up-regulated upon miR-181a/a* or miR-125b overexpression, whereas in miR-124-overexpressing cultures expression of TH was significantly decreased (Fig. 3.11 E). MicroRNA-153 and miR-324-5p/3p showed no clear influence on either TH-positive or GAD-positive neuronal subtypes (Fig. 3.11 C, D).

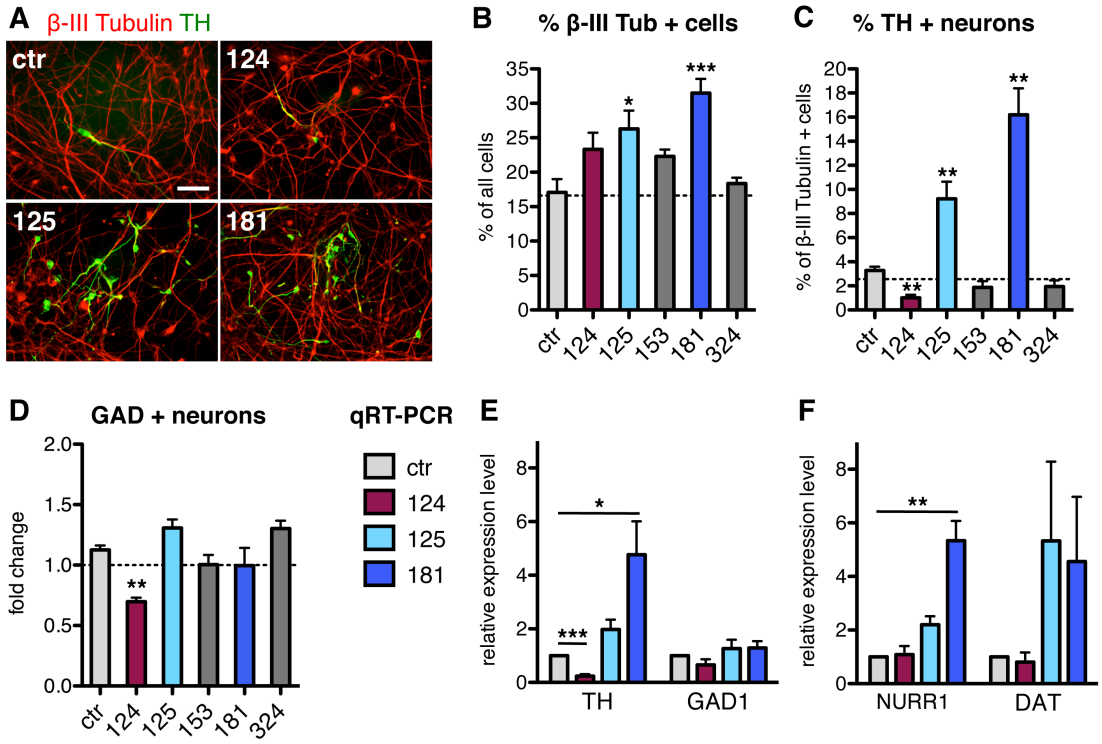

Fig. 3.11: MicroRNA-124, miR-125b and miR-181a/a* affect neuronal subtype specification during lt-NES cell differentiation. l3 lt-NES cells were transduced with pLVTHM-ctr or pLVTHM-miR-124, -miR-125b and -miR-181a/a*, respectively, and differentiated for 15 days. As an additional control, untransduced lt-NES cells were used (dashed lines). **(A)** Representative immunofluorescence stainings for β-III Tubulin plus TH in the respective cultures. Scale bar = 100 μm. **(B, C)** Percentages of β-III Tubulin-positive cells (**B**, compared to all cells) and TH-positive neurons (**C**, compared to all β-III Tubulin-positive cells). Data are presented as mean + SEM, n = 3. **(D)** Fold change in the number of GAD-positive neurons relative to the total number of neurons. Data are presented as mean + SEM compared to untransduced cells (set to 1, dashed line; n = 3). **(E, F)** Quantitative RT-PCR analysis of TH, GAD1 **(E)** and NURR1, DAT **(F)** expression in the respective cultures. Data were normalized to 18s rRNA levels and are presented as mean + SEM, relative to expression in pLVTHM-ctr expressing lt-NES cells (set to 1; n ≥ 3). *, $p \leq 0.05$; **, $p \leq 0.01$; ***, $p \leq 0.0001$.

Bona fide midbrain dopaminergic (mDA) neurons are characterized by a distinct molecular code that comprises the expression of proteins essential for dopamine synthesis and dopamine recycling (TH, AADC, DAT), region-specific markers (GIRK2, ALDH2, Corin) and fate-associated transcription factors (EN1/2, LMX1A/B, NURR1, PITX3 and FOXA2; see Smidt et al. 2007; Ono et al. 2007). The amount of TH-positive neurons generated by lt-NES cells can be increased by SHH and FGF8

treatment and, as indicated here, also by specific miRNAs. However, these TH-positive neurons fail to express the full range of DA fate markers and only express some of them like NURR1 and DAT on transcript level. Nevertheless, NURR1 and DAT expression was up-regulated upon miR-125b or miR-181a/a* overexpression (Fig. 3.11 D), indicating that these miRNAs might be able to influence the differentiation towards a dopaminergic-like TH-expressing phenotype.

3.2.5 Opposing functions of miR-181a and miR-124 on dopaminergic differentiation of hPSC-derived floor plate progenitors

In order to consolidate the role of miR-124, miR-125b and miR-181a/a* on the dopaminergic lineage, another differentiation approach specifically devised for the generation of authentic mDA neurons from hPSCs (Kriks et al. 2011) was used. The following experiments were done in collaboration with Beate Roese-Koerner and performed in two different hPSCs lines, the I3 hESCs and the in house generated iLB-C-31F-r1 iPSCs, kindly provided by Matthias Brandt. In the approach described by Kriks et al. (in the following referred to as floor plate/DA differentiation) hPSCs are first directed towards a midbrain floor plate identity – recapitulating the developmental source of mDA neurons – by dual SMAD inhibition, high levels of SHH and activation of Wnt signaling (Fig. 3.12 A; see also Fig. 2.1). The floor plate cells are then further differentiated in the presence of BDNF, GDNF, dbcAMP, TGFβ3, ascorbic acid (AA) and DAPT to generate TH-positive neurons, which co-express mDA markers, like FOXA2 and LMX1A (Fig. 3.12 A-C).

First, the endogenous expression of miR-124, miR-125b and miR-181a/a* was monitored during the time course of floor plate generation and short-term differentiation until day 13. These analyses revealed, that in line with their proposed positive function, expression of miR-181a/a* and miR-125b increased during floor plate/DA differentiation (Fig. 3.12 E). In particular, miR-181a expression levels were up-regulated by approximately 2 fold at day 9 and by 20 fold at day 13 of the protocol. However, the expression of miR-181a and miR-125b was activated several days after the induction of FOXA2 and LMX1A (Fig. 3.12 D), which suggests that these miRNAs might serve to stabilize the cell fate rather than actively inducing midbrain floor plate identity. Expression of miR-124, for which a negative impact on DA neuron lineage was proposed, did not show any substantial changes during floor plate induction (Fig. 3.12 E). Next, hPSCs (I3 hESCs and iLB-C-31F-r1 iPSCs) were transduced with lentiviral inducible miRNA constructs to overexpress the miRNAs of interest. Specifically, the doxycycline-regulated Tet-ON overexpression system (Clontech) was used, whereby the response pTRE-Tight vector was modified to express either a miR-30:non-targeting ctr shRNA hybrid as an artificial miRNA (see Fig. 2.2 in the Methods section) or the genomic miRNA locus of interest. In a proof-of-principle experiment the different miRNA-overexpression cell lines were then cultured according to the floor plate induction protocol, whereby miRNA overexpression was induced by doxycycline treatment from day 5 onwards and the cells were differentiated until day 25.

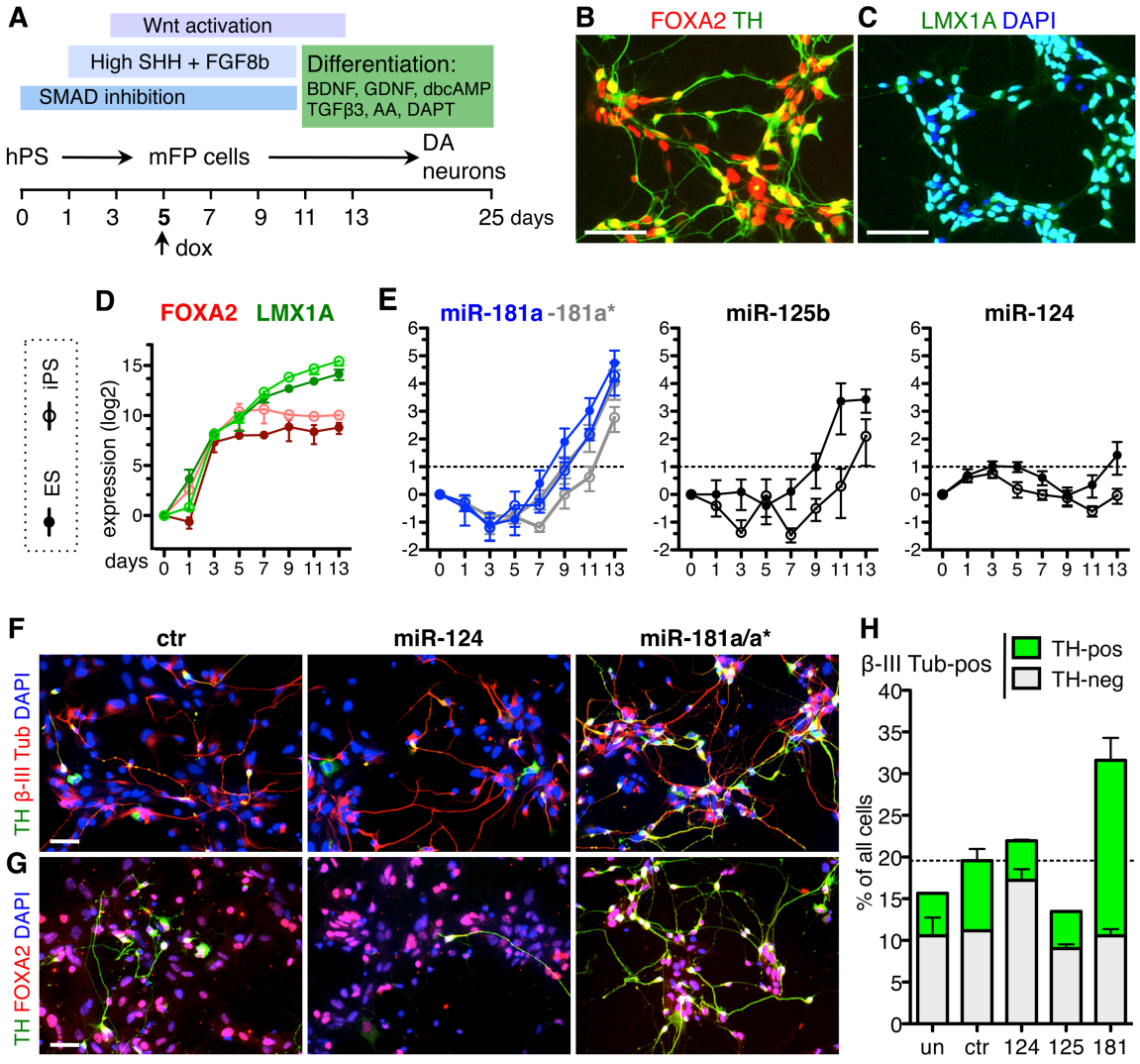

Fig. 3.12: MicroRNA-124 inhibits while miR-181a/a* promotes dopaminergic differentiation of hPSC-derived floor plate progenitor cells. (A) Scheme of the induction protocol according to Kriks et al. (2011). **(B, C)** Immunofluorescence stainings for TH, FOXA2 **(B)** and LMX1A **(C)** at day 25 of the floor plate/DA differentiation of I3 hESCs. **(D)** Quantitative RT-PCR analysis of FOXA2 and LMX1A during the time course of floor plate induction (day 0-13). Data were normalized to 18s rRNA levels and are presented as mean + SEM, relative to expression at day 0 (equal to 1; n = 3). **(E)** Quantitative RT-PCR analysis to monitor miRNA expression levels in the samples described above. Data were normalized to RNU5A snRNA levels and are presented as mean + SEM, relative to expression at day 0 (equal to 1; n = 3). Dashed line marks a 2-fold expression increase. **(F-H)** I3 hESCs and iPSCs carrying different pTight constructs were differentiated according to the floor plate/DA protocol, whereby transgene expression was activated at day 5 by doxycycline administration, before analyzing the cultures at day 25 by immunofluorescence stainings for TH plus β-III Tubulin **(F)** and TH plus FOXA2 **(G)**. Representative pictures from I3 hES cell-derived cultures are shown. **(H)** Corresponding quantification of the percentage of β-III Tubulin-positive cells being either TH-negative or TH-positive. Shown are data of two biological replicates (one per cell line). All scale bars = 100 μm. Data were obtained in collaboration with Beate Roese-Koerner.

Compared to the previous experiments (Fig. 3.12 C), the number of β-III Tubulin-positive neurons and TH-positive neurons was reduced in all conditions (miR-overexpressing and control cultures; Fig. 3.12 F). This might be due to the long-term treatment with doxycycline. However, in all conditions around 90% of all cells showed expression of FOXA2 and LMX1A, indicating that the floor plate induction itself was efficient (data not shown). Nevertheless, the number of TH-positive neurons was altered in the miRNA-overexpressing cultures. Specially, overexpression of miR-181a/a* increased the proportion of TH-positive neurons to 18.3% in the I3 hESC-derived and to 23.7% in the iPSC-derived cultures compared to the respective control cultures (ESCs: 9.8%; iPSCs: 7.0%; Fig. 3.12 F-H). In line with the previous results obtained in lt-NES cells, overexpression of miR-124 during the floor plate protocol impaired the generation of TH-positive neurons (Fig. 3.12 F-H). In contrast, overexpression of miR-125b had no strong effect on the amount of TH-positive neurons, compared to the control cultures (un, ctr; Fig. 3.12 H).

Although the floor plate/DA differentiation experiment was performed only once for each hPSC line, the consistent results observed in the two different cell lines strengthen the observations made, which further point to a positive role of miR-181a and an inhibitory effect of miR-124 on DA neuron development. However, for these experiments a stable genetic manipulation was necessary, which would not be suitable when it comes to generating mDA neurons for medical purposes. For this purpose one would rather use transient approaches, like transfecting cells with miRNA mimics or inhibitors.

3.2.6 Transfection-based modulation of miR-181a/a*, miR-125b and miR-124 shifts lt-NES cells towards TH-positive neuron differentiation

In contrast to the floor plate/DA differentiation paradigm, which requires very high cell density, lt-NES cells can be easily transfected with miRNA mimics and inhibitors (see 3.2.3). Thus, although lt-NES cells (with the protocols available at the moment) are not able to give rise to authentic mDA neurons, they were used here to establish whether transfection-based miRNA modulation is able to affect the differentiation towards a TH-expressing DA-like neuronal phenotype. For this purpose, lt-NES cells were repeatedly transfected with miRNA mimics or inhibitors in a two-weeks neuronal differentiation time course (Fig. 3.13 A). Using this protocol only around 1% of all neurons were positive for TH in mock- and ctr-transfected cultures (Fig. 3.13 B). Transfection with mimics for either miR-125b or miR-181a increased the amount of TH-positive neurons to 3.2 ± 0.9 % and 4.0 ± 0.2 %, respectively. In turn, transient inhibition of miR-125b or miR-181a strongly impaired the generation TH-positive neurons. The opposite was observed upon inhibition of miR-124, which further supports the negative function of miR-124 in this context (Fig. 3.13 B). These data indicate that transient miRNA modulation indeed suffices to manipulate neuronal subtype specification and in general confirms the previous findings obtained by lentiviral-based miRNA overexpression during lt-NES cell differentiation.

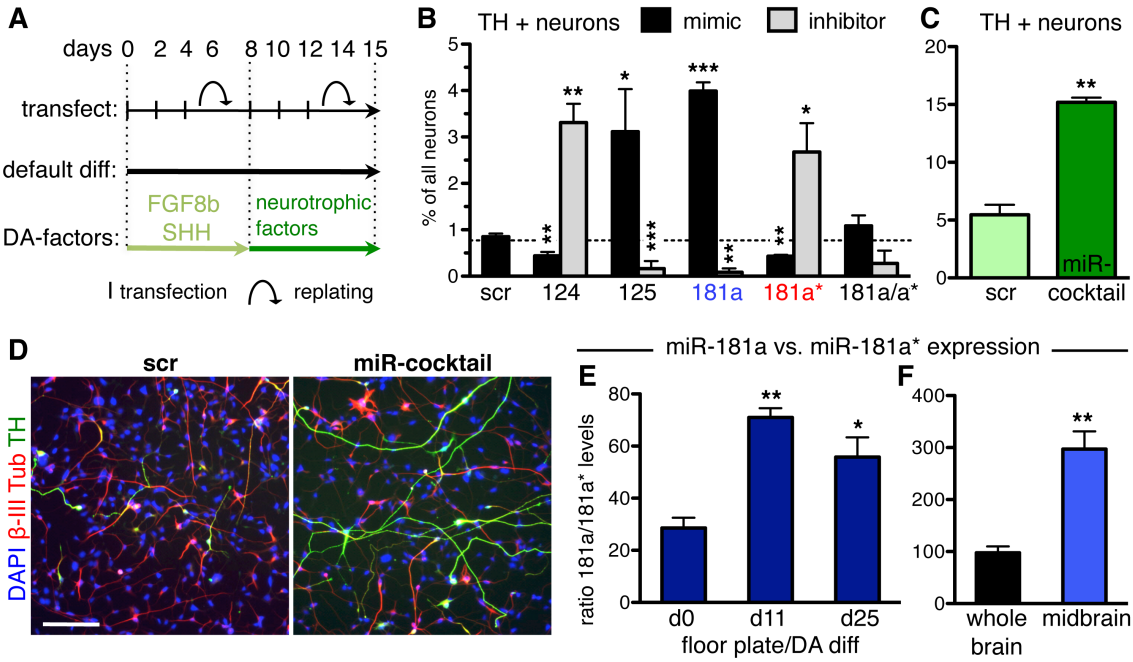

Fig. 3.13: Modulating dopaminergic differentiation of lt-NES cells with miRNA oligonucleotides; Opposing functions of miR-181a and miR-181a* on dopaminergic differentiation. (A) Scheme of the miRNA mimic and inhibitor transfection protocol: Differentiating lt-NES cells were transfected 6 times in 48 hours intervals and replated twice at the indicated days before final analysis on day 15. Lt-NES cells were either differentiated according to the standard differentiation protocol (default diff) or in presence of dopamine neuron-inducing (DA) factors. **(B, C)** Percentage of TH-positive neurons in default differentiated lt-NES cells transfected with the different oligonucleotides **(B)**, and in lt-NES cells differentiated in the presence of DA-factors and transfected with scrambled oligonucleotides or a cocktail containing miR-181a and miR-125b mimics and miR-124 inhibitor **(C)**. **(D)** Immunofluorescence staining of β-III Tubulin and TH of the samples described in C. Scale bar = 100 μm. **(E, F)** Ratio of miR-181a versus miR-181a* expression in cells derived from I3 hESCs at different time points of the floor plate/DA protocol **(E)**, and in human fetal whole brain and human fetal midbrain extracts **(F)**. The underlying qRT-PCR-data were normalized to RNU5A (for E) and SNORD25 (for F) snRNA levels. All quantification data are presented as mean + SEM; $n \geq 3$; $p \leq 0.05$; **, $p \leq 0.01$; ***, $p \leq 0.0001$.

Next, it was assessed whether the combined modulation of specific miRNAs could be used to augment the treatment with patterning signals known to induce dopaminergic differentiation such as SHH and FGF8b (Ye et al., 1998). To this end, lt-NES cells were first cultured for one week with FGF8b and active SHH signaling and further differentiated in the presence of neurotrophic factors, which will be referred to as “DA-factors” (Fig. 3.13 A; see Methods section 2.1.7). During this time, lt-NES cells were repeatedly transfected with a cocktail of miRNA modulation oligonucleotides (miR-cocktail), including a miR-124 inhibitor and mimics for miR-125 and miR-181a. The presence of DA-factors raised the proportion of TH-positive neurons to 5.5 ± 0.9 % as compared to default differentiation (Fig. 3.13 B, C). Similar to the previous experiments, modulating miRNA activities was sufficient to further increase the yield of TH-positive neurons to 15.2 ± 0.4 % even in the presence of SHH/FGF8b activators (Fig. 3.13 C). Moreover, judging by their morphology, the TH-positive neurons detected in the cultures treated with the miR-cocktail and the patterning factors seemed to be more mature than the neurons generated in the patterning-factors-only conditions (Fig. 3.13 D).

Using miRNA mimics also allows to individually study the impact of miRNA sisters like miR-181a and miR-181a*. Intriguingly, these experiments revealed that miR-181a* has an opposing function compared to miR-181a with regard to the generation of TH-positive neurons. Transfection with the miR-181a* mimic reduced the number of TH-positive neurons, while transfection with the miR-181a* inhibitor promoted the generation of this neuronal subtype (Fig. 3.13 B). In line with the observed opposite functions of the two sister strands, co-transfection with miR-181a and miR-181a* mimics did not significantly affect the number of TH-positive neurons compared to control cultures (Fig. 3.13 B). This is in apparent contrast with the data obtained from lentiviral overexpression of the miR-181a/a* locus, which was found to have a positive impact on TH-positive neurons. However, upon lentiviral-based overexpression of the genomic loci, miR-181a* levels were only increased by ~28 fold (see Fig. 3.5) while miR-181a* was over 2000 fold up-regulated, upon mimic transfection (see Fig. 3.8), which might explain the different effects observed.

As shown earlier in Fig. 3.4, miR-181a and miR-181a* have a variable expression ratio in hESCs compared to lt-NES cells. A similar discrepancy in the expression ratio was detected during the floor plate/DA differentiation protocol. Although, the expression levels of both miRNAs increased during floor plate/DA differentiation (Fig. 3.12 E), the ratio of miR-181a to miR-181a* expression seemed to vary between different stages of the protocol (Fig. 3.13 E). In the starting hPSC cultures (day 0) miR-181a expression was 28.6 ± 4.0 fold higher than that of miR-181a*. This ratio was increased upon floor plate induction and at day 11 miR-181a was 77.1 ± 3.5 fold higher expressed than miR-181a* (Fig. 3.13 E). In addition, the ratio of miR-181a to miR-181a* expression was up-regulated by approximately 3 fold in extracts from human fetal midbrain compared to commercial human whole fetal brain extracts – where tissue from forebrain is typically overrepresented (Fig. 3.13 F). These observations indicate that in analogy to the opposing functions of miR-181a and miR-181a* during DA neuron differentiation, the relative expression of these miRNAs drifts apart in samples enriched for DA neurons.

3.3 Mechanisms underlying miR-181a function on NSC maintenance and dopaminergic subdifferentiation

Given its remarkable role on neuronal differentiation and dopaminergic subdifferentiation, this part of the work aimed at the identification of *bona fide* miR-181a target genes. According to target prediction algorithms miR-181a has the potential to target several hundreds to thousands of mRNAs. Matching the list of putative miR-181a targets to Gene Ontology and pathway repositories using the DAVID Bioinformatics Resources (Huang et al. 2009) revealed an apparent bias towards genes involved in MAP kinase, Notch, TGFβ and Wnt signaling. Furthermore, many of the potential miR-181a target genes are associated with the Gene Ontology classifications “axonogenesis” and “neuron commitment”, the later including genes involved in neural stem cell (NSC) maintenance. Among those putative target genes is also GCNF/NR6A1, whose genomic locus overlaps with the MIR181A2 hostgene and for which evidence from previous studies point to a role during early neural commitment (see also Introduction section 1.4).

Thus, the potential regulatory impact of miR-181a on GCNF was validated by 3' UTR and GCNF RNA interference experiments. GCNF was further characterized for its role during lt-NES cell maintenance and dopaminergic differentiation using gain-of-function experiments. As last part, the impact of miR-181a on the Wnt pathway as an important signaling cue for dopaminergic differentiation was assessed.

3.3.1 Overexpression of miR-181a induces down-regulation of NSC-associated genes

Since it was not possible to propagate lt-NES cells constitutively overexpressing miR-181a/a*, due to the impact of miR-181a/a* on lt-NES cell self-renewal, the doxycycline-regulated pTight-miR-181a/a* overexpression system was used for the following experiments. As controls, lt-NES cells were transduced with pTight constructs carrying either a GFP cassette or the miR-30:shRNA-ctr hybrid (Fig. 3.14 A). Using this system a robust overexpression of both miR-181a (64.5 ± 5.8 fold) and miR-181a* (142.2 ± 24.6 fold) after two days of doxycycline treatment was achieved (Fig. 3.14 B). These RNA samples were then used for qRT-PCR analyses in order to assess expression changes of the candidate targets in response to miR-181a/a* overexpression. Based on target prediction analysis and literature research a shortlist of putative miR-181 targets associated with NSC maintenance and neuronal differentiation was generated. This list included several components of the Notch signaling cascade, since it has been shown that Notch activity is important for lt-NES cell maintenance (Borghese et al. 2010). Potential miR-181a binding sites were identified in the 3' UTRs of the Notch receptors NOTCH2, NOTCH3 and of the Notch target gene HEY1. NOTCH4 and HEY2 were also found to harbor potential miR-181a binding site, however both genes are absent in lt-NES cells as previously shown by Borghese et al. (2010). Quantitative RT-PCR analysis revealed that only the expression of NOTCH2 was significantly down-regulated upon miR-181a/a* overexpression compared to control cells, while the expression of the other Notch receptors and HEY1 was not changed (Fig. 3.14 C). As previously shown by experiments in megakaryotic cells, miR-181a represses LIN28A expression by direct interacting with its mRNA (Li et al. 2011b). As a consequence, the LIN28A-mediated inhibition of let-7 maturation is relieved resulting in an up-regulation of mature let-7 expression (Li et al. 2011b). LIN28A as well as its homolog LIN28B harbor potential miR-181a binding sites and were strongly down-regulated upon miR-181a/a* overexpression by 88.1 ± 2.3% and 61.3 ± 6.9%, respectively (Fig. 3.14 D). Concomitantly a significant up-regulation of let-7 expression was observed (Fig. 3.14 F), indicating that, also in lt-NES cells, this feedback loop is affected by miR-181a/a* modulation. In addition, a slight but significant increase of miR-125b expression was detected (Fig. 3.14 F), which might further contribute to the differentiation-promoting effect of miR-181a. Another important regulator of NSC maintenance is Musashi1 (MSI1), which interferes with neuronal differentiation and participates in LIN28-mediated regulation of miRNA biogenesis (Kawahara et al. 2011). While putative miR-181a binding sites were found in the 3' UTRs of both MSI1 and its homolog MSI2, only the expression of MSI2 was reduced in miR-181a/a*-overexpressing lt-NES cells compared to control cells (Fig. 3.14 E).

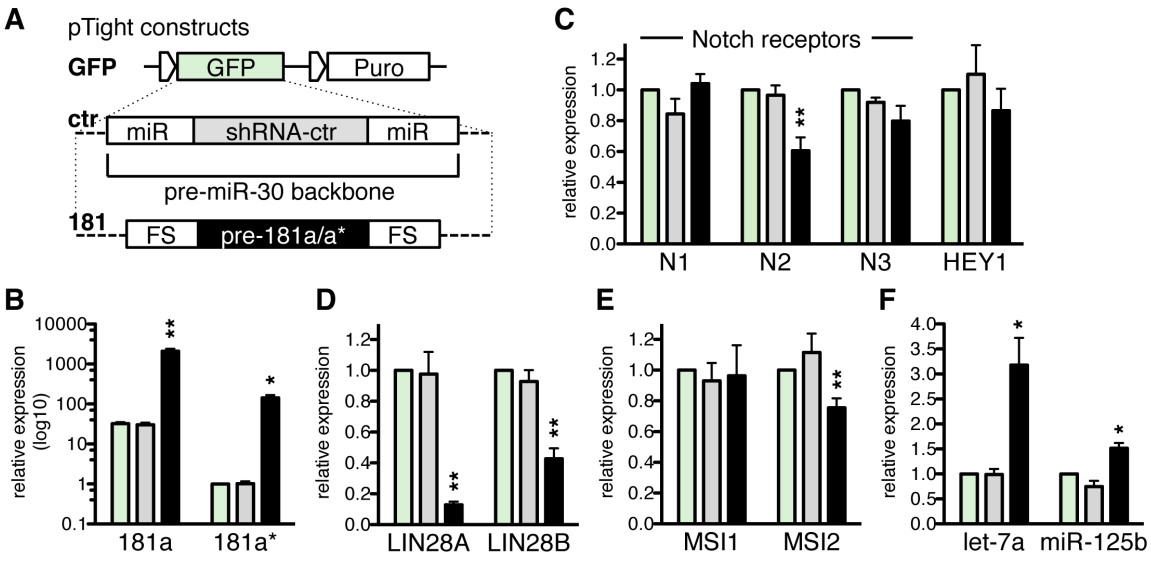

Fig. 3.14: Overexpression of miR-181a/a* induces down-regulation of genes associated with NSC maintenance. Lt-NES cells carrying different pTight constructs, i.e. pTight-GFP, pTight-ctr (encoding a miR-30:shRNA-ctr hybrid construct) or pTight-miR-181, respectively **(A)** were cultured for two days in the presence of doxycycline before isolating the RNA. **(B)** Quantitative RT-PCR analysis of miR-181a and miR-181a* expression. Data were normalized to RNU5A snRNA levels and are presented as mean + SEM relative to miR-181a* expression in pTight-GFP transduced cells (set to 1; n = 4). **(C-E)** Quantitative RT-PCR analysis of putative miR-181a target genes. Data were normalized to 18s rRNA levels and are presented as mean + SEM relative to expression in pTight-GFP transduced cells (equal to 1, $n \geq 3$). **(F)** Quantitative RT-PCR analysis of let-7 and miR-125b. Data were normalized to RNU5A snRNA levels and are presented as mean + SEM relative to expression in pTight-GFP transduced cells (equal to 1, $n \geq 4$). *, $p \leq 0.05$; **, $p \leq 0.01$.

Taken together, these data indicate that miR-181a/a* affects the expression of critical players involved in the switch of NSC self-renewal to differentiation, namely NOTCH2, Musashi2 and the LIN28/let-7 feedback loop. These data, however, need to be complemented by 3' UTR reporter assays to prove a direct interaction of miR-181a with the respective transcripts.

3.3.2 MicroRNA-181a promotes neuronal differentiation by targeting GCNF

Besides these well-known NSC-associated genes, target prediction analysis also identified the transcription repressor GCNF/NR6A1 as high-ranking target of miR-181a. This miRNA-target interaction is of high interest because of two main reasons: First, the MIR181A2 locus encoding for pri-181ab-2 is located on the antisense strand of an intron of GCNF. Second, although previous evidence mostly from mouse developmental studies have pointed to a role of GCNF during neurogenesis (Süsens et al. 1997; Chung et al. 2001b; Chung et al. 2006; Akamatsu et al. 2009), its exact function in this context has not yet been clarified. Thus, the following experiments aimed at dissecting the endogenous expression pattern of GCNF and whether this is regulated by miR-181a. Previous studies have indicated that GCNF is expressed in mouse ESCs and is transiently up-regulated upon retinoic acid-induced neuronal differentiation (Gu et al. 2005b; Akamatsu et al. 2009). Expression analyses for GCNF during hESC-based neuronal differentiation revealed that both GCNF mRNA and protein levels are down-regulated in lt-NES cells and even further decreased in their

differentiated progeny (ND15, ND30) compared to hESCs. (Fig. 3.15 A-C). This expression pattern was consistent in both I3 and H9.2 hESC-derived samples and showed an inverse correlation with the expression of mature miR-181a, which is up-regulated in neuronal differentiating cells (see Fig. 3.4). As already indicated by previous qRT-PCR analyses (see Fig. 3.4 E), pri-miR-181ab-2 expression declined from hESCs to lt-NES cells but increased again during neuronal differentiation (Fig. 3.15 A). This expression pattern is different from the one observed for GCNF pointing to an independently regulated expression of the two genes, despite their co-localization. Expression of pri-181ab-1 was constantly up-regulated in lt-NES cells and differentiating neuronal cultures (Fig. 3.15 A).

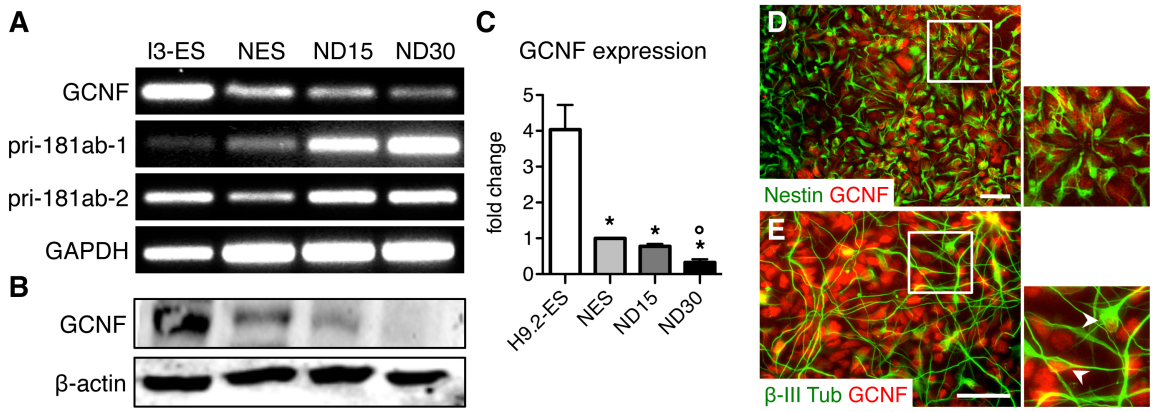

Fig. 3.15: GCNF is highly expressed in hESCs and declines upon lt-NES cell differentiation. (A) Semi-quantitative RT-PCR analysis of GCNF, pri-181ab-1 and pri-181ab-2 expression levels in hESCs, lt-NES cells, ND15 and ND30 neuronal cultures derived from the I3 hESC line. GAPDH levels were used as quantitative reference. **(B)** Western blot for GCNF. Beta-actin was used as protein loading control. **(C)** Quantitative RT-PCR analyzing GCNF expression in H9.2 hESC-derived cell samples. Data were normalized to 18s rRNA levels and are presented as mean + SEM relative to expression in NES (set to 1; $n \geq 3$; *, compared to ES; °, compared to NES; */°, $p \leq 0.05$). **(D, E)** Immunofluorescence stainings for GCNF plus Nestin in self-renewing lt-NES cells **(D)** and plus β-III Tubulin **(E)** in I3 lt-NES cells differentiated for 7 days. **(E)** Arrowheads indicate cells with co-expression of GCNF and β-III Tubulin. Scale bars = 50 μm.

The GCNF 3' UTR contains a high-scoring putative miR-181a binding site, which consists of a perfect match to the miRNA seed region and an additional stretch of nucleotides complementary to the middle part of the miRNA (Fig. 3.16 A). The reciprocal expression patterns of GCNF and mature miR-181a during lt-NES cell differentiation further points to a potential regulatory impact of miR-181a on GCNF. To test this hypothesis, first, the effect of miR-181a/a* overexpression on GCNF mRNA and protein levels was assessed. Indeed, both GCNF mRNA and protein levels were strongly reduced upon miR-181a/a* overexpression by 0.23 ± 0.03 fold and 0.32 ± 0.03 fold, respectively, compared to control cells (Fig. 3.16 B, C). A similar outcome was observed when analyzing GCNF protein levels in miR-181a/a*-overexpressing H9.2 lt-NES cells (Fig. 3.16 C').

In order to assess whether miR-181a is able to bind the putative target site, the full length 3' UTR of GCNF was cloned into a dual luciferase reporter system (psiCHECK2, Promega, Fig. 3.16 D). Lt-NES cells were then transfected with the GCNF 3' UTR reporter or the unmodified psiCHECK2 vector as control, followed by a transfection with the respective mimics and inhibitors for miR-181a and miR-181a*. The next day the cells were harvested and luciferase assays were carried out, whereby changes in the Renilla luminescence were normalized to the unregulated Firefly luciferase activity. Another batch of the cells was used for RNA preparation and qRT-PCR analysis.

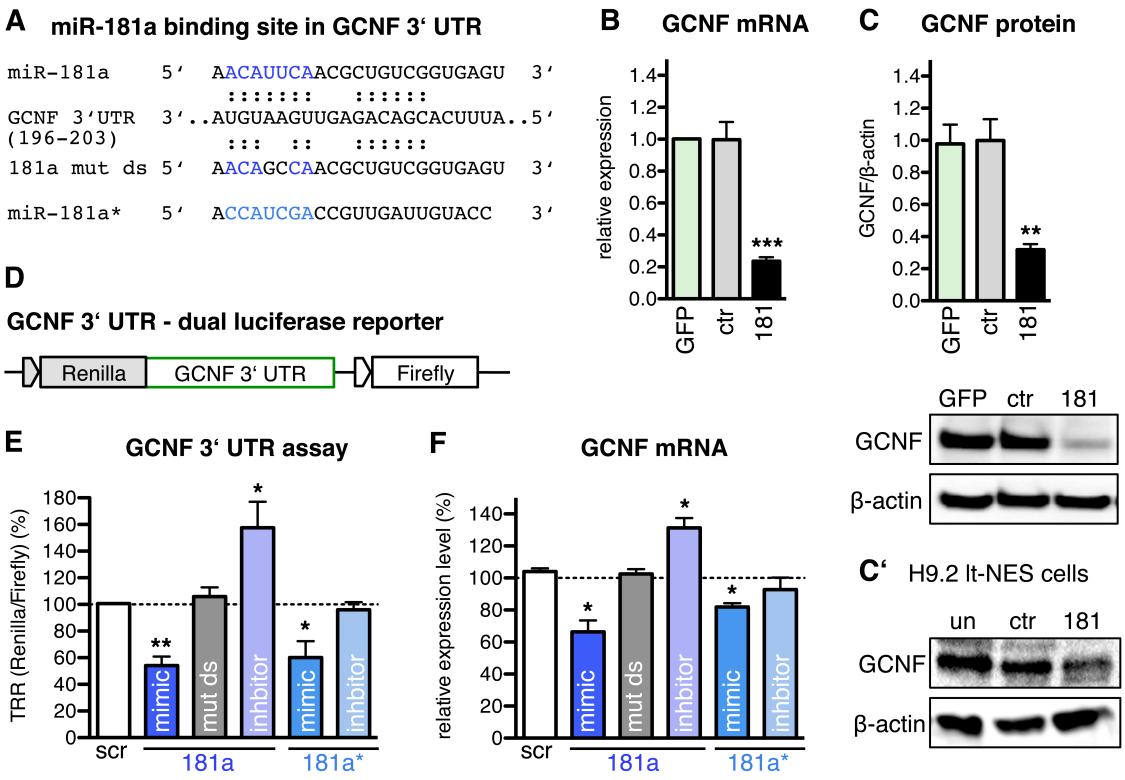

Fig. 3.16: MicroRNA-181a represses expression of GCNF by direct binding to its 3' UTR. (A) Schematic illustration of the putative miR-181a target site in the human GCNF 3' UTR according to TargetScan. Also shown are sequences of miR-181a, mutated miR-181a and miR-181a* mimics. **(B)** I3 lt-NES cells were transduced with **p**Tight-GFP, pTight-ctr or pTight-miR-181a/a* and then analyzed by qRT-PCR for GCNF expression after 48 hours of doxycycline treatment. Data were normalized to 18s rRNA levels and are presented relative to expression in pTight-GFP transduced lt-NES cells (equal to 1). **(C)** Histogram showing the densitometric GCNF/β-actin ratio as measured after Western blot analysis for GCNF and β-Actin (as loading control) in the different I3 lt-NES cell samples described in B, after 4 days of doxycycline treatment. **(C')** Western blot for GCNF in untransduced (un) H9.2 lt-NES cells or in cells transduced with pLVTHM-ctr or pLVTHM-181a/a*. Beta-Actin was used as loading control. **(D)** Scheme of the dual luciferase reporter plasmids carrying the GCNF 3' UTR down-stream of the Renilla luciferase. **(E-F)** Lt-NES cells were transfected with the GCNF 3' UTR-psiCHECK2 or the unmodified psiCHECK2 vector and subsequently transfected with different oligonucleotides (scrambled, miRNA mimics and inhibitors). The cells were then harvested for luciferase assay and RNA extraction. **(E)** Transfection-dependent Renilla/Firefly ratios (TRR) in the respective samples. Data were normalized to unmodified psiCHECK2 and are presented relative to mock-transfected cells (set to 100%, dashed line). **(F)** Quantitative RT-PCR analysis of GCNF expression. Data were normalized to 18s rRNA levels and are presented relative to the expression in mock-transfected cells (set to 100%, dashed line). All quantification data are presented as mean + SEM; n ≥ 3; *, p ≤ 0.05; **, p ≤ 0.01, ***, p ≤ 0.0001.

Transfection with the miR-181a mimic significantly suppressed the Renilla luciferase activity of the GCNF 3' UTR reporter compared to cells transfected with a scrambled oligonucleotide (scr; Fig. 3.16 E). This repression was not seen upon transfection with a mutated version of the miR-181a mimic containing a disrupted seed sequence (mut ds; Fig. 3.16 A, E). In contrast, co-transfection with a synthetic inhibitor for miR-181a resulted in an increase of Renilla luciferase activity (Fig. 3.16 E). The expression levels of GCNF mRNA upon miR-181a mimic or inhibitor transfection were in line with these observations (Fig. 3.16 F), indicating that miR-181a acts as a destabilizer of GCNF mRNA. Intriguingly, also transfection with the miR-181a* mimic reduced GCNF 3' UTR luciferase activity as well as GCNF mRNA levels (Fig. 3.16 E, F). Even though miR-181a* has been reported to regulate GCNF expression in chicken primordial germ cells (Lee et al. 2011), none of the target prediction algorithms used were able to identify a miR-181a* binding site in the human GCNF 3' UTR. In addition, inhibition of miR-181a* had no impact on GCNF expression (Fig. 3.16 F), suggesting that GCNF is not a physiological target of miR-181a*.

To address the biological relevance of the miR-181a-GCNF interaction, GCNF loss-of-function experiments using RNA interference were performed. To that end, lt-NES cells were transfected with siRNAs against GCNF, miR-181a mimic/inhibitor or with combinations of them and differentiated for one week (ND7; Fig. 3.17). Repeated transfections with a GCNF siRNA during the time course of neuronal differentiation resulted in a 59 ± 4.0% reduction of the endogenous GCNF mRNA levels (Fig. 3.17 B). Similar to the transfection with the miR-181a mimic, knock-down of GCNF increased the fraction of β-III Tubulin-positive cells to 6.0 ± 0.4% compared to 3.9 ± 0.1% in scrambled oligonucleotide-transfected cultures (Fig. 3.17 C, E). It is however important to note that transient overexpression of miR-181a was more potent than GCNF knock-down and raised the proportion of β-III Tubulin-positive neurons up to 8.4 ± 1.0%. This suggests that miR-181a may promote neuronal differentiation by targeting other genes besides GCNF, for example Notch pathway components, MSI2 and LIN28A/B. In further support of an induction of neuronal differentiation, cultures treated with the GCNF siRNAs or the miR-181a mimic contained neurons with significant longer neurites compared to control cultures (Fig. 3.17 D). As previously observed (see 3.2.3), inhibition of the miR-181a activity during lt-NES cell differentiation reduced the number of β-III Tubulin-positive cells (Fig. 3.17 C, E). Interestingly, co-transfection with a GCNF siRNA was able to rescue the impairment of neuronal differentiation induced by the miR-181a inhibitor, so that the number of neurons reached a similar level as in the control cultures (Fig. 3.17 C, E).

In summary, these results demonstrate that miR-181a represses GCNF expression through the predicted target site in the GCNF 3' UTR. They further indicate that endogenous miR-181a activity in lt-NES cells is required to down-regulate GCNF expression and thereby contributes to the commitment of lt-NES cells to neuronal differentiation.

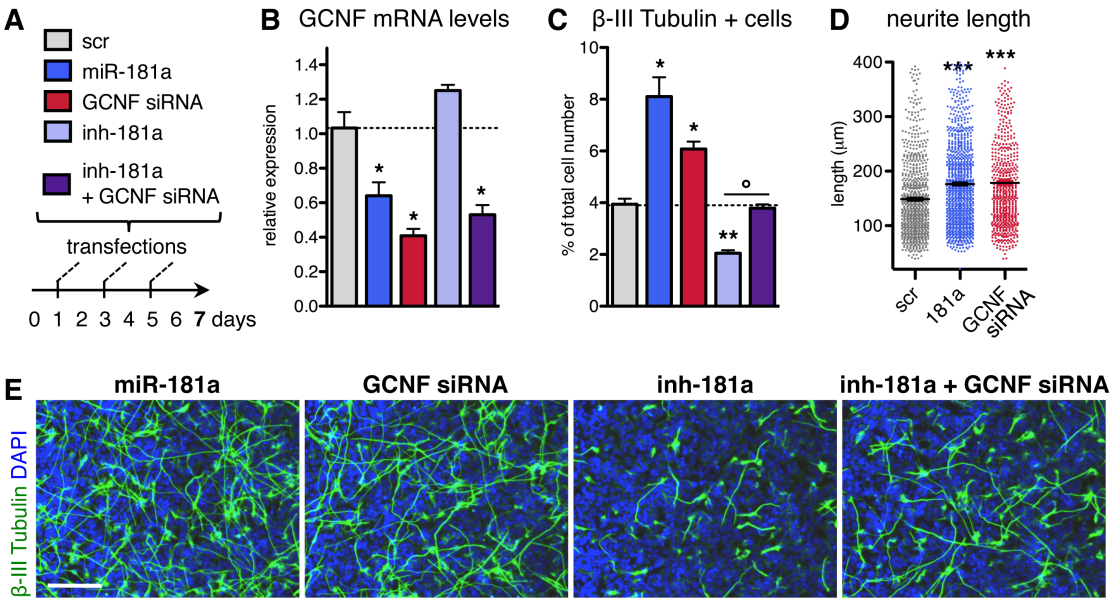

Fig. 3.17: Down-regulation of GCNF promotes neuronal differentiation and counteracts miR-181a inhibition. (A) Lt-NES cells were transfected three times during a 7 days differentiation paradigm with different combinations of GCNF siRNA, miR-181 mimic, miR-181a inhibitor or a scrambled control siRNA (scr). **(B)** Quantitative RT-PCR to analyze GCNF expression in the respective samples. Data were normalized to 18s rRNA levels and are presented as mean + SEM, relative to expression levels in mock-transfected cultures (dashed line; n = 3; *, $p \leq 0.05$). **(C)** Percentages of β-III Tubulin-positive cells. Data are presented as mean + SEM ($n \geq 3$; */°, $p \leq 0.05$; **, $p \leq 0.01$). Dashed line indicates the proportion of β-III Tubulin-positive cells in mock-transfected cultures. **(D)** Scatter plot displaying the length of single neurites (in µm) in lt-NES cells transfected with scr siRNA, miR-181 mimic or GCNF siRNA. Data from three independent replicates are shown. Black lines indicate average neurite length (mean + SEM, n = 3; ***, $p \leq 0.0001$). **(E)** Immunofluorescence images for β-III Tubulin in transfected lt-NES cells. Scale bar = 100 µm.

3.3.3 Overexpression of GCNF stabilizes neural rosette morphology and impairs neuronal differentiation

Given that knock-down of GCNF promotes neuronal differentiation, it is tempting to speculate that forced expression of GCNF would have a negative function in this context. In order to test this hypothesis and to get a deeper insight into the function of GCNF in lt-NES cell maintenance, lt-NES cells were transduced with lentiviral particles coding for a doxycycline-inducible GCNF overexpression construct (pTight-GCNF). Treatment with doxycycline for 4 days induced a strong increase of the GCNF mRNA levels in pTight-GCNF transduced lt-NES cells by up to 200 fold compared to lt-NES cells carrying the pTight-GFP or the pTight-miR-30:shRNA-ctr constructs as controls (Fig. 3.18 A). This resulted in a ~5-fold up-regulation of GCNF protein expression (Fig. 3.18 B). Although pTight-mediated transgene expression should only be activated upon doxycycline treatment, low levels of GCNF overexpression were observed even in the absence of doxycycline (Fig. 3.18 A). Since the rate of non-induced GCNF overexpression differed between different batches of independently transduced cells, the “GCNF-dox” condition was not included in the following experiments.

In line with its known nuclear localization, ectopically expressed GCNF was also exclusively confined to the nucleus (Fig. 3.18 C). As clearly shown in Fig. 3.18 C, lt-NES cell cultures transduced with pTight-GCNF are a mixture of cells with different GCNF overexpression levels.

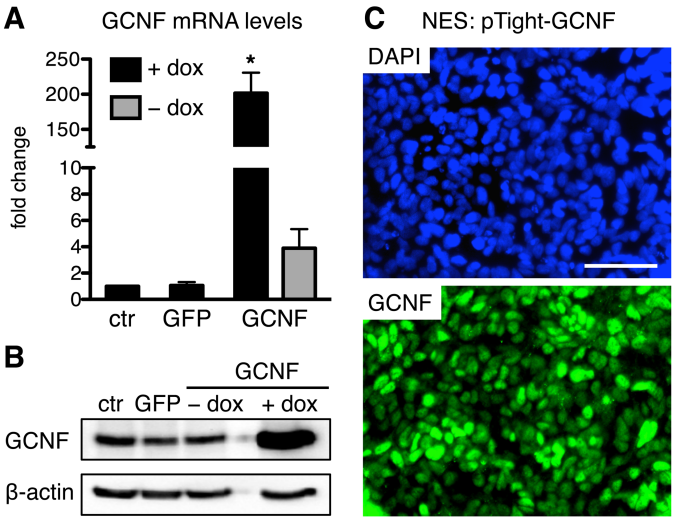

Fig. 3.18: Conditional over-expression of GCNF in lt-NES cells. (A) Quantitative RT-PCR monitoring GCNF expression in l3 lt-NES cells transduced with pTight-ctr, -GFP and -GCNF, respectively, after 4 days with or without doxycycline treatment. Data were normalized to 18s rRNA levels and are presented as mean + SEM, relative to expression in ctr-cells (set to 1; n = 3; *, $p \leq 0.05$). **(B)** GCNF Western blot in the cells described above. Beta-actin was used as loading control. **(C)** Immuno-fluorescence stainings for DAPI and GCNF in pTight-GCNF transduced lt-NES cells. Scale bar = 100 μm.

Overexpression of GCNF had no clear impact on l3 lt-NES cells cultured under self-renewing conditions (Fig 3.19 B; NES). However, when induced to enter differentiation by growth factor withdrawal, strong differences between the GCNF-overexpressing and control cultures became apparent (Fig 3.19). On the one hand, GCNF-overexpressing cultures were characterized by tightly packed cell clusters that showed expression of ZO1 in their lumen, while the cells were rather evenly distributed in control cultures and did not express ZO1 anymore (Fig 3.19 B). On the other hand, the rate of neuronal differentiation was strongly reduced upon GCNF overexpression (Fig 3.19 C). Intriguingly, both the radial organization of the cells and the polarized ZO1 expression in the GCNF-overexpressing cultures was reminiscent of the neural rosettes formed by self-renewing lt-NES cells (Koch et al. 2009b). While these rosettes are usually lost upon differentiation by growth factor withdrawal, they were still detectable in GCNF-overexpressing cultures after 4 days of differentiation (Fig. 3.19 B; ND4). This difference was even more apparent at after 7 days of differentiation (ND7), when control cultures did not contain any rosettes, whereas GCNF-overexpressing cultures still contained rosette-like structures. These structures were also bigger than the neural rosettes detected at ND4, which, together with their more longitudinal shape, might indicate that some of the rosettes might have merged upon further culturing (Fig. 3.19 B; ND7). The large neural rosettes also exhibited high expression of the neural stem cell marker PLZF/ZBTB16 and SOX2 (Fig. 3.19 D).

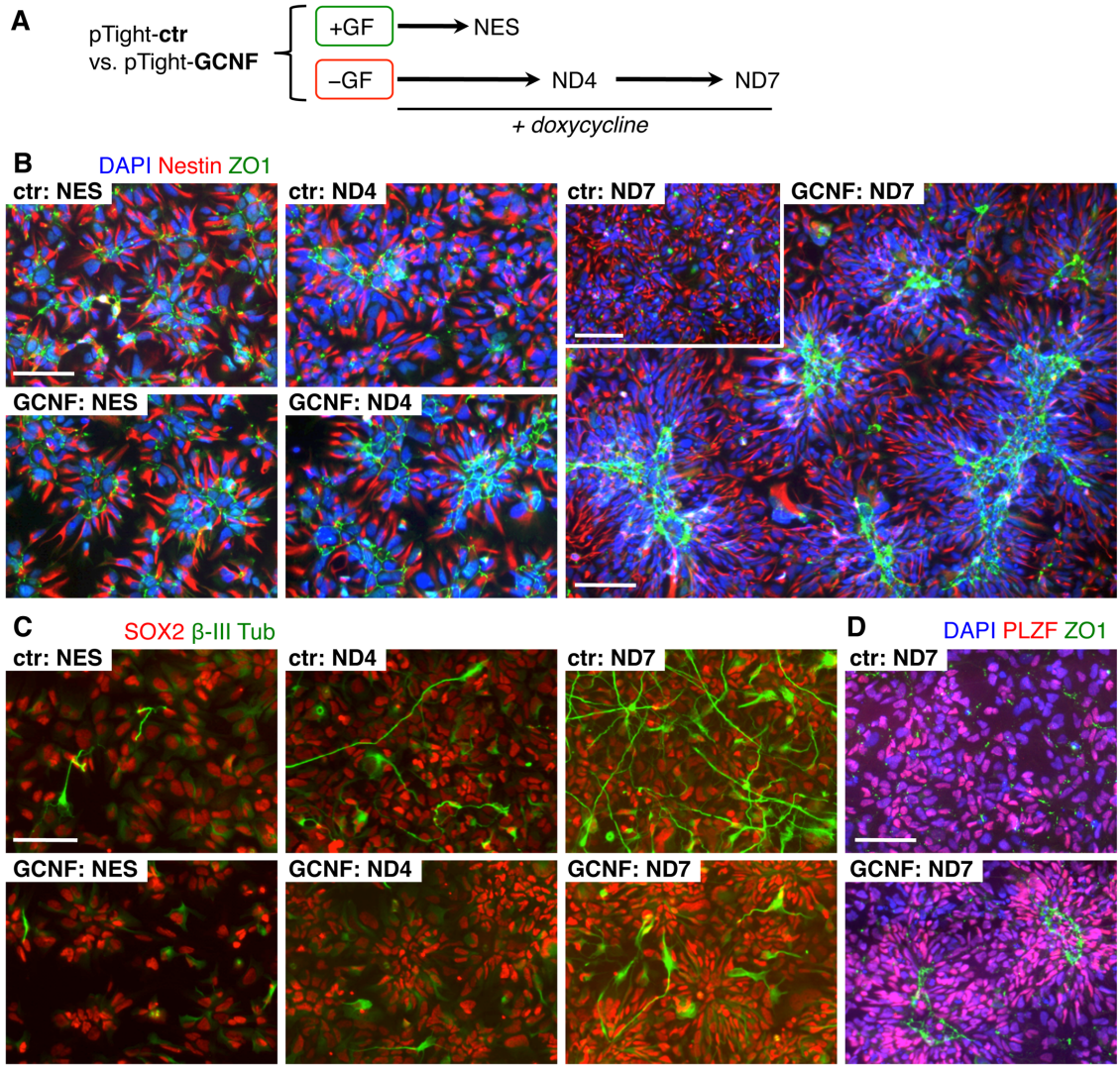

Fig. 3.19: GCNF overexpression under differentiation-inducing conditions preserves neural rosettes and inhibits neuronal differentiation. (A) I3 lt-NES carrying either pTight-ctr or pTight-GCNF were either cultured for two days in the presence of growth factors (+GF; self-renewing NES) or in their absence (–GF) to induce neuronal differentiation, which was stopped at day 4 (ND4) and day 7 (ND7), respectively. Doxycycline was present in all experimental settings. **(B, C)** Corresponding immunofluorescence stainings for Nestin plus ZO1 **(B)** and SOX2 plus β-III Tubulin **(C)**. Note the longitudinal shaped ZO1-positive cell clusters in the ND7 GCNF-cultures. **(D)** Immunofluorescence stainings for PLZF and ZO1 in ND7 cultures. All scale bars = 100 μm. Data were obtained in collaboration with Nityaa Venkatesan.

Although these experiments were done in polyclonal cultures, with cells of variable GCNF overexpression levels, the cell cluster formation induced by GCNF could be detected throughout the entire cell culture dish, as evidenced by the overview picture presented in Fig. 3.20 A, B. Furthermore, the effects of GCNF overexpression were independent of the cell line, and both the cell cluster/rosette formation and the impaired neuronal differentiation were also observed in H9.2 lt-NES cell cultures (Fig. 3.20 C, D).

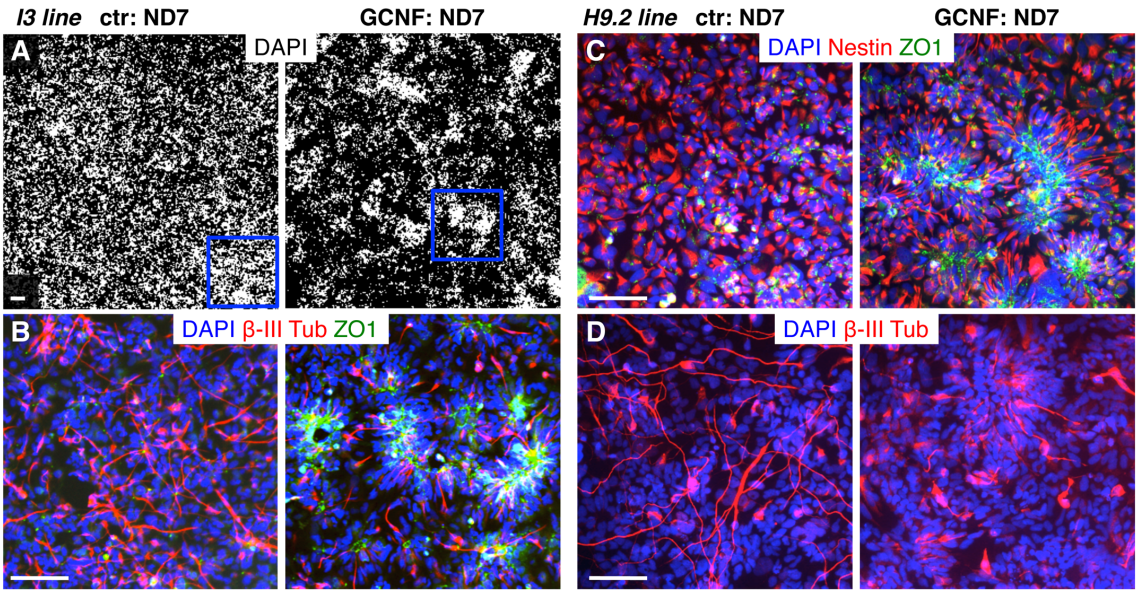

Fig. 3.20: Effects induced by GCNF overexpression are independent of the It-NES cell origin. (A-D) Immunofluorescence stainings of I3 **(A, B)** or H9.2 **(C, D)** It-NES cells transduced with either pTight-ctr or pTight-GCNF and differentiated for 7 days (ND7) in the presence of doxycycline. **(A)** Overview picture of the staining for the nuclear marker DAPI taken with an automated microscopy device and processed with ImageJ to create a binary image. The cells were also stained for β-III Tubulin and ZO1 and representative parts of the images were magnified and are shown in **(B)**. **(C, D)** Immunofluorescence stainings for Nestin plus ZO1 **(C)** and β-III Tubulin **(D)** in H9.2 It-NES cell-derived cultures. All scale bars = 100 *μ*m. Data were obtained in collaboration with Nityaa Venkatesan.

As indicated by the low amounts of β-III Tubulin-positive neurons detected in ND4 and ND7 cultures, GCNF overexpression seems to delay neuronal differentiation (Fig. 3.19 C & Fig. 3.20 B, D). In fact, quantitative analysis revealed that GCNF-overexpressing cultures contained less than half (3.9 ± 0.9%) of the β-III Tubulin-positive neurons that were detected in control cultures (ctr: 9.3 ± 0.8%; Fig. 3.21 A, B). Surprisingly, the rate of BrdU incorporation (labeling cells in S phase) was not altered upon ectopic GCNF expression (Fig. 3.21 A, B). However, the amount of cells positive for Ki67, which marks cycling cells and is present throughout all cell phases (G1, S, G2, M), was increased in GCNF-overexpressing cultures (Fig. 3.21 C, D). This might point to an effect of GCNF on cell cycle progression. The neural rosettes formed during neuronal differentiation of hESCs are characterized by a confined expression of the M phase marker Phospho-Histone H3 (PH3) to the rosette lumen (Elkabetz et al. 2008). This expression pattern was, however, not observed in the neural rosette structures detected in GCNF-overexpressing It-NES cell cultures (Fig. 3.21 C).

Next, the It-NES cells were treated with the Notch inhibitor DAPT (ND7+DAPT) to accelerate neuronal differentiation and to further assess the potency of GCNF as a negative regulator of differentiation. In agreement with previous observations (Borghese et al. 2010), DAPT treatment resulted in an increased rate of differentiation, while the rate of BrdU incorporation was reduced (Fig. 3.21 E, F). Intriguingly, DAPT treatment was not able to fully abolish the negative impact of GCNF on differentiation and GCNF-overexpressing cultures only contained about 17.0 ± 3.5% of β-III Tubulin-positive cells compared to 35.6 ± 2.3% neurons in control cultures. Nevertheless, like under normal differentiation conditions, GCNF-overexpressing cultures treated with DAPT showed a

similar BrdU incorporation rate as the corresponding control cultures (Fig. 3.21 E, F). Neuronal differentiation, in particular when accelerated by DAPT treatment, is usually accompanied by an increased rate of apoptosis. Both in normal differentiation and in the presence of DAPT, ectopic GCNF expression was able to decrease the number of apoptotic cells compared to control cultures, as measured by flow cytometry analysis for caspase activity (Fig. 3.21 G, H). This effect was even more pronounced in the presence of DAPT, which induced an increase of apoptotic cells to 14.9 ± 1.5% in control cultures, compared to 6.7 ± 1.3% in GCNF-overexpressing cultures (Fig. 3.21 G, H).

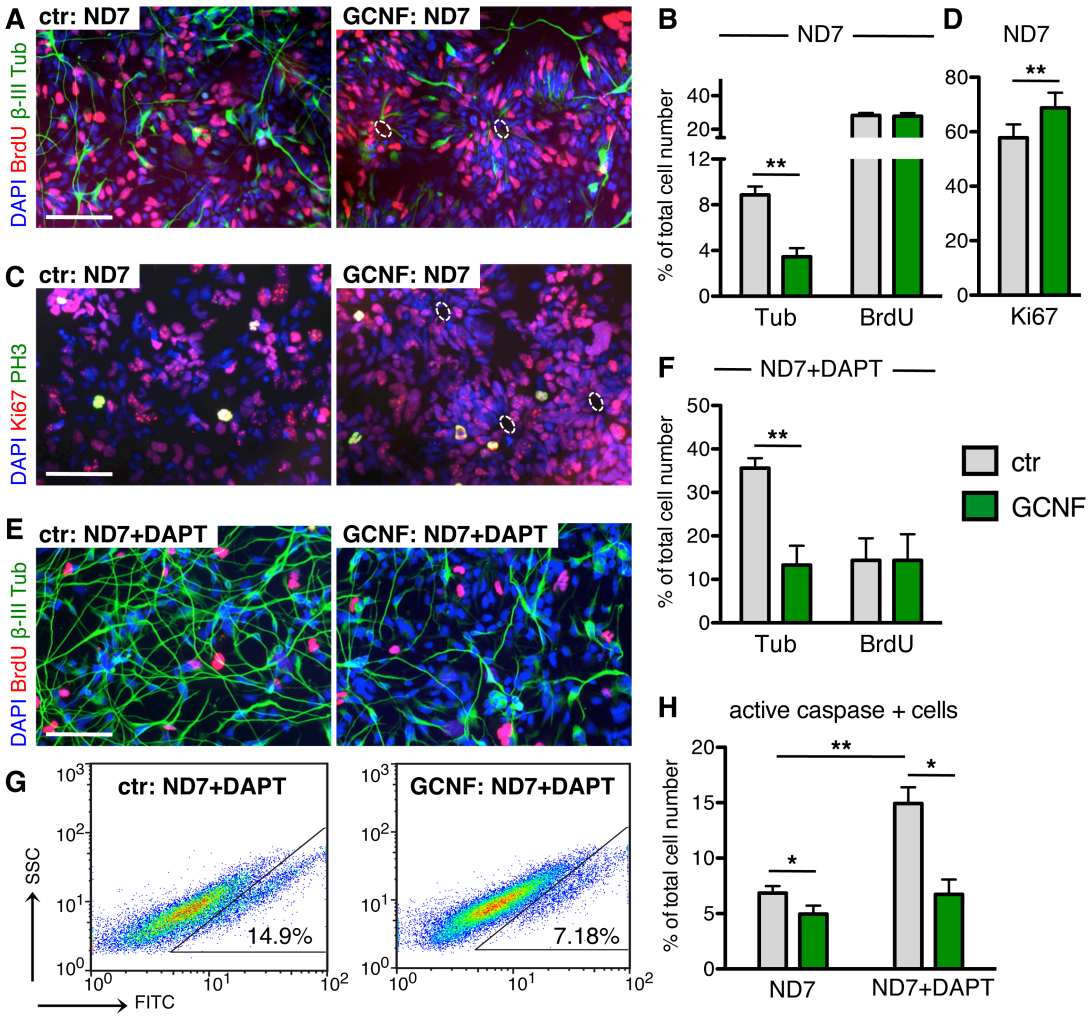

Fig. 3.21: GCNF overexpression attenuates the effects of the Notch inhibitor DAPT on neuronal differentiation and cell apoptosis. (A, C) Immunofluorescence staining for β-III Tubulin plus BrdU **(A)** and Ki67 plus PH3 **(C)** in 7 days differentiated lt-NES cells expressing either pTight-ctr or pTight-GCNF. Ovals indicate rosette lumens. **(B, D)** Quantifications of the percentages of β-III Tubulin-, BrdU-, or Ki67-positive cells, respectively. **(E)** Immunofluorescence staining for β-III Tubulin plus BrdU in lt-NES cells expressing either pTight-ctr or pTight-GCNF and differentiated for 7 days in the presence of doxycycline and DAPT (ND7+DAPT). **(F)** Corresponding quantifications of the percentages of β-III Tubulin- or BrdU-positive cells, respectively. **(G, H)** Flow cytometry-based assay to measure the amount of cells with active caspase labeled by a FITC-coupled caspase inhibitor. **(G)** Representative dot plot analysis for SSC (side scatter) and FITC in lt-NES cells expressing either pTight-ctr or pTight-GCNF after differentiation in the presence of DAPT for 7 days. Triangle indicates apoptotic cells with high FITC fluorescence signal. **(H)** Corresponding quantification of FITC-positive cells in lt-NES cell cultures differentiated for 7 days in the absence (ND7) or presence of DAPT (ND7+DAPT). All quantification data are presented as mean + SEM; n ≥ 3; *, p ≤ 0.05; **, p ≤ 0.01. All scale bars = 100 μm.

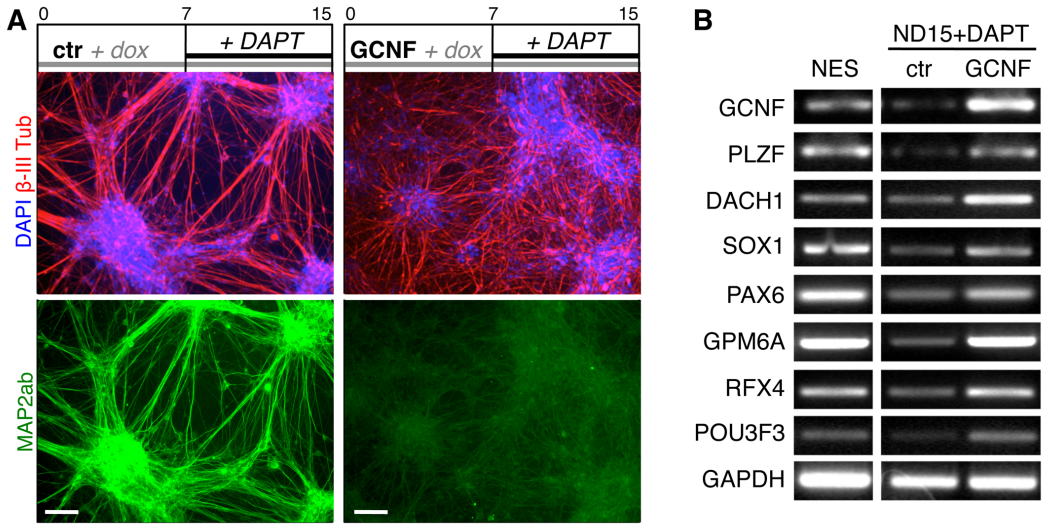

Fig. 3.22: GCNF overexpression delays neuronal maturation while preserving high expression levels of NSC-associated genes. (A) I3 lt-NES cells expressing either pTight-ctr or pTight-GCNF were cultured for 15 days in the presence of doxycycline in differentiation medium that was supplemented with DAPT for the last 7 days (ND15+DAPT). **(B)** Corresponding immunofluorescence stainings for β-III Tubulin and MAP2ab in ND15+DAPT differentiated lt-NES cell cultures. Scale bars = 100 μm. **(C)** Semi-quantitative RT-PCR analysis in self-renewing lt-NES cells and in ND15+DAPT differentiated cultures. GAPDH was used as quantitative reference.

The delay of neuronal differentiation induced by GCNF overexpression was also visible after prolonged differentiation of lt-NES cells for 15 days, whereby DAPT was added for the last 7 days (ND15+DAPT; Fig. 3.22). Under this condition, control cells formed neuronal clusters that are connected by fasciculated neurites and showed expression of the maturation marker MAP2ab (Fig. 3.22 A). In contrast to this, GCNF-overexpressing cells formed a loose and – judging by the lack of MAP2ab expression – less mature neuronal network (Fig. 3.22 A). This was accompanied by higher expression levels of NSC-associated markers, like PLZF, DACH1, SOX1 etc., in the GCNF-overexpressing cultures (Fig. 3.22 B). This finding, together with the increased stability of the neural rosette morphology, indicates that GCNF-overexpressing cells tend to longer maintain their NSC character, even under differentiation-inducing conditions.

In an attempt to corroborate this hypothesis, the clonal capacity, i.e. the capacity to generate multipotent clones at a single cell level, of the differentiated control and GCNF-overexpressing cultures was assessed. For this purpose, pre-differentiated I3 and H9.2 lt-NES cells derived from ND15+DAPT samples were replated on mouse astrocytes at a clonal density and cultured for two weeks under self-renewing conditions (Fig. 3.23 A; for more details see Methods section 2.1.8). In this NES/astrocytes co-culture paradigm both control and GCNF-overexpressing cells were able to generate Nestin-positive colonies with rosette morphology and typical ZO1 expression (Fig. 3.23 C, shown for GCNF-NES derived cultures only). Theses colonies were visualized by immunofluorescence with an antibody to human nuclear protein (anti-human Nuclei) and quantified using the CellaVista (SynenTec) automated microscopy device (Fig. 3.23 B).

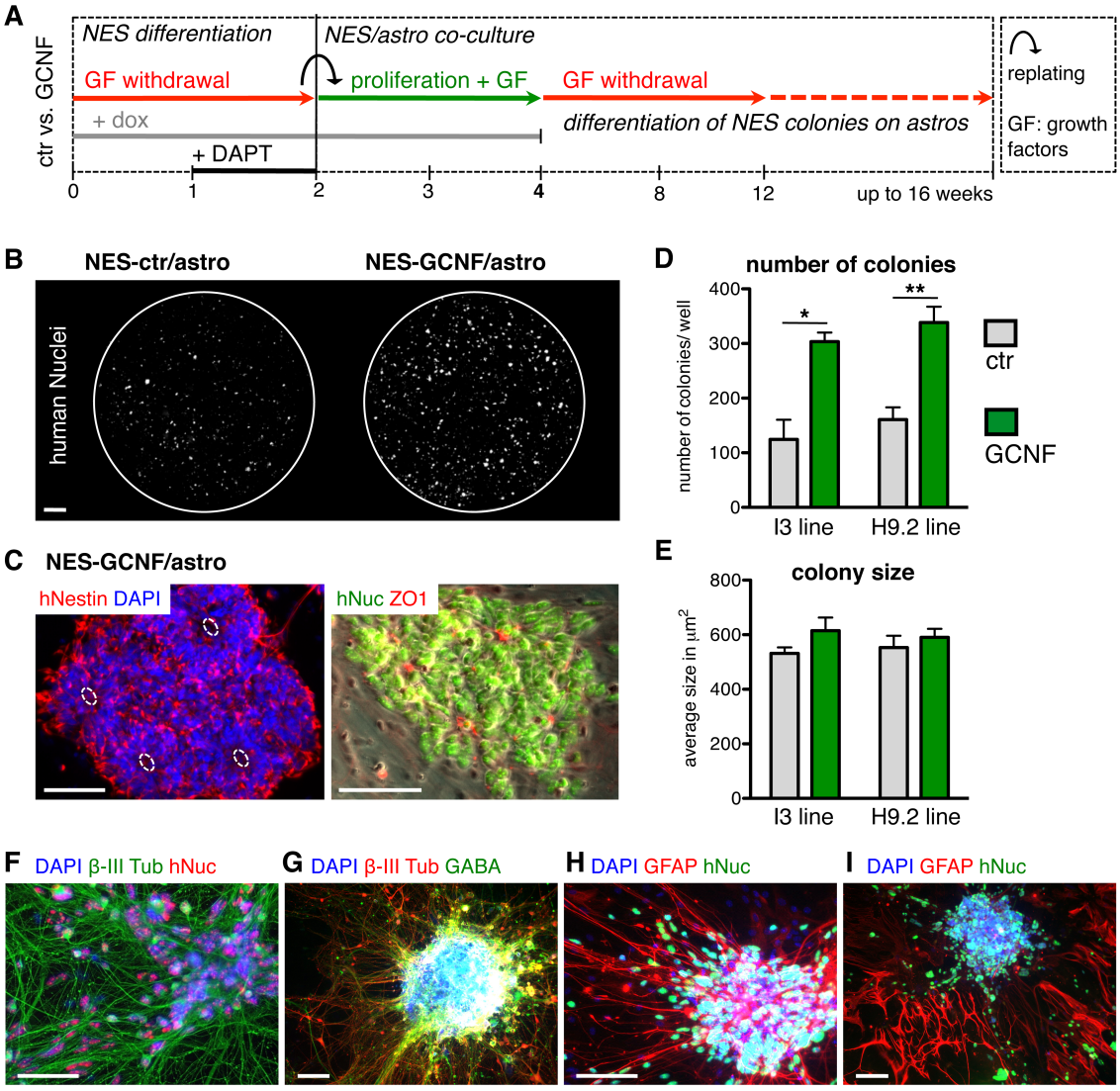

Fig. 3.23: Enhanced recovery of lt-NES cell colonies from pre-differentiated GCNF-overexpressing lt-NES cell cultures. (A) Lt-NES cells expressing either pTight-ctr or pTight-GCNF were cultured for 15 days in differentiation medium without growth factors (GF) supplemented with DAPT for the last 7 days (ND15+DAPT). The cells were replated on a mouse astrocytes layer in order to determine their clonal capacity and differentiation potential. The NES/astrocytes co-cultures were cultured for two weeks in the presence of growth factors (+ GF) to allow colony formation and subsequently differentiated again by growth factor withdrawal. **(B)** Representative whole-well images showing human lt-NES cell colonies in the I3 lt-NES/astrocytes co-cultures as indicated by human Nuclei (hNuc) immunofluorescence stainings. Pictures were taken after two weeks of culturing. Scale bar = 4 mm. **(C)** Immunofluorescence stainings for human Nestin, human Nuclei and ZO1 in I3 lt-NES cell GCNF/astrocytes co-cultures. Scale bars = 100 μm. **(D)** Number of human Nuclei-positive colonies detected per well in the co-cultures of astrocytes and pre-differentiated control or GCNF-overexpressing lt-NES cells from the I3 and H9.2 lines. Data are presented as mean + SEM; n = 3; *, $p \leq 0.05$; **, $p \leq 0.01$. **(E)** Average size of colonies in the above-described conditions. Data are presented as mean + SEM; n = 3. **(F-I)** Immunofluorescence stainings for β-III Tubulin human plus human Nuclei **(F)**, β-III Tubulin plus GABA **(G)** and GFAP plus human Nuclei **(H, I)** in colonies generated from I3 GCNF-overexpressing cells grown on mouse astrocytes and differentiated for another 4-8 weeks. Note that (H) shows a GFAP-positive human colony, while (I) shows a GFAP-negative human colony. Scale bars = 100 μm.

This analysis revealed a significant higher amount of colonies generated from GCNF-overexpressing cells compared to control cells (Fig. 3.23 D). This effect was consistently observed in I3 as well as in H9.2 lt-NES cell-derived co-culture experiments. For instance, in I3 control-lt-NES/astrocytes co-cultures approximately 124 colonies per wells were detected, whereas GCNF-overexpressing lt-NES/astrocytes co-cultures contained around 303 colonies per well. Since the average colony size was similar in both control and GCNF-overexpressing lt-NES/astrocytes co-cultures, a growth advantage of the GCNF-derived colonies can be excluded (Fig. 3.23 E). In order to address the multipotency of the clones, i.e. their ability to generate neurons, astrocytes and oligodendrocytes, the co-cultures were further differentiated for up to 3 months (see scheme in Fig. 3.23 A). This analysis revealed that all clones had been able to differentiate into β-III Tubulin- and GABA-positive neurons (Fig. 3.23 F, G). However, only a few clones contained GFAP-expressing cells and no OLIG2-positive oligodendrocytes progenitors were detected in both control and GCNF-overexpressing lt-NES cell-derived colonies (Fig. 3.23 H, I; data not shown).

Taken together, GCNF stabilizes neural rosette formation and delays neuronal differentiation. Furthermore, both control and GCNF-overexpressing cultures still contain cells with self-renewal capacity even after two weeks of pre-differentiation. The amount of proliferative cells is, however, increased upon ectopic expression of GCNF, indicating that GCNF might be involved in maintaining neural stem cell properties.

3.3.4 GCNF represses the expression of pro-neural bHLH transcription factors

GCNF is considered to act as a transcriptional repressor through binding to a response element, which is arranged as a DR0 element (direct repeat element with 0 spacing) of the core motif AG(G/T)TCA (Fig. 3.24 B). To gain more insight into the biological function of GCNF, the MAPPER platform (Marinescu et al. 2005) was used for the identification of GCNF binding sites within the promoters of human genes. Gene Ontology classification using DAVID (Huang et al. 2009) revealed that many of the putative target genes are associated with “neuronal fate commitment”, “neuron projection morphogenesis” and “synaptic transmission” (Fig. 3.24 A). Among the genes associated with “neuronal fate commitment” was also ATOH1 (also known as MATH1), which is a member of the pro-neural group of activating basic helix-loop-helix (bHLH) transcription factors (Farah et al. 2000). Since the pro-neural bHLH transcription factors are known to contribute to neuronal differentiation, the promoter sequences of ASCL1 (also known as MASH1), ATOH1, NEUROD1, NEUROD4, NEUROG1 and NEUROG2 were analyzed in detail using the Transcriptional Regulatory Element Database and the GCNF TRANSFAC annotation, which revealed the presence of several putative GCNF binding sites (Fig. 3.24 B).

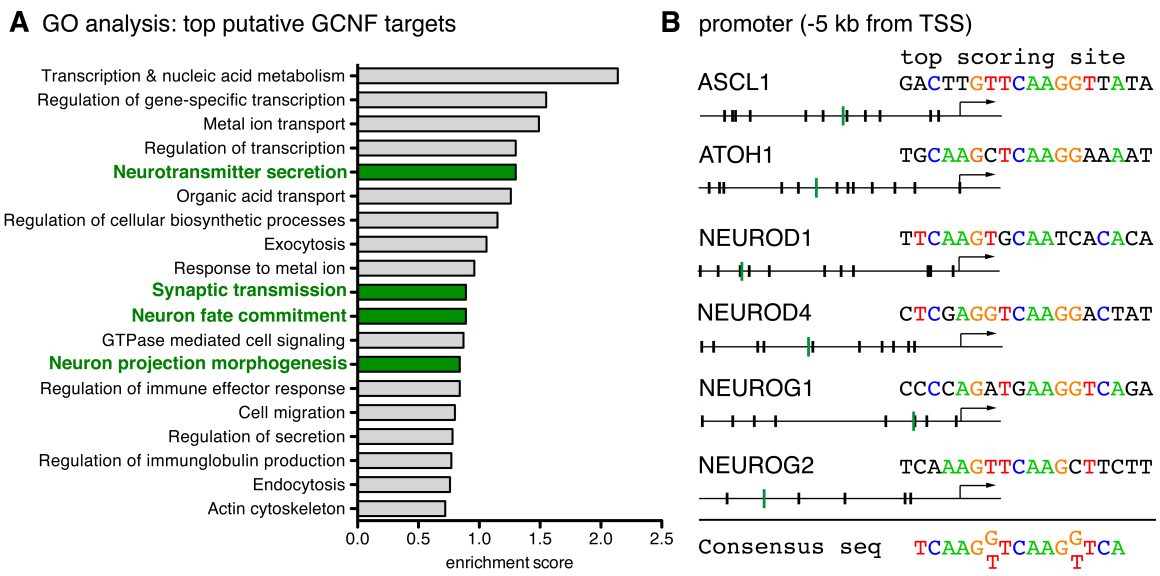

Fig. 3.24: Predicted targets of GCNF comprise genes associated with neural development and neuron function. **(A)** Gene Ontology (GO) analysis using DAVID (Huang et al. 2009) was performed to identify biological processes in which putative GCNF target gene were overrepresented. The top 16 functional clusters according to the enrichment score are shown. Clusters directly associated with neural functions are highlighted in green. **(B)** Schematic representation of the GCNF binding sites in the promoter sequences (5 kb upstream of the transcription start site (TSS)) of the indicated genes. Top-scoring binding sites are indicated by green color and their corresponding sequence is displayed in the right panel.

In order to determine whether the transcriptional activity of the pro-neural bHLH genes is directly influenced by GCNF, their expression levels were monitored in a time course. To that end, lt-NES cells were treated with doxycycline for 12 to 72 hours (12-72) or cultured for 12 hours without doxycycline (0) before harvesting them for RNA isolation (Fig. 3.25 A). Even in the absence of doxycycline, pTight-GCNF transduced lt-NES cells showed a higher level of GCNF expression compared to control cells. However, the GCNF expression level was strongly enhanced after 12 hours of doxycycline administration (Fig. 3.25 B). As shown in Fig. 3.25 B, all of the pro-neural bHLH genes investigated were slightly up-regulated over time in the control cultures. This might be due to the increasing density of the cells, which itself represents a stress factor for the cells and might, thus, promote premature differentiation. Another explanation might be that the treatment with doxycycline has an unspecific effect. In fact, there are several reports indicating that doxycycline has additional effects besides its antibiotic or transgene-inducing function (Jantzie et al. 2005; Lazzarini et al. 2013; Chang et al. 2014). Nevertheless, transcript levels of NEUROD1, NEUROD4 and NEUROG1 were rapidly reduced by 24 hours of doxycycline-activated GCNF overexpression suggesting that this down-regulation might be directly mediated by GCNF (Fig. 3.25 B). Expression levels of ASCL1 were instead not significantly affected by GCNF overexpression (data not shown). Due to their low level of expression in lt-NES cells, it was not possible to reliably determine whether GCNF would also influence expression of ATOH1 and NEUROG2 (data not shown).

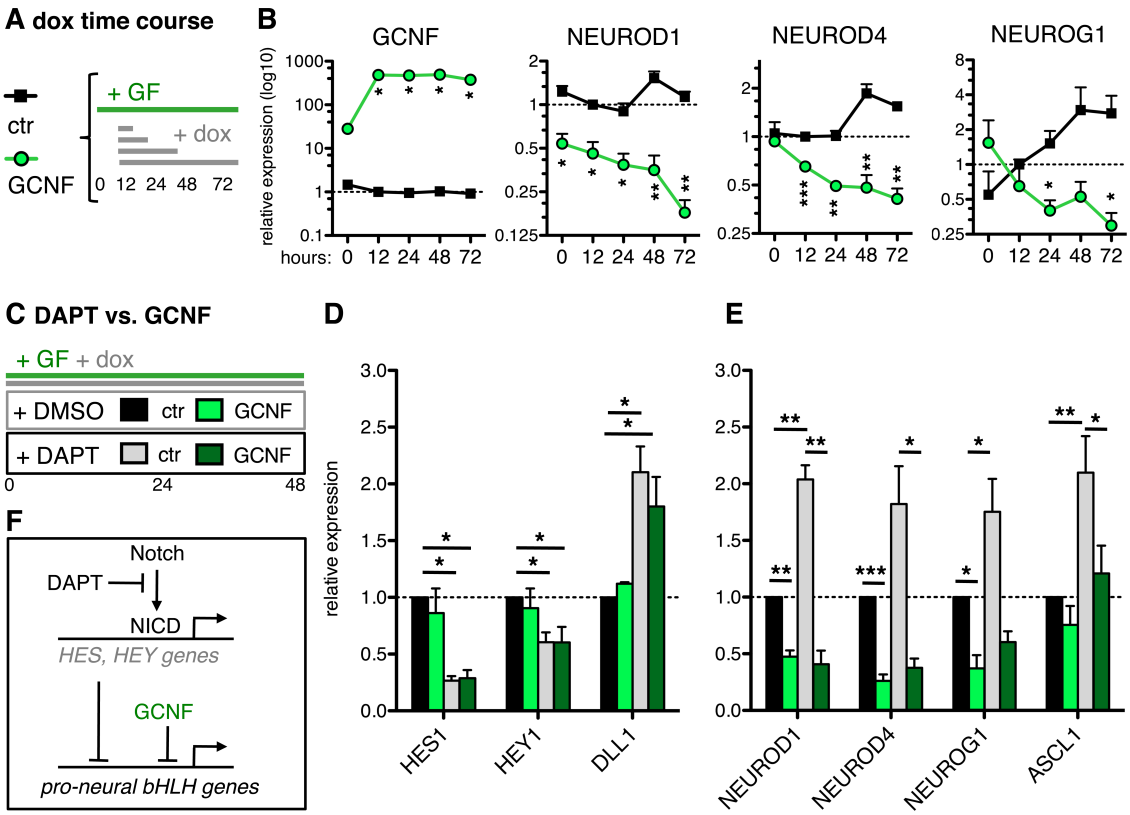

Fig. 3.25: GCNF down-regulates the expression of pro-neural bHLH transcription factors. (A, B) Self-renewing I3 lt-NES cells carrying either pTight-ctr or pTight-GCNF were treated for different time spans with doxycycline (0-72 hours) in the presence of growth factors (+ GF) and directly harvested for RNA preparation. **(B)** Corresponding qRT-PCR expression analysis of GCNF and pro-neural bHLH transcription factors. Data are shown relative to the expression in lt-NES-control cells after 12 hours of doxycycline treatment (set to 1; *, compared to the respective control condition). **(C-E)** I3 lt-NES cells were cultured for 48 hours in the presence of growth factors and doxycycline and additionally treated with either DMSO or DAPT. Corresponding qRT-PCR analysis of HES1, HEY1, DLL1 **(D)** and pro-neural bHLH transcription factors **(E)**. Data are shown relative to the expression in pTight-ctr expressing cells treated with DMSO (set to 1). Quantitative RT-PCR data were normalized to 18s rRNA levels and are presented as mean + SEM (n = 4; *, $p \leq 0.05$; **, $p \leq 0.01$; ***, $p \leq 0.0001$). **(F)** Inhibition of Notch signaling by DAPT results in the up-regulation of pro-neural bHLH genes via the down-regulation of their transcriptional repressors HES and HEY.

The fact that DAPT treatment was not able to fully counteract the GCNF-mediated impairment of neuronal differentiation suggests that GCNF might exert its function in parallel to or down-stream of Notch signaling. Notch-mediated induction of the HEY and HES transcription factors is known to lead to the repression of pro-neural bHLH genes (Kageyama et al. 2005), thus representing a point where GCNF and Notch signaling might converge (Fig. 3.25 F). As expected, upon DAPT treatment of lt-NES cells for 48 hours, the expression levels of HES1 and HEY2 were down-regulated concomitantly with an up-regulation of pro-neural bHLH genes (Fig. 3.25 C-E; compare ctr + DMSO to ctr + DAPT; see also Borghese et al. 2010). Intriguingly, GCNF overexpression interfered with DAPT-mediated induction of NEUROG1, NEUROD1, NEUROD4 and ASCL1 in lt-NES cells (Fig. 3.25 E) after 48 hours treatment. However, GCNF had no influence on the up-regulation of HES1 and HEY1 expression upon DAPT treatment (Fig. 3.25 D). Furthermore, GCNF did not affect DLL1 expression, which was

increased upon DAPT treatment in both control and GCNF-overexpressing cultures. It is known that elevated DLL1 expression activates Notch signaling in neighboring cells and thereby inhibits them from entering differentiation, a mechanism referred to as lateral inhibition (Chitnis et al. 1996). Thus, it is tempting to speculate that GCNF would only act on a subset of HES/HEY target genes that usually promote neuronal differentiation. To conclude, GCNF might contribute to the maintenance of neural stem cells by suppressing the expression of pro-neural bHLH transcription factors and other genes involved in neuronal differentiation and outgrowth.

3.3.5 GCNF overexpression inhibits the generation of TH-positive neurons

As described earlier, miR-181a promotes general neuronal differentiation, in part through targeting GCNF (see. 3.3.2). Thus it is tempting to speculate that the down-regulation of GCNF by miR-181a might be also relevant in the context of dopaminergic differentiation. In fact, co-expression of GCNF-cDNA (lacking the miRNA-regulated 3' UTR) was able to attenuate the positive impact of miR-181a on the yield of TH-positive neurons generated during default differentiation of lt-NES cells (Fig. 3.26 A).

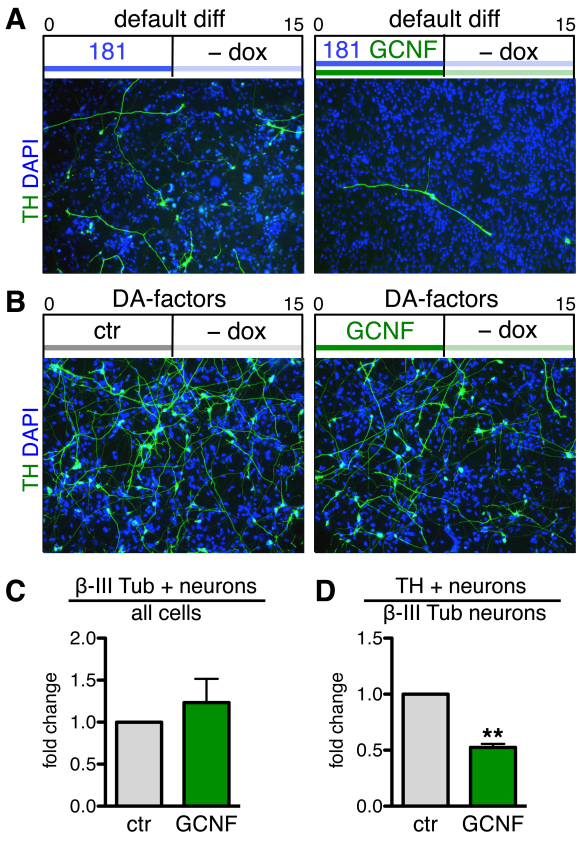

Fig. 3.26: GCNF overexpression impairs the generation of TH-positive neurons. (A) Lt-NES cells carrying either pTight-miR-181a/a* alone or pTight-miR-181a/a* plus pTight-GCNF were differentiated for 7 days in the presence of doxycycline and for another 7 days without doxycycline (– dox) according the default differentiation protocol and subsequently analyzed by immunofluorescence stainings for TH. **(B-D)** Lt-NES cells carrying either pTight-ctr or pTight-GCNF were cultured for one week in the presence of FGF8b, SHH signaling (DA-factors) and doxycycline followed by one week of differentiation without doxycycline (– dox). **(B)** Immunofluorescence stainings for TH. **(C-D)** Fold change in the numbers of neurons (β-III Tubulin-positive cells, **C**) and in the number of TH-positive neurons relative to the total number of neurons **(D)**. Data are presented as mean + SEM compared to pTight-ctr cells (set to 1; n = 3; **, $p \leq 0.01$). All scale bars = 100 μm. Data in B-D were generated in collaboration with Katharina Doll.

In order to determine the effect of GCNF overexpression more precisely, lt-NES cells expressing either pTight-ctr or pTight-GCNF were differentiated in the presence of DA-factors to enrich for TH-positive neurons. In detail, lt-NES cells were first cultured for one week with FGF8b and SHH agonists in the presence of doxycycline to activate transgene expression. Subsequently, the cells were differentiated for another week in the presence of neurotrophic factors but without doxycycline to exclude any unspecific effects due to a decreased neuronal differentiation rate. Under these conditions, overexpression of GCNF had no apparent impact on the number of β-III Tubulin-positive cells (Fig. 3.26 C), indicating that the short-term GCNF overexpressing in the presence of proliferative signals (SHH, FGF8b) did not affect general neuronal differentiation. However, the proportion of TH-positive neurons was significantly decreased by ~ 0.5 fold in GCNF-overexpressing cultures compared to control cultures (Fig. 3.26 B, D). These data point to an inhibitory effect of GCNF on the generation of dopaminergic neurons. Thus, miR-181a-mediated down-regulation of GCNF might in part explain the positive effect of miR-181a on the dopaminergic lineage.

3.3.6 MicroRNA-181a promotes the emergence of TH-positive neurons by potentiating Wnt signaling

According to target prediction analysis, miR-181a also has the potential to regulate various components of the Wnt pathway, whereby several of these putative target genes have been associated with a negative function on the Wnt signaling cascade (Fig. 3.27). In particular, the nemo-like kinase (NLK), which interferes with the β-catenin/TCF-induced activation of Wnt target genes, has been validated as miR-181a target in hepatocytes and natural killer cells (Ji et al. 2009; Cichocki et al. 2011).

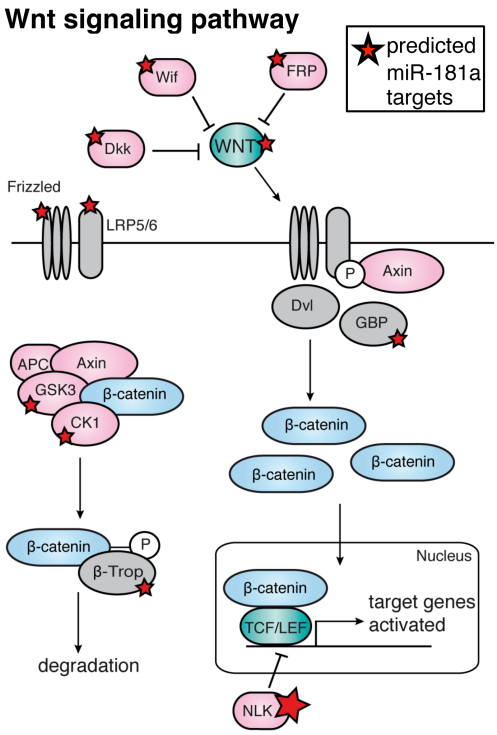

Fig. 3.27 Components of the canonical Wnt pathway potentially targeted by miR-181a. Secreted Wnt ligands bind to their cognate receptor complex consisting of the transmembrane receptor Frizzled and its co-receptor LRP. In the absence of Wnt signal, β-catenin is targeted by coordinated phosphorylation mediated by the APC/Axin/GSK3β-complex leading to its ubiquitination and proteasomal degradation. The presence of Wnt signaling leads to the activation of the intracellular protein Dishevelled (Dvl), which inhibits the action of the β-catenin destruction complex. In this setting, β-catenin accumulates in the cytosplasm and subsequently enters the nucleus where it interacts with the TCF/LEF transcription factors to activate transcription of Wnt target genes. Red stars indicate potential miR-181a targets as inferred from target prediction analysis combined with KEGG pathway annotation. Pathway components, which are believed to negatively affect Wnt signaling activity, are indicated by red color.

Wnt signaling is essentially involved in dopaminergic lineage development. Pharmacological activation of this pathway, by the GSK3 inhibitor CHIR (Ring et al. 2003) is a key mechanisms of many current protocols aiming at the *in vitro* generation of DA neurons (reviewed by Hegarty et al. 2013; Arenas 2014). Thus, one could speculate that miR-181a might promote DA neuron development by enhancing Wnt activity through the down-regulation of negative modulators of this pathway.

As a tool to test this hypothesis, a Wnt reporter lt-NES cell line was established in collaboration with Katharina Doll. For this purpose, lt-NES cells were transduced with the 7xTCF::EGFP lentiviral construct established by Fuerer & Nusse (2009), which carries an enhanced GFP (EGFP) expression cassette under the control of a promoter containing seven TCF transcription factor binding sites (7xTCF; Fig. 3.28 A). Activation of the canonical Wnt/β-catenin signaling leads to the activation of the transcription factor TCF, which in turn induces the expression of Wnt target genes (Fig. 3.27). Hence, TCF-driven EGFP expression, which is easily assessed by flow cytometry, can directly monitor canonical Wnt activity. The sensitivity of the 7xTCF::EGFP reporter in lt-NES cells was validated by a CHIR dose-response curve (Fig. 3.28 B).

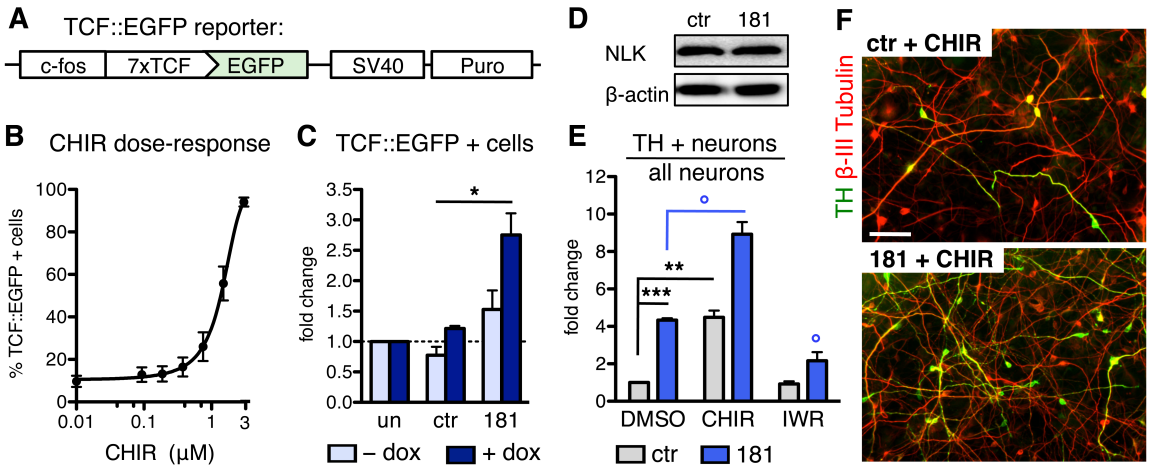

Fig. 3.28: MicroRNA-181a overexpression enhances Wnt signaling in lt-NES cells. (A) Schematic composition of the 7xTCF::EGFP reporter developed by Fuerer & Nusse et al. (2009). **(B)** Dose-response curve of CHIR treatment on the amount of EGFP-positive cells as monitored by flow cytometry. Data are presented as mean + SEM, n = 7. **(C)** Histogram showing the fold change in the percentage of EGFP-positive cells in untransduced (un) lt-NES cells or in cells transduced with pTight-ctr or pTight-miR-181a/a*, respectively, and cultured for 4 days with or without doxycycline. Data were generated by flow cytometry analysis and are presented as mean + SEM, relative to "un + dox" cells (set to 1; n = 3; *, $p \leq 0.05$). **(D)** Western blot analysis of NLK in lt-NES cells transduced with pTight-ctr or pTight-miR-181a/a* and cultured for 6 days in the presence of doxycycline. Beta-actin was used as loading control. **(E, F)** Transduced lt-NES cells carrying the pTight-ctr or the pTight-miR-181a/a* construct were differentiated for 15 days in the presence of doxycycline and co-treated with either CHIR, IWR or with DMSO as vehicle control, respectively. **(E)** Fold change in the number of TH-positive neurons relative to the total number of neurons as indicated by β-III Tubulin staining. Data are presented as mean + SEM compared to untreated pTight-ctr cells (set to 1; n = 4; *, compared to "ctr + DMSO"; ° compared to "181 + DMSO": °, $p \leq 0.05$; **, $p \leq 0.01$; ***, $p \leq 0.0001$). **(F)** Corresponding immunofluorescence stainings for TH and β-III Tubulin in pTight-ctr or -miR-181a/a*-overexpressing lt-NES cells differentiated in the presence of CHIR. Scale bar = 100 µm. Data shown in A-D were generated in collaboration with Katharina Doll.

Next, the Wnt-reporter cell line was transduced with the doxycycline-inducible pTight system to overexpress miR-181a/a*. As controls, lt-NES cells without the pTight system (untransduced) or cells transduced with the pTight-ctr construct were used. Lt-NES cells were cultured for 4 days in the presence or absence of doxycycline before monitoring EGFP fluorescence by flow cytometry. Overexpression of miR-181a/a* significantly increased the number of EGFP-positive cells by 2.7 ± 0.2 fold compared to untransduced cells (Fig. 3.28 C), confirming that miR-181a/a* enhances canonical Wnt activity in lt-NES cells. However, in contrast to what has been described in the literature, the regulatory impact of miR-181a on NLK protein synthesis could not be confirmed in lt-NES cells (Fig. 3.28 D).

To address the functional relevance of the interaction between miR-181a and Wnt signaling, the impact of pharmacological Wnt modulation on the generation of TH-positive neurons upon miR-181a/a* overexpression was analyzed. To that end, lt-NES cells were differentiated for 15 days and continuously treated with CHIR or with the Wnt inhibitor IWR (Chen et al. 2009). As expected, CHIR treatment increased the yield of TH-positive neurons in pTight-ctr transduced cultures by 4.5 ± 0.4 fold compared to pTight-ctr cultures treated with DMSO as vehicle control (Fig. 3.28 E). Interestingly, the combination of pharmacological Wnt activation and miR-181a/a* overexpression appeared to have an additive effect and further increased the number of TH-positive neurons by 8.9 ± 0.6 fold compared to CHIR-treated pTight-ctr cultures and to the overexpression of miR-181a/a* alone (181 + DMSO: 4.3 ± 0.1 fold; Fig. 3.28 E, F). On the contrary, inhibition of Wnt signaling by IWR attenuated but not completely abrogated the effect of miR-181a on the yield of TH-positive neurons (Fig. 3.28 E).

Taken together, these findings indicate that miR-181a enhances Wnt signaling, which might, at least in part, account for the positive effect of miR-181a on dopaminergic differentiation, similar to pharmacological Wnt activation. However, it is very likely that many other mechanisms, including the down-regulation of GCNF, also contribute to this function of miR-181a.

4 DISCUSSION

Numerous studies, mainly performed in animal models, have demonstrated the overall importance of miRNAs during neural development and led to the identification of specific miRNAs regulating neural stem cell self-renewal, differentiation and subtype specification (reviewed by Roese-Koerner et al. 2013; Sun & Lai 2013). However, in order to specifically evaluate the role of miRNA-based regulation on human neural development, these studies need to be extended to suitable human cell culture systems. In particular, lt-NES cells represent a versatile cellular platform for this purpose, since they are easy to maintain, have stable self-renewal and differentiation capacities and are amenable to genetic modifications (Koch et al. 2009b; Falk et al. 2012). Furthermore, lt-NES-like cells have lately been isolated from human fetal hindbrain tissue (Tailor et al. 2013), indicating that lt-NES cells do not represent an artifact due to *in vitro* culture conditions. Thus, this work mostly relied on lt-NES cells as a cell culture model in order to identify miRNAs regulating human neuronal differentiation and subtype specification. First, a comprehensive analysis of the miRNA expression changes during hESC-based neuronal differentiation using lt-NES cells as a stable intermediate was performed. Second, several miRNAs found to be up-regulated during neuronal differentiation, i.e. miR-124, miR-125b, miR-181a/a*, miR-153 and miR-324-5p/3p, were analyzed for their potential impact on neuronal differentiation and dopaminergic subdifferentiation (Fig. 4.1 A). Since miR-181a was found to have a remarkable action both on general neuronal differentiation and the differentiation into dopaminergic neurons, the third part of this thesis focused on deciphering the mechanistic functions and target genes of miR-181a (Fig. 4.1 B).

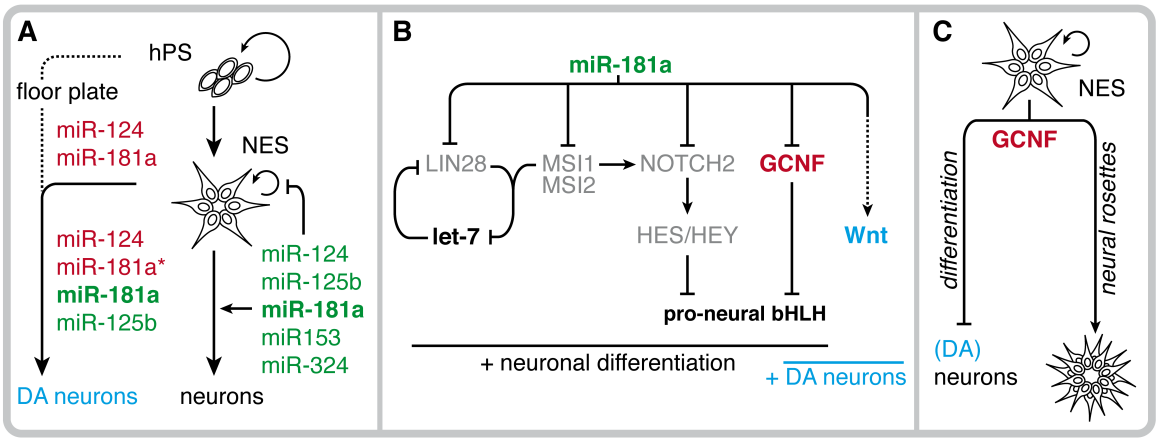

Fig. 4.1: Schematic summary of the major findings presented in this thesis. Summary of the observed impacts (green, positive; red, negative) of the investigated miRNAs. **(A)** MicroRNA-153, miR-181a/a* and miR-324-5p/3p were identified as novel miRNAs contributing to human NSCs neuronal differentiation. MicroRNA-124, miR-125b and miR-181a/a* have additionally functions during dopaminergic (DA) differentiation. **(B)** On a mechanistic level, miR-181a might promote neuronal differentiation by down-regulating NSC-associated genes. MicroRNA-181a also enhances Wnt activity, which might contribute to the increased rate of dopaminergic differentiation. Furthermore, GCNF was identified as a direct target of miR-181a, which might be relevant both in the context of general neuronal and dopaminergic differentiation. GCNF might impair neuronal differentiation by preventing premature expression of pro-neural bHLH transcription factors **(B)**. The impaired neuronal differentiation rate in GCNF-overexpressing lt-NES cell cultures was accompanied by a stabilization of the neural rosette morphology typically associated with undifferentiating lt-NES cells **(C)**.

In summary, miRNA-181a/a* as well as miR-153 and miR-324-5p/3p were identified as novel factors contributing to the shift from lt-NES cell self-renewal towards neuronal differentiation (Fig. 4.1 A). In particular, miR-181a/a* was similar potent in promoting neuronal differentiation as the neuronal-associated miR-124 and miR-125b. Overexpression of miR-181a resulted in the down-regulation of several genes involved in NSC maintenance, such as NOTCH2, LIN28A/B and Musashi1/2 (Fig. 4.1 B), which also harbor potential miR-181a binding sites. Furthermore, forced expression of miR-181a induced GCNF down-regulation via direct interaction with the GCNF 3' UTR. Sustained expression of GCNF, in turn, interfered with neuronal differentiation, while preserving the characteristic rosette morphology of undifferentiated lt-NES cells (Fig. 4.1 C). Further experiments revealed that GCNF might act in parallel to Notch signaling to maintain lt-NES cells in an undifferentiated state by preventing premature expression of pro-neural bHLH genes (Fig. 4.1 B). Indeed, GCNF overexpression was able to partially counteract the effects of the Notch inhibitor DAPT on pro-neural bHLH gene expression and neuronal differentiation.

In addition to their function on general neuronal differentiation, some of the investigated miRNAs also had specific effects on neuronal subtype specification and dopaminergic differentiation. In detail, overexpression of miR-181a and miR-125b in lt-NES cells increased the yield of TH-positive DA-like neurons, while miR-181a* and miR-124 impaired the generation of this population. These findings were integrated into a transfection-based miRNA modulation approach to further increase the generation of TH-positive neurons from lt-NES cells. Ectopic expression of the respective miRNAs in a culture system specifically devised for the generation of DA neurons using hPSC-derived floor plate progenitor cells confirmed the positive and negative impacts of miR-181a and miR-124 on this lineage. On a mechanistic level miR-181a might contribute to dopaminergic differentiation both by potentiating Wnt/β-catenin signaling and repressing the expression of GCNF, which was identified to have a negative effect on this lineage (Fig. 4.1 B).

4.1 MicroRNA expression signatures discriminate distinct stages of hESC-based neuronal differentiation

Earlier miRNA profiling studies in the developing rodent brain and during *in vitro* neuronal differentiation have demonstrated that miRNA expression is extensively regulated during neurogenesis (Miska et al. 2004; Sempere et al. 2004; Krichevsky et al. 2006; Landgraf et al. 2007; Hohjoh et al. 2007; Dogini et al. 2008). Nevertheless, when the miRNA profiling project presented here was started, the insight into miRNA expression associated with human neuronal differentiation was rather scarce. Due to the limited access to primary human neural tissue, many studies made use of the human NTera2/D1 teratomcarcinoma cell line, which can be directed towards neuronal differentiation, for miRNA expression analyses (Sempere et al. 2004; Hohjoh & Fukushima 2007; Smith et al. 2010). However, the lt-NES cells used in this thesis were expected to constitute a more suitable model system for this purpose. In detail, miRNA expression was profiled in I3 hESCs, self-renewing lt-NES cells and differentiating lt-NES cells (ND15, ND30), and selected miRNA expression profiles were validated by qRT-PCR, Northern blotting using also samples derived from the H9.2 hESC line.

Among the 330 miRNAs covered by the TaqMan Multiplex qRT-PCR array used here, 186 miRNAs were found to exhibit a minimum 2-fold expression difference in the neural cell samples compared to the hESC samples (Fig. 4.2 A). These differentially expressed miRNAs were further subdivided into three major groups (I-III) according to whether they were up-regulated (I) or down-regulated (II) during neuronal differentiation or exclusively expressed in hESCs (III; Fig. 4.2 A). The miRNAs in Group I were further assigned to three subgroups: (Ia) miRNAs with exclusive expression in neural cell samples; (Ib) miRNAs with consistently increased expression during neuronal differentiation; and (Ic) miRNAs, which were initially down-regulated in self-renewing lt-NES cells, but up-regulated again in differentiated neuronal cultures (ND15, ND30; Fig. 4.2 A). Overall, hESCs and lt-NES cells express distinct miRNA signatures, while lt-NES cells and derived neuronal cultures share similar miRNA expression profiles (Fig. 4.2 B-E). One apparent difference between hESCs and the other cell types is the number of miRNAs being expressed. Two-thirds (239) of all miRNAs analyzed were detected in hESCs, whereas the neural cell types expressed only half of the miRNAs analyzed (Fig. 4.2 B-E). This is in apparent contrast with the general concept that the overall repertoire of expressed miRNAs increases during development (Strauss et al. 2006). However, the multiplex qRT-PCR array has a bias towards the hESC-associated miRNA clusters. For instance, the large primate-specific C19MC cluster (Chromosome 19 microRNA cluster), which encodes 59 different mature miRNAs (Bentwich et al. 2005) was represented by 49 miRNAs on the multiplex qRT-PCR array. Another difference in the miRNA repertoire is that lt-NES cells expressed a subgroup (Group Ia) of neural miRNAs, including miR-153 and miR-181a*, which was lacking in hESCs according to the multiplex qRT-PCR array (Fig. 4.2 C, D). Singleplex qRT-PCR was, however, sensitive enough to detect low miR-153 and miR-181a* expression levels in hESCs. Thus, the miRNAs in Group Ia might be rather characterized by a very low expression level in hESCs and a strong up-regulation in lt-NES cells. Nevertheless, these miRNAs might be promising candidates for functional studies assessing neural lineage entry.

The observed miRNA expression patterns were in most cases consistent with previous findings of developmental- and cell-specific miRNA signatures. For instance, in agreement with previous profiling data (e.g. Laurent et al. 2008), the majority of the C19MC miRNAs was detected only in hESCs (Fig. 4.2 C). Likewise, members of the ESC-enriched miR-302/367 and miR-371-3 clusters were predominantly expressed in hESCs according to the profiling analysis (Group II and III). Intriguingly, some members of the miR-302/367 cluster as well as miR-372 and miR-373 were still expressed in lt-NES cells (Fig. 4.2 D). A similar persistent expression of ESC-enriched miRNAs during early neuronal induction has been described by other profiling studies (Wu et al. 2007; Placantonakis et al. 2009; Smith et al. 2010). However, mature miR-302 and miR-371 have been shown to specifically inhibit neural induction (Rosa et al. 2009; Rosa & Brivanlou 2011; Kim et al. 2011; Lipchina et al. 2011). Hence, it remains to be clarified whether the ESC-associated miRNAs have additional functions in neural stem or progenitor cells. In fact, according to Northern blotting, pre-miR-302b, pre-miR-371, and pre-miR-520 are expressed both in lt-NES cells and neuronal cultures indicating that their respective polycistronic miRNA loci might be still transcriptionally active (see also section 4.2.1).

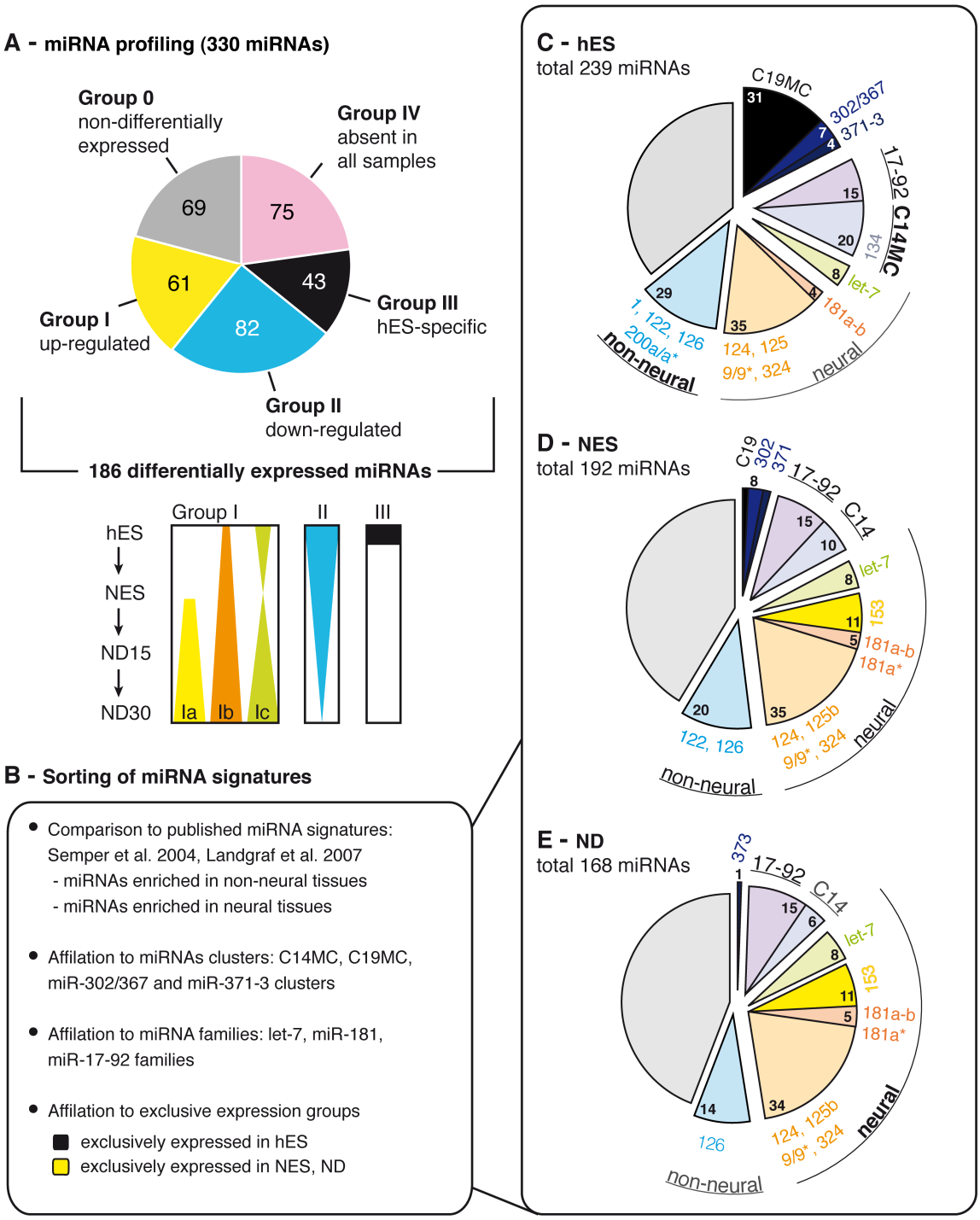

Fig. 4.2: Overview of miRNA profiling in hESCs, lt-NES cells, and neuronal cultures. (A) Schematic showing the different miRNA expression groups: Group I to III encompasses the differentially expressed miRNAs. The other miRNAs were either designated as not significantly expressed (Group IV) or as non-differentially expressed (Group 0). For more details see text. **(B-D)** MicroRNAs found to be expressed in the different cell samples were sorted according to different criteria **(B)**. In brief, miRNAs were sorted to different groups according to their overlap with previous miRNA signatures published by Semper et al. (2004) and Landgraf et al. (2007), and their affiliation to miRNA families and clusters. MicroRNAs exclusively expressed in hESCs or neural samples (NES, ND) are shown in separate pie slices. **(C-E)** Corresponding pie charts illustrating the composition of the miRNA repertoire expressed in hESCs **(C)**, lt-NES cells **(D)** and differentiated neuronal cultures (ND, **E**). MicroRNAs not sorted in to any of the categories listed in B are shown in the light grey pie slice.

However, there are also several miRNAs showing a divergent expression pattern during lt-NES cell differentiation compared to what has been described in the literature. For instance, 5 of the 8 let-7 members analyzed were down-regulated in lt-NES cells compared to hESCs (Group Ib). This expression pattern is in contrast with previous studies demonstrating a continuous up-regulation of let-7 expression during neural induction and neuronal differentiation (Viswanathan et al. 2008; Rybak et al. 2008). Since, the let-7 family members are located on different genomic regions it is unlikely that genomic alterations within the loci could be the cause for this discrepant expression patterns. Intriguingly, let-7a expression was only decreased in I3 lt-NES cells but not in H9.2 lt-NES cells compared to their respective hESC ancestors (Supplementary Fig 6.1). Furthermore, I3 lt-NES cells showed higher expression levels of LIN28A and LIN28B than their H9.2 hESC-derived counterparts (Supplementary Fig 6.1). There is a allelic variant of LIN28A carrying a single nucleotide polymorphism near the let-7 target site, which compromises let-7-mediated LIN28A suppression and, hence, shifts the LIN28/let-7 feedback loop in favor of higher LIN28A expression (Chen et al. 2011). Thus, it would be interesting to assess whether I3 hESCs or I3 lt-NES cells carry this allelic variant or other mutations influencing the LIN28/let-7 feedback loop.

Another exception is the brain-enriched miR-134 (Schratt et al. 2006), which was only detected in hESCs but not in lt-NES cells or differentiated neuronal cultures. Similarly, Wu et al. (2007) reported a strong down-regulation of miR-134 in hESC-derived NSCs and differentiated neurons. These findings are, however, in apparent contrast to the proposed positive effect of miR-134 on neural induction of mouse ESCs (Tay et al. 2008). Furthermore, miR-134 is expressed in rodent neural progenitors and mature neurons, where it promotes progenitor proliferation, attenuates neuronal migration and regulates dendritogenesis (Schratt et al. 2006; Gaughwin et al. 2011). Moreover, miR-134 is part of the large C14MC cluster (Chromosome 14 microRNA cluster, also called miR-379-656 cluster) harboring 52 different mature miRNAs. The rodent homolog of this cluster (miR-379-410) shows a brain-enriched expression pattern (Seitz et al. 2004) and is induced by the transcription factor MEF2 in response to neuronal activity (Fiore et al. 2009). Nearly all of the 20 tested C14MC miRNAs were down-regulated in lt-NES cells as well as in differentiated neuronal cultures and were, thus, classified into Group II or III. It remains to be clarified whether C14MC miRNAs and, in particular miR-134, would be again expressed in more mature lt-NES cell-derived neurons. However, these data could also point to a species-dependent expression pattern of this cluster in human and mouse.

The neuronal cultures (ND15, ND30) used for the profiling analysis exhibited a relatively high variability both with regard to the total amount of expressed miRNAs and the relative miRNA expression levels. Both effects might be due to the fact that the neuronal cultures analyzed here represent a mixture of differentiated young neurons and undifferentiated lt-NES cells. In order to overcome this variability, a good strategy would be to enrich for differentiated neurons using flow cytometry-based cell sorting (FACS). This could be done by using cell surface markers specific for neural progenitors or differentiated neurons as described by Liu et al. (2012). Furthermore, one could also use neuronal-specific fluorescent reporter lines, such as the DCX::EGFP lt-NES cells, which

express EGFP under the control of the doublecortin (DCX) promoter (Ladewig et al. 2008). The miRNA profiling analysis presented here was performed using a multiplex qRT-PCR array. Quantitative RT-PCR analysis has several advantages over miRNA microarrays, as it is more sensitive and covers a wider dynamic range (Benes et al. 2010; reviewed by Pritchard et al. 2012). Both qRT-PCR and microarray are, however, limited with regard to the number of miRNAs covered. During the least years the number of miRNAs identified has increased dramatically and to date there are 2578 different human mature miRNAs listed in the miRBase repository (www.mirbase.org, annotation v20). It is a matter of debate whether all of these annotations represent true and unique miRNAs (Chiang et al. 2010; Langenberger et al. 2011; Kozomara & Griffiths-Jones 2013). Since early miRNA research was focusing on ESC differentiation and neurogenesis (Lagos-Quintana et al. 2002; Houbaviy et al. 2003; Kim et al. 2004), the majority of the miRNAs importantly involved in these processes might have been annotated quite early. Furthermore, many of the newly identified miRNAs are characterized by relatively low expression levels and often show a low degree of evolutionary conservation, which might point to a rather subtle regulatory input of these miRNAs (Morin et al. 2008; Shao et al. 2010; Chiang et al. 2010; Inukai et al. 2012). Thus, although the profiling presented here does not capture the full miRNA repertoire, it might still provide a sufficient coverage rate to yield novel insights into the miRNAs associated with human neuronal differentiation. These data could be then validated and extended to a global scale by using small RNA deep sequencing (Pritchard et al. 2012).

4.2 MicroRNA processing intermediates and sister strands show distinct expression during neuronal differentiation

In addition to the profiling of mature miRNA expression levels, the expression of selected precursor and mature miRNAs was monitored using Northern blotting. This analysis revealed dramatic differences in the relative accumulation of precursor and mature miRNA species in the different cell types analyzed (Fig. 4.3 A).

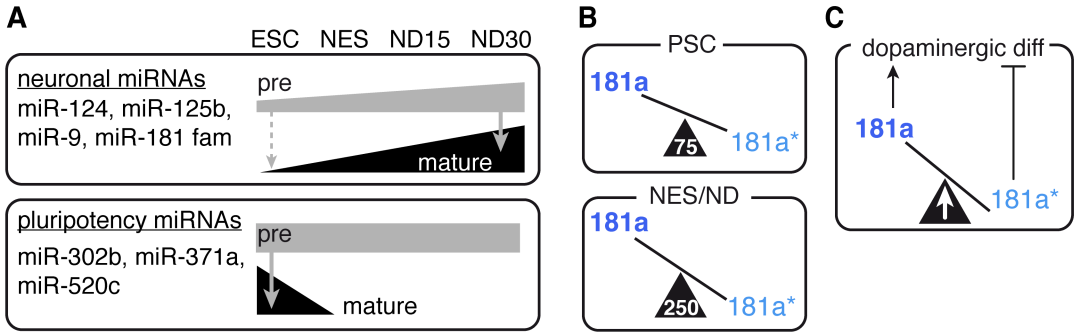

Fig. 4.3: Cell type-dependent pre-miRNA processing rates and variable miR-181a to miR-181a* expression ratios during hES cell-based neuronal differentiation. (A) Schematic summary of the relative abundance of precursor (pre) and mature miRNA species in hESCs, self-renewing lt-NES cells and neuronal cultures (ND15, ND30) as inferred from Northern blot analysis. **(B, C)** Schematic summary of the miR-181a to miR-181a* ratios in hPSCs, self-renewing lt-NES cell cultures and differentiating cultures (ND, **B**), and during dopaminergic differentiation **(C)**.

Furthermore, the relative expression levels of the sister miRNAs, miR-181a and miR-181a*, showed cell type-specific variations during the course of neuronal differentiation (summarized in Fig. 4.3 B, C). These observations are in line with other studies reporting on context-dependent patterns of miRNA processing and strand selection as delineated in the following paragraphs. Taken together, these findings point to an additional level of complexity in regulating miRNA expression and function.

4.2.1 Cell type-specific pre-miRNA processing during neuronal differentiation

Northern blot analyses in hESCs, lt-NES cells, and neuronal cultures revealed a differential expression of mature miRNAs, whereas the corresponding putative precursor forms were ubiquitously expressed (Fig. 4.3 A). This disparate expression pattern was also confirmed for the MIR181A1- and MIR181A2-derived processing intermediates by qRT-PCR. Specifically, the mature-to-precursor ratios for miR-181a was relatively low in hESCs, but was up-regulated in lt-NES cells and neuronal cultures pointing to a compromised pre-miR-181a processing rate in hESCs (Fig. 4.3 A). Conversely, in case of the pluripotency-associated miRNAs, a persistent precursor expression was observed, although the corresponding mature species were only detected at high levels in ESCs. In line with this, Choudhury et al. (2013) have recently shown that pri-miR-302a remains expressed during neuronal differentiation of SH-SY5Y neuroblastoma cells.

MicroRNA processing is tightly regulated at various levels by the concerted action of RNA-binding proteins, ribonucleases, and sequence-editing enzymes (reviewed by Slezak-Prochazka et al. 2010; Treiber et al. 2012). In fact, cell type-specific miRNA processing might be a more general phenomenon than previously thought, and was also reported to be altered in diseases, such as cancer (Thomson 2006; Lee et al. 2007; Moore et al. 2013). However, in most cases the detailed mechanisms and the biological cause of context-specific miRNA processing are still unknown. One discussed hypothesis is that regulating miRNA expression at the processing step may provide a time-saving mechanism for the rapid provision of specific active miRNAs (Slezak-Prochazka et al. 2010). For instance, the presence of precursor forms of differentiation-promoting miRNAs in PSCs might represent a mechanism that allows them to rapidly enter differentiation. In fact, the core pluripotency factors simultaneously drive the expression of pri-let-7g and LIN28A (Marson et al. 2008). Since LIN28A interferes with let-7 processing, let-7 intermediates accumulate in PSCs (Rybak et al. 2008). Upon differentiation LIN28A expression is down-regulated leading to the up-regulation of mature let-7, even in the absence of active pri-let-7g transcription. However, this theory cannot explain the persistent miRNA precursor expression of the pluripotency-associated miRNAs that was observed in the neuronal cultures. Regulation of miRNA processing may also offer a mechanism to uncouple the expression of intronic miRNAs from their host genes. One example is miR-7, which is encoded by the hnRNPK locus and is preferentially expressed in brain and pancreas, although hnRNPK is ubiquitously expressed (Choudhury et al. 2013). In non-neuronal cells, Musashi2 and HuR (ELAVL1) impair processing of pri-miR-7. During neuronal differentiation expression of Mushashi2 is down-regulated allowing expression of mature miR-7. Interestingly, all miRNAs analyzed here, besides miR-520c, are intragenic miRNAs and many of them are localized within long intergenic non-coding RNAs.

Thus, it would be interesting to determine the correlation between the miRNA processing intermediates and their host genes. Furthermore, regulation of miRNA processing is used to individually control the expression of clustered miRNAs. For instance, the RNA-binding protein hnRNPA1 specifically promotes pri-miR-18a processing, whereas the other pri-miRNAs encoded from the same polycistronic transcript (miR-17~92) are not affected (Guil et al. 2007). Another example is the let-7 family, members of which are encoded by 5 different polycistronic clusters. Let-7 maturation is obviously regulated independently from the respective co-clustered miRNAs, i.e. miR-125a/b, miR-100, miR-99a/b, through the specific action of LIN28A/B (Rybak et al. 2008; Piskounova et al. 2011).

Interestingly, three of the miRNAs analyzed here, i.e. miR-124, miR-9 and miR-181a, are subjected to post-transcriptional regulation. Processing of pre-miR-9 and pre-miR-124 in mouse brain depends on the action of the RNA-binding protein FXRP1. Loss of FXRP1 resulted in lower processing rates and consequently in the down-regulation of mature miR-9 and miR-124 expression (Xu et al. 2011b). According to Northern blot, miR-9 and miR-124 precursor processing is compromised in hESCs. Thus, it would be interesting to explore whether FXRP1 impacts on mature miR-124 and miR-9 expression during the transition of hESCs towards lt-NES cells. Expression of miR-181a was found to be induced upon TGFβ/SMAD signaling. TGFβ/SMAD might either promote miR-181a at the level of transcription (Wang et al. 2010a; Redshaw et al. 2013) or via SMAD2-dependent enhancement of pri-miRNA processing (Wang et al. 2010c). Considering that SMAD2 signaling blocks neural induction during development (Chang et al. 2007), it is however unlikely that TGFβ/SMAD has a strong impact on miR-181 expression in NSCs.

4.2.2 MicroRNA-181a and miR-181a* show cell type-dependent expression ratios

The miR-181a/a* duplex gives rise to two miRNAs, namely miR-181a, as the major product, and miR-181a*, as the minor product. Initially, the miRNA* strand, also called passenger strand, was assumed to be biologically inert and rarely expressed. However, with the advances made in deep RNA sequencing, it became clear that miRNA* species, although being less abundant than their miRNA counterparts, are expressed within the cells at quite significant levels (Ro et al. 2007; Chiang et al. 2010; Schulte et al. 2010; Yang et al. 2011; Zhou et al. 2012). Therefore, the miRNA nomenclature is currently revised and sister miRNAs should be named according to their position in the miRNA duplex, i.e. miR-X-5p (from the 5' arm) and miR-X-3p (from the 3' arm). Following the initial idea that miRNA strand selection during RISC maturation would mainly depend on thermodynamic properties (Khvorova et al. 2003), the 5p to 3p ratio for a given miRNA duplex is expected to be constant across different cell types. However, this is not always the case and many miRNA pairs show cell type- or tissue-dependent 5p to 3p strand ratios (Ro et al. 2007; Schulte et al. 2010). In fact, analyzing the expression of miR-181a versus miR-181a* in two independent differentiation paradigms (i.e. during lt-NES cell differentiation (Fig. 3.4) and during floor plate/DA differentiation (Fig. 3.13)) revealed stage-dependent changes in the expression ratio of the two strands (see also Fig. 4.3 B, C). It has been shown that miRNA pairs can even change their preferred strand during cell fate transitions

(Cloonan et al. 2011; Zhou et al. 2012). Similar to what has been described for the post-transcriptional regulation of miRNA processing, miRNA strand selection could be regulated by modulatory proteins, but those proteins still need to be identified (reviewed by Meijer et al. 2014). There is accumulating evidence pointing to a role of the Argonaute (Ago) proteins in miRNA strand selection. Higher eukaryotes have multiple Ago proteins, which form different RISCs with distinct functions and dsRNA-binding affinities (reviewed by Farazi et al. 2008). As recently shown in Drosophila, there is a specific subset of miRNA* species that is preferentially bound by Ago2 complexes, whereas their partner miRNAs are mostly incorporated into Ago1-containing RISCs (Okamura et al. 2009). In humans there are four different Ago proteins (AGO1-AGO4). Recently, AGO3 has been reported to affect the 5p to 3p ratio of let-7a by specifically binding to let-7a-3p (Winter et al. 2013). Human Ago proteins themselves show tissue-specific expression profiles and are also differentially expressed during neuronal differentiation (Gonzalez-Gonzalez et al. 2008; Potenza et al. 2009). Thus, its is tempting to speculate that loading of miRNA and miRNA* species into distinct Ago proteins might contribute to the observed divergent 5p to 3p ratio across different cell types.

Another explanation for the divergent 5p to 3p ratios might be that the stability of the two miRNA sister strands differs across different cell types. Overexpression of Argonaute proteins increased miRNA stability with a particular strong effect on miRNA* species (Winter et al. 2011). These findings suggest, that the Argonaute proteins are the limiting factors of the miRNA pathway and that not all generated mature miRNAs can be loaded into RISCs (Diederichs et al. 2007; Winter & Diederichs 2011; Zhou et al. 2012). In fact, very recently it was suggested that only 10% of the miRNAs are incorporated into RISCs (Janas et al. 2012), whereby the degree of RISC association of specific miRNAs differs between different cell lines (Flores et al. 2014). This opens the question whether the unbound miRNAs are stable and how their decay is regulated. Globally miRNAs have a relatively long half-life and are more stable than most mRNAs (Gantier et al. 2011). Some miRNAs, however, are subjected to rapid turnover, i.e. miR-9 and miR-125b (Sethi et al. 2009). Overall, the mechanisms of miRNA decay are not well understood yet and many regulatory factors identified might both promote and impair miRNA stability depending on the cellular context and the miRNA species (Kai et al. 2010; Zhang et al. 2012c). Recently, it has been shown that also target transcripts can protect their cognate miRNAs from degradation, which leads to higher miRNA expression (Chatterjee et al. 2011; Kang et al. 2013). Thus, target mRNAs may also influence miRNA strand stability and selection. Intriguingly, with regard to dopaminergic differentiation, miR-181a and miR-181a* were found to have opposing roles (see also section 4.5). Hence, these two miRNAs might constitute an intrinsic feedback mechanism and might target a distinct set of genes with essentially antagonistic roles during dopaminergic differentiation. One could further speculate that the abundance of the mRNA targets might, in turn, regulate the expression or stability of their own regulatory miRNAs. Indeed, the miR-181a to miR-181a* ratio was found to be increased during dopaminergic differentiation and was also found to be regulated in human midbrain compared to whole fetal brain (Fig. 4.3 C).

4.3 Identification of miRNAs promoting differentiation of human NSCs

Although the human CNS expresses a large amount miRNAs (Shao et al. 2010), only a few of them have been functionally associated with neurogenesis. In this work, 61 miRNAs were found to be up-regulated in lt-NES cells and differentiated neurons pointing to potential role of these miRNAs during neuronal differentiation. One objective of this thesis was to select interesting candicates from this list and to study their role during neuronal differentiation of lt-NES cells. The selected miRNAs were: (1) miR-124, which was known to be instructive for the neuronal fate (reviewed by Sun & Lai 2013) and was chosen here as a proof-of-principle; (2) miR-125b, which was previously suggested to promote neuronal differentiation (Lee 2005; Laneve et al. 2007; Ferretti et al. 2008); and (3) miR-181a, miR-153 as well as miR-324, which are known to be expressed in the neural lineage (Sempere et al. 2004; Landgraf et al. 2007; Ferretti et al. 2008; Doxakis 2010), but have not yet been functionally studied with regard to neuronal differentiation. Among those candidate neuronal miRNAs, miR-181a was studied in more detail in order to identify target genes contributing to its positive effect on neuronal differentiation. Another aim of this thesis was to establish a read-out method that could be employed to perform a miRNA screening in the context of neuronal differentiation. For this purpose the H9.2 DCX::EGFP lt-NES cell reporter line developed by Ladewig et al. (2008) was used.

4.3.1 Experiments in lt-NES cells underline the role of miR-124 and miR-125b in human neuronal differentiation and process outgrowth

Overexpression of miR-124 and miR-125b impaired the self-renewal of lt-NES cells and promoted their neuronal differentiation concomitantly with an increased average neurite length. Reciprocally, inhibition of miR-124 or miR-125b activity in differentiating lt-NES cells reduced the amount of neurons generated, indicating that the level of these miRNAs is critical for neuronal differentiation. The role of miR-124 overexpression on neuronal differentiation and target gene expression has been extensively studied and will be, therefore, not further discussed here (see also Introduction 1.2.2). The impact of miR-124 inhibition is, however, less well elaborated, and many studies have come to different conclusions depending on the time point and level of functional miR-124 loss (Krichevsky et al. 2006; Cao et al. 2007; Visvanathan et al. 2007; Cheng et al. 2009; Akerblom et al. 2012b). One discussed concept is that the inhibition of miR-124 shifts NSCs from neurogenesis to gliogenesis as shown by *in vivo* knock-down experiments in the murine subventricular zone (Akerblom et al. 2012b). Since multipotent lt-NES can also give rise to astrocytes, although only after prolonged differentiation, monitoring the rate of astrocytic versus neuronal differentiation in lt-NES cell cultures treated with miR-124 inhibitor could be used to corroborate this findings.

In contrast to miR-124, relatively little was known about the function of miR-125b during neuronal differentiation, let alone in a human context. While this work was prepared, two papers were published addressing the role of miR-125b during neural induction and neuronal differentiation (Cui et al. 2012; Boissart et al. 2012). In agreement with our data, Cui et al. (2012) showed that overexpression of miR-125b in primary mouse neural progenitors inhibits proliferation and promotes neuronal differentiation. Conversely, inhibition of miR-125b decreased the rate of neuronal

differentiation. In this context, the neural progenitor marker Nestin was identified as an important miR-125b target. Boissart et al. (2012) demonstrated that miR-125b also acts on neural lineage entry and promotes neural induction of hESCs by targeting the BMP signaling transducer SMAD4.

Overexpression of miR-124 and miR-125b not only raised the amount of lt-NES cell-derived neurons, but also increased their average neurite length. The increased neurite length might be merely a side effect of the accelerated differentiation, but there are a several reports pointing to a rather direct impact of these miRNAs on neuronal process outgrowth. In mouse primary neurons and neuronal cell lines, miR-124 has been shown to stimulate and increase the complexity of both axonal and dendritic outgrowth (Yu et al. 2008; Yoo et al. 2009; Franke et al. 2012; Schumacher et al. 2013; Gu et al. 2013). On a molecular basis, this might be explained by miR-124 targeting components of the Rho GTPase family, which is involved in actin remodeling (Yu et al. 2008; Franke et al. 2012; Schumacher & Franke 2013; Gu et al. 2013). Furthermore, miR-124 promotes the shift from BAF53a to BAF53b expression leading to the induction of genes importantly involved in dendritic development (Yoo et al. 2009). Similarly, overexpression of miR-125b in human neuroblastoma cells (SH-SY5Y) or immortalized human neural progenitors (RVM) led to an increased neurite length (Le et al. 2009). According to target prediction analysis and mRNA profiling miR-125b has the potential to regulate a number of genes associated with actin cytoskeleton. However, no specific target has been identified so far. In order to assess whether miR-124 and miR-125 also affect neurite elongation of human neurons, one could transiently modulate the activity of these miRNAs in lt-NES cell-derived neurons and measure potential changes in neurite length in a short time window.

4.3.2 General function of miR-153 and miR-324 during neuronal differentiation of non-tumorigenic human NSCs

Both miR-324-5p/3p and miR-153 have been previously shown to modulate proliferation and differentiation of brain tumor cells (Ferretti et al. 2008; Xu et al. 2010; Xu et al. 2011a). The data collected here in lt-NES cells point to an additional effect of these miRNAs in regulating neuronal differentiation in a non-neoplastic context.

MicroRNA-324-5p/3p was found to be down-regulated in human medulloblastoma (MB) cells. Re-introduction of miR-324-5p resulted in an impaired MB cell proliferation by targeting the SHH effectors Smoothened and Gli1 (Ferretti et al. 2008). Interestingly, miR-125b was also shown to attenuate proliferative SHH signaling by targeting Smoothened (Ferretti et al. 2008). In the same study, it was further demonstrated that overexpression of miR-324-5p in murine cerebellar progenitors reduces SHH-induced proliferation and attenuates the negative effect of SHH on neuronal differentiation (Ferretti et al. 2008). In analogy to these observations, overexpression of the miR-324-5p/3p locus in self-renewing lt-NES cells cultured in the presence of FGF2 and EGF impaired their proliferation rate, while enhancing the degree of spontaneous neuronal differentiation. However, overexpression of miR-324-5p/3p in lt-NES cells directed towards neuronal differentiation by growth factor withdrawal had no significant impact on the amount of neurons. This might indicate that miR-324-5p/3p merely contributes to neuronal differentiation by attenuating the proliferative signals

omitted by FGF2 and EGF, similar to its impact on SHH signaling. It would be also interesting to analyze the activity of SHH signaling in lt-NES cells and whether this is changed upon miR-324-5p/3p overexpression. Nevertheless, the average neurite length was increased in differentiating miR-324-5p/3p overexpressing lt-NES cell cultures, which might rather argue for a direct function of miR-324-5p/3p on neuronal differentiation.

MicroRNA-153 has been also linked to brain tumors and was found to be down-regulated in neoplastic compared non-neoplastic brain tissue (Gaur et al. 2007; Silber et al. 2008). While earlier studies have addressed the role of miR-153 on tumor cell proliferation and apoptosis (Xu et al. 2010; Xu et al. 2011a), it has recently been shown that overexpression of miR-153 also promotes the differentiation of glioblastoma stem cells into neurons and astrocytes (Zhao et al. 2013b). In agreement with these data, overexpression of miR-153 in lt-NES cells shifted the cells from proliferation to neuronal differentiation. Ectopic expression of miR-153 also had a positive effect on neurite length. However, it remains to be clarified whether this is caused by the induced early onset of differentiation or by a direct impact of miR-153 on neurite elongation. Given that miR-153 has been associated with the pathogenesis of Alzheimer's disease (AD), a deeper insight into its function in human neurons could even prove useful for developing novel therapeutic strategies. Expression of miR-153 was found to be reduced in a subset of AD patients (Long et al. 2012). Experiments in Hela and Neuro2A cells further revealed, that miR-153 is able to reduce APP expression by direct targeting (Liang et al. 2012). Furthermore, miR-153 may play a role during the pathogenesis of Parkinson's disease by regulating the expression of alpha synuclein (SNCA; Doxakis 2010). Considering that the expression of miR-153 itself may be induced by chromatin-modifying drugs (Xu et al. 2011a; Bao et al. 2012), modulation of miR-153 may represent an attractive therapeutic approach for AD. The potential of such an approach could be evaluated using AD patient-derived lt-NES cells and neurons, similar to the recently published paper from our institute on the impact of γ-secretase modulators on APP processing (Mertens et al. 2013b).

4.3.3 MicroRNA-181a acts on several NSC-associated mechanisms to promote neuronal differentiation

Within the CNS, the miR-181 family is expressed in neurons, astrocytes, and microglia and might regulate the interplay of these cells types under inflammatory or ischemic conditions (Ouyang et al. 2012b; Ouyang et al. 2012a; Hutchison et al. 2013). In neurons, miR-181a has been implicated in regulating synaptic plasticity (Beveridge et al. 2008; Chandrasekar et al. 2009; Chandrasekar et al. 2011; Saba et al. 2012). Furthermore, miR-181 has been shown to act as tumor suppressor in human glioma and impairs tumor cell proliferation and migration, while enhancing their sensitivity towards anti-tumor treatment (Chen et al. 2010; Wang et al. 2011; Wang et al. 2013a; Shi et al. 2013; Tao et al. 2013). Although miR-181 is considered as a general regulator of differentiation and is up-regulated during neural development, its actual impact on neural differentiation has not yet been investigated. Based on the data presented here, miR-181a seems to promote neuronal differentiation of human NSCs. Specifically, overexpression of the bifunctional

miR-181a/a* locus impaired lt-NES cell proliferation while promoting their neuronal differentiation, similar to the impact of miR-124 and miR-125b. MicroRNA mimic and inhibitor experiments revealed that the enhanced neuronal differentiation induced by miR-181a/a* might be mostly due to the action of miR-181a. Nevertheless, both miR-181a* and miR-181a seem to be importantly involved in neuronal differentiation, since prolonged inhibition of these miRNAs in differentiating lt-NES cells resulted in a reduced neuronal yield. The sequences of the major miR-181 isoforms are very similar indicating a high degree of functional redundancy. Indeed, combined overexpression of the four major miR-181 isoforms had an additional impact on neuronal differentiation compared to miR-181a alone (data not shown). Considering that the miR-181 family is expressed in both neurons and astrocytes (Ouyang et al. 2012a; Hutchison et al. 2013), it would be interesting to determine whether overexpression of miR-181a/a* would also increase astrocytic differentiation. Furthermore, the miR-181 family has been shown to promote apoptosis of transformed cells by targeting anti-apoptotic factors of the BCL2 family (Zhu et al. 2010; Wang et al. 2011). Preliminary data, however, suggest that overexpression of miR-181a/a* in lt-NES cells does not induce cell apoptosis (data not shown).

According to mRNA expression analyses, miR-181a appears to down-regulate several genes implicated in NSC maintenance (see Fig. 4.1 B for an overview). These genes include the already validated target gene LIN28A/B, as well as Musashi2 and NOTCH2, which harbor potential miR-181a binding sites that still need to be experimentally validated. In addition to these well-known NSC-associated genes, miR-181a also targets the orphan nuclear receptor GCNF (NR6A1) as demonstrated in this work and further discussed in section 4.4. The interaction of miR-181a and LIN28A has been previously validated in megakaryotic cells (Li et al. 2011b). Besides its function in pluripotency (Yu et al. 2007), the RNA-binding protein LIN28A is also involved in regulating NSC plasticity (Balzer et al. 2010; Cimadamore et al. 2013). Part of the functions of LIN28A and presumably also of its paralog LIN28B can be attributed to their role as negative regulators of let-7 maturation (reviewed by Thornton et al. 2012; see also Introduction 1.2.1). As shown here, miR-181a represses the expression of LIN28A as well as LIN28B in lt-NES cells resulting in a shift of the LIN28/let-7 feedback loop towards higher let-7 expression levels. Elevated let-7 levels, in turn, contribute to neuronal differentiation (Schwamborn et al. 2009; Zhao et al. 2010; Zhao et al. 2013a). In addition, miR-181a has the potential to target the RNA-binding proteins Musashi1 (MSI1) and Musashi2 (MSI2), which have been associated with neural progenitor cells (reviewed by Horisawa et al. 2012). Musashi1 regulates NSC maintenance by repressing the translation of the Notch inhibitor Numb1 among other target genes (Imai et al. 2001; reviewed by Horisawa & Yanagawa 2012). Furthermore, Musashi1 cooperates with LIN28A to repress the maturation of miR-98, which is a member of the let-7 family (Kawahara et al. 2011). Overexpression of miR-181a/a* had no impact on Musashi1 transcript levels but it might be still possible that miR-181a only affects Musashi1 translation, which could be addressed by Western blot analysis. Nevertheless, ectopic expression of miR-181a/a* was able to reduce Musashi2 transcript levels. It is believed that Musashi2 has similar RNA-binding properties and, thus, overlapping functions with Musashi1 (Sakakibara et al. 2001). As recently shown, Musashi2 might be also involved in regulating miRNA processing. In non-neuronal cells and neuronal

progenitors, processing of pri-miR-7, which is co-transcribed with its ubiquitously expressed protein-coding host gene, is blocked by Musashi2 in conjunction with HuR (ELAVL1) (Choudhury et al. 2013). According to the miRNA profiling presented here, expression of miR-7 is up-regulated during lt-NES cell differentiation, and Beate Roese-Koerner has shown in her PhD thesis, that overexpression of this miRNA promotes neuronal differentiation. Thus, miR-181a might contribute to neuronal differentiation not only by up-regulating let-7 but also other neuronal-associated miRNAs, such as miR-7. In addition, a slight up-regulation of miR-125b expression was observed in miR-181a/a* overexpressing lt-NES cells.

Lt-NES cells depend on Notch signaling in order to maintain their self-renewal capacity, and pharmacological blockage of Notch activity by the γ-secretase inhibitor DAPT induces neuronal differentiation (Borghese et al. 2010). Similarly, miRNA-mediated attenuation of Notch signaling, for instance by overexpression of miR-9/9*, shifts lt-NES cells towards neuronal differentiation (Roese-Koerner et al. in submission). Expression of NOTCH2 mRNA, which also contains a miR-181a binding site, is down-regulated upon miR-181a/a* overexpression. Notwithstanding that this finding needs to be complemented with 3' UTR luciferase and protein analysis, it may point to a negative impact of miR-181a on Notch signaling. In addition, miR-181a might indirectly influence Notch signaling by targeting Musashi1, which represses expression of the Notch inhibitor Numb1 (Imai et al. 2001). Furthermore, HES1 and HEY2 have been shown to interact with SIRT1 (Takata et al. 2003) which is also targeted by miR-181 (Saunders et al. 2010). As discussed in more detail in section 4.4.2, the transcriptional repressor GCNF might act on a similar set of pro-neural target genes as Notch/HES signaling to preserve NSC maintenance. Hence, there is an emerging picture in which miR-181 targets several factors that are either directly linked to the Notch pathway (NOTCH2), or act as modulators (SIRT1, MSI1) or in parallel to Notch signaling (GCNF). Intriguingly, miR-181a has been previously demonstrated to rather enhance Notch signaling in mouse T cell progenitors by targeting the Notch inhibitor Nrarp (Fragoso et al. 2012).

However, it is known that the miR-181 family has diverse functions depending on the cellular context, which might be due to a cell type-dependent miR-181a target repertoire. Interestingly, miR-181 has been also shown to regulate TGFβ and Wnt signaling (Bhushan et al. 2013; Judson et al. 2013). Furthermore, miR-181 expression itself might be regulated by these pathways (Ji et al. 2009; Wang et al. 2010b; Wang et al. 2010c; Redshaw et al. 2013). Although obtained from different cellular systems, these data indicate that miR-181 might serve as regulatory node for different signaling pathways. In fact, miR-181a seems to promote Wnt signaling in lt-NES cells as discussed in section 4.5.2 and it would be interesting to explore wether miR-181a also impacts on TGFβ signaling in these cells.

4.3.4 Towards establishing a functional miRNA screening in lt-NES cells

Lt-NES cells are easy to handle in culture, which makes them an excellent system for throughput screenings. In fact, lt-NES cells have been already used for functional screenings of chemical libraries (McLaren et al. 2013; Mertens et al. 2013b). After having established the methods to modify miRNA activities in lt-NES cells, the next step would be to transfer these to a larger cohort of miRNAs in order to identify additional miRNAs involved in human neuronal differentiation. To that purpose commercially available miRNA mimic or inhibitor libraries could be used (Lemons et al. 2013). As shown in this work, lt-NES cells tolerate serial transfections with miRNA oligonucleotides using lipofectamine. However, in order to perform such a miRNA screening, it is necessary to develop a suitable read-out assay to monitor the degree of neuronal differentiation in a rapid and unbiased manner. This could be achieved by using cell type-specific reporter lines. Here, the neuronal reporter DCX::EGFP H9.2 lt-NES cell line developed by Ladewig et al. (2008), which relies on the induction of endogenous doublecortin (DCX) expression in young neurons was used. In brief, the H9.2 DCX::EGFP lt-NES cells were transfected twice with miRNA oligonucleotides followed by a flow cytometry-based quantification of the DCX::EGFP-expressing neuronal cells. As another read-out for functional miRNA screeings one could also use an automated high-content microscopy device, which would allow assessing additional parameters such as the neurite length. First attempts to set-up such an automated imaging in combination with miRNA modulation were performed by Nina Groß as part of her diploma thesis at our institute (Groß 2012).

4.4 The miR-181a target gene GCNF regulates neural stem cell maintenance

Germ cell nuclear factor GCNF/NR6A1 has been previously proposed to be regulated by miR-181a according to target prediction analyses (John et al. 2004; Gu et al. 2008). Interestingly, the MIR181A2 host gene encoding miR-181a-2 and miR-181b-2 is located on the opposite strand of in an intron of the GCNF/NR6A1 locus in both mouse and humans. As shown for other antisense oriented intronic miRNAs, the MIR181A2 host gene is believed to have its own promoter (Marson et al. 2008). Indeed, the divergent expression pattern of pri-miR-181ab-2 and NR6A1 during hESC-based neuronal differentiation indicates that both genes are independently expressed from each other. Upon transition towards lt-NES cells, and during further differentiation, GCNF is down-regulated, whereas expression of the mature miR-181 family members is up-regulated, pointing to an interaction between these factors. Indeed, miR-181a and probably also the other major miR-181 isoforms, recognize a specific site in the GCNF 3' UTR and down-regulate GCNF transcript levels. Knock-down of GCNF by siRNA mimicked the impact of miR-181a overexpression in that it resulted in an increased rate of differentiation and longer neurites. Reciprocally, interfering with GCNF down-regulation by blocking endogenous miR-181a activity impaired neuronal differentiation. This indicates that miR-181a-mediated down-regulation of GCNF is necessary to allow the transition of lt-NES cells towards neuronal differentiation.

Indeed, the data collected in this thesis, suggest that the orphan nuclear receptor GCNF might act as a repressor of neuronal differentiation in human NSCs. Three lines of evidence support this hypothesis. First, as discussed above, GCNF was strongly down-regulated in lt-NES cells compared to hESCs and further declined in differentiating lt-NES cell cultures. Second, knock-down of GCNF in lt-NES cells using siRNAs resulted in an increased neuronal differentiation. Third, direct overexpression of GCNF attenuated neuronal differentiation, while stabilizing neural rosette morphology and increasing the rate of cell proliferation. Furthermore, GCNF overexpression in differentiating cells led to a reduced rate of apoptosis (Fig 4.4 A). However, these findings are in apparent contrast with an earlier study reporting on a positive impact of GCNF on neuronal differentiation of mouse embryonic carcinoma cells (Sattler et al. 2004).

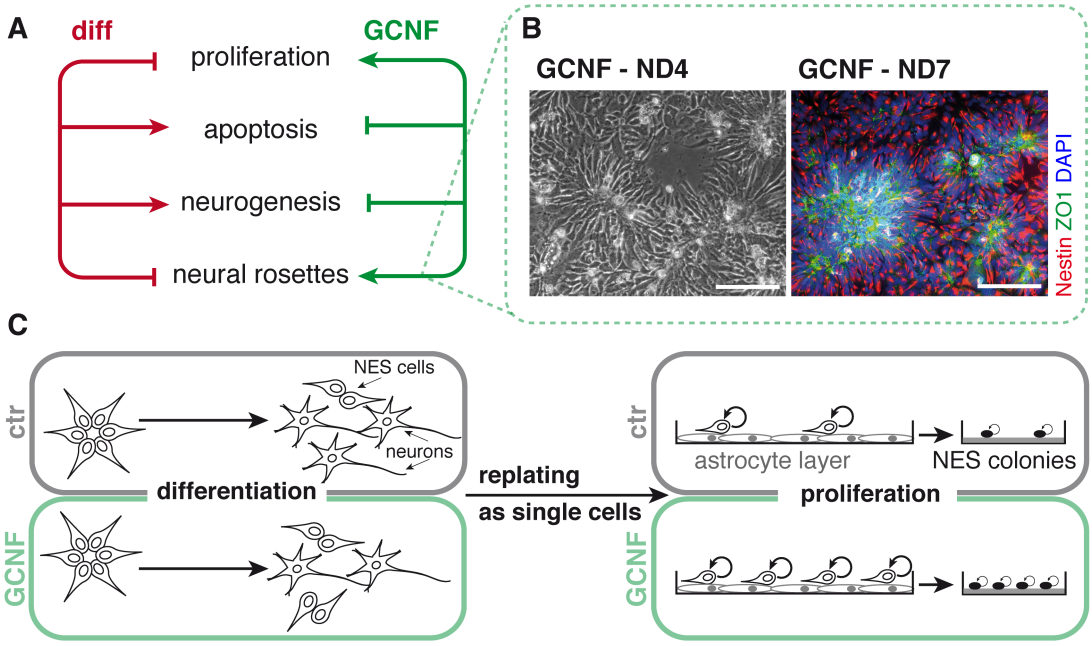

Fig. 4.4: GCNF overexpression impairs neuronal differentiation and differentiation-induced apoptosis, while preserving neural rosette formation and enhancing cell proliferation. (A) GCNF overexpression counteracts the effects of differentiation (diff) stimuli with regard to neurogenesis, neural rosette architecture, apoptosis and proliferation. **(B)** GCNF-overexpressing cultures form large neural rosettes when cultured in differentiation-inducing conditions. Scale bars = 200 μm. **(C)** Compared to control cultures, pre-differentiated GCNF-overexpressing cultures show higher recovery rate of lt-NES colonies when replated in a clonal density on mouse astrocytes.

4.4.1 GCNF preserves neural stem cell properties and inhibits premature neuronal differentiation

While GCNF overexpression did not have an apparent effect on self-renewing lt-NES cells, it had a strong impact when the cells were directed towards differentiation. One intriguing difference observed during the differentiation of GCNF-overexpressing cultures was the persistent neural rosette morphology, which is normally associated with undifferentiated lt-NES cells. In fact, these neural rosettes normally disappear upon differentiation. However, in GCNF-overexpressing cultures, the neural rosettes seemed to have rather grown over time or merged with other rosettes and were

characterized by an increased extent of ZO1 expression (Fig. 4.4 B). The stabilized neural rosette morphology might be a side effect of the impaired neuronal differentiation, but it might be also due to a more direct role of GCNF on the rosette cytoarchitecture. In this context, several features like cell polarity, cell-cell and cell-matrix adhesion might be regulated by GCNF. In fact, data obtained during Xenopus development point to a role of GCNF during cell-matrix adhesion (David et al. 1998; Barreto et al. 2003b). GCNF knock-down in Xenopus embryos affected neural plate cell migration and radial intercalation, which resulted in a irregular-shaped neural tube and a failure of neural tube closure (Barreto et al. 2003b). Molecularly, depletion of GCNF led to a decreased expression of the integrins itga5 and itga6, as well as an impaired fibronectin deposition (Barreto et al. 2003b). Conversely, overexpression of GCNF caused an up-regulation of fibronectin transcription (David et al. 1998). The fact that the neural rosettes detected in the GCNF-overexpressing cultures consisted of several cell layers, might also argue for a positive effect on GCNF on proliferation. Indeed, an increased rate of Ki67-positive cells was observed in differentiated GCNF-overexpressing cultures. However, the rate of BrdU incorporation – as an indicator of cells in the S-phase – was not changed, indicating that GCNF might have an impact on cell cycle progression. As very recently shown, GCNF represses the expression of miR-302a, which targets CyclinD1, an important regulator of cell cycle progression (Wang et al. 2014). This leads to an increased CyclinD1-independent proliferation in self-renewing as well as differentiating GCNF-depleted mouse ESCs (Wang et al. 2014). Self-renewing lt-NES cells still express miR-302b and it would be interesting to assess whether GCNF can also modulate miR-302b and CyclinD1 expression in these cells. However, it is likely that GCNF has a different function on proliferation in ESCs versus lt-NES cells. In fact, inhibition of GCNF in differentiating lt-NES cells resulted in a reduced proliferation rate as indicated by preliminary data (data not shown). GCNF overexpression also resulted in a reduced rate of apoptosis, probably as a side effect of the impaired neuronal differentiation. However, according to GCNF binging site search Caspase3 (CASP3) was identified as one of the 1000 best-scoring putative GCNF targets, suggesting that GCNF might also have a direct impact on cell survival.

Since the neural rosette morphology is a distinctive feature of undifferentiated lt-NES cells, it was assessed whether GCNF is able to preserve the lt-NES cell fate under prolonged differentiation-inducing conditions using the Notch inhibitor DAPT. Intriguingly, even under these conditions, GCNF overexpression was sufficient to delay neuronal differentiation. It has been previously shown that lt-NES cells differentiate asynchronously and 20% of the cells are still undifferentiated after 15 days of differentiation in the presence of DAPT (Falk et al. 2012). These undifferentiated cells are able to form lt-NES cell colonies when replated on mouse astrocytes and cultured again under self-renewing conditions (Fig. 4.4 C). Interestingly, the GCNF-overexpressing cultures apparently contained more of these cells as indicated by the increased recovery rate of lt-NES cell colonies (Fig. 4.4 C). However, the size of the colonies formed was not different between GCNF-overexpressing and control cells, excluding a GCNF-induced growth advantage under the recovery condition.

Taken together, these data point to a role of GCNF in regulating the balance between NSC maintenance and differentiation. It remains to be clarified whether the effects on neural rosette morphology and neuronal differentiation are directly associated or are rather two independent functions of GCNF. Interestingly, the reduced neuronal differentiation rate is also apparent in cultures exhibiting low GCNF overexpression, whereas the effect on cell cluster/rosette formation could be only observed upon high GCNF overexpression (data not shown). In order to distinguish between these two phenotypes, one could study the impact of GCNF in self-renewing lt-NES cells treated with compounds known to impair neural rosette integrity, such as Y27632 (ROCK inhibitor) or Cytochalasin D as described by Main et al. (2013). Furthermore, it would be interesting to assess whether GCNF plays a role during early neural rosette formation from hESCs, similar to the experiments described by Lo Sardo et al. (2012), or during the transition of pre-rosette cells to rosette-forming NSCs (Reinhardt et al. 2013). Furthermore, one could monitor the dynamics of neural rosette assembly and disintegration in GCNF-overexpressing lt-NES cell cultures using live time-lapse imaging. Preliminary data also suggest that the effect of GCNF might be non-cell autonomous, since culturing control lt-NES cells with conditioned medium from GCNF-overexpressing cells resulted in an impaired neuronal differentiation. This might point to an impact of GCNF in regulating the levels of secreted factors contributing to the NSC niche. Indeed, according to GCNF binding site search and Gene Ontology annotation, GCNF has the potential to regulate various genes associated with “exocytosis” and “regulation of secretion”. Furthermore, many of the putative GCNF targets genes are associated with “neurite morphogenesis”, “synaptic transmission” and “neuron fate commitment” (see Fig. 3.24 A). In order to dissect the underlying mechanisms, future work should aim at identifying the GCNF target gene program by experimental means.

4.4.2 GCNF acts in parallel to Notch to repress the expression of pro-neural bhLH genes

According to mRNA expression analysis, GCNF appears to directly repress the expression of a subset of pro-neural bHLH transcription factors, i.e. NEUROG1, NEUROD1, NEUROD4 and eventually ASLC1. The pro-neural bHLH gene family includes ASCL1, ATOH1 as well as several Neurogenins (NEUROGs) and Neurogenic differentiation genes (NEURODs), all of which are expressed in the nervous system (reviewed by Wilkinson et al. 2013). Due to the low basal expression level of ATOH1 and NEUROG2 in proliferating lt-NES cells, it remains unknown whether GCNF targets these genes under such conditions. However, the loci encoding ATOH1 and NEUROG2 harbor potential GCNF binding sites and ATOH1 was among the top 1000 target hits. Pro-neural bHLH genes are considered as generic neurogenic factors and are both essential and sufficient to activate a neuronal differentiation program. Furthermore, they are involved in directing neural progenitor cells towards specific neuronal subtypes (reviewed by Bertrand et al. 2002; Wilkinson et al. 2013). ASCL1, NEUROG2 and NEUROD1 are even able to convert fibroblasts into neuronal cells – a process called direct neural conversion – upon ectopic expression in conjunction with other neuronal transcription factors (reviewed by Ladewig et al. 2013). In this context, ASCL1 has been suggested to act as a pioneer transcription factor binding to several genomic sites and recruiting the other neurogenic

factors, BRN2 (POU3F2) and MYT1L (Wapinski et al. 2013). Ectopic expression of NEUROG2, as sole transcription factor, in combination with small molecules is also sufficient to convert human fibroblast into cholinergic neurons (Liu et al. 2013). Forced expression of NEUROG2 or NEUROD1 accelerates neuronal differentiation of hESCs resulting in the emergence of functional neurons already after few weeks (Zhang et al. 2013).

The expression of the pro-neural bHLH genes is tightly regulated by various mechanisms, one of them is the Notch signaling pathway. Activation of Notch signaling leads to the induction of another group of bHLH genes – the repressor-type transcription factors, including the HES and HEY genes (Kageyama et al. 2005). These genes can then bind to the promoters of the pro-neural bHLH genes to repress their expression. Notch inhibition by DAPT in lt-NES cells leads to a down-regulation of HES1, HES5 and HEY1 concomitantly with an increase of ASCL1, ATOH1, NEUROGs and NEURODs (Borghese et al. 2010 and shown here). Intriguingly, in the presence of GCNF overexpression, DAPT-mediated inhibition of Notch signaling was not able to induce the expression of NEUROD1, NEUROD4, NEUROG1 as well as ASCL1. The respective promoters are probably occupied by ectopic GCNF, which emits a repressive signal strong enough to compensate for the loss HES- and HEY-mediated repression. This might explain why GCNF can partially counteract DAPT-induced neuronal differentiation. Since, the Notch effector HES1 has prominent role in regulating the expression of pro-neural bHLH genes (Shimojo et al. 2008), it would be interesting to directly compare the impact of GCNF overexpression with HES1 overexpression in lt-NES cells. Furthermore, one could assess whether forced expression of GCNF can compensate for the loss of HES1 expression. In addition, it would be worth to study the overlap between the target gene program of GCNF and HES/HEY. It is also possible that GCNF and HES/HEY physically interact with each other or share some of their binding partners. Indeed, HEY1 and HEY2 recruit the co-repressor N-CoR (Iso et al. 2001), which is also bound by GCNF (Yan & Jetten 2000). Considering that Notch signaling is critically for maintaining NSCs in an undifferentiated state (Hitoshi et al. 2002; Borghese et al. 2010), both GCNF and Notch signaling might act in parallel in this regard. Notch signaling is also involved in regulating the balance between neurogenesis and gliogenesis and it would be interesting to assess the role of GCNF in this context. In fact, reduced pro-neural bHLH gene expression, as observed upon GCNF overexpression, has been associated with an increased gliogenesis (Bertrand et al. 2002).

Taken together, a picture emerges, in which GCNF is involved both in early NSC progression, as indicated by data from Akamatsu et al. (2009), and NSC maintenance, as indicated by our own data. Furthermore, GCNF may impede neuronal differentiation in part by inhibiting the induction of the pro-neural bHLH genes that is normally observed upon differentiation stimuli.

4.4.3 Antagonistic roles of GCNF, let-7 and miR-181a as regulators of developmental timing

During early mouse embryonic development GCNF acts as a repressor of the pluripotency genes Oct4 and Nanog (Gu et al. 2005a; Gu et al. 2011). While in mouse ESCs, expression of GCNF is only transiently induced upon retinoic acid treatment (Gu et al. 2005b), human ESCs show already relatively high GCNF expression. This might be attributed to the fact, that human ESCs are less naive

than mouse ESCs and more prone to differentiation (reviewed by Nichols et al. 2009; Martello et al. 2014). Nevertheless, it remains to be clarified, why the relatively high endogenous GCNF levels in hESCs does not affect OCT4 expression and pluripotency. One explanation might be that the GCNF binding site in the OCT4 proximal promoter is blocked by the nuclear receptors and transcription activators SF-1 (NR5A1) and LRH-1 (NR5A2) (Barnea & Bergman 2000; Gu et al. 2005a). GCNF also represses miR-302 expression (Wang et al. 2014), which is induced by Oct4 and Sox2 (Marson et al. 2008; Card et al. 2008). Thus, GCNF might down-regulate the expression of protein-coding genes and miRNA genes within the pluripotency network to promote differentiation and NSC progression (Akamatsu et al. 2009). However, once the NSC fate has been consolidated, GCNF may inhibit neuronal differentiation by repressing differentiation-associated genes, such as pro-neural bHLH transcription factors. Taken together, these findings indicate that GCNF might be involved in regulating the timing of development and might have a dual role during neural development. This hypothesis is supported by the finding that expression of GCNF during mouse development peaks at E8.5, when NSCs down-regulate Oct4 expression and are fully committed to the neural lineage (Akamatsu et al. 2009). With ongoing development GCNF expression decreases and is diminished at E10.5 according to *in situ* hybridization analyses (Chung et al. 2001b; Chung & Cooney 2001a) or at E14.5 as indicated by microarray analysis (Gurtan et al. 2013, Fig. 4.5 B). A similar decline of GCNF expression was observed during lt-NES cell differentiation and this down-regulation seems to be necessary to allow neurogenesis to proceed. This might be in part mediated by the concerted action of let-7, as shown by Gurtan et al. (2013), and miR-181a, as demonstrated in this work. In this context, it would be interesting to assess, how GCNF transcription is regulated in the first place and how this regulation changes with ongoing development. Another open question is whether GCNF, as in mouse ESCs, is transiently up-regulated during human ESC differentiation.

In support of our hypothesis of a dual role of GCNF in neural development, Gurtan et al. (2013) proposed that GCNF and let-7 might have reciprocal functions in regulating developmental timing. Let-7 is a well known regulator of cell fate progression in C. elegans and targets several genes, that are involved in coordinating developmental transcription programs, among them LIN28A (reviewed by Ambros 2011). Considering that miR-181 targets both LIN28A and GCNF, it is tempting to speculate that miR-181a might as well act as a so-called heterochronic regulator. Intriguingly, GCNF has orthologs in C. elegans (nhr-91) and Drosophila (HR4) (Sluder et al. 2001; Enmark et al. 2001; Wang & Cooney 2013c). In both animals, these nuclear receptors play important roles in linking the developmental timing to nutrition supply (King-Jones et al. 2005; Ou et al. 2011; Kasuga et al. 2013).

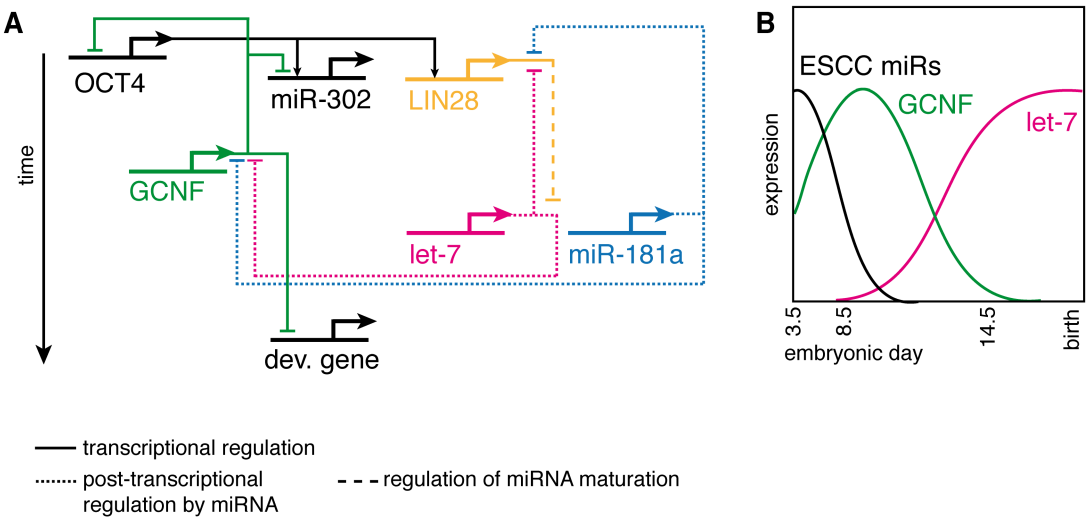

Fig. 4.5: GCNF as a regulator of developmental timing. (A) Schematic depiction showing a draft of the gene regulatory network around GCNF. GCNF might have a dual function during development and might first promote differentiation by repressing pluripotency-associated factors (i.e. OCT4 and miR-302), while later on repressing the expression of developmental (dev) genes. Expression of GCNF itself might be controlled at the post-transcriptional level by let-7 and miR-181a, which promote differentiation and also regulate the expression of another heterochronic gene – LIN28. However, it remains to be investigated how GCNF transcription is regulated. **(B)** Summary of the expression of ESCC miRNAs (including miR-302), let-7 and GCNF in the developing mouse embryo from E3.5 to birth. Graphic is redrawn from Gurtan et al. (2013).

The theory of a dual function of GCNF during neural development could also explain the divergent impact of GCNF observed in embryonic carcinoma (EC) cells and lt-NES cells. In mouse PCC7-Mz1 EC cells, GCNF seems to promote neuronal differentiation (Sattler et al. 2004), which is in apparent contrast with its role in lt-NES cells. In brief, Sattler et al. (2004) found an increased and accelerated neuronal differentiation upon conditional overexpression of sense GCNF mRNA, whereas neuronal differentiation was delayed upon GCNF knock-down using antisense RNA. Conversely, GCNF was found to have a negative effect on neuronal differentiation of human NT2/D1 EC cells (Schmitz 2000) and lt-NES cells. Obviously the contradictory findings described by these two studies and in the work presented here, could reflect a species-dependent function of GCNF. However, the human GCNF is 98% identical to the mouse GCNF and both human and mouse GCNF bind to the same consensus site and therefore probably regulate a similar set (Kapelle et al. 1997; Hentschke et al. 2006). Another explanation is that the NT2/D1 cell line – similar to lt-NES cells – is already determined towards the neuronal fate (Pleasure et al. 1993), while the PCC7-Mz1 EC line also differentiates into non-neural cell types in the presence of retinoic acid and is considered closer to the pluripotent stage (Jostock et al. 1998). Thus, the observed differences might be also due to the cell lines used and their differential commitment to the neural lineage.

4.5 MicroRNA modulation as a tool to regulate the emergence of dopaminergic neurons

Theoretically, miRNAs could be envisaged as tools to direct the differentiation of pluripotent stem cells towards medically relevant neuronal subtypes, such as midbrain dopaminergic (mDA) neurons. First evidence pointing to this came from two studies, which showed that the amount of TH-positive neurons generated during dopaminergic differentiation of mouse ESCs can be increased by inhibiting either miR-133b or miR-132 (Kim et al. 2007a; Yang et al. 2012). However, the actual function of miR-133b during mDA differentiation is unclear, since miR-133b knock-out mice display normal midbrain development (Heyer et al. 2012). There is one very recent study on the role of miR-135a during murine midbrain development, which showed that miR-135a defines the dorso-ventral extent of dopaminergic progenitors by targeting Lmx1b (Anderegg et al. 2013). Another very recent publication has reported on a negative function of miR-218 during DA differentiation of mouse ESCs (Baek et al. 2014). Although these findings indicate that miRNAs play essential roles during DA fate specification, a direct experimental link between miRNAs and human DA neuron differentiation was still missing.

4.5.1 MicroRNA-181a promotes while miR-124 inhibits dopaminergic differentiation

Lt-NES cells show a strong differentiation bias towards GABAergic interneurons (Koch et al. 2009b). Nevertheless, they can also give rise to other neuronal phenotypes and produce small amounts of TH-positive dopaminergic-like neurons. Upon exposure to FGF8b and SHH signaling, the fraction of TH-positive neurons can be further increased and occasionally cells co-expressing FOXA2 and LMX1A emerge (Falk et al. 2012). However, lt-NES cells fail to express the full range of mDA fate markers. As shown in this work, modulation of distinct miRNAs resulted in an either increased (miR-125b, miR-181a) or decreased (miR-124, miR-181a*) amount of TH-positive neurons generated from lt-NES cells. In particular, overexpression of miR-181a had a strong impact on the generation of TH-positive neurons and tripled their amount compared to the control conditions. However, the overall yield of TH-positive neurons was still relatively low, and no expression of FOXA2 or LMX1A could be detected. The yield of TH-positive neurons was further increased upon combining miRNA modulation (miR-124 inhibition, miR-125 and miR-181a overexpression) with SHH/FGF8 patterning. The combination of the two approaches resulted in higher amounts of TH-positive neurons compared to their individual impacts. This suggests that miRNA mimics or inhibitors could be theoretically used to complement the current repertoire of small molecules and recombinant factors used for DA neuron differentiation.

In order to test whether these findings could be translated to a protocol specifically tailored for the generation of mDA neurons, the floor plate-based differentiation paradigm developed by Kriks et al. (2011) was used. In line with its proposed role as a promoter of DA neuron fate, expression of miR-181a increased during floor plate induction and subsequent DA neuron differentiation. Accordingly, ectopic expression of miR-181a/a* in floor plate progenitors increased the amount of TH-positive neurons, which were also positive for FOXA2 and LMX1A. Conversely, ectopic expression of miR-124 impaired the differentiation of floor plate cells into TH-positive neurons, whereas miR-125b

seemed to have no specific impact. However, neither miR-181a/a* nor miR-124 had an influence on the proportion of FOXA2/LMX1A-positive progenitors, which in all conditions exceeded 90% of all cells. This might due to the late time point of miRNA overexpression at day five of the protocol, when the midbrain floor plate identity might be already consolidated. Nevertheless, both miR-181a and miR-124 seem to be able to affect the subsequent dopaminergic differentiation of floor plate progenitors. Future work should continue to recapitulate these findings and to determine whether overexpression of these miRNAs would influence the maturation of mDA neurons, e.g. affecting neurite elongation and dopamine release. According to the protocol developed by Kriks et al. (2011), floor plate progenitors cells need to be differentiated for additional 40 days in the presence of DAPT to generate appropriate amounts of TH-positive mDA neurons. It would be interesting to assess whether miR-181a overexpression could be used to accelerate this process.

The finding that miR-133b inhibits DA differentiation of mouse ESCs (Kim et al. 2007a) has caught a lot of attention. However, it was later shown that miR-133b null mice have a normal mDA neuron development (Heyer et al. 2012). This illustrates that *in vitro* generated data have to be interpreted carefully and cannot necessary be translated to the *in vivo* situation. Studying the function of miR-124 or miR-181 *in vivo* by classical knock-out-strategies might be difficult, due the fact that there exist multiple isoforms located on separate genomic regions (reviewed by Akerblom et al. 2012a). In order to determine the role of miR-181 during midbrain development and function, it might be necessary to deplete all three miR-181 loci. However – although it was possible to generate single miR-181 knock-outs – so far all attempts to generate triple knock-out mice have failed, presumably due to an early lethality of the embryos (Fragoso et al. 2012; Henao-Mejia et al. 2013). With regard to the *in vivo* situation, it would be interesting to first study the expression of miR-181 and miR-124 across different brain regions. Indeed a previous profiling analysis in different human brain samples has indicated an enrichment of the miR-181 family in the human midbrain (Landgraf et al. 2007).

Further *in vitro* experiments should aim at identifying the *bona fide* miRNA targets responsible for the observed effects. Intriguingly, miR-124 has been demonstrated to target FoxA2 in mouse pancreatic β-cells (Baroukh et al. 2007). Thus, it would be interesting to assess the impact of ectopic miR-124 expression during early floor plate specification. Surprisingly, miR-181a has been recently shown to repress the expression of a subset of transcription factors known to be expressed in mDA neurons, i.e. EN1, EN2 and LMX1A, in HPRT-deficient human dopaminergic SH-SY5Y neuroblastoma cells (Guibinga et al. 2012). While these findings are in apparent contrast to the proposed positive effect of miR-181a on DA neurons, they could also reflect differences between the cellular model-systems employed. Another possibility is that miR-181a may act as a fine-tuner of mDA-associated transcription factors to ensure their proper expression. Given that its sister – miR-181a* – was found to have a negative effect on dopaminergic differentiation, it would be interesting to compare the target gene program of miR-181a and miR-181a*. However, most target prediction algorithms do not yet cover the miRNA* strands. As presented in this work, miR-181a might contribute to mDA neuron differentiation by enhancing Wnt signaling and by targeting GCNF.

4.5.2 Wnt activity is critical for dopaminergic differentiation and is enhanced by miR-181a

Target prediction analysis for miR-181a suggested an apparent bias towards genes involved in Wnt signaling, whereby several negative modulators of the signaling cascade were found to harbor potential miR-181 binding sites in their 3' UTR. Among them are for instance, components of the β-catenin destruction complex (GSK3, CK1), secreted Wnt antagonists (DKK, WIF, FRP) and the TCF inhibitor NLK. Based on this target profile it has already been suggested that miR-181a might potentiate Wnt signaling (Qin et al. 2010). As shown in this work, miR-181a indeed enhances Wnt/β-catenin activity in lt-NES cells. In the meantime it has been demonstrated that miR-181a also activates Wnt/β-catenin signaling during cellular reprogramming (Judson et al. 2013). Although NLK has been validated as a miR-181a target in human hepatocytes and natural killer cells (Ji et al. 2009; Cichocki et al. 2011), it seems not be regulated by miR-181a in lt-NES cells. Hence, the next step would be to identify which components of the Wnt pathway are actually regulated by miR-181a. Wnt signaling plays a crucial role for the instruction and differentiation of mDA neurons and the pharmacological activation this pathway has become an important concept of many *in vitro* mDA differentiation paradigms (reviewed by Hegarty et al. 2013; Arenas 2014). For instance, the GSK3 inhibitor CHIR mimicking Wnt//β-catenin signaling, is a key component of the patterning cocktails used to direct hPSCs towards the mDA fate (e.g. Kriks et al. 2011; Kirkeby et al. 2012; Xi et al. 2012). In particular, the acquisition of the midbrain floor plate identity from hPSCs seems to depend on Wnt signaling (Kriks et al. 2011). However, the dosage of CHIR is critical and excess of Wnt signaling has been shown to be detrimental for mDA neuron generation (Tang et al. 2010; Xi et al. 2012). Treating lt-NES cells with CHIR also resulted in a higher yield of TH-positive dopaminergic-like neurons and the combination of pharmacological Wnt activation with miR-181a/a* overexpression had an even stronger effect. Conversely, blockage of Wnt signaling was able to partially counteract the promoting impact of miR-181a/a* on TH-positive neurons. This suggests that miR-181a and Wnt might act additively to induce TH-positive neurons but it also indicates that more miR-181a target might be at play.

Different Wnt molecules, are secreted from the isthmic organizer and the developing midbrain, which have divergent functions with regard to progenitor proliferation and mDA differentiation (reviewed by Hegarty et al. 2013; Arenas 2014). The most studied Wnt molecules in this context are Wnt1 and Wnt5a, which activate distinct Wnt signaling branches but seem to cooperatively contribute to mDA neuron development. Wnt1-dependent Wnt/β-catenin signaling is required both for mDA progenitor proliferation as well as mDA neuron differentiation and only a few mDA neurons emerge in Wnt1- or β-catenin-depleted mice (Prakash 2006; Joksimovic et al. 2009; Tang et al. 2009). Wnt5a activates the Wnt/Calcium signaling cascade and acts as a repressor of mDA progenitor proliferation and is required for correct midbrain morphogenesis (Andersson et al. 2008). Combined deletion of Wnt1 and Wnt5a resulted in an aggravation compared to the effects of the single deletions on midbrain and mDA neuron development. Accordingly, combined activation of Wnt/β-catenin signaling by Wnt3a and administration of Wnt5a was able to further increase the yield and DA neurons from mouse ESCs (Andersson et al. 2013). Based on these findings the group of Prof. Arenas (Laboratory of Molecular Neurobiology, Karolinska Institute, Sweden) is currently testing the efficacy of

combined Wnt modulation on the generation of DA neurons from lt-NES cells (personal communication). In this context, it would be interesting to assess whether miR-181a also has an impact on the other Wnt signaling branches besides the Wnt/β-catenin cascade. Another question is whether miR181a in general enhances the responsiveness of cells towards Wnt molecules or pharmacological activators by reducing negative feedback/buffering mechanism present in the cells.

4.5.3 Specific inhibitory effect of the miR-181a target GCNF on dopaminergic differentiation

In this work, GCNF was identified as a relevant miR-181a target in the context of neuronal differentiation as discussed before. Based on this finding it was tempting to speculate that down-regulation of GCNF would also contribute to the positive impact of miR-181a on DA neuron fate. Indeed, overexpression of GCNF (lacking the miRNA-regulated 3 'UTR) was able to attenuate the effects of SHH/FGF8 treatment as well as of miR-181a/a* overexpression and decreased the yield of TH-positive neurons in both conditions. To exclude that this phenotype might be merely caused by the impact of GCNF on neuronal differentiation, GCNF was only overexpressed during the first week of the two-weeks patterning paradigm. This short-term GCNF overexpression in the presence of SHH/FGF8b had no effect on the amount of β-III Tubulin-positive neurons, but specifically decreased the number of TH-positive neurons. To consolidate these finding, one could also design an experiment, in which the DA fate is first induced before activating the overexpression of GCNF. Furthermore it would be interesting to assess the efficacy of GCNF siRNAs in the context of DA neuron differentiation.

Previous data have pointed to a role of GCNF in regulating CNS regionalization. In both mouse and Xenopus, depletion of GCNF impairs the formation of the midbrain-hindbrain boundary (MHB). (Song et al. 1999; Barreto et al. 2003a; Chung et al. 2006). The MHB, also known as isthmic organizer, regulates the patterning of the midbrain and the anterior hindbrain via Wnt and FGF signaling (Wurst et al. 2001). Depletion of xGCNF by morpholino injection in two-cell Xenopus embryos resulted in a more posterior repositioning of the MHB as indicated by a shift of the Otx2 and Gbx2 expression domains (Barreto et al. 2003a). In GCNF-depleted mice, expression of Fgf8 was diminished along with a reduced expression of MHB markers and a higher rate of cell apoptosis at the isthmus (Chung et al. 2006). Since GCNF knock-out mice die at E10.5, Chung et al. could not determine whether GCNF also plays a role during later midbrain development and DA neuron differentiation. However, there are data pointing to an impact of GCNF on the expression of MHB and DA fate-associated transcription factors. On the one hand, in Xenopus GCNF was found to promote the expression of En2, which might point to a positive impact of GCNF on DA neuron fate (Song et al. 1999). On the other hand, several DA determinants (Nurr1, FoxA2, En1 and En2) were pulled-down by GCNF chromatin immunoprecipitation in mouse mesenchymal stem cells (Gurtan et al. 2013). Since GCNF is considered to act as transcriptional repressor, these findings would argue for a negative impact of GCNF on DA neuron fate and support our data. Taken together, GCNF might have a specific function during midbrain and DA neuron development. In this context, it might be worth to compare the expression patterns of miR-181a and GCNF by *in situ* hybridization in different brain regions.

4.6 Implications and future prospects

The findings presented in this work provide novel insights into the role of miRNAs regulating human neuronal differentiation and subtype specification and could be exploited to develop novel strategies for the *in vitro* derivation of human NSCs and mature neurons. The generation of medically relevant neural cell types still represents one of the main challenges in applied stem cell research. Another challenge is the stable expansion of appropriate neural stem cell or progenitor populations without altering their differentiation potential. During the last years our knowledge on the transcriptional mechanisms and extrinsic patterning cues driving cell fate choices has increased dramatically, but we have just started to explore the role of miRNAs and other non-coding RNAs in this context. First studies, including the here presented one, indicate that miRNAs could be envisioned as tools for the *in vitro* modulation of cell fates. For instance, miR-181a/a* and miR-124 were here identified as novel regulators of dopaminergic differentiation. Furthermore, miRNA research and target identification may lead to the discovery of entire regulatory mechanisms, as shown here with miR-181a and GCNF. In the following, some of the key findings of the thesis will be discussed in more detail with regard to future experiments and potential applications.

Combining miRNA profiling with functional screenings to identify neural-associated miRNAs

This work concentrated on analyzing the function of a subset of miRNAs and identified miR-153, miR-181a/a* as well as miR-324-5p/3p as novel factors contributing to neuronal differentiation of human NSCs. Nevertheless, the functions of the majority of the neural-associated miRNAs are still unknown. The combination of a comprehensive miRNA profiling to identify cell fate-associated miRNA signatures with functional screening assays represents a good strategy to approach this problem. As shown here, in a proof-of-principle analysis, the DCX::EGFP lt-NES cell line responds well to miRNA mimics/inhibitor transfections and could be, thus, used as a cellular platform to analyze a larger cohort of miRNAs for their potential impact on neuronal differentiation. It would be also interesting to assess the function of miRNAs during neural lineage entry. For this purpose one could use the protocol developed by Boissart et al. (2012) to transiently modulate miRNA activity during neural induction of hPSCs.

Transient miRNA-modulation to direct neuronal differentiation into defined neuronal subtypes

Intriguingly, some of the miRNAs under study were found to have a specific impact on the generation of dopaminergic-like neurons from lt-NES cells. Although these cells may not represent the ideal source for authentic mDA neurons, data collected in this cell population might be transferrable to other more appropriate cell cultures systems. Indeed, experiments using hPSC-derived floor plate progenitors, a cell population close to the developmental origin of mDA neurons (Fasano et al. 2010; Kriks et al. 2011), confirmed the positive and negative effect of miR-181a and miR-124 on dopaminergic differentiation. Nevertheless, a more direct approach to identify miRNAs regulating the dopaminergic lineage would be to perform a miRNA profiling analysis of mDA differentiation paradigms or to annotate region-specific human brain miRNA signatures.

Given their small size and their broad target repertoire, miRNAs have a great potential to be used as cell fate modulators or therapeutic targets (reviewed in van Rooij et al. 2014). However, with the exception of a few “blockbusters”, most miRNAs might rather act as cell fate stabilizers (reviewed in Ebert et al. 2012). This means that miRNA oligonucleotides may not be as potent as pharmacological signaling modulators with regard to cell fate manipulation. Nevertheless, miRNA modulation may still be an asset to the currently used patterning protocols. Indeed, as shown in this work, application of a miRNA-cocktail was able to further promote dopaminergic differentiation even in the presence of SHH/FGF8 signaling activators. Furthermore, as indicated by the example of miR-181a and Wnt signaling, miRNAs may also have a direct impact on the responsiveness of cells to patterning signals. One drawback of transfection-based miRNA modulation approaches is that low cell densities are necessary to ensure high transfection efficiencies. However, this is not feasible for the generation of mDA neurons from floor plate progenitors, where a high cell density is critical. Therefore, one would rather opt for NSC-based DA differentiation paradigms, which should be more amenable to miRNA oligonucleotides. There are promising data indicating that lt-NES cells might be able generate midbrain dopaminergic neurons when treated with CHIR and Wnt5a (J. Carlos Villaescusa and Ernest Arenas, personal communication). As an alternative progenitor population one could also use the pre-rosette NSCs developed by Li et al. (2011a) and Reinhardt et al. (2013), which are believed to have a broader differentiation potential than lt-NES cells. Thus, the next step would be to integrate the findings made here and to study the efficacy of combined miRNA/Wnt modulation and/or GCNF inhibition during dopaminergic differentiation of different NSC culture systems.

Using GCNF as target for the in vitro propagation of human neural stem cells

In this work, GCNF was identified as important factor for human neural stem cell maintenance, which probably acts via repressing a neuronal transcription program. Notwithstanding that these initial findings need to be extended, they indicate that GCNF might be a promising target to optimize the derivation and propagation of human NSCs. In this context, the activity of GCNF as a nuclear receptor could even become amenable to pharmacological modulation. So far, no cognate ligand for GCNF has been identified, but there is a group of benzodiazepines that potentially regulates GCNF function (Roughten et al. 2007). It would be interesting to validate the impact of these benzodiazepines derivates on GCNF function and to investigate their potential effect on neural stem cell fate. To understand the biological function of GCNF in more detail, we are currently establishing a *GCNF chromatin immunoprecipitation followed by DNA-sequencing* (ChIP-seq) assay in a joint project with the Institute for Stem Cell Research and Regenerative Medicine in Düsseldorf. Combining the ChIP-seq data with data generated by RNA-sequencing analysis in response to GCNF overexpression will provide a solid basis to identify and functionally test GCNF target genes. Further experiments should aim at deciphering whether GCNF has a direct function on the self-organization of the neural rosette architecture. In this context, the role of GCNF during neural development starting from neural induction going to pre-rosette and then rosette-forming NSCs should be assessed in more detail.

5 REFERENCES

Abranches E, Silva M, Pradier L, Schulz H, Hummel O, Henrique D et al. (2009). Neural differentiation of embryonic stem cells in vitro: a Road map to neurogenesis in the embryo. PLoS ONE 4, e6286.

Akamatsu W, DeVeale B, Okano H, Cooney AJ & van der Kooy D (2009). Suppression of Oct4 by germ cell nuclear factor restricts pluripotency and promotes neural stem cell development in the early neural lineage. J Neurosci 29, 2113–2124.

Akerblom M & Jakobsson J (2013). MicroRNAs as neuronal fate determinants. Neuroscientist 10.1177/1073858413497265.

Akerblom M, Sachdeva R & Jakobsson J (2012a). Functional studies of microRNAs in neural stem cells: problems and perspectives. Front Neurosci 6, 14.

Akerblom M, Sachdeva R, Barde I, Verp S, Gentner B, Trono D et al. (2012b). MicroRNA-124 is a subventricular zone neuronal fate determinant. J Neurosci 32, 8879–8889.

Ambasudhan R, Talantova M, Coleman R, Yuan X, Zhu S, Lipton SA et al. (2011). Direct reprogramming of adult human fibroblasts to functional neurons under defined conditions. Cell Stem Cell 9, 113–118.

Ambros V (2011). MicroRNAs and developmental timing. Current Opinion in Genetics & Development 21, 511–517.

Amit M & Itskovitz-Eldor J (2002). Derivation and spontaneous differentiation of human embryonic stem cells. J Anat 200, 225–232.

Amit M, Carpenter MK, Inokuma MS, Chiu CP, Harris CP, Waknitz MA et al. (2000). Clonally derived human embryonic stem cell lines maintain pluripotency and proliferative potential for prolonged periods of culture. Dev Biol 227, 271–278.

Anderegg A, Lin HP, Chen JA, Caronia-Brown G, Cherepanova N, Yun B et al. (2013). An Lmx1b-miR135a2 regulatory circuit modulates Wnt1/Wnt signaling and determines the size of the midbrain dopaminergic progenitor pool. PLoS Genet 9, e1003973.

Andersson ER, Prakash N, Cajanek L, Minina E, Bryja V, Bryjova L et al. (2008). Wnt5a regulates ventral midbrain morphogenesis and the development of A9–A10 dopaminergic cells in vivo. PLoS ONE 3, e3517.

Andersson ER, Saltó C, Villaescusa JC, Cajanek L, Yang S, Bryjova L et al. (2013). Wnt5a cooperates with canonical Wnts to generate midbrain dopaminergic neurons in vivo and in stem cells. Proc Natl Acad Sci U S A 110, E602–E610.

Arenas E (2014). Wnt signaling in midbrain dopaminergic neuron development and regenerative medicine for Parkinson's disease. Journal of Molecular Cell Biology 6, 42–53.

Baek S, Choi H & Kim J (2014). Ebf3-miR218 regulation is involved in the development of dopaminergic neurons. Brain Research.

Bain DL, Heneghan AF, Connaghan-Jones KD & Miura MT (2007). Nuclear receptor structure: implications for function. Annu Rev Physiol 69, 201–220.

Balzer E, Heine C, Jiang Q, Lee VM & Moss EG (2010). LIN28 alters cell fate succession and acts independently of the let-7 microRNA during neurogliogenesis in vitro. Development 137, 891–900.

Bao B, Rodriguez-Melendez R & Zempleni J (2012). Cytosine methylation in miR-153 gene promoters increases the expression of holocarboxylase synthetase, thereby increasing the abundance of histone H4 biotinylation marks in HEK-293 human kidney cells. J Nutr Biochem 23, 635–639.

Bar M, Wyman SK, Fritz BR, Qi J, Garg KS, Parkin RK et al. (2008). MicroRNA discovery and profiling in human embryonic stem cells by deep sequencing of small RNA libraries. STEM CELLS 26, 2496–2505.

Barnea E & Bergman Y (2000). Synergy of SF1 and RAR in activation of Oct-3/4 promoter. J Biol Chem 275, 6608–6619.

Baroukh N, Ravier MA, Loder MK, Hill EV, Bounacer A, Scharfmann R et al. (2007). MicroRNA-124a regulates Foxa2 expression and intracellular signaling in pancreatic β-cell lines. J Biol Chem 282, 19575–19588.

Barreto G, Borgmeyer U & Dreyer C (2003a). The germ cell nuclear factor is required for retinoic acid signaling during Xenopus development. Mechanisms of Development 120, 415–428.

Barreto G, Reintsch W, Kaufmann C & Dreyer C (2003b). The function of Xenopus germ cell nuclear factor (xGCNF) in morphogenetic movements during neurulation. Developmental Biology 257, 329–342.

Bauer UM, Schneider-Hirsch S, Reinhardt S, Pauly T, Maus A, Wang F et al. (1997). Neuronal cell nuclear factor--a nuclear receptor possibly involved in the control of neurogenesis and neuronal differentiation. Eur J Biochem 249, 826–837.

Bayart E & Cohen-Haguenauer O (2013). Technological overview of iPS induction from human adult somatic cells. Curr Gene Ther 13, 73–92.

Behm-Ansmant I, Rehwinkel J, Doerks T, Stark A, Bork P & Izaurralde E (2006). mRNA degradation by miRNAs and GW182 requires both CCR4:NOT deadenylase and DCP1:DCP2 decapping complexes. Genes & Development 20, 1885–1898.

Benchoua A & Peschanski M (2013). Pluripotent stem cells as a model to study non-coding RNAs function in human neurogenesis. Front Cell Neurosci 7, 140.

Benes V & Castoldi M (2010). Expression profiling of microRNA using real-time quantitative PCR, how to use it and what is available. Methods 50, 244–249.

Bentwich I, Avniel A, Karov Y, Aharonov R, Gilad S, Barad O et al. (2005). Identification of hundreds of conserved and nonconserved human microRNAs. Nat Genet 37, 766–770.

Berezikov E, Chung WJ, Willis J, Cuppen E & Lai EC (2007). Mammalian mirtron genes. Mol Cell 28, 328–336.

Bertrand N, Castro DS & Guillemot F (2002). Proneural genes and the specification of neural cell types. Nat Rev Neurosci 3, 517–530.

Beveridge NJ, Tooney PA, Carroll AP, Gardiner E, Bowden N, Scott RJ et al. (2008). Dysregulation of miRNA 181b in the temporal cortex in schizophrenia. Human Molecular Genetics 17, 1156–1168.

Bhushan R, Grünhagen J, Becker J, Robinson PN, Ott CE & Knaus P (2013). miR-181a promotes osteoblastic differentiation through repression of TGF-β signaling molecules. The International Journal of Biochemistry & Cell Biology 45, 696–705.

Bian S, Xu TL & Sun T (2013). Tuning the cell fate of neurons and glia by microRNAs. Current Opinion in Neurobiology 23, 928–934.

Bohnsack MT, Czaplinski K & Gorlich D (2004). Exportin 5 is a RanGTP-dependent dsRNA-binding protein that mediates nuclear export of pre-miRNAs. RNA 10, 185–191.

Boissart C, Nissan X, Giraud-Triboult K, Peschanski M & Benchoua A (2012). miR-125 potentiates early neural specification of human embryonic stem cells. Development 139, 1247–1257.

Bonev B, Stanley P & Papalopulu N (2012). MicroRNA-9 modulates Hes1 ultradian oscillations by forming a double-negative feedback loop. Cell Reports 2, 10–18.

Borghese L, Dolezalova D, Opitz T, Haupt S, Leinhaas A, Steinfarz B et al. (2010). Inhibition of Notch signaling in human embryonic stem cell-derived neural stem cells delays G1/S phase transition and accelerates neuronal differentiation in vitro and in vivo. STEM CELLS 28, 955–964.

Borgmeyer U (1997). Dimeric binding of the mouse germ cell nuclear factor. Eur J Biochem 244, 120–127.

Brennecke J, Stark A, Russell R & Cohen S (2005). Principles of microRNA-target recognition. PLoS Biol 3, e85–e85.

Breunig JJ, Haydar TF & Rakic P (2011). Neural stem cells: historical perspective and future prospects. Neuron 70, 614–625.

Cai X, Hagedorn CH & Cullen BR (2004). Human microRNAs are processed from capped, polyadenylated transcripts that can also function as mRNAs. RNA 10, 1957–1966.

Cao X, Pfaff SL & Gage FH (2007). A functional study of miR-124 in the developing neural tube. Genes & Development 21, 531–536.

Card DAG, Hebbar PB, Li L, Trotter KW, Komatsu Y, Mishina Y et al. (2008). Oct4/Sox2-regulated miR-302 targets cyclin D1 in human embryonic stem cells. Molecular and Cellular Biology 28, 6426–6438.

Chambers SM, Fasano CA, Papapetrou EP, Tomishima M, Sadelain M & Studer L (2009). Highly efficient neural conversion of human ES and iPS cells by dual inhibition of SMAD signaling. Nat Biotechnol 27, 275–280.

Chandrasekar V & Dreyer JL (2009). microRNAs miR-124, let-7d and miR-181a regulate Cocaine-induced Plasticity. Molecular and Cellular Neuroscience 42, 350–362.

Chandrasekar V & Dreyer JL (2011). Regulation of miR-124, let-7d, and miR-181a in the accumbens affects the expression, extinction, and reinstatement of cocaine-induced conditioned place preference. Neuropsychopharmacology 36, 1149–1164.

Chang C & Harland RM (2007). Neural induction requires continued suppression of both Smad1 and Smad2 signals during gastrulation. Development 134, 3861–3872.

Chang MY, Rhee YH, Yi SH, Lee SJ, Kim RK, Kim H et al. (2014). Doxycycline enhances survival and self-renewal of human pluripotent stem cells. Stem Cell Reports 3, 353–364.

Chatterjee S, Fasler M, Büssing I & Großhans H (2011). Target-mediated protection of endogenous microRNAs in C. elegans. Dev Cell 20, 388–396.

Chen AX, Yu KD, Fan L, Li JY, Yang C, Huang AJ et al. (2011). Germline genetic variants disturbing the let-7/LIN28 double-negative feedback loop alter breast cancer susceptibility. PLoS Genet 7, e1002259.

Chen B, Dodge ME, Tang W, Lu J, Ma Z, Fan CW et al. (2009). Small molecule-mediated disruption of Wnt-dependent signaling in tissue regeneration and cancer. Nat Chem Biol 5, 100–107.

Chen CZ, Li L, Lodish HF & Bartel DP (2004). MicroRNAs modulate hematopoietic lineage differentiation. Science 303, 83–86.

Chen F, Cooney AJ, Wang Y, Law SW & O'Malley BW (1994). Cloning of a novel orphan receptor (GCNF) expressed during germ cell development. Molecular Endocrinology 8, 1434–1444.

Chen G, Zhu W, Shi D, Lv L, Zhang C, Liu P et al. (2010). MicroRNA-181a sensitizes human malignant glioma U87MG cells to radiation by targeting Bcl-2. Oncology reports 23, 997–1003.

Chendrimada TP, Finn KJ, Ji X, Baillat D, Gregory RI, Liebhaber SA et al. (2007). MicroRNA silencing through RISC recruitment of eIF6. Nature 447, 823–828.

Cheng LC, Pastrana E, Tavazoie M & Doetsch F (2009). miR-124 regulates adult neurogenesis in the subventricular zone stem cell niche. Nat Neurosci 12, 399–408.

Chiang HR, Schoenfeld LW, Ruby JG, Auyeung VC, Spies N, Baek D et al. (2010). Mammalian microRNAs: experimental evaluation of novel and previously annotated genes. Genes & Development 24, 992–1009.

Chitnis A & Kintner C (1996). Sensitivity of proneural genes to lateral inhibition affects the pattern of primary neurons in Xenopus embryos. Development 122, 2295–2301.

Choudhury NR, de Lima Alves F, de Andres-Aguayo L, Graf T, Caceres JF, Rappsilber J et al. (2013). Tissue-specific control of brain-enriched miR-7 biogenesis. Genes & Development 27, 24–38.

Chung AC & Cooney AJ (2001a). Germ cell nuclear factor. International Journal of Biochemistry and Cell Biology 33, 1141–1146.

Chung ACK, Katz D, Pereira FA, Jackson KJ, DeMayo FJ, Cooney AJ et al. (2001b). Loss of orphan receptor germ cell nuclear factor function results in ectopic development of the tail bud and a novel posterior truncation. Molecular and Cellular Biology 21, 663–677.

Chung ACK, Xu X, Niederreither KA & Cooney AJ (2006). Loss of orphan nuclear receptor GCNF function disrupts forebrain development and the establishment of the isthmic organizer. Developmental Biology 293, 13–24.

Cichocki F, Felices M, McCullar V, Presnell SR, Al-Attar A, Lutz CT et al. (2011). Cutting edge: MicroRNA-181 promotes human NK cell development by regulating notch signaling. The Journal of Immunology 187, 6171–6175.

Cimadamore F, Amador-Arjona A, Chen C, Huang CT & Terskikh AV (2013). SOX2-LIN28/let-7 pathway regulates proliferation and neurogenesis in neural precursors. Proc Natl Acad Sci U S A 110, E3017–E3026.

Cloonan N, Wani S, Xu Q, Gu J, Lea K, Heater S et al. (2011). MicroRNAs and their isomiRs function cooperatively to target common biological pathways. Genome Biol 12, R126–R126.

Coles-Takabe BLK, Brain I, Purpura KA, Karpowicz P, Zandstra PW, Morshead CM et al. (2008). Don't look: growing clonal versus nonclonal neural stem cell colonies. STEM CELLS 26, 2938–2944.

Conaco C, Otto S, Han JJ & Mandel G (2006). Reciprocal actions of REST and a microRNA promote neuronal identity. Proc Natl Acad Sci U S A 103, 2422–2427.

Conti L & Cattaneo E (2010). Neural stem cell systems: physiological players or in vitro entities? Nat Rev Neurosci 11, 176–187.

Conti L, Pollard SM, Gorba T, Reitano E, Toselli M, Biella G et al. (2005). Niche-independent symmetrical self-renewal of a mammalian tissue stem cell. PLoS Biol 3, e283.

Coolen M, Katz S & Bally-Cuif L (2013). miR-9: a versatile regulator of neurogenesis. Front Cell Neurosci 7, 220.

Cooney AJ, Hummelke GC, Herman T, Chen F & Jackson KJ (1998). Germ cell nuclear factor is a response element-specific repressor of transcription. Biochem Biophys Res Commun 245, 94–100.

Cremisi F (2013). MicroRNAs and cell fate in cortical and retinal development. Front Cell Neurosci 7, 1–8.

Cui Y, Xiao Z, Han J, Sun J, Ding W, Zhao Y et al. (2012). MiR-125b orchestrates cell proliferation, differentiation and migration in neural stem/progenitor cells by targeting Nestin. BMC Neurosci 13, 116.

David R, Joos TO & Dreyer C (1998). Anteroposterior patterning and organogenesis of Xenopus laevis require a correct dose of germ cell nuclear factor (xGCNF). Mech Dev 79, 137–152.

Davis BN, Hilyard AC, Lagna G & Hata A (2008). SMAD proteins control DROSHA-mediated microRNA maturation. Nature 454, 56–61.

Davis BN, Hilyard AC, Nguyen PH, Lagna G & Hata A (2010). Smad proteins bind a conserved RNA sequence to promote microRNA maturation by Drosha. Molecular Cell 39, 373–384.

de Hoon MJ, Imoto S, Nolan J & Miyano S (2004). Open source clustering software. Bioinformatics 20, 1453–1454.

Denli AM, Tops BBJ, Plasterk RHA, Ketting RF & Hannon GJ (2004). Processing of primary microRNAs by the Microprocessor complex. Nature 432, 231–235.

Diederichs S & Haber DA (2007). Dual role for Argonautes in microRNA processing and posttranscriptional regulation of microRNA expression. Cell 131, 12–12.

Dogini DB, Ribeiro PAO, Rocha C, Pereira TC & Lopes-Cendes I (2008). MicroRNA expression profile in murine central nervous system development. J Mol Neurosci 35, 331–337.

Doxakis E (2010). Post-transcriptional regulation of alpha-synuclein expression by mir-7 and mir-153. Journal of Biological Chemistry 285, 12726–12734.

Du ZW, Ma LX, Phillips C & Zhang SC (2013). miR-200 and miR-96 families repress neural induction from human embryonic stem cells. Development 140, 2611–2618.

Dweep H, Sticht C, Pandey P & Gretz N (2011). miRWalk – Database: Prediction of possible miRNA binding sites by “walking” the genes of three genomes. Journal of biomedical informatics.

Ebert MS & Sharp PA (2012). Roles for MicroRNAs in conferring robustness to biological processes. Cell 149, 515–524.

Eisen MB, Spellman PT, Brown PO & Botstein D (1998). Cluster analysis and display of genome-wide expression patterns. Proc Natl Acad Sci U S A 95, 14863–14868.

Elkabetz Y, Panagiotakos G, Shamy Al G, Socci ND, Tabar V & Studer L (2008). Human ES cell-derived neural rosettes reveal a functionally distinct early neural stem cell stage. Genes & Development 22, 152–165.

Enmark E & Gustafsson JA (2001). Comparing nuclear receptors in worms, flies and humans. Trends Pharmacol Sci 22, 611–615.

Esteller M (2011). Non-coding RNAs in human disease. Nat Rev Genet 12, 861–874.

Eulalio A, Behm-Ansmant I & Izaurralde E (2006). P bodies: at the crossroads of post-transcriptional pathways. Nat Rev Mol Cell Biol 8, 9–22.

Evans MJ & Kaufman MH (1981). Establishment in culture of pluripotential cells from mouse embryos. Nature 292, 154–156.

Falk A, Koch P, Kesavan J, Takashima Y, Ladewig J, Alexander M et al. (2012). Capture of neuroepithelial-like stem cells from pluripotent stem cells provides a versatile system for in vitro production of human neurons. PLoS ONE 7, e29597.

Farah MH, Olson JM, Sucic HB, Hume RI, Tapscott SJ & Turner DL (2000). Generation of neurons by transient expression of neural bHLH proteins in mammalian cells. Development 127, 693–702.

Farazi TA, Juranek SA & Tuschl T (2008). The growing catalog of small RNAs and their association with distinct Argonaute/Piwi family members. Development 135, 1201–1214.

Farrell BC, Power EM & Dermott KWM (2011). Developmentally regulated expression of Sox9 and microRNAs 124,128 and 23 in neuroepithelial stem cells in the developing spinal cord. International Journal of Developmental Neuroscience 29, 6–6.

Fasano CA, Chambers SM, Lee G, Tomishima MJ & Studer L (2010). Efficient derivation of functional floor plate tissue from human embryonic stem cells. Cell Stem Cell 6, 336–347.

Ferretti E, De Smaele E, Miele E, Laneve P, Po A, Pelloni M et al. (2008). Concerted microRNA control of Hedgehog signalling in cerebellar neuronal progenitor and tumour cells. EMBO J 27, 2616–2627.

Fiore R, Khudayberdiev S, Christensen M, Siegel G, Flavell SW, Kim TK et al. (2009). Mef2-mediated transcription of the miR379–410 cluster regulates activity-dependent dendritogenesis by fine-tuning Pumilio2 protein levels. EMBO J 28, 697–710.

Flores O, Kennedy EM, Skalsky RL & Cullen BR (2014). Differential RISC association of endogenous human microRNAs predicts their inhibitory potential. Nucleic Acids Research.

Fragoso R, Mao T, Wang S, Schaffert S, Gong X, Yue S et al. (2012). Modulating the strength and threshold of NOTCH oncogenic signals by mir-181a-1/b-1. PLoS Genet 8, e1002855.

Franke K, Otto W, Johannes S, Baumgart J, Nitsch R & Schumacher S (2012). miR-124-regulated RhoG reduces neuronal process complexity via ELMO/Dock180/Rac1 and Cdc42 signalling. EMBO J 31, 2908–2921.

Fuerer C & Nusse R (2009). Lentiviral vectors to probe and manipulate the Wnt signaling pathway. PLoS ONE 5, e9370–e9370.

Fuhrmann G, Chung AC, Jackson KJ, Hummelke G, Baniahmad A, Sutter J et al. (2001). Mouse germline restriction of Oct4 expression by germ cell nuclear factor. Dev Cell 1, 11–11.

Gantier MP, McCoy CE, Rusinova I, Saulep D, Wang D, Xu D et al. (2011). Analysis of microRNA turnover in mammalian cells following Dicer1 ablation. Nucleic Acids Research 39, 5692–5703.

Gaspard N & Vanderhaeghen P (2010). Mechanisms of neural specification from embryonic stem cells. Current Opinion in Neurobiology 20, 37–43.

Gaughwin P, Ciesla M, Yang H, Lim B & Brundin P (2011). Stage-specific modulation of cortical neuronal development by mmu-miR-134. Cerebral Cortex 21, 1857–1869.

Gaur A, Jewell DA, Liang Y, Ridzon D, Moore JH, Chen C et al. (2007). Characterization of microRNA expression levels and their biological correlates in human cancer cell lines. Cancer Research 67, 2456–2468.

Geekiyanage H & Chan C (2011). MicroRNA-137/181c regulates serine palmitoyltransferase and in turn amyloid β, novel targets in sporadic Alzheimer's disease. J Neurosci 31, 14820–14830.

Glaser T, Pollard SM, Smith A & Brüstle O (2007). Tripotential differentiation of adherently expandable neural stem (NS) cells. PLoS ONE 2, e298.

Godnic I, Zorc M, Jevsinek Skok D, Calin GA, Horvat S, Dovc P et al. (2013). Genome-wide and species-wide in silico screening for intragenic microRNAs in human, mouse and chicken. PLoS ONE 8, e65165.

Gonzalez-Gonzalez E, Lopez-Casas PP & del Mazo J (2008). The expression patterns of genes involved in the RNAi pathways are tissue-dependent and differ in the germ and somatic cells of mouse testis. Biochim Biophys Acta 1779, 306–311.

Gorris R, Fischer J, Erwes KL, Kesavan J, Alexander M, Nöthen M et al. Pluripotent stem cell-derived radial glia-like cells as stable intermediate for efficient generation of human oligodendrocytes. *in submission*.

Götz M & Barde YA (2005). Radial glial cells. Neuron 46, 369–372.

Greve TS, Judson RL & Blelloch R (2013). MicroRNA control of mouse and human pluripotent stem cell behavior. Annu Rev Cell Dev Biol 29, 213–239.

Grimson A, Farh KKH, Johnston WK, Garrett-Engele P, Lim LP & Bartel DP (2007). MicroRNA targeting specificity in mammals: determinants beyond seed pairing. Mol Cell 27, 91–105.

Groß NA (2012). Analysis of the impact of microRNA activity modulation in human pluripotent stem cell-derived neural stem cells. Diplomarbeit.

Gu P, Goodwin B, Chung ACK, Xu X, Wheeler DA, Price RR et al. (2005a). Orphan nuclear receptor LRH-1 is required to maintain Oct4 expression at the epiblast stage of embryonic development. Molecular and Cellular Biology 25, 3492–3505.

Gu P, Le Menuet D, Chung ACK, Mancini M, Wheeler DA & Cooney AJ (2005b). Orphan nuclear receptor GCNF is required for the repression of pluripotency genes during retinoic acid-induced embryonic stem cell differentiation. Molecular and Cellular Biology 25, 8507–8519.

Gu P, Reid JG, Gao X, Shaw CA, Creighton C, Tran PL et al. (2008). Novel microRNA candidates and miRNA-mRNA pairs in embryonic stem (ES) cells. PLoS ONE 3, e2548.

Gu P, Xu X, Le Menuet D, Chung ACK & Cooney AJ (2011). Differential recruitment of methyl CpG-binding domain factors and DNA methyltransferases by the orphan receptor germ cell nuclear factor initiates the repression and silencing of Oct4. STEM CELLS 29, 1041–1051.

Gu X, Meng S, Liu S, Jia C, Fang Y, Li S et al. (2013). miR-124 represses ROCK1 expression to promote neurite elongation through activation of the PI3K/Akt signal Pathway. J Mol Neurosci.

Guibinga GH, Hrustanovic G, Bouic K, Jinnah HA & Friedmann T (2012). MicroRNA-mediated dysregulation of neural developmental genes in HPRT deficiency: clues for Lesch-Nyhan disease? Human Molecular Genetics 21, 609–622.

Guil S & Cáceres JF (2007). The multifunctional RNA-binding protein hnRNP A1 is required for processing of miR-18a. Nat Struct Mol Biol 14, 591–596.

Guo Y, Chen Y, Ito H, Watanabe A, Ge X, Kodama T et al. (2006). Identification and characterization of lin-28 homolog B (LIN28B) in human hepatocellular carcinoma. Gene 384, 51–61.

Gurtan AM, Ravi A, Rahl PB, Bosson AD, JnBaptiste CK, Bhutkar A et al. (2013). Let-7 represses Nr6a1 and a mid-gestation developmental program in adult fibroblasts. Genes & Development 27, 941–954.

Han J, Lee Y, Yeom KH, Kim YK, Jin H & Kim VN (2004). The Drosha-DGCR8 complex in primary microRNA processing. Genes & Development 18, 3016–3027.

He X, Yu Y, Awatramani R & Lu QR (2012). Unwrapping myelination by microRNAs. Neuroscientist 18, 45–55.

Hegarty SV, Sullivan AM & O'Keeffe GW (2013). Midbrain dopaminergic neurons: A review of the molecular circuitry that regulates their development. Developmental Biology 379, 123–138.

Henao-Mejia J, Williams A, Goff LA, Staron M, Licona-Limón P, Kaech SM et al. (2013). The microRNA miR-181 is a critical cellular metabolic rheostat essential for NKT cell ontogenesis and lymphocyte development and homeostasis. IMMUNI 38, 984–997.

Hentschke M, Kurth I, Borgmeyer U & Hübner CA (2006). Germ cell nuclear factor is a repressor of CRIPTO-1 and CRIPTO-3. J Biol Chem 281, 33497–33504.

Heo I, Joo C, Kim YK, Ha M, Yoon MJ, Cho J et al. (2009). TUT4 in concert with Lin28 suppresses microRNA biogenesis through pre-microRNA uridylation. Cell 138, 696–708.

Herranz H & Cohen SM (2010). MicroRNAs and gene regulatory networks: managing the impact of noise in biological systems. Genes & Development 24, 1339–1344.

Heyer MP, Pani AK, Smeyne RJ, Kenny PJ & Feng G (2012). Normal midbrain dopaminergic neuron development and function in miR-133b mutant mice. J Neurosci 32, 10887–10894.

Hirose T, O'Brien DA & Jetten AM (1995). RTR: a new member of the nuclear receptor superfamily that is highly expressed in murine testis. Gene 152, 247–251.

Hitoshi S, Alexson T, Tropepe V, Donoviel D, Elia AJ, Nye JS et al. (2002). Notch pathway molecules are essential for the maintenance, but not the generation, of mammalian neural stem cells.
Genes & Development 16, 846–858.

Hohjoh H & Fukushima T (2007). Marked change in microRNA expression during neuronal differentiation of human teratocarcinoma NTera2D1 and mouse embryonal carcinoma P19 cells.
Biochem Biophys Res Commun 362, 8–8.

Horisawa K & Yanagawa H (2012). Musashi proteins in neural stem/progenitor cells. In *Neural Stem Cells and Therapy*. InTech, pp. 21–34.

Houbaviy HB, Murray MF & Sharp PA (2003). Embryonic stem cell-specific microRNAs. Dev Cell 5, 351–358.

Huang DW, Sherman BT & Lempicki RA (2009). Systematic and integrative analysis of large gene lists using DAVID bioinformatics resources. Nat Protoc 4, 44–57.

Hummelke GC & Cooney AJ (2004). Reciprocal regulation of the mouse protamine genes by the orphan nuclear receptor germ cell nuclear factor and CREMtau. Mol Reprod Dev 68, 394–407.

Humphreys DT, Westman BJ, Martin DIK & Preiss T (2005). MicroRNAs control translation initiation by inhibiting eukaryotic initiation factor 4E/cap and poly(A) tail function. Proc Natl Acad Sci U S A 102, 16961–16966.

Hutchison ER, Kawamoto EM, Taub DD, Lal A, Abdelmohsen K, Zhang Y et al. (2013). Evidence for miR-181 involvement in neuroinflammatory responses of astrocytes. Glia 61, 1018–1028.

Hutvagner G & Simard MJ (2007). Argonaute proteins: key players in RNA silencing.
Nat Rev Mol Cell Biol 9, 22–32.

Imai T, Tokunaga A, Yoshida T, Hashimoto M, Mikoshiba K, Weinmaster G et al. (2001). The neural RNA-binding protein Musashi1 translationally regulates mammalian numb gene expression by interacting with its mRNA. Molecular and Cellular Biology 21, 3888–3900.

Inukai S, de Lencastre A, Turner M & Slack F (2012). Novel microRNAs differentially expressed during aging in the mouse brain. PLoS ONE 7, e40028.

Iso T, Sartorelli V, Poizat C, Iezzi S, Wu HY, Chung G et al. (2001). HERP, a novel heterodimer partner of HES/E(spl) in Notch Signaling.
Molecular and Cellular Biology 21, 6080–6089.

Ivey KN & Srivastava D (2010). MicroRNAs as regulators of differentiation and cell fate decisions.
Cell Stem Cell 7, 36–41.

Ivey KN, Muth A, Arnold J, King FW, Yeh RF, Fish JE et al. (2008). MicroRNA regulation of cell lineages in mouse and human embryonic stem cells.
Cell Stem Cell 2, 219–229.

Jaenisch R & Young R (2008). Stem sells, the molecular circuitry of pluripotency and nuclear reprogramming.
Cell 132, 567–582.

Janas MM, Wang B, Harris AS, Aguiar M, Shaffer JM, Subrahmanyam YVBK et al. (2012). Alternative RISC assembly: Binding and repression of microRNA-mRNA duplexes by human Ago proteins. RNA 18, 2041–2055.

Jantzie LL, Cheung PY & Todd KG (2005). Doxycycline reduces cleaved caspase-3 and microglial activation in an animal model of neonatal hypoxia-ischemia. J Cereb Blood Flow Metab 25, 314–324.

Ji J, Yamashita T, Budhu A, Forgues M, Jia HL, Li C et al. (2009). Identification of microRNA-181 by genome-wide screening as a critical player in EpCAM-positive hepatic cancer stem cells. Hepatology 50, 472–480.

Jiang C, Xuan Z, Zhao F & Zhang MQ (2007). TRED: a transcriptional regulatory element database, new entries and other development.
Nucleic Acids Research 35, D137–D140.

John B, Enright AJ, Aravin A, Tuschl T, Sander C & Marks DS (2004). Human MicroRNA targets.
PLoS Biol 2, e363.

Joksimovic M, Yun BA, Kittappa R, Anderegg AM, Chang WW, Taketo MM et al. (2009). Wnt antagonism of Shh facilitates midbrain floor plate neurogenesis.
Nat Neurosci 12, 125–131.

Jones-Villeneuve EM, Rudnicki MA, Harris JF & McBurney MW (1983). Retinoic acid-induced neural differentiation of embryonal carcinoma cells.
Molecular and Cellular Biology 3, 2271–2279.

Joos TO, David R & Dreyer C (1996). xGCNF, a nuclear orphan receptor is expressed during neurulation in Xenopus laevis. Mech Dev 60, 45–57.

Jostock, RentropMaelicke (1998). Cell fate specification in an in vitro model of neural development.
Eur J Cell Biol 76, 14–14.

Judson RL, Greve TS, Parchem RJ & Blelloch R (2013). MicroRNA-based discovery of barriers to dedifferentiation of fibroblasts to pluripotent stem cells.
Nat Struct Mol Biol 20, 1227–1235.

Kageyama R, Ohtsuka T, Hatakeyama J & Ohsawa R (2005). Roles of bHLH genes in neural stem cell differentiation. Experimental Cell Research 306, 343–348.

Kai ZS & Pasquinelli AE (2010). MicroRNA assassins: factors that regulate the disappearance of miRNAs.
Nat Struct Mol Biol 17, 5–10.

Kamanu TKK, Radovanovic A, Archer JAC & Bajic VB (2013). Exploration of miRNA families for hypotheses generation. Sci Rep 3.

Kane NM, Howard L, Descamps B, Meloni M, McClure J, Lu R et al. (2012). Role of microRNAs 99b, 181a, and 181b in the differentiation of human embryonic stem cells to vascular endothelial cells. STEM CELLS 30, 643–654.

Kang SM, Choi JW, Hong SH & Lee HJ (2013). Up-regulation of microRNA* strands by their target transcripts.
Int J Mol Sci 14, 13231–13240.

Kapelle M, Kratzschmar J, Husemann M & Schleuning WD (1997). cDNA cloning of two closely related forms of human germ cell nuclear factor (GCNF). Biochim Biophys Acta 1352, 13–17.

Karus M, Blaess S & Brüstle O (2014). Self-organisation of neural tissue architectures from pluripotent stem cells. J Comp Neurol.

Kasuga H, Fukuyama M, Kitazawa A, Kontani K & Katada T (2013). The microRNA miR-235 couples blast-cell quiescence to the nutritional state. Nature 497, 503–506.

Kataoka N, Fujita M & Ohno M (2009). Functional association of the Microprocessor complex with the spliceosome. Mol Cell Biol 29, 3243–3254.

Kawahara H, Okada Y, Imai T, Iwanami A, Mischel PS & Okano H (2011). Musashi1 cooperates in abnormal cell lineage protein 28 (Lin28)-mediated let-7 family microRNA biogenesis in early neural differentiation. J Biol Chem 286, 16121–16130.

Kawahara Y, Zinshteyn B, Chendrimada TP, Shiekhattar R & Nishikura K (2007). RNA editing of the microRNA-151 precursor blocks cleavage by the Dicer-TRBP complex. EMBO Rep 8, 763–769.

Kazenwadel J, Michael MZ & Harvey NL (2010). Prox1 expression is negatively regulated by miR-181 in endothelial cells. Blood 116, 2395–2401.

Khvorova A, Reynolds A & Jayasena SD (2003). Functional siRNAs and miRNAs exhibit strand bias. Cell 115, 209–216.

Kim DS, Lee JS, Leem JW, Huh YJ, Kim JY, Kim HS et al. (2010). Robust enhancement of neural differentiation from human ES and iPS cells regardless of their innate difference in differentiation propensity. Stem Cell Rev and Rep 6, 270–281.

Kim H, Lee G, Ganat Y, Papapetrou EP, Lipchina I, Socci ND et al. (2011). miR-371-3 expression predicts neural differentiation propensity in human pluripotent stem cells. Cell Stem Cell 8, 695–706.

Kim J, Inoue K, Ishii J, Vanti WB, Voronov SV, Murchison E et al. (2007a). A MicroRNA feedback circuit in midbrain dopamine neurons. Science 317, 1220–1224.

Kim J, Krichevsky A, Grad Y, Hayes GD, Kosik KS, Church GM et al. (2004). Identification of many microRNAs that copurify with polyribosomes in mammalian neurons. Proc Natl Acad Sci U S A 101, 360–365.

Kim YK & Kim VN (2007b). Processing of intronic microRNAs. EMBO J 26, 775–783.

King-Jones K, Charles JP, Lam G & Thummel CS (2005). The Ecdysone-Induced DHR4 orphan nuclear receptor coordinates growth and maturation in Drosophila. Cell 121, 773–784.

Kiriakidou M, Tan GS, Lamprinaki S, De Planell-Saguer M, Nelson PT & Mourelatos Z (2007). An mRNA m^7G cap binding-like motif within human ago2 represses translation. Cell 129, 11–11.

Kirkeby A, Grealish S, Wolf DA, Nelander J, Wood J, Lundblad M et al. (2012). Generation of regionally specified neural progenitors and functional neurons from human embryonic stem cells under defined conditions. Cell Reports 1, 703–714.

Klein ME, Lioy DT, Ma L, Impey S, Mandel G & Goodman RH (2007). Homeostatic regulation of MeCP2 expression by a CREB-induced microRNA. Nat Neurosci 10, 1513–1514.

Koch P, Breuer P, Peitz M, Jungverdorben J, Kesavan J, Poppe D et al. (2011). Excitation-induced ataxin-3 aggregation in neurons from patients with Machado-Joseph disease. Nature 480, 543–546.

Koch P, Kokaia Z, Lindvall O & Brüstle O (2009a). Emerging concepts in neural stem cell research: autologous repair and cell-based disease modelling. The Lancet Neurology 8, 819–829.

Koch P, Opitz T, Steinbeck JA, Ladewig J & Brüstle O (2009b). A rosette-type, self-renewing human ES cell-derived neural stem cell with potential for in vitro instruction and synaptic integration. Proc Natl Acad Sci U S A 106, 3225–3230.

Koch P, Siemen H, Biegler A, Itskovitz-Eldor J & Brüstle O (2006). Transduction of human embryonic stem cells by ecotropic retroviral vectors. Nucleic Acids Research 34, e120–e120.

Koch P, Tamboli IY, Mertens J, Wunderlich P, Ladewig J, Stuber K et al. (2012). Presenilin-1 L166P mutant human pluripotent stem cell-derived neurons exhibit partial loss of gamma-secretase activity in endogenous amyloid-beta generation. Am J Pathol 180, 2404–2416.

Kozomara A & Griffiths-Jones S (2013). miRBase: annotating high confidence microRNAs using deep sequencing data. Nucleic Acids Research 42, D68–D73.

Kozomara A & Griffiths-Jones S (2011). miRBase: integrating microRNA annotation and deep-sequencing data. Nucleic Acids Research 39, D152–7.

Krichevsky AM, Sonntag KC, Isacson O & Kosik KS (2006). Specific microRNAs modulate embryonic stem cell-derived neurogenesis. STEM CELLS 24, 857–864.

Kriks S, Shim JW, Piao J, Ganat YM, Wakeman DR, Xie Z et al. (2011). Dopamine neurons derived from human ES cells efficiently engraft in animal models of Parkinson's disease. Nature 480, 547–551.

Krützfeldt J, Rajewsky N, Braich R, Rajeev KG, Tuschl T, Manoharan M et al. (2005). Silencing of microRNAs in vivo with 'antagomirs'. Nature 438, 685–689.

Kutner RH, Zhang XY & Reiser J (2009). Production, concentration and titration of pseudotyped HIV-1-based lentiviral vectors. Nat Protoc 4, 495–505.

Kwak PB & Tomari Y (2012). The N domain of Argonaute drives duplex unwinding during RISC assembly. Nat Struct Mol Biol 19, 145–151.

Ladewig J, Koch P & Brüstle O (2013). Leveling Waddington: the emergence of direct programming and the loss of cell fate hierarchies. Nat Rev Mol Cell Biol 14, 225–236.

Ladewig J, Koch P, Endl E, Meiners B, Opitz T, Couillard-Despres S et al. (2008). Lineage selection of functional and cryopreservable human embryonic stem cell-derived neurons. STEM CELLS 26, 1705–1712.

Lagos-Quintana M, Rauhut R, Yalcin A, Meyer J, Lendeckel W & Tuschl T (2002). Identification of tissue-specific microRNAs from mouse. Curr Biol 12, 735–739.

Lan ZJ, Gu P, Xu X & Cooney AJ (2002). Expression of the orphan nuclear receptor, germ cell nuclear factor, in mouse gonads and preimplantation embryos. Biology of Reproduction 68, 282–289.

Landgraf P, Rusu M, Sheridan R, Sewer A, Iovino N, Aravin A et al. (2007). A mammalian microRNA expression atlas based on small RNA library sequencing. Cell 129, 1401–1414.

Laneve P, Di Marcotullio L, Gioia U, Fiori ME, Ferretti E, Gulino A et al. (2007). The interplay between microRNAs and the neurotrophin receptor tropomyosin-related kinase C controls proliferation of human neuroblastoma cells. Proc Natl Acad Sci U S A 104, 7957–7962.

Langenberger D, Bartschat S, Jana Hertel, Steve Hoffmann, Hakim Tafer & Stadler PF (2011). MicroRNA or not microRNA? Advances in Bioinformatics and Computational Biology Lecture Notes in Computer Science Volume 6832, 2011, pp 1-9

Lao K, Xu NL, Sun YA, Livak KJ & Straus NA (2007). Real time PCR profiling of 330 human micro-RNAs. Biotechnol J 2, 33–35.

Laurent LC, Chen J, Ulitsky I, Mueller FJ, Lu C, Shamir R et al. (2008). Comprehensive microRNA profiling reveals a unique human embryonic stem cell signature dominated by a single seed sequence. STEM CELLS 26, 1506–1516.

Lazzarini M, Martin S, Mitkovski M, Vozari RR, Stühmer W & Bel ED (2013). Doxycycline restrains glia and confers neuroprotection in a 6-OHDA Parkinson model. Glia 61, 1084–1100.

Le MT, Xie H, Zhou B, Chia PH, Rizk P, Um M et al. (2009). MicroRNA-125b promotes neuronal differentiation in human cells by repressing multiple targets. Mol Cell Biol 29, 5290–5305.

Lee EJ, Baek M, Gusev Y, Brackett DJ, Nuovo GJ & Schmittgen TD (2007). Systematic evaluation of microRNA processing patterns in tissues, cell lines, and tumors. RNA 14, 35–42.

Lee RC, Feinbaum RL & Ambros V (1993). The C. elegans heterochronic gene lin-4 encodes small RNAs with antisense complementarity to lin-14. Cell 75, 843–854.

Lee SI, Lee BR, Hwang YS, Lee HC, Rengaraj D, Song G et al. (2011). MicroRNA-mediated posttranscriptional regulation is required for maintaining undifferentiated properties of blastoderm and primordial germ cells in chickens. Proc Natl Acad Sci U S A 108, 10426–10431.

Lee Y, Jeon K, Lee JT, Kim S & Kim VN (2002). MicroRNA maturation: stepwise processing and subcellular localization. EMBO J 21, 4663–4670.

Lee Y, Kim M, Han J, Yeom KH, Lee S, Baek SH et al. (2004). MicroRNA genes are transcribed by RNA polymerase II. EMBO J 23, 4051–4060.

Lee YS (2005). Depletion of Human Micro-RNA miR-125b reveals that it is critical for the proliferation of differentiated cells but not for the down-regulation of putative targets during differentiation. Journal of Biological Chemistry 280, 16635–16641.

Lemons D, Maurya MR, Subramaniam S & Mercola M (2013). Developing microRNA screening as a functional genomics tool for disease research. Front Physiol 4, 223.

Lessard J, Wu JI, Ranish JA, Wan M, Winslow MM, Staahl BT et al. (2007). An essential switch in subunit composition of a chromatin remodeling complex during neural development. Neuron 55, 201–215.

Lewis BP, Burge CB & Bartel DP (2005). Conserved seed pairing, often flanked by adenosines, indicates that thousands of human genes are microRNA targets. Cell 120, 6–6.

Li W, Sun W, Zhang Y, Wei W, Ambasudhan R, Xia P et al. (2011a). Rapid induction and long-term self-renewal of primitive neural precursors from human embryonic stem cells by small molecule inhibitors. Proc Natl Acad Sci U S A 108, 8299–8304.

Li X, Zhang J, Gao L, McClellan S, Finan MA, Butler TW et al. (2011b). MiR-181 mediates cell differentiation by interrupting the Lin28 and let-7 feedback circuit. Cell Death Differ 19, 378–386.

Liang C, Zhu H, Xu Y, Huang L, Ma C, Deng W et al. (2012). MicroRNA-153 negatively regulates the expression of amyloid precursor protein and amyloid precursor-like protein 2. Brain Research 1455, 103–113.

Lim LP, Lau NC, Garrett-Engele P, Grimson A, Schelter JM, Castle J et al. (2005). Microarray analysis shows that some microRNAs downregulate large numbers of target mRNAs. Nature 433, 769–773.

Lindvall O (2013). Developing dopaminergic cell therapy for Parkinson's disease-give up or move forward? Mov Disord 28, 268–273.

Lipchina I, Elkabetz Y, Hafner M, Sheridan R, Mihailovic A, Tuschl T et al. (2011). Genome-wide identification of microRNA targets in human ES cells reveals a role for miR-302 in modulating BMP response. Genes & Development 25, 2173–2186.

Lipchina I, Studer L & Betel D (2012). The expanding role of miR-302–367 in pluripotency and reprogramming. Cell Cycle 11, 1517–1523.

Liu ML, Zang T, Zou Y, Chang JC, Gibson JR, Huber KM et al. (2013). Small molecules enable neurogenin 2 to efficiently convert human fibroblasts into cholinergic neurons. Nat Comms 4.

Livak KJ & Schmittgen TD (2001). Analysis of Relative Gene Expression Data Using Real-Time Quantitative PCR and the 2−ΔΔCT Method. Methods 25, 402–408.

Long JM, Ray B & Lahiri DK (2012). MicroRNA-153 physiologically inhibits expression of amyloid-precursor protein in cultured human fetal brain cells and is dysregulated in a subset of Alzheimer disease patients. Journal of Biological Chemistry 287, 31298–31310.

Louvi A & Artavanis-Tsakonas S (2006). Notch signalling in vertebrate neural development. Nat Rev Neurosci 7, 93–102.

Main H, Radenkovic J, Jin SB, Lendahl U & Andersson ER (2013). Notch signaling maintains neural rosette polarity. PLoS ONE 8, e62959.

Makeyev EV, Zhang J, Carrasco MA & Maniatis T (2007). The MicroRNA miR-124 promotes neuronal differentiation by triggering brain-specific alternative pre-mRNA splicing. Mol Cell 27, 435–448.

Marinescu VD, Kohane IS & Riva A (2005). MAPPER: a search engine for the computational identification of putative transcription factor binding sites in multiple genomes. BMC Bioinformatics 6, 79.

Marson A, Levine SS, Cole MF, Frampton GM, Brambrink T, Johnstone S et al. (2008). Connecting microRNA genes to the core transcriptional regulatory circuitry of embryonic stem cells. Cell 134, 521–533.

Martello G & Smith A (2014). The Nature of Embryonic Stem Cells. Annu Rev Cell Dev Biol 30, 647–675.

McLaren D, Gorba T, Marguerie de Rotrou A, Pillai G, Chappell C, Stacey A et al. (2013). Automated large-scale culture and medium-throughput chemical screen for modulators of proliferation and viability of human induced pluripotent stem cell-derived neuroepithelial-like stem cells. Journal of Biomolecular Screening 18, 258–268.

Mehta DV, Kim YS, Dixon D & Jetten AM (2002). Characterization of the expression of the retinoid-related, testis-associated receptor (RTR) in trophoblasts. Placenta 23, 281–287.

Meijer HA, Smith EM & Bushell M (2014). Regulation of miRNA strand selection: follow the leader? Biochem Soc Trans 42, 1135–1140.

Meijering E, Jacob M, Sarria JC, Steiner P, Hirling H & Unser M (2004). Design and validation of a tool for neurite tracing and analysis in fluorescence microscopy images. Cytometry A 58, 167–176.

Melton C, Judson RL & Blelloch R (2010). Opposing microRNA families regulate self-renewal in mouse embryonic stem cells. Nature 463, 621–626.

Mertens J, Stüber K, Poppe D, Doerr J, Ladewig J, Brüstle O et al. (2013a). Embryonic stem cell-based modeling of tau pathology in human neurons. Am J Pathol 182, 1769–1779.

Mertens J, Stüber K, Wunderlich P, Ladewig J, Kesavan JC, Vandenberghe R et al. (2013b). APP processing in human pluripotent stem cell-derived neurons is resistant to NSAID-based γ-secretase modulation.
Stem Cell Reports 5;1(6):491-8 1–8.

Miska EA, Alvarez-Saavedra E, Townsend M, Yoshii A, Šestan N, Rakic P et al. (2004). Microarray analysis of microRNA expression in the developing mammalian brain.
Genome Biol 5, R68.

Moore LM, Kivinen V, Liu Y, Annala M, Cogdell D, Liu X et al. (2013). Transcriptome and small RNA deep sequencing reveals deregulation of miRNA biogenesis in human glioma. J Pathol 229, 449–459.

Moreau MP, Bruse SE, Jornsten R, Liu Y & Brzustowicz LM (2013). Chronological changes in microRNA expression in the developing human brain. PLoS ONE 8, e60480.

Morin RD, O'Connor MD, Griffith M, Kuchenbauer F, Delaney A, Prabhu AL et al. (2008). Application of massively parallel sequencing to microRNA profiling and discovery in human embryonic stem cells.
Genome Research 18, 610–621.

Muertz L (2009). MicroRNA profiling in ES cell derived neural cells. Diplomarbeit, 1–140.

Naguibneva I, Ameyar-Zazoua M, Polesskaya A, Ait-Si-Ali S, Groisman R, Souidi M et al. (2006). The microRNA miR-181 targets the homeobox protein Hox-A11 during mammalian myoblast differentiation.
Nature 8, 278–284.

Nasu M, Takata N, Danjo T, Sakaguchi H, Kadoshima T, Futaki S et al. (2012). Robust formation and maintenance of continuous stratified cortical neuroepithelium by laminin-containing matrix in mouse ES cell culture.
PLoS ONE 7, e53024.

Nat R, Nilbratt M, Narkilahti S, Winblad B, Hovatta O & Nordberg A (2007). Neurogenic neuroepithelial and radial glial cells generated from six human embryonic stem cell lines in serum-free suspension and adherent cultures.
Glia 55, 385–399.

Nichols J & Smith A (2009). Naive and Primed Pluripotent States. Cell Stem Cell 4, 487–492.

Nunez-Iglesias J, Liu CC, Morgan TE, Finch CE & Zhou XJ (2010). Joint genome-wide profiling of miRNA and mRNA expression in Alzheimer's disease cortex reveals altered miRNA regulation. PLoS ONE 5, e8898.

O'Loghlen A, Muñoz-Cabello AM, Gaspar-Maia A, Wu HA, Banito A, Kunowska N et al. (2012). MicroRNA regulation of Cbx7 mediates a switch of polycomb orthologs during ESC differentiation. Cell Stem Cell 10, 33–46.

Okabe S, Forsberg-Nilsson K, Spiro AC, Segal M & McKay RD (1996). Development of neuronal precursor cells and functional postmitotic neurons from embryonic stem cells in vitro. Mech Dev 59, 89–102.

Okamura K, Liu N & Lai EC (2009). Distinct mechanisms for microRNA strand selection by Drosophila Argonautes.
Molecular Cell 36, 431–444.

Okamura K, Phillips MD, Tyler DM, Duan H, Chou YT & Lai EC (2008). The regulatory activity of microRNA* species has substantial influence on microRNA and 3' UTR evolution. Nat Struct Mol Biol 15, 354–363.

Ono Y, Nakatani T, Sakamoto Y, Mizuhara E, Minaki Y, Kumai M et al. (2007). Differences in neurogenic potential in floor plate cells along an anteroposterior location: midbrain dopaminergic neurons originate from mesencephalic floor plate cells.
Development 134, 3213–3225.

Otto C (2008). Bioinformatisches Praktikum Evolution von microRNAs.

Otto SJ, McCorkle SR, Hover J, Conaco C, Han JJ, Impey S et al. (2007). A new binding motif for the transcriptional repressor REST uncovers large gene networks devoted to neuronal functions.
J Neurosci 27, 6729–6739.

Ou Q, Magico A & King-Jones K (2011). Nuclear receptor DHR4 controls the timing of steroid hormone pulses during Drosophila development. PLoS Biol 9, e1001160.

Ouyang YB, Lu Y, Yue S & Giffard RG (2012a). miR-181 targets multiple Bcl-2 family members and influences apoptosis and mitochondrial function in astrocytes.
MITOCH 12, 213–219.

Ouyang YB, Lu Y, Yue S, Xu LJ, Xiong XX, White RE et al. (2012b). miR-181 regulates GRP78 and influences outcome from cerebral ischemia in vitro and in vivo.
Neurobiology of Disease 45, 555–563.

Ozsolak F, Poling LL, Wang Z, Liu H, Liu XS, Roeder RG et al. (2008). Chromatin structure analyses identify miRNA promoters. Genes & Development 22, 3172–3183.

Packer AN, Xing Y, Harper SQ, Jones L & Davidson BL (2008). The bifunctional microRNA miR-9/miR-9* regulates REST and CoREST and is downregulated in Huntington's disease. J Neurosci 28, 14341–14346.

Paddison PJ, Cleary M, Silva JM, Chang K, Sheth N, Sachidanandam R et al. (2004). Cloning of short hairpin RNAs for gene knockdown in mammalian cells.
Nat Meth 1, 163–167.

Pang X, Hogan EM, Casserly A, Gao G, Gardner PD & Tapper AR (2014). Dicer expression is essential for adult midbrain dopaminergic neuron maintenance and survival.
Molecular and Cellular Neuroscience 58, 22–28.

Pang ZP, Yang N, Vierbuchen T, Ostermeier A, Fuentes DR, Yang TQ et al. (2011). Induction of human neuronal cells by defined transcription factors. Nature. 476(7359): 220–223. doi:10.1038

Parker R & Sheth U (2007). P bodies and the control of mRNA translation and degradation.
Mol Cell 25, 635–646.

Peng Z, Li J, Li Y, Yang X, Feng S, Han S et al. (2013). Downregulation of miR-181b in mouse brain following ischemic stroke induces neuroprotection against ischemic injury through targeting heat shock protein A5 and ubiquitin carboxyl-terminal hydrolase isozyme L1.
J Neurosci Res. (10):1349-62. doi: 10.1002/jnr.23255.

Perrier AL, Tabar V, Barberi T, Rubio ME, Bruses J, Topf N et al. (2004). Derivation of midbrain dopamine neurons from human embryonic stem cells.
Proc Natl Acad Sci U S A 101, 12543–12548.

Petersen CP, Bordeleau ME, Pelletier J & Sharp PA (2006). Short RNAs repress translation after initiation in mammalian cells. Mol Cell 21, 10–10.

Pietersen AM & van Lohuizen M (2008). Stem cell regulation by polycomb repressors: postponing commitment. Current Opinion in Cell Biology 20, 201–207.

Piskounova E, Polytarchou C, Thornton JE, LaPierre RJ, Pothoulakis C, Hagan JP et al. (2011). Lin28A and Lin28B inhibit let-7 microRNA biogenesis by distinct mechanisms. Cell 147, 1066–1079.

Placantonakis DG, Tomishima MJ, Lafaille F, Desbordes SC, Jia F, Socci ND et al. (2009). BAC transgenesis in human embryonic stem cells as a novel tool to define the human neural lineage.
STEM CELLS 27, 521–532.

Pleasure SJ & Lee VM (1993). NTera 2 cells: a human cell line which displays characteristics expected of a human committed neuronal progenitor cell.
J Neurosci Res 35, 585–602.

Potenza N, Papa U & Russo A (2009). Differential expression of Dicer and Argonaute genes duringthe differentiation of human neuroblastoma cells.
Cell Biology International 33, 734–738.

Prakash N (2006). A Wnt1-regulated genetic network controls the identity and fate of midbrain-dopaminergic progenitors in vivo. Development 133, 89–98.

Pritchard C, Cheng H & Tewari M (2012). MicroRNA profiling: approaches and considerations.
Nat Rev Genet 13, 358–369.

Qin L, Chen Y, Niu Y, Chen W, Wang Q, Xiao S et al. (2010). A deep investigation into the adipogenesis mechanism: Profile of microRNAs regulating adipogenesis by modulating the canonical Wnt/β-catenin signaling pathway.
BMC Genomics 11, 320.

Rajkovic M, Iwen KAH, Hofmann PJ, Harneit A & Weitzel JM (2010). Functional cooperation between CREM and GCNF directs gene expression in haploid male germ cells. Nucleic Acids Research 38, 2268–2278.

Rajkovic M, Middendorff R, Wetzel MG, Frkovic D, Damerow S, Seitz HJ et al. (2004). Germ cell nuclear factor relieves cAMP-response element modulator tau-mediated activation of the testis-specific promoter of human mitochondrial glycerol-3-phosphate dehydrogenase.
Journal of Biological Chemistry 279, 52493–52499.

Ramkissoon SH, Mainwaring LA, Sloand EM, Young NS & Kajigaya S (2006). Nonisotopic detection of microRNA using digoxigenin labeled RNA probes.
Mol Cell Probes 20, 1–4.

Redshaw N, Camps C, Sharma V, Motallebipour M, Guzman-Ayala M, Oikonomopoulos S et al. (2013). TGF-β/Smad2/3 signaling directly regulates several miRNAs in mouse ES cells and early embryos. PLoS ONE 8, e55186.

Reinhardt P, Glatza M, Hemmer K, Tsytsyura Y, Thiel CS, Höing S et al. (2013). Derivation and expansion using only small molecules of human neural progenitors for neurodegenerative disease modeling.
PLoS ONE 8, e59252.

Reinhart BJ, Slack FJ, Basson M, Pasquinelli AE, Bettinger JC, Rougvie AE et al. (2000). The 21-nucleotide let-7 RNA regulates developmental timing in Caenorhabditis elegans. Nature 403, 901–906.

Reubinoff BE, Itsykson P, Turetsky T, Pera MF, Reinhartz E, Itzik A et al. (2001). Neural progenitors from human embryonic stem cells.
Nat Biotechnol 19, 1134–1140.

Reynolds BA & Weiss S (1992). Generation of neurons and astrocytes from isolated cells of the adult mammalian central nervous system. Science 255, 1707–1710.

Ring DB, Johnson KW, Henriksen EJ, Nuss JM, Goff D, Kinnick TR et al. (2003). Selective glycogen synthase kinase 3 inhibitors potentiate insulin activation of glucose transport and utilization in vitro and in vivo.
Diabetes 52, 588–595.

Ro S, Park C, Young D, Sanders KM & Yan W (2007). Tissue-dependent paired expression of miRNAs. Nucleic Acids Research 35, 5944–5953.

Rodriguez A, Griffiths-Jones S, Ashurst JL & Bradley A (2004). Identification of mammalian microRNA host genes and transcription units. Genome Research 14, 1902–1910.

Roese-Koerner B, Stappert L, Koch P, Brüstle O & Borghese L (2013). Pluripotent stem cell-derived somatic stem cells as tool to study the role of microRNAs in early human neural development. Curr Mol Med 13, 707–722.

Roese-Koerner B, Borghese L, Stappert L, D'Araio S, Evert BO, Peitz M, Brüstle O. A feedback loop between miR-9/9* and its direct transcriptional modulator Notch regulating human neural stem cell self-renewal and differentiation. *in submission*

Rosa A & Brivanlou AH (2011). A regulatory circuitry comprised of miR-302 and the transcription factors OCT4 and NR2F2 regulates human embryonic stem cell differentiation. EMBO J 30, 237–248.

Rosa A, Spagnoli FM & Brivanlou AH (2009).
The miR-430/427/302 family controls mesendodermal fate specification via species-specific target selection.
Dev Cell 16, 517–527.

Roughten A, Rong Y, Quintero J, Ohlmeyer M, Kultgen S, Kingsbury C et al. (2007). Benzodiazepine GCNF modulators for stem cell modulation. WO2007/095495.

Ruby JG, Jan CH & Bartel DP (2007). Intronic microRNA precursors that bypass Drosha processing.
Nature 448, 83–86.

Rybak A, Fuchs H, Smirnova L, Brandt C, Pohl EE, Nitsch R et al. (2008). A feedback loop comprising lin-28 and let-7 controls pre-let-7 maturation during neural stem-cell commitment. Nat Cell Biol 10, 987–993.

Saba R, Storchel PH, Aksoy-Aksel A, Kepura F, Lippi G, Plant TD et al. (2012). The dopamine-regulated microRNA, miR-181a, controls GluA2 surface expression in hippocampal neurons.
Molecular and Cellular Biology 32, 619–632.

Sakakibara SI, Nakamura Y, Satoh H & Okano H (2001). RNA-binding protein Musashi2: Developmentally regulated expression in neural precursor Cells and subpopulations of neurons in mammalian CNS.
J Neurosci 15;21(20):8091-107.

Saldanha AJ (2004). Java Treeview--extensible visualization of microarray data.
Bioinformatics 20, 3246–3248.

Sardo Lo V, Zuccato C, Gaudenzi G, Vitali B, Ramos C, Tartari M et al. (2012). An evolutionary recent neuroepithelial cell adhesion function of huntingtin implicates ADAM10-Ncadherin. Nat Neurosci 15, 713–721.

Sattler U, Samochocki M, Maelicke A & Zechel C (2004). The expression level of the orphan nuclear receptor GCNF (germ cell nuclear factor) is critical for neuronal differentiation. Molecular Endocrinology 18, 2714–2726.

Saunders LR, Sharma AD, Tawney J, Nakagawa M, Okita K, Yamanaka S et al. (2010). miRNAs regulate SIRT1 expression during mouse embryonic stem cell differentiation and in adult mouse tissues.
Aging (Albany NY) 2, 415–431.

Schmitz TP (2000). Funktion des Germ Cell Nuclear Factor (GCNF) in der neuronalen Differenzierung humaner Zellen, Mensch-und-Buch-Verlag.

Schneider CA, Rasband WS & Eliceiri KW (2012). NIH Image to ImageJ: 25 years of image analysis. Nat Meth 9, 671–675.

Schonrock N, Ke YD, Humphreys D, Staufenbiel M, Ittner LM, Preiss T et al. (2010). Neuronal microRNA deregulation in response to Alzheimer's disease amyloid-β. PLoS ONE 5, e11070.

Schratt GM, Tuebing F, Nigh EA, Kane CG, Sabatini ME, Kiebler M et al. (2006). A brain-specific microRNA regulates dendritic spine development. Nature 439, 283–289.

Schulte JH, Marschall T, Martin M, Rosenstiel P, Mestdagh P, Schlierf S et al. (2010). Deep sequencing reveals differential expression of microRNAs in favorable versus unfavorable neuroblastoma. Nucleic Acids Research 38, 5919–5928.

Schumacher S & Franke K (2013). miR-124-regulated RhoG: A conductor of neuronal process complexity. smallgtpases 4, 42–46.

Schwamborn JC, Berezikov E & Knoblich JA (2009). The TRIM-NHL protein TRIM32 activates microRNAs and prevents self-renewal in mouse neural progenitors. Cell 136, 913–925.

Seitz H, Royo H, Bortolin ML, Lin SP, Ferguson-Smith AC & Cavaillé J (2004). A large imprinted microRNA gene cluster at the mouse Dlk1-Gtl2 domain. Genome Research 14, 1741–1748.

Sempere LF, Freemantle S, Pitha-Rowe I, Moss E, Dmitrovsky E & Ambros V (2004). Expression profiling of mammalian microRNAs uncovers a subset of brain-expressed microRNAs with possible roles in murine and human neuronal differentiation. Genome Biol 5, R13.

Seoudi AM, Lashine YA & Abdelaziz AI (2012). MicroRNA-181a – a tale of discrepancies. Expert Rev Mol Med 14, e5.

Sethi P & Lukiw WJ (2009). Micro-RNA abundance and stability in human brain: Specific alterations in Alzheimer's disease temporal lobe neocortex. Neuroscience Letters 459, 100–104.

Shao NY, Hu HY, Yan Z, Xu Y, Hu H, Menzel C et al. (2010). Comprehensive survey of human brain microRNA by deep sequencing. BMC Genomics 11, 409.

Shi L, Cheng Z, Zhang J, Li R, Zhao P, Fu Z et al. (2008). hsa-mir-181a and hsa-mir-181b function as tumor suppressors in human glioma cells. Brain Research 1236, 185–193.

Shi W, Du J, Qi Y, Liang G, Wang T, Li S et al. (2012). Aberrant expression of serum miRNAs in schizophrenia. Journal of Psychiatric Research 46, 198–204.

Shi ZM, Wang XF, Qian X, Tao T, Wang L, Chen QD et al. (2013). MiRNA-181b suppresses IGF-1R and functions as a tumor suppressor gene in gliomas. RNA 19, 552–560.

Shimojo H, Ohtsuka T & Kageyama R (2008). Oscillations in Notch Signaling Regulate Maintenance of Neural Progenitors. Neuron 58, 52–64.

Silber J, Lim DA, Petritsch C, Persson AI, Maunakea AK, Yu M et al. (2008). miR-124 and miR-137 inhibit proliferation of glioblastoma multiforme cells and induce differentiation of brain tumor stem cells. BMC Med 6, 14.

Slezak-Prochazka I, Durmus S, Kroesen BJ & van den Berg A (2010). MicroRNAs, macrocontrol: regulation of miRNA processing. RNA 16, 1087–1095.

Sluder AE & Maina CV (2001). Nuclear receptors in nematodes: themes and variations.

Trends Genet 17, 206–213.

Smidt MP & Burbach JPH (2007). How to make a mesodiencephalic dopaminergic neuron. Nat Rev Neurosci 8, 21–32.

Smith B, Treadwell J, Zhang D, Ly D, McKinnell I, Walker PR et al. (2010). Large-scale expression analysis reveals distinct microRNA profiles at different stages of human neurodevelopment. PLoS ONE 5, e11109.

Song K, Takemaru KI & Moon RT (1999). A role for xGCNF in midbrain-hindbrain patterning in Xenopus laevis. Dev Biol 213, 170–179.

Stadler B, Ivanovska I, Mehta K, Song S, Nelson A, Tan Y et al. (2010). Characterization of microRNAs involved in embryonic stem cell states. Stem Cells and Development 19, 935–950.

Stappert L, Roese-Koerner B & Brüstle O (2014). The role of microRNAs in human neural stem cells, neuronal differentiation and subtype specification. Cell Tissue Res. 10.1007/s00441-014-1981-y (2014)

Stergiopoulos A & Politis PK (2013). The role of nuclear receptors in controlling the fine balance between proliferation and differentiation of neural stem cells. Archives of Biochemistry and Biophysics 534, 27–37.

Stern CD (2005). Neural induction: old problem, new findings, yet more questions. Development 132, 2007–2021.

Strauss WM, Chen C, Lee CT & Ridzon D (2006). Nonrestrictive developmental regulation of microRNA gene expression. Mamm Genome 17, 833–840.

Suh MR, Lee Y, Kim JY, Kim SK, Moon SH, Lee JY et al. (2004). Human embryonic stem cells express a unique set of microRNAs. Developmental Biology 270, 488–498.

Sun K & Lai EC (2013). Adult-specific functions of animal microRNAs. Nat Rev Genet 14, 535–548.

Suzuki HI, Arase M, Matsuyama H, Choi YL, Ueno T, Mano H et al. (2011). MCPIP1 ribonuclease antagonizes Dicer and terminates microRNA biogenesis through precursor microRNA degradation. Molecular Cell 44, 424–436.

Suzuki HI, Yamagata K, Sugimoto K, Iwamoto T, Kato S & Miyazono K (2009). Modulation of microRNA processing by p53. Nature 460, 529–533.

Süsens U & Borgmeyer U (1996). Characterization of the human germ cell nuclear factor gene. Biochim Biophys Acta 1309, 179–182.

Süsens U, Aguiluz JB, Evans RM & Borgmeyer U (1997). The germ cell nuclear factor mGCNF is expressed in the developing nervous system. Dev Neurosci 19, 410–420.

Tailor J, Kittappa R, Leto K, Gates M, Borel M, Paulsen O et al. (2013). Stem cells expanded from the human embryonic hindbrain stably retain regional specification and high neurogenic potency. J Neurosci 33, 12407–12422.

Takahashi K & Yamanaka S (2006). Induction of pluripotent stem cells from mouse embryonic and adult fibroblast cultures by defined factors. Cell 126, 663–676.

Takahashi K, Tanabe K, Ohnuki M, Narita M, Ichisaka T, Tomoda K et al. (2007). Induction of pluripotent stem cells from adult human fibroblasts by defined factors. Cell 131, 861–872.

Takata T & Ishikawa F (2003). Human Sir2-related protein SIRT1 associates with the bHLH repressors HES1 and HEY2 and is involved in HES1- and HEY2-mediated transcriptional repression. Biochemical and Biophysical Research Communications 301, 250–257.

Tang M, Miyamoto Y & Huang EJ (2009). Multiple roles of beta-catenin in controlling the neurogenic niche for midbrain dopamine neurons. Development 136, 2027–2038.

Tang M, Villaescusa JC, Luo SX, Guitarte C, Lei S, Miyamoto Y et al. (2010). Interactions of Wnt/β-Catenin signaling and Sonic Hedgehog regulate the neurogenesis of ventral midbrain dopamine neurons.
J Neurosci 30, 9280–9291.

Tao T, Wang Y, Luo H, Yao L, Wang L, Wang J et al. (2013). Involvement of FOS-mediated miR-181b/miR-21 signalling in the progression of malignant gliomas.
European Journal of Cancer, 1–9.

Tay YMS, Tam WL, Ang YS, Gaughwin PM, Yang H, Wang W et al. (2008). MicroRNA-134 modulates the differentiation of mouse embryonic stem cells, where it causes post-transcriptional attenuation of Nanog and LRH1. STEM CELLS 26, 17–29.

Thomson JA, Itskovitz-Eldor J, Shapiro SS, Waknitz MA, Swiergiel JJ, Marshall VS et al. (1998). Embryonic stem cell lines derived from human blastocysts.
Science 282, 1145–1147.

Thomson JM (2006). Extensive post-transcriptional regulation of microRNAs and its implications for cancer.
Genes & Development 20, 2202–2207.

Thornton JE & Gregory RI (2012). How does Lin28 let-7 control development and disease?
Trends in Cell Biology 22, 474–482.

Treiber T, Treiber N & Meister G (2012). Regulation of microRNA biogenesis and function.
Thromb Haemost 107, 605–610.

Tropepe V, Hitoshi S, Sirard C, Mak TW, Rossant J & van der Kooy D (2001). Direct neural fate specification from embryonic stem cells: a primitive mammalian neural stem cell stage acquired through a default mechanism.
Neuron 30, 65–78.

Tzur G, Levy A, Meiri E, Barad O, Spector Y, Bentwich Z et al. (2008). MicroRNA expression patterns and function in endodermal differentiation of human embryonic stem cells.
PLoS ONE 3, e3726.

van Rooij E & Kauppinen S (2014). Development of microRNA therapeutics is coming of age.
EMBO Mol Med 6, 851–864.

Várallyay É, Burgyán J & Havelda Z (2008). MicroRNA detection by northern blotting using locked nucleic acid probes. Nat Protoc 3, 190–196.

Villa-Diaz LG, Ross AM, Lahann J & Krebsbach PH (2012). Concise Review: The Evolution of human pluripotent stem cell culture: From feeder cells to synthetic coatings. STEM CELLS 31, 1–7.

Visvanathan J, Lee S, Lee B, Lee JW & Lee SK (2007). The microRNA miR-124 antagonizes the anti-neural REST/SCP1 pathway during embryonic CNS development.
Genes & Development 21, 744–749.

Viswanathan SR, Daley GQ & Gregory RI (2008). Selective blockade of microRNA processing by Lin28.
Science 320, 97–100.

Wagner RT & Cooney AJ (2013). Minireview: The diverse roles of nuclear receptors in the regulation of embryonic stem cell pluripotency.
Molecular Endocrinology 27, 864–878.

Wang B, Hsu SH, Majumder S, Kutay H, Huang W, Jacob ST et al. (2010a). TGFb-mediated upregulation of hepatic miR-181b promotes hepatocarcinogenesis by targeting TIMP3. Oncogene 29, 1787–1797.

Wang H, Wang X, Archer TK & Zwaka TP (2014). GCNF-dependent activation of cyclin D1 expression via repression of Mir302a during ES cell differentiation.
STEM CELLS 32(6):1527-37.

Wang H, Wang X, Xu X, Zwaka TP & Cooney AJ (2013a). Epigenetic re-programming of the germ cell nuclear factor gene is required for proper fifferentiation of induced pluripotent cells. STEM CELLS 31(12):2659-66.

Wang J, Sai K, Chen FR & Chen ZP (2013b). miR-181b modulates glioma cell sensitivity to temozolomide by targeting MEK1.
Cancer Chemother Pharmacol 72, 147–158.

Wang Q & Cooney AJ (2013c). Revisiting the role of GCNF in embryonic development.
Semin Cell Dev Biol 24(10-12):679-86.

Wang S, Aurora AB, Johnson BA, Qi X, McAnally J, Hill JA et al. (2008). The rndothelial-specific microRNA miR-126 governs vascular integrity and angiogenesis.
Dev Cell 15, 261–271.

Wang XF, Shi ZM, Wang XR, Cao L, Wang YY, Zhang JX et al. (2011). MiR-181d acts as a tumor suppressor in glioma by targeting K-ras and Bcl-2.
J Cancer Res Clin Oncol 138, 573–584.

Wang Y, Li Z, He C, Wang D, Yuan X, Chen J et al. (2010b). MicroRNAs expression signatures are associated with lineage and survival in acute leukemias.
Blood Cells, Molecules, and Diseases 44, 191–197.

Wang Y, Yu Y, Tsuyada A, Ren X, Wu X, Stubblefield K et al. (2010c). Transforming growth factor-b regulates the sphere-initiating stem cell-like feature in breast cancer through miRNA-181 and ATM.
Oncogene, 1–11.

Wapinski OL, Vierbuchen T, Qu K, Lee QY, Chanda S, Fuentes DR et al. (2013). Hierarchical mechanisms for direct reprogramming of fibroblasts to neurons.
Cell 155, 621–635.

Watanabe K, Ueno M, Kamiya D, Nishiyama A, Matsumura M, Wataya T et al. (2007). A ROCK inhibitor permits survival of dissociated human embryonic stem cells. Nat Biotechnol 25, 681–686.

Wilkinson G, Dennis D & Schuurmans C (2013). Proneural genes in neocortical development.
Neuroscience 253, 256–273.

Winter J & Diederichs S (2011). Argonaute proteins regulate microRNA stability: Increased microRNA abundance by Argonaute proteins is due to microRNA stabilization. RNA Biol 8 (6), 1149–1157.

Winter J & Diederichs S (2013). Argonaute-3 activates the let-7a passenger strand microRNA.
RNA Biol 10 (10):1631-43.

Wiznerowicz M & Trono D (2003). Conditional suppression of cellular genes: lentivirus vector-mediated drug-inducible RNA interference.
Journal of Virology 77, 8957–8961.

Wu H, Xu J, Pang ZP, Ge W, Kim KJ, Blanchi B et al. (2007). Integrative genomic and functional analyses reveal neuronal subtype differentiation bias in human embryonic stem cell lines.
Proc Natl Acad Sci U S A 104, 13821–13826.

Wu J & Xie X (2006a). Comparative sequence analysis reveals an intricate network among REST, CREB and miRNA in mediating neuronal gene expression.
Genome Biol 7, R85–R85.

Wu L, Fan J & Belasco JG (2006b). MicroRNAs direct rapid deadenylation of mRNA.
Proc Natl Acad Sci U S A 103, 4034–4039.

Wulczyn FG, Smirnova L, Rybak A, Brandt C, Kwidzinski E, Ninnemann O et al. (2007). Post-transcriptional regulation of the let-7 microRNA during neural cell specification. The FASEB Journal 21, 415–426.

Wurst W & Bally-Cuif L (2001). Neural plate patterning: upstream and downstream of the isthmic organizer.
Nat Rev Neurosci 2, 99–108.

Xi J, Liu Y, Liu H, Chen H, Emborg ME & Zhang SC (2012). Specification of midbrain dopamine neurons from primate pluripotent stem cells.
STEM CELLS 30, 1655–1663.

Xu C, Zhou ZY, Guo QS & Wang YF (2004). Expression of germ cell nuclear factor in mouse germ cells and sperm during postnatal period. Asian J Androl 6, 217–222.

Xu J, Liao X & Wong C (2010). Downregulations of B-cell lymphoma 2 and myeloid cell leukemia sequence 1 by microRNA 153 induce apoptosis in a glioblastoma cell line DBTRG-05MG. Int J Cancer 126, 1029–1035.

Xu J, Liao X, Lu N, Liu W & Wong CW (2011a). Chromatin-modifying drugs induce miRNA-153 expression to suppress Irs-2 in glioblastoma cell lines.
Int J Cancer 129, 2527–2531.

Xu XH & Zhong Z (2013a). Disease modeling and drug screening for neurological diseases using human induced pluripotent stem cells. Acta Pharmacol Sin 34, 755–764.

Xu XL, Zong R, Li Z, Biswas MH, Fang Z, Nelson DL et al. (2011b). FXR1P but not FMRP regulates the levels of mammalian brain-specific microRNA-9 and microRNA-124.
J Neurosci 31, 13705–13709.

Xu Z, Jiang J, Xu C, Wang Y, Sun L, Guo X et al. (2013b). MicroRNA-181 regulates CARM1 and histone aginine methylation to promote differentiation of human embryonic stem cells. PLoS ONE 8, e53146.

Yamagata K, Fujiyama S, Ito S, Ueda T, Murata T, Naitou M et al. (2009). Maturation of microRNA is hormonally regulated by a nuclear receptor.
Molecular Cell 36, 340–347.

Yan Z & Jetten AM (2000). Characterization of the repressor function of the nuclear orphan receptor retinoid receptor-related testis-associated receptor/germ cell nuclear factor. J Biol Chem 275, 35077–35085.

Yan ZH, Medvedev A, Hirose T, Gotoh H & Jetten AM (1997). Characterization of the response element and DNA binding properties of the nuclear orphan receptor germ cell nuclear factor/retinoid receptor-related testis-associated receptor. J Biol Chem 272, 10565–10572.

Yang D, Li T, Wang Y, Tang Y, Cui H, Zhang X et al. (2012). miR-132 regulates the differentiation of dopamine neurons by directly targeting Nurr1 expression.
Journal of Cell Science 125, 1673–1682.

Yang JS, Phillips MD, Betel D, Mu P, Ventura A, Siepel AC et al. (2011). Widespread regulatory activity of vertebrate microRNA* species. RNA 17, 312–326.

Yang W, Chendrimada TP, Wang Q, Higuchi M, Seeburg PH, Shiekhattar R et al. (2005). Modulation of microRNA processing and expression through RNA editing by ADAR deaminases. Nat Struct Mol Biol 13, 13–21.

Ye W, Shimamura K, Rubenstein JL, Hynes MA & Rosenthal A (1998). FGF and Shh signals control dopaminergic and serotonergic cell fate in the anterior neural plate. Cell 93, 755–766.

Yoo AS, Staahl BT, Chen L & Crabtree GR (2009). MicroRNA-mediated switching of chromatin-remodelling complexes in neural development. Nature 460, 642–646.

Yoo AS, Sun AX, Li L, Shcheglovitov A, Portmann T, Li Y et al. (2011). MicroRNA-mediated conversion of human fibroblasts to neurons. Nature 476, 228–231.

Yoon K & Gaiano N (2005). Notch signaling in the mammalian central nervous system: insights from mouse mutants. Nat Neurosci 8, 709–715.

Yu J, Vodyanik MA, Smuga-Otto K, Antosiewicz-Bourget J, Frane JL, Tian S et al. (2007). Induced pluripotent stem cell lines derived from human somatic cells. Science 318, 1917–1920.

Yu JY, Chung KH, Deo M, Thompson RC & Turner DL (2008). MicroRNA miR-124 regulates neurite outgrowth during neuronal differentiation.
Exp Cell Res 314, 2618–2633.

Zechel C (2005). The germ cell nuclear factor (GCNF). Mol Reprod Dev 72, 550–556.

Zhang H, Kolb FA, Brondani V, Billy E & Filipowicz W (2002). Human Dicer preferentially cleaves dsRNAs at their termini without a requirement for ATP.
EMBO J 21, 5875–5885.

Zhang H, Kolb FA, Jaskiewicz L, Westhof E & Filipowicz W (2004a). Single processing center models for human Dicer and bacterial RNase III. Cell 118, 12–12.

Zhang H, Shykind B & Sun T (2012a). Approaches to manipulating microRNAs in neurogenesis.
Front Neurosci 6, 196.

Zhang L, Dong LY, Li YJ, Hong Z & Wei WS (2012b). The microRNA miR-181c controls microglia-mediated neuronal apoptosis by suppressing tumor necrosis factor.
J Neuroinflammation 9, 211.

Zhang QY, Qiu SD & Yang J (2004b). Expression of germ cell nuclear factor in rat epididymis during postnatal development. Zhonghua Yi Xue Za Zhi 84, 1126–1129.

Zhang SC, Wernig M, Duncan ID, Brüstle O & Thomson JA (2001). In vitro differentiation of transplantable neural precursors from human embryonic stem cells.
Nat Biotechnol 19, 1129–1133.

Zhang Y, Pak C, Han Y, Ahlenius H, Zhang Z, Chanda S et al. (2013). Rapid single-step induction of functional neurons from human pluripotent stem cells.
Neuron 78, 785–798.

Zhang YL, Akmal KM, Tsuruta JK, Shang Q, Hirose T, Jetten AM et al. (1998). Expression of germ cell nuclear factor (GCNF/RTR) during spermatogenesis.
Mol Reprod Dev 50, 93–102.

Zhang Z, Qin YW, Brewer G & Jing Q (2012c). MicroRNA degradation and turnover: regulating the regulators. WIREs RNA 3, 593–600.

Zhao C, Huang C, Weng T, Xiao X, Ma H & Liu L (2012). Computational prediction of MicroRNAs targeting GABA receptors and experimental verification of miR-181, miR-216 and miR-203 targets in GABA-A receptor. BMC Research Notes 5, 91.

Zhao C, Sun G, Li S & Shi Y (2009). A feedback regulatory loop involving microRNA-9 and nuclear receptor TLX in neural stem cell fate determination. Nat Struct Mol Biol 16, 365–371.

Zhao C, Sun G, Li S, Lang MF, Yang S, Li W et al. (2010). MicroRNA let-7b regulates neural stem cell proliferation and differentiation by targeting nuclear receptor TLX signaling. Proc Natl Acad Sci U S A 107, 1876–1881.

Zhao C, Sun G, Ye P, Li S & Shi Y (2013a). MicroRNA let-7d regulates the TLX/microRNA-9 cascade to control neural cell fate and neurogenesis. Sci Rep 3.

Zhao S, Deng Y, Liu Y, Chen X, Yang G, Mu Y et al. (2013b). MicroRNA-153 is tumor suppressive in glioblastoma stem cells. Mol Biol Rep 40, 2789–2798.

Zheng K, Li H, Huang H & Qiu M (2012). MicroRNAs and glial cell development. Neuroscientist 18, 114–118.

Zhong X, Li N, Liang S, Huang Q, Coukos G & Zhang L (2010). Identification of microRNAs regulating reprogramming factor LIN28 in embryonic stem cells and cancer cells. Journal of Biological Chemistry 285, 41961–41971.

Zhou H, Arcila ML, Li Z, Lee EJ, Henzler C, Liu J et al. (2012). Deep annotation of mouse iso-miR and iso-moR variation. Nucleic Acids Research 40, 5864–5875.

Zhou J, Su P, Li D, Tsang S, Duan E & Wang F (2010). High-efficiency induction of neural conversion in human ESCs and human induced pluripotent stem cells with a single chemical inhibitor of transforming growth factor beta superfamily receptors. STEM CELLS 28, 1741–1750.

Zhu W, Shan X, Wang T, Shu Y & Liu P (2010). miR-181b modulates multidrug resistance by targeting BCL2 in human cancer cell lines. Int J Cancer 127, 2520–2529.

6 APPENDIX

6.1 Supplementary figure

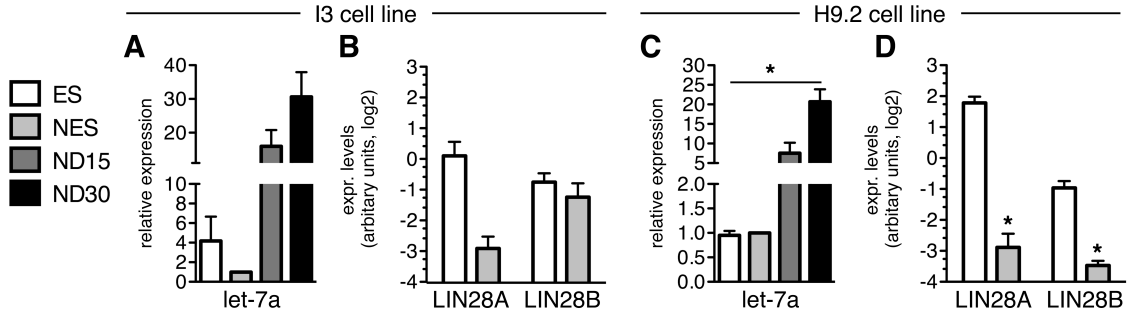

Fig. 6.1: Lt-NES cells derived from the I3 and H9.2 hESC lines exhibit different let-7a and LIN28 expression levels. (A, C) Quantitative RT-PCR analysis of let-7a expression in human ESCs (ES), lt-NES cells (NES) and differentiated neuronal cultures (ND15, ND30) derived from the I3 **(A)** and the H9.2 **(C)** lines. Data were normalized to RNU5A snRNA levels and are presented relative to expression in lt-NES cells (equal to 1, n = 3). **(B, D)** Quantitative RT-PCR analysis of LIN28A and LIN28B in hESCs and lt-NES cells derived form the I3 **(B)** and the H9.2 **(D)** lines. Data were normalized to 18S rRNA levels and are presented as expression data (2^{-dCt}). All data are presented as mean + SEM; *, compared to ES, $p \leq 0.05$.

6.2 Publications

Parts of this thesis have been published by the author:

Stappert L*, Borghese L*#, Roese-Koerner B, Weinhold S, Koch P, Terstegge S, Uhrberg M, Wernet P, Brüstle O# (2013).
MicroRNA-based promotion of human neuronal differentiation and subtype specification.
PLoS One 8(3):e59011
(* equal contribution; # shared corresponding authorship)

Roese-Koerner B*, **Stappert L***, Koch P, Brüstle O#, Borghese L# (2013).
Pluripotent stem cell-derived somatic stem cells as tool to study the role of microRNAs in early human neural development.
Curr Mol Med 13(5):707-722
(* equal contribution; # shared corresponding authorship)

Stappert L, Roese-Koerner B, Brüstle O (2014).
The role of microRNAs in human neural stem cells, neuronal differentiation and subtype specification.
Cell and Tissue Research doi:10.1007/s00441-014-1981-y

6.3 Abbreviations

Abbreviation	Full name	Abbreviation	Full name
3' UTR	Three prime untranslated region	ICC	Immunocytochemistry
AA	Ascorbic acid	ICM	Inner cell mass
Ago	Argonaute protein	inh	MicroRNA inhibitor
Amp	Ampicillin	iPS cells	Induced pluripotent stem cells
Astro	Astrocytes	LBD	Ligand-binding domain
ATP	Adenosine triphosphate	LN	Laminin
BDNF	Brain-derived neurotrophic factor	(lt-)NES cells	(Long-term self-renewing) neuroepithelial like stem cells
bHLH	Basic helix-loop-helix	MCS	Multiple cloning site
BMP	Bone morphogenetic protein	mDA neurons	Midbrain dopaminergic neurons
BrdU	Bromdesoxyuridin	MEF	Mouse embryonic fibroblast
BS	Biosensor	MG	Matrigel
C14MC	Chromosome 14 microRNA cluster	miRNA, miR	MicroRNA
C19MC	Chromosome 19 microRNA cluster	MHB	Midbrain-hindbrain boundary
cDNA	Complementary DNA	mRNA	Messenger RNA
CNS	Central nervous system	ncRNAs	Non-coding RNAs
Ct	Threshold cycle	ND(n)	neuronal cultures generated after n days of differentiation
ctr	control	NICD	Notch intracellular domain
DA-factors	Factors inducing dopaminergic neurons	NP	Neural progenitors
DAPI	4',6-diamidino-2-phenylindole	NR	Nuclear receptor
DAPT	N-[N-(3,5-difluorophenacetyl)-L-alanyl]- S-phenylglycine t-butyl ester	NR6A1	Nuclear receptor subfamily 6, group A, member 1
DBD	DNA-binding domain	NSCs	Neural stem cells
DCX	Doublecortin	ns	Not significantly expressed
DEPC	Diethylpyrocarbonate	PMA	Purmorphamin
(db)cAMP	(Dibuturyl) cyclic adenosine mono-phosphate	PO	Poly-L-Ornithine
		Pre-miRNA	Precursor microRNA
DIG	Digoxigenin	Pri-miRNA	Primary microRNA
DMSO	Dimethyl sulfoxide	PSCs	Pluripotent stem cells
dNTPs	Deoxynucleotide triphosphates	qRT-PCR	(Quantitative) Reverse Transcription PCR
dox	Doxycycline	R-NSCs	Rosette-forming NSCs
DR0	Direct repeat element with 0 spacing	RA	Retinoic acid
dsRNA	Double-stranded RNA	RISC	RNA-induced silencing complex
E6.5	Embryonic day 6.5	RNase	Ribonuclease enzyme
EBs	Embryoid bodies	rpm	Rounds per minute
EC cells	Embryonic carcinoma (EC) cells	rRNA	Ribosomal RNA
EGF	Epidermal growth factor	SAG	Smoothened agonist
ESCs	Embryonic stem cells	scr	Scrambled control oligonucleotide
ESCC miRNAs	ES cell cycle regulating miRNAs	SEM	Standard error of the mean
FACS	Fluorescence activated cell sorting	SHH	Sonic Hedgehog
FBS	Fetal bovine serum	siRNA	Small interfering RNA
FGF	Fibroblast growth factor	snoRNA	Small nucleolar RNA
FSC	Forward Scatter	SR	Serum replacement
G418	Geneticin	SSC	Sideward scatter
GAD	Glutamate decarboxylase	TC dish	Tissue culture dish
GCNF	Germ cell nuclear factor	TGF	Transforming growth factor
GCNF-RE	GCNF response element	TH	Tyrosine Hydroxylase
GDNF	Glial cell-derived neurotrophic factor	TRIF complex	Transiently retinoid acid-induced factor complex
GO	Gene Ontology	TSS	Transcription start site
h, hsa	Human, Homo sapiens	UTP	Uridine triphosphate
HEK cells	Human embryonic kidney cells	WB	Western blot

6.4 Acknowledgement

First of all, I would like to express my gratitude to Prof. Dr. Oliver Brüstle for his support and guidance throughout my PhD thesis. I would also like to thank him for putting the trust in me to follow my own ideas and to take the lead on the miRNA research at our Institute. I wish to thank my second supervisor Prof. Dr. Michael Hoch and the other thesis committee members for they interest in my work and for taking the time to examine my PhD thesis.

I am deeply grateful to Dr. Lodovica Borghese, who inspired me to work with miRNAs in the first place and guided me through the first half of my PhD thesis. My thanks also go to the former members of the "AG Lodo" Katja Hamann, Sergio D'Araio and Nina Groß for their support and the great working atmosphere. Special thanks go to my colleague Beate Roese-Koerner for the fruitful collaboration and for making conference visits even more enjoyable. I also wish to thank Monika Veltel, not only for her excellent technical assistance, but also for her emotional support and for helping me to run the miRNA lab. Furthermore, I would like to thank my students Katharina Doll, Nityaa Venkatesan, Nils Christian Braun and Thomas Berger for their help and for giving me the opportunity to see my research from a different perspective.

I thank all current and former members of the Institute of Reconstructive Neurobiology for creating an inspiring and cooperative scientific environment as well as for sharing many beautiful moments with me, in and outside of the lab. In particular, I want to thank Beatrice Weykopf, Dr. Gabriela Bodea, Dr. Jérôme Mertens, Johannes Jungverdorben, Dr. Micheal Peitz, Dr. Michael Karus and PD. Dr. Sandra Blaess for sharing their knowledge and for valuable scientific discussions. Furthermore, I would like to thank PD. Dr. Phillip Koch, Dr. Julia Ladewig, Dr. Jona Doerr, Dr. Jaideep Kesavan and Matthias Brandt for providing cells and Dr. Lars Nolden for helping me cloning the pTight-miRNA constructs. I also wish to thank my long-term office mates Monika Endl, Rachel Konang and Dr. Jaideep Kesavan for the nice atmosphere.

I would like to use this opportunity to appreciate the support that I have received from external collaborators. The miRNA profiling analysis presented in this work was performed in a joint project with Dr. Sandra Weinhold and Prof. Dr. Wernet from the Institute of Transplantation Diagnostics and Cell Therapeutics at the University of Düsseldorf, and I am deeply grateful for this valuable collaboration. I would also like to thank PD. Dr. Bernd Evert from the Department of Neurology at the University of Bonn for his help with the luciferase reporter assays. Many thanks go to Steven Lisgo and the Human Developmental Resource (HDBR) at Newcastle University for providing the human fetal brain samples.

While writing this thesis I have received a lot of help from my colleagues and friends. In particular, I want to thank Dr. Michael Karus, Dr. Lodovica Borghese, Kristina Dobrindt and Dr. Dominik Stappert for proof-reading my thesis. Moreover, I would like to thank Beate Roese-Koerner, Beatrice Weykopf, Dr. Tom Lickiss and Dr. David Ryan Ormond for their helpful comments.

I thank my friends and family with all my heart for keeping my spirits up, distracting me when needed, and for always being there for me. My husband and favorite travel companion Dominik has earned the very last words here: The current work could have only been completed, since you supported me with your brilliant scientific mind, your fantastic cooking skills, and most importantly with your love. Thank you!